STUDIES ON THE REGULATORY ROLES OF MICRORNA-27A AND MICRORNA-200B IN ACTIVATED RODENT MICROGLIA

SHWETA PRADIP JADHAV

(M.Sc.)

A THESIS SUBMITTED FOR THE DEGREE OF

DOCTOR OF PHILOSOPHY

DEPARTMENT OF ANATOMY

YONG LOO LIN SCHOOL OF MEDICINE

NATIONAL UNIVERSITY OF SINGAPORE

2015

DECLARATION

I hereby declare that this thesis is my original work and it has been written by me in its entirety. I have duly acknowledged all the sources of information which have been used in the thesis. This thesis has also not been submitted for any degree in any university previously.

NAME: SHWETA PRADIP JADHAV

DATE: 21/01/15

ACKNOWLEDGEMENTS

I would like to express my deepest gratitude to my supervisor, Associate Professor S. Thameem Dheen, Department of Anatomy, Assistant Dean (Graduate studies), Yong Loo Lin School of Medicine, National University of Singapore, for believing in me. His constructive criticism, patience and motivation through the years have helped me immensely. By pushing me to "think out of the box" Prof Dheen has helped me develop my potential as an independent researcher. I am greatly indebted to him.

I would like to thank my co-supervisor Associate Professor Mahesh Choolani for his encouragement, Associate Professor Samuel Tay Sam Wah (Deputy Head, Department of Anatomy), for his support and Professor Bay Boon Huat, Head, Department of Anatomy, NUS for providing me with an opportunity to be a part of "Team Anatomy". I thank NUS for the research scholarship for aiding my stay in Singapore. I am grateful to Dr Vivek Tanavde, Bioinformatics Institute, A*STAR for providing IPA software and Associate Professor Lu Jia from DSO laboratories, for help with the laser capture microdissection analysis.

I extend my gratitude to all staff and students of the Department of Anatomy for providing a wonderful work environment. I would like to acknowledge the technical assistance provided by Mrs. Ng Geok Lan, Mrs. Yong Eng Siang and Mrs. Chan Yee Gek and the administrative assistance provided by Mdm. Carolyne Ang, Ms Violet Teo and Mrs. Diljit Kaur d/o Bachan Singh. I would like to thank my labmates Sukanya, Parakalan, Janani, Nimmi, Sandhya and Radhika for their help and friendship through these years.

I am grateful to my dear friends Shruthi, Soumya, Sharvari, Srinath, Robert and Rohith for being there for me and sharing my fun and crazy times.

I would like to thank my mom Dr Shailaja Jadhav and dearest sister Preeti, for being a constant pillar of strength and a source of inspiration in my life and my dad Dr Pradeep Jadhav for his encouragement and blessings. Lastly, heartfelt thanks to my loving husband Aneesh, for his constant support, love and encouragement and without whom this thesis would not have been possible.

DEDICATION

I dedicate this thesis to my beloved family.

PUBLICATIONS

Various portions of this thesis have been published or submitted for publication.

International Journals:

Jadhav SP, Kamath SP, Choolani M, Lu J, Dheen ST. microRNA-200b modulates microglia-mediated neuroinflammation via the cJun/MAPK pathway. *J. Neurochem* (2014) 130, 388-401DOI: 10.1111/jnc.12731

Jadhav SP, Tanavde V, Dheen ST. (2014) microRNA-27a targets TGF-β signaling *via* repression of TβR1, SMAD2 and Runx1 in microglia (manuscript in preparation).

Shyamasundar S, **Jadhav SP**, Bay BH, Tay SSW, Kumar SD, et al. (2013) Analysis of Epigenetic Factors in Mouse Embryonic Neural Stem Cells Exposed to Hyperglycemia. *PLoS ONE* 8(6): e65945. doi:10.1371/journal.pone.0065945

CONFERENCE PRESENTATIONS

Oral Presentations:

1. **Jadhav SP***, Tanavde V, Dheen ST. "microRNA-27a targets TGF-β signaling via repression of TβR1, SMAD2 and Runx1 in microglia".

Proceedings of YLL SoM Graduate Scientific Congress (2015), 27th January 2015.

2. **Jadhav SP***, Tanavde V, Dheen ST. "microRNA-27a targets Smad2, a key mediator of TGF-β signalling in microglia". Neuroscience 2014, Washington DC, United States, November 15-19th 2014.
3. **Jadhav SP***, Choolani M, Lu J, Dheen ST. "miRNA-200b modulates microglia-mediated neuroinflammation by targeting the cJun/MAPK pathway". Proceedings of the SNA Symposium 2012, ed. Samuel Tay Sam Wah (2012): 008. SNA Symposium 2012, Singapore. 19th April 2012.
4. **Jadhav SP***, Dheen ST. "Analyzing promoter methylation". University of Madras-National University of SingaporeWorkshop on Epigenetics an**d** Gene Expression, Chennai, India, 19th-22nd December 2012.

Poster Presentations:

5. **Jadhav SP*,** M Choolani, E A Ling, J Lu, Dheen ST. "microRNA-200 family modulates microglia-mediated neuroinflammation". Proceedings of YLL SoM Graduate Scientific Congress (2012), 15th February 2012.

6. **Jadhav SP*,** M Choolani, E A Ling, J Lu, Dheen ST. "miRNA-200b modulates microglia-mediated neuroinflammation". *Glia in Health and Disease conference*, ed. Dwight Bergles, William Talbot (2012): 44.

New York: Cold Spring Harbor Laboratories, New York, 19th – 23rd July, 2012.

7. **Jadhav SP*,** M Choolani, E A Ling, J Lu, Dheen ST. "Analysis of microRNA functions in activated microglia". Proceedings of YLL SoM Graduate Scientific Congress (2013). 30th January 2013.
8. **Jadhav SP*,** M Choolani, E A Ling, J Lu, Dheen ST. "Regulatory roles of microRNAs in microglia-mediated neuroinflammation". Proceedings of ANS 2013 (2013). Melbourne: Australian Neuroscience Society. (Federation of Asian-Oceanian Neuroscience Societies) Conference 2013 2nd -6th February 2013.
9. **Jadhav SP*,** Kamath SP, M Choolani, E A Ling, J Lu, Dheen ST. "Analysis of miRNA signature in activated microglia". Proceedings of SNA Symposium 2013 (2013). Singapore Neuroscience Association (SNA). Singapore Neuroscience Association Symposium, Singapore, April 26th 2013.
10. Jadhav SP, Kamath SP, M Choolani, E A Ling, J Lu, Dheen ST*. "Understanding the role of microRNAs in microglia-mediated neuroinflammation". Glia, 61 (2013):S94. Berlin: Wiley Periodicals. XI European Meeting on Glia Cells in Health and Disease, Berlin, July 3-6, 2013.
11. **Jadhav SP*,** Kamath SP, M Choolani, E A Ling, J Lu, Dheen ST. "Understanding the role of microRNAs in microglia-mediated Immune response". Proceedings of the 8th International Conference for Neurons and Brain Diseases (2013). NUS: SFN Singapore Chapter. The 8th

International Conference for Neurons and Brain Diseases, Singapore 2nd-4th July 2013.

12. **Jadhav SP*,** Kamath SP, M Choolani, E A Ling, J Lu, Dheen ST. "microRNA-200b modulates microglia-mediated neuroinflammation by regulating the cJun/MAPK pathway". 10th Biennial Conference of the Chinese Neuroscience Society, Beijing, September 19th – 22nd, 2013.
13. **Jadhav SP*,** Kamath SP, M Choolani, E A Ling, J Lu, Dheen ST. "microRNA-200b regulates the cJun/MAPK pathway in activated microglia". Proceedings of YLL SoM Graduate Scientific Congress 2014, NUS. YLL SoM Graduate Congress 11th March 2014.

AWARDS

- **Anatomy Graduate student award 2013**
- **NUS Medicine FY 2014** "**Best Oral Presentation award**"- for presentation at International Conference, SfN, **Washington D.C** 15-19th Nov 2014
- **1st Runner-up** Oral Presentation Award at YLLSoM 5th Annual Graduate Scientific Congress 2015, Singapore

POSTER AWARDS

1. **Jadhav SP*,** M Choolani, E A Ling, J Lu, Dheen ST. YLLSoM 2nd Annual Graduate Scientific Congress 2012, Singapore, 15th February 2012.
2. **Jadhav SP*,** M Choolani, E A Ling, J Lu, Dheen ST. YLLSoM 3rd Annual Graduate Scientific Congress 2013, Singapore 30th January 2013.
3. **Jadhav SP*,** M Choolani, E A Ling, J Lu, Dheen ST. SNA Symposium 2013, Singapore, April 26th 2013.
4. **Jadhav SP*,** M Choolani, E A Ling, J Lu, Dheen ST. YLLSoM 4th Annual Graduate Scientific Congress 2014, Singapore, 11th March 2014.

TRAVEL AWARDS

1. NUS-India Research Initiative travel award to attend the "Epigenetics and Gene Expression" workshop, Chennai, India, 19th-22nd December 2012.

2. Federation of Asian-Oceanian Neuroscience Societies travel award for attending FAONS-ANS 2013 symposium, Melbourne, 2nd -6th February 2013.
3. Chinese Neuroscience Society travel award for attending 10th Biennial Conference of the Chinese Neuroscience Society, Beijing, 19th – 22nd September, 2013.
4. Singapore Neuroscience Association (SNA) travel award for attending Neuroscience 2014, Washington DC, United States, 15th-19th November, 2014.

TABLE OF CONTENTS

ABBREVIATIONS

AD	Alzheimer’s disease
Aβ	amyloid beta
CC	Corpus Callosum
CNS	Central Nervous system
IL-1β	Interleukin-1 beta
IL6	Interleukin 6
iNOS	inducible nitric oxide synthase
ISH	*in situ* hybridization
JNK	cJun-N terminal kinase
LCM	Laser capture microdissection
LNA	Locked nucleic acid
LPS	Lipopolysaccharide
MAPK	Mitogen activated protein kinase
miRNA	microRNA
NO	nitric oxide
PD	Parkinson’s disease
Runx1	Runt-related transcription factor 1
SMAD2	Mothers against decapentaplegic homolog 2
TBI	Traumatic brain injury
TGFβ	Transforming growth factor beta
TNFα	Tumor necrosis factor alpha
TβR1	Transforming growth factor receptor 1

SUMMARY

The Central Nervous System (CNS) consists of neuron and glial cells which include astrocytes, oligodendrocytes and microglia. Microglia, while traditionally known as the "immune cells" of the CNS are now known to possess multiple effector functions ranging from immune surveillance, synaptic plasticity and pruning to playing roles in higher order functions such as learning and memory. As part of their immune effector function, microglia continuously scan the surrounding brain parenchyma for perturbations resulting from injury or other pathological conditions. Upon stimulation in pathological conditions, microglia undergo morphological and functional changes, become activated, migrate to the site of injury and release several cytotoxic molecules such as superoxides, nitric oxide (NO), reactive oxygen species (ROS), proinflammatory cytokines and chemokines. However, in neuropathologies including neurodegenerative diseases such as Alzheimer's disease, and Parkinson's disease, microglia are chronically activated releasing excessive amount of the proinflammatory mediators, resulting in exacerbation of the neuroinflammation and neuronal damage. Thus, it has been widely suggested that understanding the mechanism of microglia-mediated inflammation is crucial towards developing neurodegenerative disease therapies.

MicroRNAs (miRNAs) function as epigenetic regulators of gene expression by binding to the 3' UTR of their target mRNAs resulting in gene silencing either by mRNA translational inhibition or mRNA degradation. MiRNAs influence a number of biological processes including immune-

mediated pathologies. About 70% of all known miRNAs are expressed by human and rodent brains with dynamic changes in their expression pattern during development and disease processes. MiRNAs have been shown to regulate microglial functions, however a catalogue documenting the altered expression of miRNAs in activated microglia is lacking. It is hypothesized that microglial activation in neuropathological conditions is regulated by molecular and epigenetic mechanisms. In order to understand the altered expression profile of miRNAs contributing to microglial activation, a global miRNA microarray was carried out using control and activated primary microglia (activation by LPS and β-amyloid). This screen identified several differentially expressed miRNAs in activated microglia in response to LPS and β-amyloid. The microarray was followed by pathway analysis using Ingenuity Pathway Analysis (IPA) software for identification of specific pathways targeted by selected (up/down regulated) miRNAs. Quantitative PCR analysis was used to validate the expression of selected miRNAs from the microarray screen in primary and BV2 microglia. In order to understand the miRNA-mediated regulation of microglial functions, 2 miRNAs were chosen for further analysis: 1. miR-27a which was found to be upregulated in activated microglia; 2. miRNA-200b which was found to be repressed in activated microglia.

MiR-27a was predicted to target SMAD2, TβR1 and Runx1, members of the TGFβ signalling pathway in microglia. TGFβ1 is an anti-inflammatory cytokine and TGFβ signalling *via* SMAD2/3 has been shown to lead to microglial quiescence. Thus, it was hypothesized that miR-27a promotes the proinflammatory response of microglia by suppressing TGFβ-SMAD signalling in microglia. On the other hand, miR-200b was predicted to target

cJun, a member of the mitogen activated protein kinase (MAPK) signalling pathway. MAPK pathways regulate production of proinflammatory cytokines and cytotoxic molecules by activated microglia. Thus it was hypothesized that miR-200b inhibits microglia activation by suppressing the cJun/MAPK pathway in microglia.

MiR-27a was identified as a novel miRNA upregulated in activated primary microglia *in vitro* as well as in activated microglia isolated using laser-capture microdissection from traumatic brain injury (TBI) rat model *in vivo*. Bioinformatic analysis had predicted miR-27a to target the TGFβ pathway in microglia. TGFβ1 cytokine was found to be upregulated in activated microglia *in vivo* whereas TGFβ receptor 1 (TβR1) and SMAD2, key mediators of TGFβ signalling were found to be downregulated in activated microglia *in vitro*. On the other hand, Runx1, a target of TGF-β- SMAD signalling was found to be upregulated in activated microglia. Gain-of-function, loss-of-function studies using miR-27a mimic and inhibitor respectively, confirmed TβR1, SMAD2 and Runx1 as the targets of miR-27a. MiR-27a inhibition resulted in an increase in SMAD2 activity as measured by the expression of phospho-SMAD2. Further, miR-27a was observed to positively regulate the inflammatory response of microglia with overexpression of miR-27a resulting in a decrease in the expression of alternative activation genes such as Ym1 and Arginase1 and an increase in the expression of the proinflammatory cytokines TNFα, IL6, IL-1β and iNOS. Furthermore, miR-27a overexpression also resulted in increased NF-κB nuclear translocation in microglia, correlating with increased inflammatory response. Lastly, treatment of MN9D neurons with microglia conditioned

medium (CM) obtained after overexpression of miR-27a in microglia appeared to be neurotoxic as it had a cytotoxic effect on survival of the neurons as evidenced by Annexin V FACS analysis. These results demonstrate how miRNAs can regulate the expression of specific genes thereby promoting the proinflammatory actions of microglia.

MiR-200b was found to be repressed in activated microglia *in vitro* as well as in activated microglia isolated using laser-capture microdissection from traumatic brain injury (TBI) rat model *in vivo*. MiR-200b was shown to target cJun, the substrate of JNK MAPK (mitogen-activated protein kinase) which mediates the release of proinflammatory cytokines. Loss-of-function and gain-of-function studies using miR-200b inhibitor and mimic respectively, in microglia confirmed cJun to be the target of miR-200b. Luciferase assay confirmed the binding of miR-200b to the 3'UTR of cJun gene demonstrating that cJun is a direct target of miR-200b. Overexpression of miR-200b resulted in a decrease in JNK expression and activity, thus dysregulating the MAPK-JNK pathway. Further, miR-200b was shown to negatively regulate the inflammatory response of microglia. Knockdown of miR-200b resulted in an increase in the pro-inflammatory cytokines, TNF-α, IL-1β and IL6, as well as iNOS expression and NO production. Conversely, overexpression of miRNA-200b led to a decrease in the pro-inflammatory cytokines, iNOS and NO. Furthermore, overexpression of miR-200b impaired the migratory potential of activated microglia. Lastly, treatment of MN9D neurons with microglia conditioned medium after miR-200b knockdown resulted in increased cell death as compared to control as a result of increased secretion of proinflammatory cytokines and NO in the culture medium.

In conclusion, this study provides a database of differentially expressed miRNAs in activated microglia. Further, the author attempts to understand the miRNA regulation of microglial function *via* 2 differentially expressed miRNAs in activated microglia. It is concluded that miRNAs altered different aspects of microglial functions including inflammatory response, migration and neuronal survival by regulating the TGFβ and MAPK signalling pathways in microglia.

LIST OF TABLES

LIST OF ILLUSTRATIONS

1 INTRODUCTION

The Central Nervous System (CNS) consists of neurons and non-neuronal glial cells. Glia consist of macroglia constituting astrocytes and oligodendrocytes and microglia. Microglial cells which account for 5–20% of the total glial cell population within the CNS parenchyma are distributed throughout the brain and spinal cord (Lawson *et al.* 1990). Microglia have been shown to originate from the yolk sac and populate the CNS prior to vasculogenesis (Ginhoux *et al.* 2010) and are involved in maintaining the internal milieu of the CNS in both health and disease (Perry *et al.* 2010).

Microglia appear round or amoeboid in shape in early postnatal stage and undergo functional and morphological transformation to form "ramified" or "resting" microglia in adult stage (Ling and Wong 1993). Resting microglia in the adult brain have a small cell body and are highly ramified with multiple fine processes. "Resting" is a misnomer because these cells continuously scan the surrounding parenchyma with their processes and communicate directly with neurons and astrocytes (Davalos *et al.* 2005; Nimmerjahn *et al.* 2005; Graeber 2010). This perpetual state of motion allows them to respond swiftly to neuronal damage or infection by transforming into an activated phenotype and performing inflammatory functions. They are remarkably plastic and capable of responding to a vast array of challenges in the CNS. Upon detection of specific factors generated by parenchymal injury, degeneration, or infection, microglia undergo morphological transformations and respond rapidly through induction of genetic programs designed to overcome and repair CNS insults (Kreutzberg 1996). Transformations of microglial morphology, phenotype and

function are observed during almost all neuropathological conditions (e.g., degenerative diseases, infection, stroke, tumors and brain injury) (Banati and Graeber 1994; Stoll and Jander 1999; Streit *et al.* 1999). Initially thought to be the immune effectors of the CNS, microglia are now known to perform several neurological functions including regulation of synaptic activity (Nayak *et al.* 2014). Thus, microglia play a major role in maintaining the overall health of the CNS.

1.1 Microglia Origin and Development

Neurons, astrocytes and oligodendrocytes arise from the neuroectoderm during embryogenesis. However, microglia are distinct from the other CNS cell types as they have been shown to originate from the mesoderm.

Although microglia were believed to have neuroectoderm origin in early days, their non-neuroectodermal origin was first suggested in 1932 (Rezaie and Male 2002). Subsequently, it was shown that the precursor cells of monocyte lineage or the circulating monocytes enter brain during the embryonic, fetal or postnatal stages of development and differentiate into microglia (Ling and Wong 1993; Kaur *et al.* 2001). Recent *in vivo* fate mapping study of yolk-sac-derived cells in mice revealed that microglia are derived from extra embryonic yolk sac macrophages that populate the brain during early fetal development (Ginhoux *et al.* 2010). This finding was further confirmed by Schulz and his colleagues, since the transcription factor Myb, which is required for hematopoiesis and the generation of hematopoietic stem cells (HSCs), was found to be not essential for the generation of microglia (Schulz *et al.* 2012). $Myb^{-/-}$ mice are deficient in hematopoietically derived

monocytes/macrophages but had normal numbers of microglia in the CNS, indicating that yolk sac-derived macrophages are distinct from HSC derived progeny. Further studies revealed that microglia are derived from CD45^{-}/c-kit+ erythromyeloid progenitor cells (Kierdorf *et al.* 2013). These precursors developed into CD45+/c-kit^{low}/CX3CR1− immature cells, which finally matured into CD45+/c-kit−/CX3CR1+ microglia and invaded the brain rudiment using matrix metalloproteinases (MMPs), such as MMP-8 and MMP-9. Collectively, these studies support the concept that microglia are derived from embryonic yolk sac. During neonatal development, primitive yolk-sac-derived microglial progenitors appear amoeboid. However, they eventually progress through a developmental program that includes proliferation and subsequent acquisition of ramified processes, which give rise to the ramified microglial phenotype commonly observed in the adult CNS (Ling and Wong 1993) (Illustration 1).

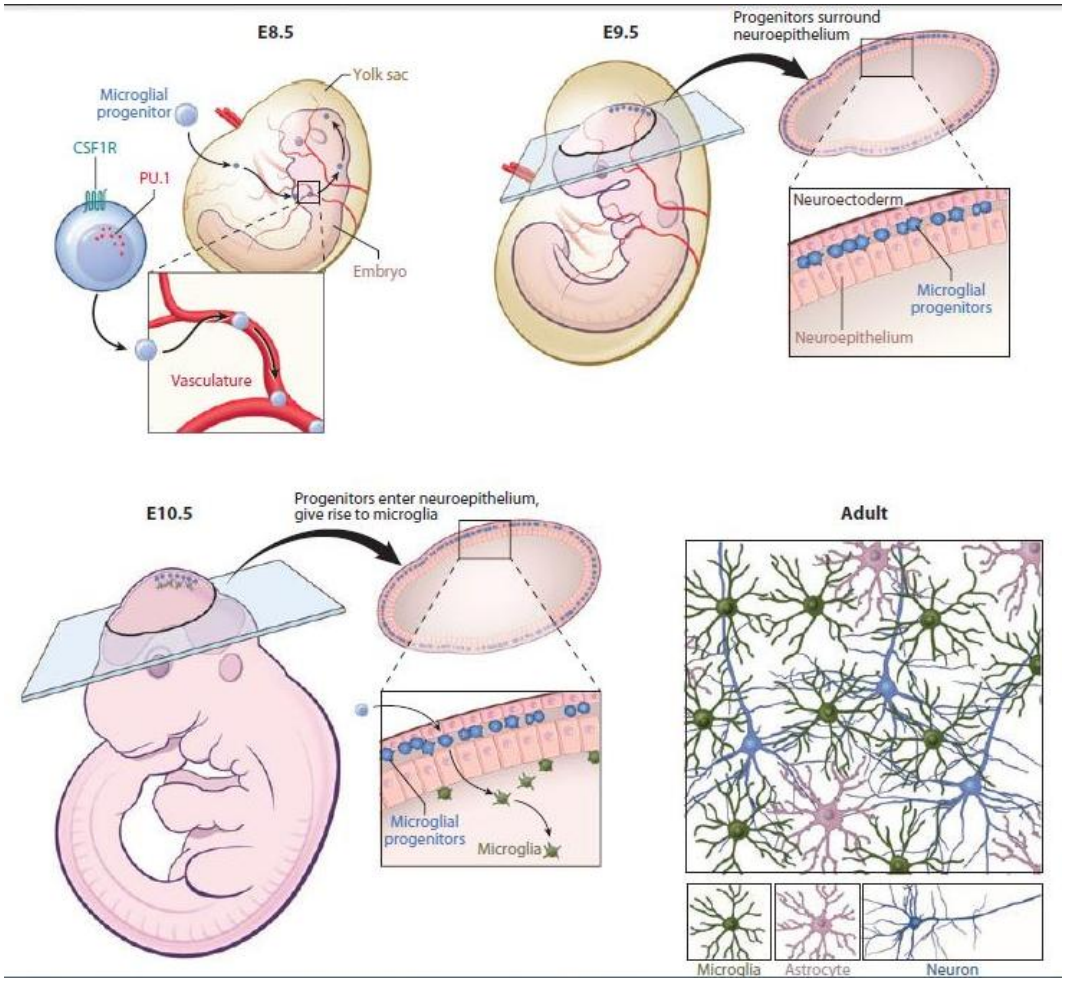

Illustration 1: Adapted from Nayak *et al*, 2014 (Nayak *et al.* 2014).

1.2 Homeostatic functions of microglia

1.2.1 Neurogenesis

During development there is a need for precise generation of neurons and glia (astrocytes and oligodendrocytes) from neural precursors. Interestingly microglial precursors have been co-localised in neuroepithelia with neural progenitors indicating a role for these cells in neurogenesis (Kaur *et al.* 2001; Chan *et al.* 2007; Ginhoux *et al.* 2010). Further, microglia are known to secrete trophic factors such as hepatocyte growth factor, basic fibroblast

growth factor (bFGF), brain-derived neurotrophic factor (BDNF), insulin-like-growth-factor-1 (IGF-1), which support the formation of neural circuits and promote their survival (Yamagata 1995; Tuan Trang, Simon Beggs 2011; Ueno *et al.* 2013) (Illustration 2).

1.2.2 Programmed Cell Death in developing CNS

Excessive immature neurons formed during development are eliminated through programmed cell death (Buss *et al.* 2006). In addition, neurons that form weaker neuronal circuits or that perform only transient functions also undergo apoptosis. Microglia initiate this cell death by releasing "death-inducing factors" and phagocytose the resulting debris (Ueno and Yamashita 2014) . Several molecular mechanisms by which microglia initiate neuronal apoptosis in distinct regions of the CNS have been identified: 1) releasing superoxide ions in the cerebellum (Jose Luis Marin-Teva *et al.* 2004), 2) through nerve growth factor in the retina which induces cell death *via* p75 neurotrophin receptor (Jose Maria Frade 1998), 3) through TNFα in the spinal cord (Sedel *et al.* 2004), 4) through induction of the complement system *via* complement receptor 3 (CR3) in the hippocampus (Schafer *et al.* 2012).

In addition to initiating apoptosis, microglia help clean up the CNS parenchyma by phagocytising the dead and dying neurons without initiating an inflammatory response (Marín-Teva *et al.* 2011). Non inflammatory phagocytosis proceeds through triggering receptor expressed on myeloid cells-2 (TREM2) signaling (Takahashi *et al.* 2005). TREM2 signaling activates DAP12, a transmembrane immune receptor protein, which induces cytoskeletal reorganization and phagocytosis (Campbell and Colonna 1999;

Linnartz *et al.* 2010). In this manner, both, numbers of neural precursors as well as differentiated neurons are regulated by microglia (Cunningham *et al.* 2013).

1.2.3 Synaptic pruning

Microglial phagocytic activity is essential for synaptic homeostasis (Paolicelli *et al.* 2011; Wake *et al.* 2013). Proper synaptic function is dependent on several trophic factors and synaptogenic signals released by microglia. It has been demonstrated that DAP12 signaling is essential for synaptic function and plasticity (Roumier *et al.* 2004). In the mouse brain, the expression of DAP12 is restricted to microglia. Loss of DAP12 leads to reduction of tyrosine kinase receptor B (TRK-B), a receptor for brain-derived neurotrophic factor (BDNF), leading to aberrant synaptic function. Further, studies on *ex-vivo* organotypic hippocampal slice cultures revealed that microglia can influence synaptic function by regulating synaptic densities and dendritic spine numbers (Ji *et al.* 2013). Microglial engulfment of pre- and post-synaptic proteins has also been observed (Paolicelli *et al.* 2011). Microglia mediate synaptic pruning *via* CX3CR1 signaling. CX3CR1 is a chemokine receptor expressed solely by microglia in the CNS (Hughes *et al.* 2002; Limatola and Ransohoff 2014). CX3CR1 deficient mice show increased dendritic spines thereby indicating aberrant synaptic pruning (Paolicelli *et al.* 2011) (Illustration 2).

The complement system is also known to mediate microglial synaptic pruning. Neurons express the complement protein C1q which activates C3. Since microglia express C3 receptor (CR3), it is possible that microglia mediate synaptic pruning and phagocytosis through the complement system.

Indeed, mice deficient in C1q or C3 retained excessive synaptic connections (Stevens *et al.* 2007). Moreover it has been shown that microglia phagocytose retinogeniculate synapses *via* CR3 signaling. Collectively these studies indicate that microglia participate in synaptic development and maintenance (Schafer *et al.* 2012).

1.2.4 Synaptic maturation

In addition to synaptic pruning, microglia are required for proper synaptic maturation. Around postnatal day 13, as compared to wildtype littermates, the amplitude and frequency of miniature excitatory post-synaptic currents (mEPSCs) are increased in CX3CR1 null mice (Paolicelli *et al.* 2011). CX3CR1 null mice also display alterations in excitatory transmission (Zhang et al., 2014). Since CX3CR1 is expressed solely by microglia in the CNS, these studies are suggestive of a role of microglia in maturation of synapses. Consistent with this hypothesis, mice harbouring DAP12 mutation display abnormal synapses by postnatal day 18-25 (Roumier *et al.* 2004).

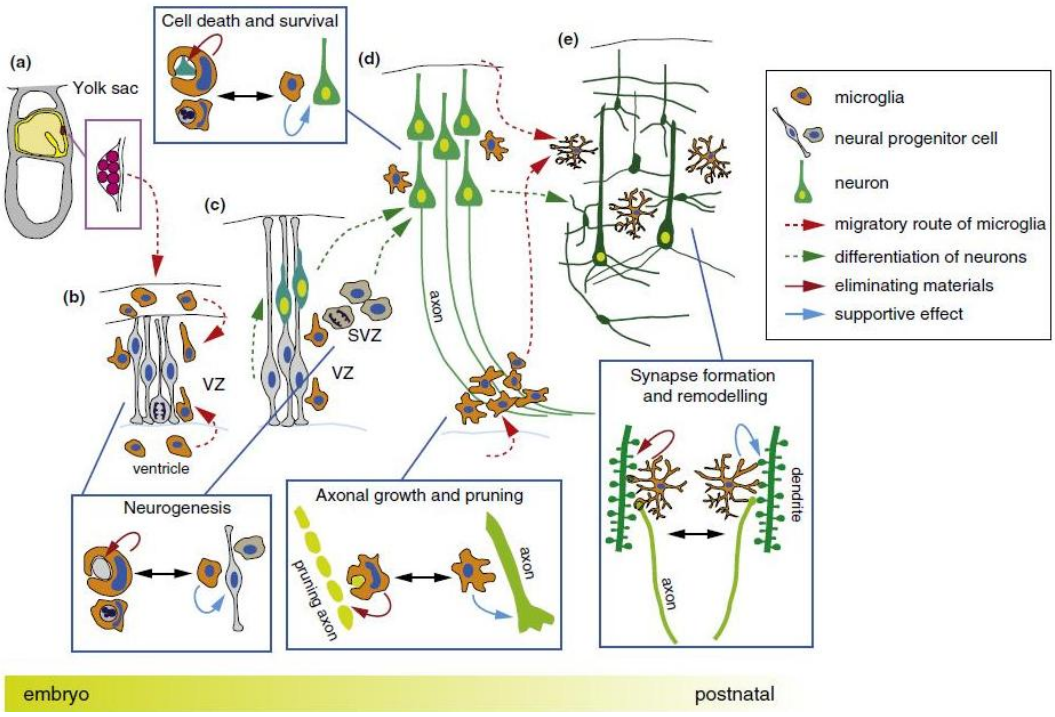

Illustration 2 showing the regulation of neurogenesis and synaptic maturation by microglia. Adapted from Ueno M *et al*, 2014 (Ueno and Yamashita 2014). License number-3546811398453.

1.2.5 Synaptic plasticity involved in learning and memory in the adult

Synaptic plasticity involves activity-triggered persistent changes in synaptic efficacy and is the fundamental mechanism underlying learning and memory. Such persistent activity-triggered synaptic inputs may result in an increase or decrease in synaptic efficacy referred to as long-term potentiation (LTP) or long-term depression (LTD) respectively. Learning and memory is dependent on neurogenesis, which occurs in the developing and adult brain. Microglia are regulators of activity-driven synaptic plasticity (Rogers *et al.* 2011; Schafer *et al.* 2013), adult neurogenesis (Gemma and Bachstetter 2013) and learning and memory (Rogers *et al.* 2011; Tremblay 2011; Parkhurst *et al.* 2013). Microglia through CR3 affect activity independent LTD (J. Zhang et al., 2014). CNS-TGFβ1 deficient mice which lack microglia display altered synaptic plasticity

with reduced LTP but increased LTD at the Schafer collateral-CA1 synapses in the hippocampus (Butovsky *et al.* 2014). These observations are consistent with those in CX3CR1 null mice in which LTP is almost eliminated with the mice displaying deficits in hippocampal-dependent learning and memory (Rogers *et al.* 2011). Using $CX3CR1^{CreER}$:$R26^{iDTR}$ mice (transgenic mice in which a selected depletion of microglia is possible) it has been observed (Parkhurst *et al.* 2013) that microglia-depleted mice showed deficits in contextual fear conditioning, novel object recognition, tests of hippocampal dependant learning and motor learning. In addition, reduction in both elimination and formation of dendritic spines was observed in microglia-depleted animals, indicating the essential role of microglia in synaptic plasticity and learning in the normal adult CNS. Further, it has been shown BDNF, a neurotrophin known to regulate synaptic plasticity (Korte *et al.* 1995) is expressed in microglia which regulate learning and memory through BDNF signaling (Parkhurst *et al.* 2013).

1.3 Activation of microglia

1.3.1 Different activation states of microglia

In response to different stimuli, microglia and peripheral macrophages are known to display different reactive phenotypes. These activation states are broadly classified into 2 types:

M1/Classical activation: Activation of microglia and macrophages in response to infection resulting in the expression of high levels of

proinflammatory cytokines and an enhanced microbicidal capacity is defined as the M1 or classical activation phenotype. Interferon-γ (IFNγ) and LPS trigger an M1 phenotype in microglia which are characterized by a high expression of TNFα, Toll-like-receptors (TLRs), co-stimulatory molecules for antigen presentation and cytotoxic molecules like reactive oxygen species (ROS). The M1 phenotype has been shown to be neurotoxic (Boche *et al.* 2013). This classical activation of microglia has been clearly demonstrated in a number of neuropathologies such as experimental autoimmune encephalomyelitis (EAE)-induced demyelination, and neurodegenerative diseases, such as Alzheimer's disease (AD), Parkinson's disease (PD) and amyotrophic lateral sclerosis (ALS) (Colton 2009; Luo and Chen 2012).

M2/Alternative activation: M2 phenotype in microglia is defined as the response elicited in response to cytokines, interleukin-4 (IL-4) or interleukin-13 (IL-13) and is characterized by the expression of anti-inflammatory cytokines such as interleukin-10 (IL-10) and TGFβ and high expression of scavenger receptors such as RAGE and CD36 (Aguzzi *et al.* 2013). Thus this phenotype microglia are neuroprotective as they exert anti-inflammatory effects, resolve inflammation and promote tissue repair (Hanisch 2013). It has been observed that *in vitro* stimulation of microglia with anti-inflammatory cytokines induced expression of alternative activation genes such as arginase 1 (Arg1), mannose receptor, found in inflammatory zone I (FIZZ1) and chitinase 3-like protein 3 (Ym1) (Colton 2009). Microglia and peripheral macrophages have also been shown to switch from one phenotype to another influencing the outcome of CNS repair (Kigerl *et al.* 2009). For example, during infection,

microglia assume a M1 phenotype and switch to M2 as the response matures (Hanisch and Kettenmann 2007). In an oxygen-glucose deprivation model (OGD), M1 primed microglia aggravated neuronal cell death while M2 primed microglia enhanced neuronal survival (X. Hu et al., 2012). In EAE, the mouse model of multiple sclerosis, microglia were found to be exclusively M2 primed as evidenced by the expression of YM1. Further, infiltrating macrophages were also positive for Ym1 (Ponomarev *et al.* 2007).

A third activation phenotype has been proposed, M3, with IL-10 and TGFβ being the inducers of this phenotype. While direct evidence supporting the existence of this phenotype in microglia is lacking, it should however be noted that delivery of IL-10 in APP/PS1 mice (transgenic mouse model of AD with apolipoprotein mutation) has been shown to reduce astrogliosis/microgliosis, increase neurogenesis and restore spatial learning abilities (Kiyota *et al.* 2012). Further, TGFβ has been shown to enhance the anti-inflammatory effects of IL-4 including induction of Arg1 and YM1, the alternative activation markers in microglia *in vitro*. Moreover blocking of the TGFβ receptor 1 (TβR1) resulted in a reduction of Arg1 and YM1 in microglia (Zhou *et al.* 2012) suggesting that TGFβ enhances IL-4 mediated M2/Alternative activation in microglia. These results point towards the presence of a third "deactivated" state of microglia with microglia returning to the same functional state as the resting phenotype. This "deactivated state" may be genetically and/or epigenetically different from the native/resting state and holds tremendous therapeutic potential (Hanisch and Kettenmann 2007).

1.3.2 **Proliferation**

In early postnatal period, amoeboid microglia undergo rapid proliferation and develop into mature ramified microglia. Only about 30% of the total amoeboid microglia transform into ramified form with the rest undergoing apoptosis (Imamoto and Leblond 1978; Ling and Wong 1993). In order to document the molecular changes governing microglial transformation, a microarray analysis performed using laser capture microdissected microglia from 5 day and 28 day rat brain revealed several genes involved in cell proliferation to be highly expressed in amoeboid microglia (Parakalan *et al.* 2012). Runx1t1 (Runt-related transcription factor 1, translocated to 1), a gene found to be expressed in amoeboid microglia from this microarray, has been established as a novel transcriptional repressor of microglial proliferation (Baby *et al.* 2014). Further, Runt-related transcription factor 1(Runx1) has been identified as a regulator of transformation of amoeboid microglia into ramified microglia by controlling microglial proliferation in early postnatal stage *in vivo* (Zusso *et al.* 2012). Further, Runx1 has been shown to be induced in adult microglia during nerve injury (Zusso *et al.* 2012) and traumatic brain injury (Logan *et al.* 2013) to control microgliosis occurring as a result of microglial proliferation.

Microglia have been shown to undergo rapid proliferation in several CNS pathologies. In human brain from AD patients, proliferating microglia were observed. Further, it occurred in close proximity of plaque pathology, and may contribute to the neuroinflammation common in AD (Marlatt *et al.* 2014). In another neurodegenerative disease, incidental Lewy body disease (iLBD), a prodromal state of PD, increased number of proliferating microglia were observed in hippocampus of patients as compared to healthy controls.

However, proliferating microglia were not observed in established PD patients suggesting an early microglial response to developing PD pathology (Doorn *et al.* 2014). Using immunohistology and *in vivo* two-photon imaging, rapid proliferation of the resident microglia was detected around the ischemic core of the stroke brain. Further reactive microglia were also recruited to the ischemic area continuously during the first week after stroke induction (T. Li et al., 2013).

A number of receptors expressed by microglia are known to play a role in microglial proliferation. An important molecule governing microglial proliferation is CSF1R, the receptor for colony stimulating factor (CSF). CSF1R is solely expressed by microglia in the CNS. CSF1 is upregulated in the AD brain and promotes the proliferation of microglia by binding to the CSF1R (Erblich *et al.* 2011).

1.3.3 Phagocytosis

Phagocytosis is an important function of microglia enabling it to clear cellular debris in healthy and diseased conditions. The mechanism of phagocytosis by microglia is relatively unknown. However recent studies suggest a three step process of phagocytosis by microglia: “find-me”, “eat-me” and “digest-me” (Sierra *et al.* 2013) (Illustration 3).

1. **Find-me:** when the motile processes of microglia encounter signals released by a target (dying neurons or infective pathogens), the phagocytosis process is initiated. For example, uridine diphosphate (UDP), acts on P2Y6 receptors on the microglial surface to facilitate phagocytosis (Koizumi *et al.* 2007). Microglia also expresses the

fractalkine receptor/CX3CR1 which binds to its ligand fractalkine/CX3CL1 released by apoptotic cells which promote their phagocytosis (Noda *et al.* 2011).

2. **Eat-me:** depending on their targets, phagocytes such as microglia, express two types of cell surface receptors enabling them to recognise distress signals from either invading pathogens or apoptotic cells (Ravichandran 2010). Phosphatidylserine (PS), which is a component of cellular membrane and is expressed on apoptotic cell membrane, is the most distinguished "eat me" signal (Ravichandran 2010). Microglia express various P2X and P2Y receptors, nucleotide receptors, which regulate phagocytosis and are also considered as "eat me" signal (Franke *et al.* 2007; Koizumi *et al.* 2007). Another important receptor that signals internalization is TREM2, whose loss-of-function prevents microglial phagocytosis (Takahashi *et al.* 2005). In order to initiate phagocytosis, microglia express various receptors including lipopolysaccharide (LPS) receptor, CD14 (Reed-Geaghan *et al.* 2009), the scavenger receptor, CD36 and the toll-like receptors (TLRs) (Yu and Ye 2014). In addition to direct recognition of target by microglia receptors, antibodies such as IgG and complement proteins such as C3 can also bind to Fc receptors and complement receptors (CR3) respectively, present on microglial cell surface, triggering internalization. Microglia have also been shown to phagocytose weaker synapses and dendrites *via* CX3CR1 and CR3 mediated mechanisms (Tremblay 2011; Schafer *et al.* 2012).

3. **Digest-me:** a number of hydrolytic enzymes such as cathepsins, ATP proton pumps to acidify the medium, are required for degradation of the internalized target (Garin *et al.* 2001). A live-cell imaging study in *Caenorhabditis elegans* has revealed that nematode microglia possess ATP proton pumps for target degradation (Peri and Nüsslein-Volhard 2008). Further, phagocytosis is not limited to amoeboid or activated microglia alone, but is carried out by ramified microglia as well (Peri and Nüsslein-Volhard 2008; Sierra *et al.* 2010).

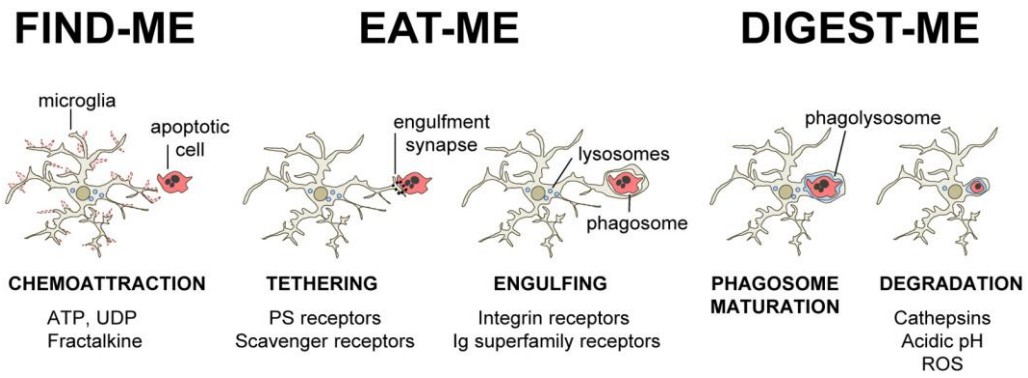

Illustration 3 Adapted from Sierra *et al*, 2013 (Sierra *et al.* 2013).

1.3.4 Production of cytokines and chemokines

Cytokines are signaling molecules produced by a cell for specific biological functions. Microglia are known to secrete several cytokines including IL6, IL-1β, TNFα, TGFβ, IL-10 and CSFs (Benveniste 1992). Microglia release cytokines which in turn activate microglia as a part of their immune response in the CNS (Hanisch 2002). Several exogenous factors including viral envelop protein, bacterial cell wall components such as LPS, bacterial DNA, and prions stimulate the release of cytokines by microglia (Heppner *et al.* 2001). Endogenous factors triggering microglia to secrete cytokines are lipids, serum

factors, complement proteins or disturbance in ATP or K^+ levels (Hanisch 2002).

Cytokines are of two types- pronflammatory- or anti-inflammatory (Benveniste 1992). As the name suggests proinflammatory cytokines including IL6, IL-1β, and TNFα aid in the activation of microglia and peripheral macrophages in inflammatory conditions (Benveniste 1992; Merrill 1992) . Anti-inflammatory cytokines include TGFβ, and IL-10 and are released in order to reduce inflammation and assist in tissue growth and repair (Hanisch 2002). The cytokine, IFN-γ is a well-known inducer of antimicrobial, pro-inflammatory, and antigen-presenting functions of microglia (Benveniste 1992). Upon activation of microglia, IFN-γ binds to its receptor which is readily expressed in microglia (Vass and Lassmann 1990). This activates the transcription factor STAT-1 further activating the downstream target genes (Leonard and O'Shea 1998; Nguyen and Benveniste 2000).

TNFα is another pro-inflammatory cytokine, promoting phagocytosis and secretion of pro- and anti-inflammatory cytokines by activated microglia (ChaoHuShengand Peterson 1995; ChaoHuShengTsang*et al.* 1995). TNFα is a major autocrine activator produced by microglia during CNS inflammation (Becher *et al.* 2000). The TNFα receptors, TNFRI and TNFRII have been shown to be expressed in microglia *in vitro* (Dopp *et al.* 1997). TNFα activates several transcription factors including NFkB (Cao *et al.* 1999) to promote the transcription of many immune genes.

IL-1 is another pro-inflammatory cytokine produced by microglia (Même *et al.* 2006) involved in the initiation of neuroinflammation by

inducing the expression of cytokines (Chao and Peterson 1995) and chemokines (McManus *et al.* 1998). IL-1 can also serve as an autocrine activator (Janabi *et al.* 1996; Saud *et al.* 2005).

Microglia produce a number of anti-inflammatory cytokines, such as IL-10, TGFβ (Palin *et al.* 2001; Rasley *et al.* 2006), which down-regulate the expression of proinflammatory cytokines, chemokines and cytotoxic molecules such as ROS (Aloisi *et al.* 1999; O'Keefe *et al.* 1999).

Chemokines are small peptides playing crucial role in cell migration and cellular communication(Fernandez and Lolis 2002). Chemokines act by binding to chemokine receptors expressed on target cells (Rollins 1997). Signaling of chemokines through various chemokines receptors present on microglial surface is important for microglial proliferation, migration, cytoskeletal reorganization and cytokine production (Boddeke *et al.* 1999; Trebst *et al.* 2003; de Jong *et al.* 2008). Microglia are known to upregulate chemokine receptors during development CXCL1, (Filipovic *et al.* 2003) as well as in neuropathological conditions such as ischemia (CXCL8/IL-8) (Popivanova *et al.* 2003), AD (CCL2/MCP-1) (Ishizuka *et al.* 1997), multiple sclerosis (CCL3/MIP-1α) (Balashov *et al.* 1999) and in different bacterial and viral infections (CCL4/MIP-1) (McManus *et al.* 1998).

1.3.5 Migration

Migration is an important aspect of microglial function in immune response. Ramified microglia sense the contiguous parenchyma using their fine processes. Amoeboid microglia can migrate within brain parenchyma (Rezaie

and Male 1999). A number of candidate molecules serve as triggers for microglial migration including neurotransmitters such as ATP and purinergic receptors (P2Y12) (Irino *et al.* 2008), AMPA and metabotropic glutamate receptors (Liu *et al.* 2009), chemokines such as CCL21 (Rappert *et al.* 2002), CX3CL1 released by neurons which bind to receptors CXCR3 and CX3CR1 (Liang *et al.* 2009) on microglia, lysophosphatidic acid (Schilling *et al.* 2004), bradykinin (Ifuku *et al.* 2007) and β-amyloid (Heneka *et al.* 2010). In addition, components associated with actin cytoskeleton such as ion channels and transporters including K^+ channels, Cl^- channels, Na^+/H^+ exchanger, $Cl^-/HCO3^-$ exchanger also play an important role in cell migration (Schwab 2001). Impaired microglial migration leads to several brain diseases such as Prion disease (Ciesielski-Treska *et al.* 2004), PD (Park *et al.* 2008) and AD (Mizuno 2012) and inhibit axonal regeneration during acute CNS injuries (Vargas and Barres 2007).

1.4 Important signalling pathways that regulate microglia functions

1.4.1 Mitogen-activated protein kinase (MAPK) pathway

Mitogen-activated protein kinase (MAPK) signal transduction pathways are ubiquitously expressed, highly evolutionarily conserved mechanisms that enable cells to respond to a variety of stimuli, thereby regulating cellular functions (Kyriakis and Avruch 2012). MAPK pathways coordinate cellular responses to diverse stimuli including hormones, growth factors, cytokine, G

protein-coupled receptors and environmental stresses among others (Kyriakis and Avruch 2001). Mammals express multiple MAPK pathways with a majority of these being triggered by stress and inflammatory stimuli. The three major MAPK pathways are the extracellular signal-regulated kinases (ERK 1/2 or MAPKs1/3 or p44/42), cJun NH2-terminal kinases (JNKs) and p38 MAPK (Oliver and Jamur 2010). It has been shown that p38 and ERK MAPKs regulate the production of TNFα and iNOS in LPS activated glial cells including microglia and astrocytes (Zhang *et al.* 1998). p38 MAPK-mediated release of TNFα and NO was further observed in LPS activated rat and human microglia (Lee *et al.* 2000; Xing *et al.* 2008). JNK signaling is known for promoting cytokine production from LPS-stimulated or hypoxia-exposed microglia *in vitro* (Waetzig *et al.* 2005). Activation of all three MAPK cascades has been reported in LPS-stimulated BV2 microglia (Kim *et al.* 2004). In activated BV2 microglia, p38 and JNK pathways are upregulated, leading to ROS production *via* activation of NADPH oxidase (Sun *et al.* 2008; Wang *et al.* 2011). Moreover, in the rat model of white matter damage induced by hypoxia, activation of microglia was found to be associated with upregulation of JNK signaling while inhibition of JNK activation significantly reduced neuroinflammation (Wang *et al.* 2012). *In vivo* evidence also implicates MAPK pathways to aid microglial activation in brain pathologies such as stroke and AD. Activated MAPK signaling pathways contribute to AD pathogenesis through neuronal apoptosis (Tamagno *et al.* 2003), transcriptional activation of β and γ-secretases (Tamagno *et al.* 2005) and phosphorylation and stabilization of the amyloid precursor protein (Colombo

et al. 2009). α-synuclein a key protein in the pathogenesis of PD has been shown to activate p38, ERK, and JNK pathways in human microglial cells, thus inducing inflammation by promoting the production of IL-1β and TNFα (Klegeris *et al.* 2008). The MAPKs have also been implicated in causing neuronal death in PD by various other mechanisms such as phosphorylation of p53 by p38 MAPK (Chipuk *et al.* 2008) and activation of JNK (Vila *et al.* 2004; Brecht *et al.* 2005). Further, abberant MAPKs function in motor neurons and microglia, (Bendotti *et al.* 2005). p38 triggers NO production contributing to the Fas-dependent apoptosis of motor neurons in ALS (Raoul *et al.* 2002). The above evidence suggests that MAPKs signaling is triggered in activated microglia *in vivo* and *in vitro* and mediates neuroinflammation *via* microglial activation.

1.4.2 Transforming growth factor beta (TGF-β) pathway

TGFβ1 is a pleiotrophic cytokine involved in different biological processes including gliosis, inflammation, cell survival and proliferation (Dünker and Krieglstein 2000) . TGFβ initiates responses by activating transmembrane serine-threonine kinase receptors: I (TβRI) and II (TβRII) (Massagué 2000). The activated TβRI then interacts with the SMAD2 and/or SMAD3 transcription factors (Khalil *et al.* 2001). After activation by phosphorylation, SMAD2 and SMAD3 associate with SMAD4 and translocate to the nucleus to activate transcription of target genes (Massagué 2000; Massagué *et al.* 2005). In microglia, TGFβ1 acts as an anti-inflammatory cytokine having a variety of immunomodulatory functions including inhibition of production of proinflammatory cytokines (Lodge 1996; Kim, Won-Ki *et al.* 2004; Spittau *et*

al. 2013), chemokines (Hu *et al.* 1999; Paglinawan *et al.* 2003) and reactive oxygen intermediates by microglia (Chao and Peterson 1995; Hu *et al.* 1995). In the ischemic brain, overexpression of TGFβ1 has been shown to inhibit microglial activation and the release of proinflammatory chemokines (Gross *et al.* 1993). Further, TGFβ1 is induced after Traumatic Brain Injury (TBI) presumably to control microglial proliferation and increase neurogenesis (Logan *et al.* 2013). These data suggest that TGFβ1 and its signaling members and/or target genes could serve as potential targets for therapeutic manipulations to control microglia- mediated neuroinflammation in various CNS pathologies.

1.5 Regulation of microglia quiescence by extrinsic and intrinsic signals

1.5.1 Extrinsic signals

Under homeostatic conditions, microglia are maintained in "resting" condition by a number of CNS parenchymal factors. These environmental signals are of two types, "On" and "Off" signals (van Rossum and Hanisch 2004; Hanisch and Kettenmann 2007). "On" signals are molecules that trigger microglial activation. These molecules include bacterial cell wall components, viral RNAs, neurotransmitters and intracellular proteins (Kettenmann *et al.* 2011). These "On" signals molecules are recognised by a number of receptors present on microglial cell surface (Kawai and Akira 2010). Damaged neurons secrete nucleotides such as UTP and ATP in high concentrations, also forming a part

of “on” signals. These nucleotides are recognised by purinergic receptors present on microglia enabling microglial migration and subsequent phagocytosis (Koizumi *et al.* 2007). Excessive glutamate released in neurodegenerative conditions also function as ‘On’ signal molecule activating microglia (Pocock and Kettenmann 2007).

“Off” signals are those that trigger microglia when they are no longer received by microglia (van Rossum and Hanisch 2004; Hanisch and Kettenmann 2007). Microglia and neurons interact through cell surface molecules such as CD200/CD200R, CD47-SIRPα, CX3XL1/CX3CR1 or CD22/CD45 and TREM2b (Hoek *et al.* 2000; Schmid *et al.* 2002; Cardona *et al.* 2006; Neumann *et al.* 2009). Microglia are activated when they no longer receive signals from neurons *via* these receptors.

1.5.2 Intrinsic signals

Epigenetic factors constitute intrinsic signals regulating microglial activation. Recent study has demonstrated that processes involving histone modification and noncoding RNAs have important roles in modulating neuroinflammation (Garden 2013). It has been demonstrated that acetylation and deacetylation of histone proteins regulate the expression of target genes. In general, histone acetylation catalyzed by histone acetyl-transferases (HAT) activates gene expression by addition of acetyl groups to target proteins whereas histone deacetylation catalyzed by histone deacetylases (HDACs) downregulate gene expression by removal of the acetyl group from the target protein (Kuo and Allis 1998). HDACs have been shown to modulate the inflammatory response

of microglia, whereas HDAC inhibitors (HDACi) influence innate immune activity (Kim *et al.* 2007; Kannan *et al.* 2013).

HDACs are enzymes that catalyze the removal of an acetyl group from the target proteins (Kuo and Allis 1998). The effect of HDACi on microglial activation is not yet clear. In some experimental settings, HDACi potentiate the inflammatory response of activated microglia, where in other studies the opposite effect was observed (Suuronen *et al.* 2003, 2006; Faraco *et al.* 2009).

Recently, microRNAs (miRNAs) have been identified as important epigenetic regulators of microglia differentiation and activation. miRNAs are a class of small non-coding RNA molecules that either promote degradation and/or inhibit translation of their target mRNAs. A discussion on miRNA mediated modulation of microglial functions is detailed in subsequent sections.

1.6 Microglia in CNS diseases

1.6.1 Microglia in neurodegenerative diseases

1.6.1.1 Alzheimer's disease (AD)

Alzheimer's disease (AD) is characterized by 1) neuritic plaques (NPs) consisting of β-amyloid aggregates, 2) neurofibrillary tangles (NFTs) formed as a result of hyperphosphorylation of microtubule-associated protein tau; and 3) neuroinflammation induced by activated microglia. In AD, activated

microglia and astrocytes secrete excessive amount of proinflammatory cytokines, IL-1, TNFα and IL6, (Lue *et al.* 2001; Tuppo and Arias 2005), further stimulating microglia to produce neurotoxins such as ROS and excitatory amino acids, thereby amplifying microglial activation (Giulian 1999). In culture, in response to β amyloid, microglia produce excessive amount of reactive oxygen species, proinflammatory cytokines and chemokines (Lue *et al.* 2001).

1.6.1.2 Parkinson's disease (PD)

Loss of dopaminergic neurons in the substantia nigra pars compacts (SN) and their projection fibers in the striatum are the characteristic features of PD. Microglial phagocytosis of dopaminergic neurons is thought to be an early inducer of PD (Kim and Joh 2006). Degenerative dopaminergic neurons secrete proteins such as α-synuclein, matrix metalloproteinase 3 (MMP-3) and neuromelanin. Dopaminergic neurons secrete MMP-3, which activate microglia, leading to production of superoxide, TNFα, IL6 and NO (Wilms *et al.* 2003; Kim *et al.* 2005; Zhang *et al.* 2005; Kim and Joh 2006).

1.6.2 HIV-associated neuropathology

The human immunodeficiency virus (HIV) entry into the CNS is mediated *via* the chemokine receptor, CCR5 expressed on the surface of microglia and leads to HIV-associated dementia (HAD) (Moore *et al.* 2004). The neuronal loss accompanying HAD is thought to be a result of microglial activation (Adle-

Biassette *et al.* 1999). HAD is characterized by the formation of multinucleated giant cell (MNGC). MNGC which form from the fusion of microglia and/or macrophages are activated cells and produce excessive amounts of ROS and viral proteins (Epstein and Gendelman 1993; Jones *et al.* 2000). Further, viral proteins such as, viral HIV-I Tat, gp120 and Vpr stimulate inflammation and associated neuronal damage (Ghafouri *et al.* 2006).

1.6.3 Brain Injury

Brain injury refers to mechanical disruption of brain tissue. Neuronal loss accompanying brain injury may be a result of direct mechanical threat to the brain or due to indirect secondary mechanisms (McIntosh *et al.* 1998; Stoica and Faden 2010). A strong inflammatory response involving microglia is mounted after brain injury (Morganti-Kossmann *et al.* 2007; Kumar and Loane 2012; Schwarzmaier and Plesnila 2014). Activated microglia are known to persist in animal models of brain injury for upto a year after injury (Smith *et al.* 1997; Nagamoto-Combs *et al.* 2007). Furthermore, the presence of activated microglia was observed in patients of brain injury up to 17 years after injury, indicating a chronic inflammatory state (Ramlackhansingh *et al.* 2011). The role of microglia in brain injury may be both neuroprotective and neurotoxic. Microglia, in regions distant from the injury site are known to secrete BDNF, which helps in neuronal growth and survival (Nagamoto-Combs *et al.* 2007). However, chronic activation of microglia leads to production of reactive oxygen species (ROS) in the injured CNS, thereby leading to neuronal damage (Dohi *et al.* 2010).

1.6.4 Glioma

Glioma is a form of brain tumor consisting of tumor cells and a variety of immune cells including microglia or macrophages (Graeber *et al.* 2002). Several studies demonstrated that the glioma microenvironment converts the glioma-associated microglia into glioma-supportive cells (Ghosh and Chaudhuri 2010). Glioma-conditioned medium has also been shown to activate microglia in a form that is distinct from the inflammatory phenotype. Glioma associated activation leads to the upregulation of metalloprotease 2, IL-10 and VEGF from microglia (Markovic *et al.* 2005; Sliwa *et al.* 2007; Li and Graeber 2012). However, it does not lead to production of proinflammatory cytokines. Further, glioma cells secrete TGFβ to maintain microglial quiescence and promote glioma growth and invasion (Li and Graeber 2012).

1.7 MicroRNAs

MicroRNAs are small nonprotein-coding RNA molecules ranging from 18-22 nucleotides that act as important regulators of post translational gene expression (Kim and Nam 2006). MicroRNAs (miRNAs) influence gene function by targeting the 3'UTR of mRNAs, thus leading to mRNA degradation and the subsequent inhibition of protein translation (Mattick 2009; Taft *et al.* 2010). Typically, a miRNA can bind to several target mRNAs and conversely one mRNA can be targeted by several miRNAs (Pasquinelli 2012). Recent studies have shown miRNAs to display cell-type specific functions and

also play a role in disease pathogenesis and progression (Bartel 2009; Fabian and Sonenberg 2012). This highlights the potential of miRNAS as therapeutic targets and diagnostic tools (Noori-daloii and Nejatizadeh n.d.; Garzon and Marcucci 2012). Recent years have witnessed considerable amount of research interest in studies on miRNA-mediated modulation of gene function during neuroinflammation (Thounaojam *et al.* 2013). However, changes in miRNA expression occurring during microglial activation in pathological conditions have not been documented on a genome wide scale till date and should be the focus of future research.

1.7.1 Mechanism of action of miRNA

The miRNA is loaded onto a RNA-induced silencing complex (RISC), which mediates the degradation of target mRNAs. MicroRNAs direct the RISC to downregulate gene expression by either of two post-transcriptional mechanisms: 1) Degradation of target mRNA 2) Translational repression. The bases 2-8 of a miRNA are known as the "seed sequence" of the miRNA (Ameres and Zamore 2013). Interaction between this seed sequence and the 3' untranslated region (UTR) of the target mRNA negatively impacts its protein output. The strength of this interaction determines if the mRNA will be degraded or undergo translational repression due to destabilization of its structure (Pasquinelli 2012; Ameres and Zamore 2013).

1.7.2 Identifying mRNA targets of miRNAs

A number of computational tools predicting putative mRNA targets of miRNAs have been developed using distinct as well as overlapping algorithms

(Min and Yoon 2010). Among the popular algorithms are miRanda, Targetscan, PicTar, PITA and miRWALK.

1.7.2.1 miRanda

The miRanda algorithms include the following parameters (Enright *et al.* 2003; John *et al.* 2004): *1*) an alignment score for complementarity between the seed sequence of the miRNA and the 3'UTR of target mRNA *2*) determining the degree of conservation between seed sequence of miRNA and 3'UTR of target mRNA for human and rodents.

1.7.2.2 Targetscan

Targetscan includes the following parameters for miRNA target prediction (Lewis *et al.* 2003): *1*) an alignment score for complementarity between the target mRNA 3'UTR and miRNA seed sequence; *2*) presence of a adenosine nucleotide at position 1 and/or a Watson-Crick (W-C) match at the eighth position, *3*) AU content ~30 nucleotides on either sides of the targeted site, as well as the target's distance from the end of the 3'UTR; and *4*) degree of conservation between target mRNA 3'UTR and miRNA seed sequence for different species including human, mouse, rat dog and chicken.

1.7.2.3 PicTar

PicTar prediction is based on (Grün *et al.* 2005) 1) perfect complementarity between the seed sequence of the miRNA and the 3'UTR of target mRNA at position 1–7 or 2–8. 2) binding energy of the miRNA-mRNA duplex and 3) the degree of conservation between seed sequence of miRNA and 3'UTR of target mRNA for a number of species including human, mouse, rat dog, chicken, chimpanzee, pufferfish, and zebrafish.

1.7.2.4 PITA

PITA (Probability of Interaction by Target Accessibility) considers a very important criterion overlooked in the above-mentioned programs during miRNA target prediction that is, the accessibility of the target site (Kertesz *et al.* 2007). Target sites that are embedded in a closed stem or secondary structures are inaccessible to the miRNA RISC complex. PITA provides probability of interaction by first checking the seed sequence complimentarity with the target mRNA 3'UTR as the other algorithms. This is further followed by calculating the energy required to unwind any secondary structures and substracting it from the free binding energy to provide a final value of the probability of interaction.

1.7.2.5 MiRWalk

Apart from the above mentioned bioinformatic programs, miRWalk is a very popular and useful tool of choice for miRNA target prediction (Dweep *et al.* 2011). MiRWalk boasts the following features: 1) predicts miRNA binding sites on the complete sequence of all known genes of human and rodents 2) presents the results together with those from *8 different prediction programs* including miRanda, PITA and Targetscan among others. 3) provides information on both predicted and experimentally validated targets along the references. The validated target database is updated every month to incorporate any new information. 4) provides information on experimentally validated miRNA-mRNA interactions.

1.7.3 MiRNAs in the brain

The nervous system expresses most of the known miRNAs (around 70%) of all known miRNAs (Fineberg *et al.* 2009). They are involved in neuronal cell formation, differentiation, brain patterning and their dysregulation is shown to contribute to a number of neuropathologies (Follert *et al.* 2014). However, very few microRNAs are expressed in a brain specific or brain-enriched manner (Nowak and Michlewski 2013). Along with miRNAs, miRNA biogenesis enzymes are also important for brain development. Several brain abnormalities have been documented in Dicer deficient mice and mouse model of schizophrenia (Stark *et al.* 2008). MiR-9 and miR-124 are brain-specific miRNAs with extensive roles in neurogenesis. MiR-9 has been shown to regulate both neural progenitor proliferation and differentiation (Delaloy *et al.* 2010; Shibata *et al.* 2011). MiR-124 is mostly expressed in post-mitotic neurons (Åkerblom *et al.* 2012) with increase in expression during brain development (Sempere *et al.* 2004). MiR-124 targets several genes to regulate neurogenesis (Cao *et al.* 2007; Visvanathan *et al.* 2007). In addition, miR-124 regulates neuronal maturation (Rajasethupathy *et al.* 2009; Gu *et al.* 2014), synaptic transmission and cognition (Yang *et al.* 2012; Wang *et al.* 2013). Several miRNAs such as miR-132/miR-212 (Edbauer *et al.* 2010; Magill *et al.* 2010), miR-134 and miR-138 (Schratt *et al.* 2006) have also been reported to play roles in adult neurogenesis, synaptic plasticity and LTP.

1.7.4 MiRNAs and microglia

Recent years have witnessed considerable amount of research interest in studies on miRNA-mediated modulation of gene function during

neuroinflammation (Thounaojam *et al.* 2013). Several miRNAs have been shown to target mRNAs influencing microglial functions, thereby modulating microglial mediated inflammatory response. A genome wide miRNA expression screen to identify differentially expressed miRNAs in the four cell types in the CNS, namely: neurons, astrocytes, oligodendrocytes and microglia using rat primary culture identified several miRNAs such as miR-126, miR-146a and miR-150 specifically enriched in microglia as compared to the other cell types in the brain (Jovičić *et al.* 2013). These findings suggested that there exist a specific subset of miRNAs enriched in microglia distinct from the other neuroglial subtypes presumably to regulate microglial functions in the CNS.

1.7.4.1 MiRNAs in microglia development

CEBPα, PU.1, Runx1 and M-CSF are required for differentiation of peripheral macrophages and microglia development (Nayak *et al.* 2014). Recently, miR-124, a brain enriched miRNA has been shown to be essential in maintaining quiescent state of microglia (Ponomarev *et al.* 2011). MiR-124 reduced cell proliferation by targeting the cyclins CDK4 and CDK6. Further, miR-124 targeted the transcription factor CEBPα to reduce expression of its downstream targets PU.1 and M-CSF receptor leading to differentiation of macrophages to adult microglia in the brain. Further, amoeboid microglia (isolated from 5-day old mice pups) exhibited low miR-124 expression level along with high CD45 and MHC II expression levels, indicating active proliferative state of microglia (Ponomarev *et al.* 2011, 2013). Ramified microglia in the adult brain, on the other hand displayed high miR-124 expression levels. Furthermore, miR-124 expression was found to be

significantly downregulated in activated microglia during experimental autoimmune encephalomyelitis (EAE) and knockdown of miR-124 in microglia resulted in a transformation of these cells from a resting to an activated state *in vitro* and *in vivo*. These results indicate that miRNAs are involved in the 1) formation of microglia by targeting key transcriptions factors such as CEBPα and PU.1, 2) transformation of microglia from amoeboid to resting ramified state and 3) transformation of adult resting microglia to activated form in neuropathology (Ponomarev *et al.* 2011).

1.7.4.2 MiRNAs in microglia activation

MiRNAs are now known to influence the polarization of microglia and peripheral macrophages towards either the M1 or M2 phenotype (Illustration 4). Commonly known as a proinflammatory miRNA, the expression of miR-155 is upregulated in microglia and peripheral macrophages in response to several proinflammatory stimuli, such as LPS, IFNγ, and TNFα (Wang *et al.* 2010; Bala *et al.* 2011; Cardoso *et al.* 2012). Recently miR-155 has been shown to target M2-associated genes, such SMAD2 (Louafi *et al.* 2010), and CEBPα, a transcription factor important for the expression of IL-10, arginase 1, and CD206 (Ruffell *et al.* 2009), further supporting the hypothesis that miR-155 can influence the activation of microglia towards M1-like phenotypes. Similarly, LPS-responsive miR-27a/b was identified as an M1 polarizing miRNA in human monocyte-derived macrophages (Graff *et al.* 2012). MiR-27a/b targets the anti-inflammatory cytokine IL-10 and peroxisome proliferator-activated receptor γ (PPARγ), the nuclear hormone receptor, which represses iNOS resulting in suppression of NO production in peripheral

macrophages. MiR-27a overexpression results in an increase in proinflammatory cytokines, thereby polarizing macrophages towards the M1 phenotype (Jennewein *et al.* 2010; Xie *et al.* 2014). Further, miR-27a has also been shown to repress members of the TGFβ pathway, Runx1 and SMAD2 thereby reducing inflammation and helping polarize microglia to M1-like phenotype (Feng *et al.* 2009; Bao *et al.* 2014). Recently miR-27a was identified in a miRNA microarray screen carried out in activated primary microglia (Jadhav SP et al, unpublished data) indicating a role for miR-27a in microglia activation and polarization. Several other miRNAs such as miR-101 and miR-125b have been shown to play a role on the M1-polarization of microglia and peripheral macrophages (Zhu *et al.* 2010; Chaudhuri *et al.* 2011). MiR-101 was observed to be upregulated in response to several TLR ligands in peripheral macrophages (Zhu *et al.* 2010). Further, by targeting and downregulating MAPK phosphatase 1 (MKP-1), miR-101 mediated the activation of MAPK and expression of proinflammatory cytokines in peripheral macrophages. Another miRNA, miR-125b targeted interferon regulatory factor 4 (IRF4) and mediated the upregulation of MHC class II, CD40, CD80, and CD86, thereby bringing about the polarization of peripheral macrophages towards the M1 phenotype (Chaudhuri *et al.* 2011). On the other hand, miRNAs -200b and -92a were recently shown to be downregulated in microglia and peripheral macrophages respectively, in response to activation by TLRs such as LPS. Overexpression of miR-200b in microglia inhibited the cJun/MAPK-mediated release of proinflammatory cytokines and NO in activated microglia (Jadhav SP *et al.* 2014). Similarly, miR-92a targeted mitogen-activated protein kinase kinase 4 (MKK4) to inhibit the JNK/cJUN

pathway in peripheral macrophages thus contributing to the M1 phenotype (Lai *et al.* 2013). Recently, miR-124 has been reported to contribute to the M2 phenotype of peripheral macrophages and microglia (Ponomarev *et al.* 2013). Treatment of microglia and peripheral macrophages with cytokines IL-4 and Il-13 which are M2 phenotype inducing stimuli, resulted in an upregulation of miR-124 expression. Further miR-124 expression contributed to the expression of the M2 markers TGFβ, arginase-1 and FIZZ1 and downregulation of M1-associated markers, such as IL-6, TNFα and iNOS in the polarized macrophages.

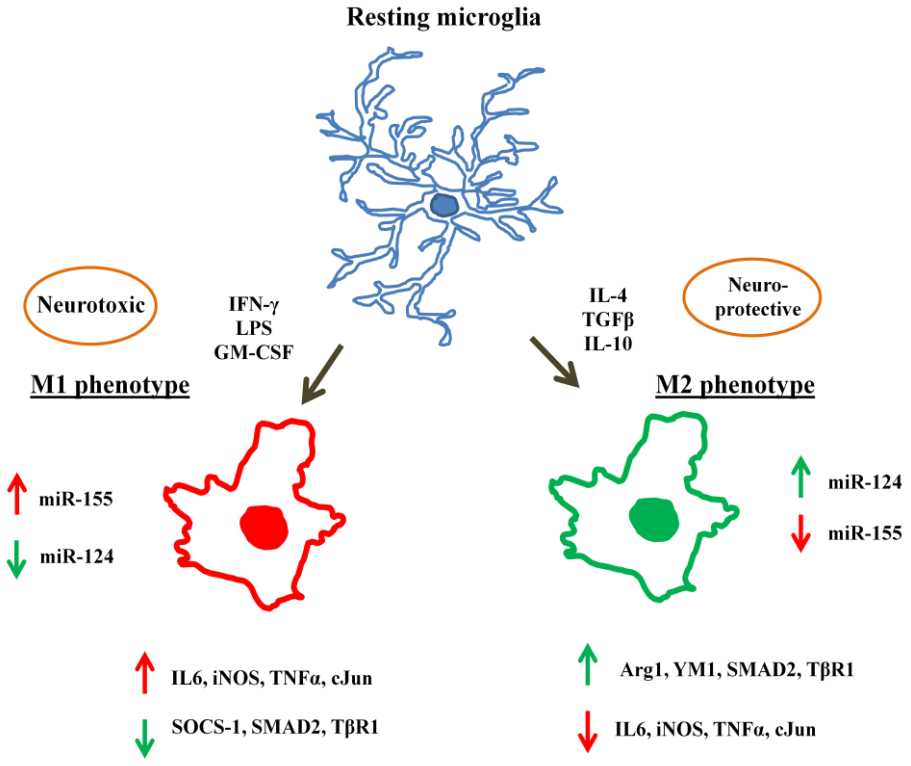

Illustration 4: Polarization of resting microglia towards the M1 (red) or M2 (green) phenotype and the associated molecules.

1.7.4.3 MiRNAs regulate microglia-mediated neuroinflammation and neuropathology

Recently, several miRNAs have been shown to be involved in microglial activation in various CNS pathologies (see Illustration 5) such as HIV-1 infection (Mishra *et al.* 2012; Jadhav *et al.* 2014), Japanese encephalities virus infection (Pareek *et al.* 2014; Thounaojam *et al.* 2014), Alzheimer's disease (Guedes *et al.* 2014), ischemia (Zhao *et al.* 2013; Kong *et al.* 2014), prion disease (Saba *et al.* 2012), normal physiological processes such as ageing (Fenn *et al.* 2013) and signalling pathways such as MAPK signalling (Jadhav SP *et al.* 2014), thus modulating neuroinflammation.

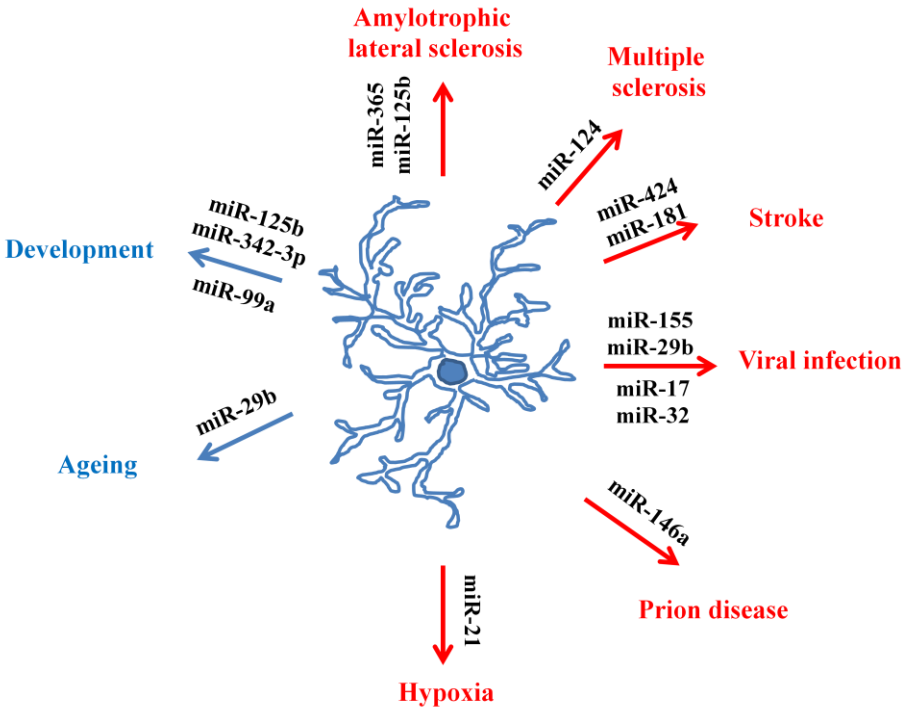

9

Illustration 5: MiRNAs involved in microglial activation in various CNS pathologies (red) and miRNAs aiding normal physiological process such as microglial development and ageing (blue).

The ability of miRNAs to regulate diverse cellular processes with negligible adverse events qualifies them as extremely potent therapeutic agents. Indeed the evidence reviewed above suggests using miRNAs as novel "Epidrugs" with a view to reduce microglia-mediated neurotoxicity. For example, overexpressing anti-inflammatory miRNAs (such as miR-124) and suppressing proinflammatory miRNAs (such as miR-155) could reduce microglia activation and subsequently neuroinflammation. This could be useful for the treatment of CNS inflammatory diseases such as multiple sclerosis (MS). However, altered miRNA expression occurring during microglial activation in pathological conditions has not been documented on a genome wide scale till date and this should be the focus of future research. Thus, disease-specific miRNA profile can be used for diagnosis, prognosis, and treatment of various neuroinflammatory conditions and will facilitate the development of small RNA molecules in anti-inflammatory therapy with an attempt to ameliorate the damage caused by chronic activation of microglia in CNS infection, injury and neurodegenerative diseases.

1.8 LPS as tool for microglial activation

Lipopolysaccharide (LPS) is a constituent of the cell wall of Gram negative bacteria (Kulp and Kuehn 2010). LPS is a prominent inducer of microglial activation both *in vivo* and *in vitro* (Dheen *et al.* 2007; Cazareth *et al.* 2014). LPS binds to the CD14 protein expressed on microglial cell surface (Kitchens *et al.* 2000). CD14 expression is upregulated in microglia upon stimulation

with LPS or TNFα (Nadeau and Rivest 2000). CD14 acts as a co-activator along with Toll like receptor 4 (TLR4) for the detection of LPS (Zanoni *et al.* 2011). TLRs are a class of pattern recognition receptors (PRRs) that recognize conserved moieties from pathogens that are different from host molecules and are thus important members of the innate immune response (Akira and Takeda 2004). Binding of LPS to the TLR4 on microglia activates the MAPK and NFκB pathways (Lu *et al.* 2008) leading to production of proinflammatory mediators like TNFα, and interleukins perpetuating microglial activation (Qin *et al.* 2007).

1.9 Traumatic brain injury model of neuropathology

Application of an external mechanical force to the brain leads to brain trauma, leading to a temporary or permanent impairment in cognitive, behavioral, or physical functions (Maas *et al.* 2008). TBI leads to a broad spectrum of neurological defects some of which are irreversible severely influencing the quality of life (Saatman *et al.* 2008). Though the underlying pathophysiology of TBI is not well known, it is now appreciated that multiple molecular and cellular mechanisms involving inflammation, apoptosis and altered neuronal plasticity may play a role. Of particular importance is the microglia-mediated inflammation in the hippocampus leading to increased neuronal cell death, thus contributing to increased cognitive dysfunction (Hernandez-Ontiveros *et al.* 2013). Several animal models of TBI have been developed with the fluid percussion injury model (FPI) being popular due to its reproducibility (Xiong *et al.* 2013).

1.10 Culture of microglial cells

1.10.1 Culture of primary microglia

Primary microglia are grown as a mixed culture of cortical glial cells isolated from neonatal rodent pups. Usually, primary dissociated mouse brain and rat brain cultures after 2 weeks *in vitro* culture develop a confluent layer of fibroblast-like astrocytes above which microglia, are seen distributed throughout the culture. Following 10-14 days in culture, microglia are purified from the other cells by mild trypsinization. This method selectively removes the astrocytic layer and retains the microglia. Highly pure (>95%) microglial cells can be obtained by this method with microglial purity being assessed by OX-42/Cd11b staining (Hassan *et al.* 1991). Cultured microglia display properties of mononuclear phagocytic cells such as nonspecific esterase activity, display of the macrophage surface antigens MAC-l and MAC-3, and acetylated low-density lipoprotein receptors. Cultured microglia also display functions similar to microglia *in vivo* such as the ability to engulf 5 pm latex beads, to secrete proinflammatory cytokines such as interleukins and TNFα in response to LPS treatment (Giulian and Baker 1986).

1.10.2 BV-2 cell line

BV-2 cells were developed from raf/myc-immortalised murine neonatal microglia and are the most frequently used substitute for primary microglia. It has been shown that BV2 microglia behave very similar to primary microglia

in terms of cytokine secretion, MAP kinase signalling and phagocytosis (Hirt and Leist 2003). It has also been demonstrated that 90% of the genes induced in BV-2 by LPS were also found in primary microglia, and around 50% were even found in hippocampal microglia after *in vivo* stimulation of mice by intracerebroventricular injection of LPS (Henn *et al.* 2009). Furthermore, BV-2, stimulated by LPS, can also trigger activation in astrocytes as assessed by translocation of the transcription factor NF-κB and secretion of the cytokine Il-6 (Henn *et al.* 2009). BV-2 cell line was used for miRNA functional analyses due to the difficulty in transfecting primary microglial cells.

2 AIMS OF THE STUDY

2.1 To perform a miRNA microarray of control and LPS-activated, amyloid β-activated primary microglia

MiRNAs are novel epigenetic factors regulating gene expression by degrading their target mRNA or inhibition of protein translation. Altered miRNA expression has been observed in microglia in various CNS pathologies. However a comprehensive catalogue showing the miRNA expression in activated microglia is lacking. The main objectives of this study are as follows-

a. To identify the differentially expressed miRNAs in activated microglia.
b. To perform pathway analysis to understand miRNAs involved in the signaling pathways affecting microglial activation.

2.2 To understand the role of miR-27a in regulating TGFβ signaling pathway in microglia

MiR-27a was predicted to target SMAD2, TβR1 and Runx1, members of the TGFβ signalling pathway in microglia. TGFβ1 is an anti-inflammatory cytokine and TGFβ signalling *via* SMAD2/3 has been shown to lead to microglial quiescence. Thus it is hypothesized that miR-27a promotes the proinflammatory response of microglia by suppressing TGFβ-SMAD signalling in microglia.

The main objectives of this study are as follows-

a. To check the expression of miR-27a in LPS and TGFβ activated microglia *in vitro*
b. To verify if SMAD2, TβR1 and Runx1 are the targets of miR-27a by knockdown and overexpression of miR-27a in BV2 microglia
c. To perform functional studies such as expression of proinflammatory cytokines after knockdown and overexpression of miR-27a in BV2 microglia
d. To check neuronal apoptosis mediated by microglia conditioned medium after knockdown and overexpression of miR-27a in BV2 microglia

2.3 To understand the role of miR-200b in regulating cJun/MAPK signaling pathway in microglia

MiR-200b was predicted to target cJun, a member of the mitogen activated protein kinase (MAPK) signalling pathway. MAPK pathways regulate production of proinflammatory cytokines and cytotoxic molecules by activated microglia. Thus it is hypothesized that miR-200b inhibits microglia activation by suppressing the cJun/MAPK pathway in microglia.

The main objectives of this study are as follows-

a. To check the expression of miR-200b in LPS activated microglia *in vitro*
b. To verify if cJun is the target of miR-200b by knockdown and overexpression of miR-200b in BV2 microglia

c. To perform functional studies such as expression of proinflammatory cytokines after knockdown and overexpression of miR-200b in BV2 microglia
d. To check neuronal apoptosis mediated by microglia conditioned medium after knockdown and overexpression of miR-200b in BV2 microglia.

3 MATERIALS AND METHODS

3.1 Animals

In this study, wistar rats of different ages were used as tabulated below (Table 1). The animals were procurred from Laboratory Animals Centre, National University of Singapore (NUS). This study was approved by the National University of Singapore Institutional Animal Care & Use Committee (IACUC) and DSO National Laboratories Institutional Animal Care & Use Committee (protocol number 059\11 and 080/10). All efforts were made to minimize pain and the number of animals used. The rats used in this study are tabulated below.

Table 1: Animals used for the study.

Experiment	Age	Number
Primary culture of microglia	3-day	120
LPS treatment	5-day	6
Laser-capture microdissection	2 month	6
Total		132

3.2 Collection of fresh brain samples

To collect brain samples, 2-month old wistar rats were anaesthetized by intraperitonial injection of pentobarbitone (50mg/kg body wt). An incision was made along the midline to cut open the skull. The whole brain was

removed carefully followed by washing twice in sterile ice-cold PBS. Following washing, the tissue was rapidly frozen in liquid nitrogen in optimal cutting temperature compound (OCT)-containing moulds. The tissue was stored at -80ºC freezer to inhibit denaturation of samples until further use.

3.3 Treatment of animals with drug

3.3.1 Materials

- Lipopolysaccharide (LPS) (Cat No. L6529; Sigma-Aldrich, St. Louis, MO, USA)

3.3.2 Procedure

To inject animals with LPS, it was first diluted in saline (250µl of saline per injection). 5-day old rat pups were injected with two doses of LPS intraperitoneally (i.p.) (1mg/kg body weight) with an interval of 6h. To serve as control, the rat pups were injected with saline (250µl per injection) instead of LPS.

3.4 Perfusion

3.4.1 Principle

Perfusion is defined as a technique of pouring a liquid on or through an organ. Animal perfusion involves injecting a fixative such as formaldehyde or alcohol through the body to preserve the structure of the organs and tissue. A fixative cross-links the proteins thereby protecting them from degradation (Oliver and Jamur 2010). Transcardiac perfusion involves injecting the fixative through the heart when the animal is still alive. This allows pumping

of the fixative to all parts of the body including the brain, through the action of the heart (Paul *et al.* 2008)**.**

3.4.2 Materials

- NaH_2PO_4 (sodium di-hydrogen phosphate) (Cat no S8282, Sigma-Aldrich, St. Louis, MO, USA)
- Na_2HPO_4 (di-sodium hydrogen phosphate) (Cat no 255793, Sigma-Aldrich, MO, USA)
- Paraformaldehyde (PF) (Cat. No. P001, TAAB Laboratories, UK)

3.4.3 Preparation of Fixative

Before preparation of the fixative, the buffers sodium di-hydrogen phosphate and di-sodium hydrogen phosphate were prepared. To prepare 1000 ml of 0.1M di-sodium hydrogen phosphate buffer, 14.1g of Na_2HPO_4 powder was dissolved in 1000 ml of distilled water (DW). To prepare 0.1M of sodium di-hydrogen phosphate buffer, 11.9g of NaH_2PO_4 powder was dissolved in 1000ml of DW. Further, to prepare 1 liter of phosphate buffer, 800 ml of the above prepared Na_2HPO_4 solution was mixed with 200 ml of NaH_2PO_4 solution. 40g paraformaldehyde powder was dissolved in 1 liter of phosphate buffer prepared as described above, by heating, until the PF had completely dissolved, to prepare the 4% fixative solution. The fixative was filtered using Whatmann paper and chilled prior to use.

3.4.4 Procedure

For perfusion the animal was anaesthetized with pentobarbitone (i.p., 30mg/kg body wt) followed by the toe pinch test to ensure unresponsiveness. With its ventral side facing upward, the body cavity of the rat was exposed by cutting

through the thoracic and abdominal wall along the midline and the diaphragm using a scalpel. A needle was put in the left ventricle of the heart and the right auricle was clipped with the help of forceps. Ringer's solution was used to flush out the blood. Fixative substituted Ringer's solution after the liver turned pale. The brain tissue was isolated and incubated in PF for 2-3h at 4ºC. Once post-fixation was over the tissue was transferred to 15% sucrose solution overnight at 4ºC for cryoprotection.

3.5 Traumatic brain injury (TBI) rat model

Fluid percussion model was used to induce brain trauma in rodents (Dixon *et al.* 1987). Anesthesia was applied to male wistar rats (ketamine (75mg/kg) and xylazine (10mg/kg)). Craniotomy was performed midway between bregma and lambda by preserving dural layers and a fluid pressure pulse was applied to produce brief displacement of neural tissue. Sham operated rats received only anaesthetic agent following a midline incision. After injury or sham operation, the scalp was sutured, and the animal was allowed to recover from anaesthesia and returned to their home cages. 24h after surgery, fresh brain tissue was collected and stored at -80ºC for LCM analysis.

3.6 Preparation of gelatinized slides

3.6.1 Materials

- Gelatin (Cat no 1.04080, Merck Millipore, Germany)
- Chrome alum (Chromium (III) potassium sulfate (Cat no 1.01036, Merck Millipore, Germany)

3.6.2 Procedure

To prepare gelatin solution, 9g of gelatin was dissolved in 600 ml distilled water by constant stirring with heat until gelatin had completed dissolved. The slides were washed with alcohol and air dried. Once the gelatin solution had cooled, 0.9g chrome alum was mixed in the gelatin solution and filtered using Whatman's filter paper. The washed slides were gelatin coated by immersing in the gelatin solution for 1 min followed by air drying and storage at 37°C.

3.7 Cryosectioning of brain tissue

3.7.1 Materials and equipment

- Cryostat (Leica CM 3050 S, Leica-Microsystems, Nussloch, GmbH, Germany)

3.7.2 Procedure

For cryosectioning of brain tissue, the brain sample was attached onto a metal chuck by application of optimal cutting temperature compound followed by quick freezing in liquid nitrogen. Following this the sample was left in the cryostat for a period of 10-15 min until the entire tissue froze completely. The brain tissue was then cut at 30 µm thickness for immunohistochemistry and arranged on gelatin slides. The corpus callosum was chosen for further experiments. For LCM, the brain samples were cut at 10 µm thickness and placed on MMI metal slides. The hippocampus was selected for LCM experiment. The sections for immunohistochemistry were stored at -20 ºC

while those for laser capture microdissection were stored at -80 ºC until further use.

3.8 Immunohistochemistry

3.8.1 Principle of immunohistochemistry

Immunohistochemistry defined as detecting a protein of interest on a particular tissue. For this purpose, a primary antibody raised against the protein of interest is used followed by using a secondary antibody raised against the primary antibody. The secondary antibody is usually tagged with an enzyme such as horseradish peroxidase or with a fluorophore such as cy3 or FITC allowing visualization either by color development or under a confocal microscope (Fritschy Jean-marc 2001; Matos *et al.* 2010).

3.8.2 Materials

- Phosphate buffered saline (PBS; BUF-2041-1x1L, 1st Base, Singapore)
- Peroxidase conjugated isolectin (Cat # L5391, Sigma-Aldrich, MO, USA)
- Water, Diethylpyrocarbonate (DEPC) treated, Biotechnology Grade, 1L (BUF-1170-1L, 1st Base, Singapore)
- 30% Hydrogen peroxide (H_2O_2) solution
- DAB solution

3.8.3 Procedure for staining microglia on fresh brain sections

IHC on fresh frozen tissue for LCM analysis was carried out rapidly to minimize RNA degradation of the samples. The sections were fixed in 75%

ethanol for 1 min followed by incubation with peroxidase conjugated isolectin for 15 min at room temperature. This was followed by dehydration using a graded series of ethanol. For color development, the sections were incubated in DAB solution in the dark. Lectin-marked microglia were stained in brown.

3.8.4 Materials

- Rabbit-anti-SMAD2 antibody (Cat # D43B4, Cell Signaling Tech, USA)
- Rabbit anti-TGFβ1 antibody (Cat # sc 28679, Santa Cruz Biotechn., Texas, USA)
- Rabbit anti-TβR1 antibody (Cat # sc 398, Santa Cruz Biotechn., Texas, USA)
- Mouse anti-Integrin-αM/Cd11b antibody (Cat # CBL1512, Merck Millipore, Billerica, MA, USA)
- goat anti-rabbit IgG Cy3 (Prod # AP132B, Merck Millipore, Billerica, MA, USA)
- Goat anti-mouse IgG FITC (Prod # AP132F, Merck Millipore, Billerica, MA, USA)
- DAPI (Cat # D3571, Molecular Probes, Invitrogen, Life Technologies, Thermo Fisher Scientific Inc, MA, USA)
- Phosphate buffered saline (PBS; BUF-2041-1x1L, 1st Base, Singapore)
- Mounting Medium (Cat # S302380, Dako, Agilent Technologies, USA)
- Goat serum (Cat # S-1000, Vector Laboratories, Burlingame, USA)

- Olympus FV100 confocal laser-scanning microscope (FV-1000, Olympus Optical Co., Japan)

3.8.5 Procedure for immunofluorescence on fixed brain tissues

For tissue staining, the fixed frozen tissue sections given a quick wash in 1XPBS followed by blocking in 10% goat serum for 1h at room temperature. Care was taken to ensure that the sections do not dry out during the entire procedure. Following blocking, the sections were incubated with a primary antibody mixture of anti-Cd11b and either anti-SMAD2 or anti-TGFβ1 or anti-TβR1 antibodies, overnight at 4ºC. The next day, tissue sections were washed in 1XPBS. This was followed by incubation with a mixture of anti-mouse FITC and anti-rabbit Cy3 secondary antibodies for 1h at room temperature. Following secondary antibody incubation, nuclei were stained using DAPI. Nuclear staining was followed by a further 3 washes with 1XPBS. Finally, the sections were mounted in DAKO fluorescent mounting medium. Images were captured using an Olympus confocal microscope.

3.9 Laser-capture microdissection of microglia from adult rat brain tissue

3.9.1 Principle of LCM

Laser capture microdissection enables isolation of specific cells from a mixed population, under microscopic visualization. These samples can be further used for various biological analysis including downstream next-generation sequencing, Sanger sequencing, PCR, and proteomics. LCM is an important technique as it allows for the isolation of a specific cell type from a

heterogeneous cell population, thereby allowing us to understand the effect of the tissue microenvironment on the cell under consideration.

3.9.2 Materials

- MMI Transparent caps (Cat # 50208, Molecular Machines & Industries, Switzerland)
- MMI CellCut (Molecular Machines & Industries, Glattbrugg, Switzerland)

3.9.3 Procedure

Laser-capture microdissection of microglia was carried out by arranging the metal slides with lectin stained microglial sections on the stage of the laser-capture microdissection microscope. The isolation caps were arranged above the hippocampus and cells were identified and cut using the laser. A minimum of 800 cells were isolated per sample.

3.10 Extraction of RNA from laser-captured microglia

3.10.1 Principle of RNA extraction

Two important aspects of RNA isolation are maintenance of RNA integrity during the extraction process and a complete removal of contaminating protein and DNA. Single step RNA isolation procedure using guanidine thiocyanate combined with phenol gives the best results including increased RNA yield from the tissue/cell preparation (Chomczynski and Sacchi 2006). Recently, the miRNeasy kit developed by Qiagen combines the above-mentioned procedure along with a downstream silica-membrane based purification process to yield highly pure total RNA including small RNA and miRNA.

3.10.2 Material

- QIAzol Lysis Reagent (Qiagen, Prod # 79306, Germany)
- miRNeasy mini kit (Qiagen, Prod # 74106, Germany)
- Nanodrop (Thermo Scientific, Model No. ND1000, MA, USA)

3.10.3 Procedure

The QIAzol reagent, which is a combination of phenol and guanidine-thiocyanate was used for lysing the laser-captured microglial cells. The lysate was mixed with chloroform and separated into upper aqueous, interphase and lower organic phases. The upper aqueous phase containing RNA was carefully pipetted out. This was put together with 70% ethanol and added to the miRNeasy column to "capture" the RNA on the membrane in the column. The flow through was discarded. After washing the column with wash buffer provided in the kit, total RNA along with small and miRNAs was eluted in 15µl of warm nuclease-free water. The RNA quality and concentration were measured using a nanodrop. An aliquot of RNA was prepared for cDNA conversion while the rest was immediately stored at -80°C.

3.11 Synthesis of cDNA from LCM-extracted RNA

3.11.1 Principle

Complementary DNA (cDNA) is reverse transcribed from RNA using an enzyme known as reverse transcriptase. Reverse transcriptase is a RNA-dependent DNA polymerase, which uses mRNA as a template, to produce its complementary DNA based on the pairing of RNA base pairs.

3.11.2 Materials

- SuperScript® VILO™ cDNA Synthesis Kit (Cat #11754050, Invitrogen, Life Technologies, Carlsbad, CA, USA)
- Mastercycler gradient thermal cycler (Cat # 950000015, Hamburg, Germany)

3.11.3 Procedure

Since the amount of RNA obtained using LCM is very low, cDNA conversion was achieved using a thermostable reverse transcriptase enzyme which improves cDNA yield, and qRTPCR results. About 300ng of total RNA was mixed with 4 μl of 5X reaction mix containing random primers, MgCl2, and dNTPs, 2 μl of 10X SuperScript® VILO™ enzyme. Appropriate volume of DEPC water was used to bring up the reaction volume to 20 μl. This mixture was incubated according to the following protocol in a Mastercycler gradient thermal cycler: 42°C for 60 min and 85°C for 5min. The resulting cDNA was stored at -20°C until further use.

3.12 Cell Culture

3.12.1 Primary culture of microglia

3.12.1.1 Materials

- DMEM (Prod # 11965-092, Gibco, USA)
- Fetal bovine serum (Prod # 10100-147, Gibco, USA)
- Dnase I from bovine pancreas (Prod # D4527, Sigma-Aldrich, MO, USA)

- Phosphate buffered saline (PBS; BUF-2041-1x1L, 1st Base, Singapore)
- Trypsin-EDTA solution (Sigma-Aldrich, Prod # T4049, USA)
- 70µm cell strainer (BD Biosciences, Prod # 352350, USA)
- 0.5M EDTA (Sigma-Aldrich, Prod # E-7889, USA)
- Insulin (Bovine) (Sigma-Aldrich, Prod # I0305000, USA)
- Antibiotic antimycotic solution 100X (Sigma-Aldrich, Prod # A5955, USA)

3.12.1.2 Procedure

Complete medium for primary microglia culture was prepared using 450 ml DMEM, 5 ml of antibiotics, 50 ml of FBS, 5 ml of non-essential amino acids, and 625 µl of insulin. Brain cortices from 3-day-old rat pups were removed and cleaned in ice-cold sterile PBS followed by removal of the meninges. The tissues were mechanically minced followed by enzymatic digestion with TE and DNase at 250rpm for 15min in a humidified atmosphere of 37ºC. Further, the cell suspension was filtered through a 70 µm cell strainer followed by seeding in complete medium. The cells were cultured at 37°C in an incubator with 5% CO_2 and 95% air incubator. Mixed glial cells were cultured for 10-12 days and the medium was changed every other day. Microglia purification from the mixed glial culture was carried out using the trypsination method. Briefly, the cultures were given a warm 1X PBS wash. The trypsin solution was prepared by mixing 1 ml of 10X trypsin with 20 µl of 0.5mM EDTA in 39 ml of DMEM without serum. The cells were incubated with the trypsin solution for 10 min. Astrocyte and oligodendrocyte cell layer was detached

from the flask and discarded. Microglial cells remaining in the flask were washed with PBS. The cells were allowed to rest in complete medium for 24h followed by further analyses.

3.12.2 BV-2 cell culture

3.12.2.1 Materials

- Dulbecco's Modified Eagle's Medium (Cat # 11965-092, Gibco, Life Technologies, CA, USA)
- Fetal bovine serum (Cat # 10100-147, Gibco, Life Technologies, CA, USA)
- Phosphate buffered saline (PBS; BUF-2041-1x1L, 1st Base, Singapore)
- Trypsin/EDTA solution (Cat # R001100, Life Technologies, CA, USA)

3.12.2.2 Procedure

A widely used murine microglial cell line, BV-2 microglial cells were maintained in complete medium consisting of, DMEM and 10% FBS, and cultured in an incubator at 37°C with 5% CO_2 and 95% air. For subculturing, the cells were washed with PBS followed by treatment with 1X trypsin-EDTA solution in PBS for 5min at 37°C. The enzymatic reaction was neutralized by complete medium and cells were collected by centrifugation at 1000 rpm for 5min at 4°C. The pellet was re-suspended in fresh complete medium. Cells were seeded on 96 well plates at a density of 1.0×10^3 for cell viability assay, and on 6-well plates at a density of 2.0×10^5 per well for protein and RNA isolation. For functional studies and immunofluorescence, 2.0×10^5 or

2.0×10^4 cells were used per well in six well plates or 24 well plates, respectively. BV-2 cells were treated with LPS at 1 μg/ml for 1 to 6h to activate microglia.

3.12.3 Neuronal Cell Culture

3.12.3.1 Materials

- Dulbecco's Modified Eagle's Medium (Cat # 11965-092, Gibco, Life Technologies, CA, USA)
- Fetal bovine serum (Cat # 10100-147, Gibco, Life Technologies, CA, USA)
- Phosphate buffered saline (PBS; BUF-2041-1x1L, 1st Base, Singapore)
- Trypsin/EDTA solution (Cat # R001100, Life Technologies, CA, USA)
- Sodium butyrate (Cat # B5887, Sigma Aldrich, MO, USA)

3.12.3.2 Procedure

MN9D dopaminergic neuronal cell line was grown in DMEM and 10% FBS, cultured at 37°C with 5% CO_2. The cells were differentiated into dopaminergic neurons by adding 1 mM sodium butyrate to complete medium for 6 days.

3.13 MiRNA profiling

3.13.1 Principle

MiRNA microarray is a high-throughput method for screening genome-wide miRNA expression profile across samples. Using this method, large sample collection can be processed in parallel. MiRNA oligo probes designed on the sense strand of the miRNA for the detection of either mature miRNA or precursor miRNA are used as "capture" probes. Either biotinylated or fluorescently labelled RNA samples are hybridized to the capture probes followed by detection of the signal by a laser. The Exiqon miRCURY LNA™ microRNA Array slides contain capture probes complementary to mature microRNAs registered in miRBase.

3.13.2 Procedure

Prior to miRNA microarray analysis, quality of RNA samples was assessed using an Agilent 2100 Bioanalyzer profile. The bioanalyzer provides a RIN value (RNA Integrity Number ranging from 0 to 10), which gives a reliable impression of the quality of the RNA (Schroeder *et al.* 2006). RIN value for all samples was above 7, which is indicative of good quality, unfragmented RNA. Total RNA (400ng) from control and activated microglia samples was labeled with Hy3™ and Hy5™ fluorescent label, respectively, using the miRCURY LNA™ microRNA Hi-Power Labeling Kit (Exiqon, Denmark) following manufacturer's instructions. The Hy3™-labeled and Hy5™- labeled reference RNA samples were mixed pair-wise and hybridized to the miRCURY LNA™ microRNA Array 7th (Exiqon, Denmark). This microRNA

microarray chip contains capture probes targeting all microRNAs for human, mouse or rat registered in the miRBASE 18.0. A Tecan HS 4800™ hybridization station (Tecan, Austria) was used to perform the hybridization reaction. The microarray slides were scanned using the Agilent G2565BA Microarray Scanner System (Agilent Technologies, Inc., USA). Analysis of the data obtained was carried out using the ImaGene 9.0 software (BioDiscovery, Inc., USA). The quantified signals were background corrected (Ritchie *et al.* 2007) and normalized using the global Lowess (LOcally WEighted Scatterplot Smoothing) regression algorithm. The microRNA microarray experiment was conducted at Exiqon, Denmark.

3.14 MiRNA pathway analysis

MiRNA pathway analysis was carried out using the Ingenuity pathway analysis (IPA) software. MiRNAs identified from the microarray analysis as having the highest fold change across samples were fed into the software which identified the mRNAs targeted by these miRNAs. Highly predicted and experimentally verified targets as per the Targetscan database were considered for further analyses.

3.15 MiRNA functional analysis

3.15.1 miRNA knock down

3.15.1.1 Principle

miRNA inhibitors or anti-miRs are chemically modified antisense oligonucleotides, which sequester the mature miRNA leading to functional

inhibition of the miRNA and increased expression of the direct target genes (Stenvang *et al.* 2012). Beacuase of the small size of these chemical inhibitors, anti-miRNAs can be easily transfected in mammalian cells where they bind to the endogenous miRNA. This leads to a reduction of the levels of the specific miRNA under consideration. The functional activity of a miR inhibitor can be checked by assessing the mRNA expression of its target gene by qRT-PCR or protein expression by western blot. However, predominantly the mRNA expression of a target gene may not be affected since miRNAs regulate gene expression post-transcriptionally (Valastyan and Weinberg 2009).

3.15.1.2 Materials

- miRCURY LNA™ microRNA inhibitor (Exiqon, Vedbaek, Denmark)
- OptiMEM medium (Cat # 31905070, Invitrogen, Life technologies)
- X-tremeGENE siRNA transfection reagent (Cat. No. 04476093001, Roche Applied Sciences)

3.15.1.3 Procedure

For functional analysis of miRNAs in microglia, BV2 cells were seeded in 6 well plates at a density of 2×10^5. Transfection was carried out using X-tremeGENE siRNA transfection reagent. 5'fluorescent labelled miRCURY LNA^{TM} microRNA inhibitors and control scrambled miRNA were purchased from Exiqon. Table 2 summarizes the sequences of the inhibitors. MiRNA inhibitors were diluted in opti-MEM medium and added to the cells at final concentration of 40nM of the inhibitors. Western blot analysis was used to evaluate the protein expression of the target mRNA 48h after transfection.

Table 2: Sequence of miRNA inhibitors purchased from Exiqon (Vedbaek, Denmark)

Catalogue No	miRNA name	Sequence	Label
199006-011	Scrambled miR/ Negative control A	TAACACGTCTATACGCCCA	5' flourescein
4102898-001	Mmu-miR-200b	TCATCATTACCAGGCAGTA	5' flourescein
4101960-001	Mmu-miR-27a	CGGAACTTAGCCACTGTGA	Unlabelled

3.15.2 miRNA overexpression

3.15.2.1 Principle

MiRNA mimics are small, chemically modified double-stranded RNAs. These molecules mimic endogenous miRNAs, leading to up-regulation of miRNA activity. Use of chemical miRNA mimics is advantageous as it enables targeting of a specific mRNA and provides a possibility of *in vivo* delivery using lipid- or polymer-based nanoparticles (Wang 2011).

3.15.2.2 Materials

- *mir*VANA^{TM} miRNA mimic (Ambion, Life Technologies)
- X-tremeGENE siRNA transfection reagent (Cat. No. 04476093001, Roche Applied Sciences)
- OptiMEM medium (Cat # 31905070, Invitrogen, Life technologies)

3.15.2.3 Procedure

For overexpression of miRNAs in microglia, BV2 cells were seeded in 6 well plates at a density of 2×10^5. Transfection was carried out using X-tremeGENE siRNA transfection reagent. Non-labelled *mir*VANA™ miRNA mimic and scrambled negative control were purchased from Ambion (Life Technologies). Table 3 summarizes the sequences of miRNA mimics. MiRNA mimics were diluted in opti-MEM medium at final concentration of 20 nM. Western blot analysis was used to evaluate the protein expression of the target mRNA 48h after transfection.

Table 3: Sequence of miRNA mimics purchased from Ambion (Life Technologies).

Catalogue No	miRNA name	Sequence	Label
4464058	mirVana miRNA mimic Neg control	TAACACGTCTATACGCCCA	Unlabelled
4464066	mirVana miRNA mimic mmu-miR-200b	TCATCATTACCAGGCAGTA	Unlabelled
4464066	mirVana miRNA mimic mmu-miR-27a	CGGAACTTAGCCACTGTGA	Unlabelled

3.16 Cell Viability Assay

3.16.1 Principle

Cell viability was measured using a calorimetric assay known as MTS assay. NADPH generated by dehydrogenases in viable cells converts tetrazolium compound (Owen's reagent, [3-(4,5-dimethylthiazol-2-yl)-5-(3-carboxymethoxyphenyl)-2-(4-sulfophenyl)-2H-tetrazolium, inner salt;) to a colored formazan product and thus is a direct measure of cell viability. The quantity of formazan is measured colorimetrically by absorbance at 490nm.

3.16.2 Materials

- CellTiter 96^{R} AQ_{ueous} Non-Radioactive Cell Proliferation Assay (Prod # G5421, Promega, WI, USA)

3.16.3 Procedure

Cell viability post transfection was measured using the colorimetric MTS assay, which is non-radioactive cell proliferation assay, as per manufacturer's instructions. Briefly 5000 BV2 cells were seeded in 96 well plates and transfected as mentioned above. 24h post transfection, 20µl of MTS/PMS solution was added to each well. Next, the plate was incubated in 37°C in a humidified atmosphere of 5% CO_2 and 95% air incubator for 3h and the absorbance was measured using a microplate spectrophotometer at 490 nm. The percentage of cell viability was plot as a function of the absorbance.

3.17 Luciferase Assay

3.17.1 Principle

The luciferase reporter assay is a tool to assess transcriptional activity. Luciferases are oxidative enzymes found in several species such as fireflies allowing the organisms to emit light (Gould and Subramani 1988). For the reporter assay, the regulatory region of gene-of-interest is cloned upstream of the luciferase gene in an expression vector. This is known as a reporter plasmid. This plasmid is transfected into cells. The luciferase enzyme activity can be measured using a spectrophotometer after addition of the substrate luciferin. Since the gene of interest is fused to the luciferase reporter gene, the luciferase activity can be directly correlated with the activity of this gene.

3.17.2 Materials

- pMiRTarget luciferase reporter containing the 3'UTR of cJun (custom made, OriGene Technologies, Rockville, MD, USA)
- ONE-Glo™ Luciferase assay (Cat # E6110, Promega, Madison, WI, USA)

3.17.3 Procedure

pMiRTarget luciferase reporter vector containing the 3'UTR of cJun cloned into the multiple cloning site was purchased from OriGene Technologies (custom made). BV2 cells were cotransfected with 80ng of the luciferase reporter plasmid along with miRNA mimics (final concentration 20 nM). 48h post transfection, luciferase activity was evaluated using the ONE-Glo™ Luciferase assay system. pMiRTarget luciferase reporter vector also encodes for red fluorescent protein (RFP) which was used as a reporter for transfection

monitoring and normalization. Each experiment was repeated twice in triplicate.

3.18 *In situ* hybridization

3.18.1 Principle

In situ hybridization is a technique to obtain temporal and spatial expression pattern of gene of interest by localizing specific nucleic acid targets within fixed tissues and cells (Jin and Lloyd 1997). A labeled complementary DNA or RNA strand (i.e., probe) is used to localize a specific DNA or RNA sequence in a tissue (*in situ*), or cells. This technique is very useful in revealing the location of specific nucleic acids sequences on chromosomes or in tissues which is a important for understanding the organization, regulation and function of genes. This technique is further extended to study the localization of miRNAs in tissue or cells.

3.18.2 Materials

- miRCURY LNA™ microRNA ISH Buffer Set (Prod No. 90000, Exiqon)
- miRCURY LNA ™ probe mmu-miR-200b (Prod No. 88080-04, Exiqon)
- miRCURY LNA ™ probe U6 (Prod No. 99002-04, Exiqon)
- DAPI (Cat # D1306, Molecular probes, Invitrogen, Life Technologies)
- Mounting Medium (Cat # S302380, Dako, Agilent Technologies, USA)

3.18.3 **Procedure**

In situ hybridisation was carried out to localze miR-200b in microglia using Exiqon's miRCURY LNA™ microRNA ISH Buffer Set. BV2 cells were seeded at a cell density of 2×10^4 on poly lysine coated cover slips overnight. The cells were fixed with freshly prepared 4% PF and permeabilized using the ISH buffer provided in the kit. 5' fluorescein labelled miRCURY LNA ^{TM} probe mmu-miR-200b (Prod No. 88080-04, Exiqon) was used to localise the mature miR-200b while 5' fluorescein labelled miRCURY LNA ^{TM} probe mouse U6 (Prod No. 99002-04, Exiqon) served as a positive control. Further, the nucleus was stained with DAPI (1µg/ml) and coverslips were mounted on glass slides with fluorescent mounting medium. Images were captured using an Olympus confocal FV1000 microscope. The sequences for the probes used are listed in table 4.

Table 4: Sequence of miRNA *in situ* probes purchased from Exiqon (Vedbaek, Denmark).

Catalogue No	miRNA name	Sequence	Label
99004-04	Scrambled-miR	GTGTAACACGTCTATACGCCCA	5' flourescein
88080-04	mmu-miR-200b	TCATCATTACCAGGCAGTATTA	5' flourescein
99002-04	U6, hsa/mmu/rno	CACGAATTTGCGTGTCATCCTT	Unlabelled

3.19 RNA isolation and quantitative real-time RT-PCR (qRTPCR)

3.19.1 Isolation of total and small RNA

3.19.2 Material

- QIAzol Lysis Reagent (Prod# 79306, Qiagen, Germany)
- miRNeasy mini kit (Prod# 74106, Qiagen, Germany)
- 70% ethanol
- β-mercaptoethanol (Prod# M6250, Sigma Aldrich, MO, USA)

3.19.3 Procedure

For RNA isolation from LPS treated primary and BV2 cells, 700 µl Qiazol reagent was added to each sample. After vigorous mixing, the lysate was mixed with chloroform and separated into upper aqueous, interphase and lower organic phases. The upper aqueous phase containing RNA was pipetted out. This was put together with 70% ethanol and added to the miRNeasy column to "capture" the RNA on the membrane in the column. The flow through was discarded. After washing the column twice with wash buffer provided in the kit, total RNA along with small and miRNAs was eluted in 15 µl of nuclease-free water. The RNA quality and concentration were measured using a sphectrophotometer. An aliquot of RNA was prepared for cDNA conversion while the rest was immediately stored at -80°C.

3.20 Reverse transcription of RNA into cDNA

3.20.1 Material

- dNTP mix (Cat # U1511, Promega, Madison, USA)
- Moloney murine leukemia virus reverse transcriptase (Prod # M1705, Promega, Madison, USA)
- Moloney murine leukemia virus reverse transcriptase buffer pack (Prod # M5313, Promega, Madison, USA)
- RNase inhibitor (Cat # AM2694, Invitrogen, USA)
- Oligo (dT) (Cat # AM5730G, Invitrogen, USA)

3.20.2 Procedure

For the first step of cDNA conversion, 2µg RNA from each sample was mixed with 2 µl of oligodT primer and incubated at 70ºC for 5min. A master mix of 5 µl M-MLV buffer, 1µl M-MLV enzyme, 1.5 µl dNTP mix and 0.7 µl of Rnase inhibitor were prepared for each sample. After cooling the RNA oligodT mix on ice for 5min, the above master mix was added to the samples. The cDNA mixture was incubated according to the following protocol in a Mastercycler gradient thermal cycler: 42°C for 60’ and 95°C for 5 min. The resulting cDNA was stored at -20°C until further use.

3.21 Quantitative real time RT-PCR

3.21.1 Principle

Real time polymerase chain reaction (RTPCR) is a biochemical process used to amplify a specific region of DNA or gene of interest from a small amount of starting material. This method involves the following steps:

- Melting or denaturation of DNA to yield a single strand of DNA from the duplex
- Annealing of primers to the single stranded region of interest
- Elongation of the DNA strand by addition of dNTPS, Taq polymerase enzyme and forward and reverse oligonucleotides (primers) specific to that region.

RTPCR has the advantage of allowing the quantitation of the DNA formed after each cycle by the use of double-stranded DNA intercalating dyes such as SYBR green or fluorescent probes (TaqMan chemistry). The SYBR green method measures the amount of intercalated dye in the double stranded DNA and provides a number known as the cycle threshold (Bustin 2000). The $2^{-[\Delta\Delta Ct]}$ method is used to calculate the fold change in gene expression of gene of interest when compared to control (Livak and Schmittgen 2001).

3.21.2 Material and instrument

- Fast SYBR® green master mix (Prod # 4385617, ThermoFisher Scientific, Applied Biosystems, USA)
- 7900HT Fast real-time PCR system (Thermo Fisher Scientific, Applied Biosystems, USA)
- MicroAmp® Optical 96-Well Reaction Plate (Prod # 4306737, Life Technologies, USA)

3.21.3 Procedure

The qRTPCR reaction mixture (10µl) included the following reagents:

- Fast SYBR green master mix (containing ROX dye and dNTPs) 5µl
- Forward primer (0.5µM) 0.5 µl

- Reverse primer (0.5µM) 0.5 µl

The cDNA used for qRTPCR was diluted 1:10 with nuclease-free water to a final volume of 10µl. Table 5 summarizes the primer sequences of the genes under consideration. The PCR reaction was as follows:

95°C 1s

60°C 20s

PCR products were subjected to agarose gel electrophoresis to ensure primer specificity by detection of the presence of a single band.

Table 5: Sequence of primers used for qRT-PCR analysis (mouse)

Gene	Forward primer	Reverse primer
cJun	5’-AAAACCTTGAAAGCGCAAAA-3’	5’-CGCAACCAGTCAAGTTCTCA-3’
IL6	5'-AGTTGCCTTCTTGGGACTGA-3'	5'-TCCACGATTTCCCAGAGAAC-3'
IL-1β	5'- GCC CAT CCT CTG TGA CTCAT-3'	5'-AGG CCA CAG GTA TTT TGT CG-3'
TNF-α	5'-CATCACAACCACTCCCACTG-3'	5'-GTTCTGCCAGTTCCTTCTGC-3'
Arg1	5’-GGAAAGCCAATGAAGAGCTG-3’	5’-CTGGTTGTCAGGGGAGTGTT-3’
YM1	5’-CCAGCATATGGGCATACCTT-3’	5’-CAGACCTCAGTGGCTCCTTC-3’
SMAD2	5’-GTGACGCTGAGGTCTTGTC	5’-CACCCAGGGTAAGTCAGGA

	A-3’	A-3’
SMAD3	5’-CTGGGCCTACTGTCCAATGT-3’	5’-GCAGCAAATTCCTGGTTGTT-3’
TβR1	5’-ACCTTCTGATCCATCGGTTG-3’	5’-TTCCTGTTGGCTGAGTTGTG-3’
Runx1	5’-GTG ATG CGT ATC CCC GTA GA-3’	5’- GCC AGG GTG GTC AGC TAG TA-3’
B actin	5’-GAAGAGCTATGAGCTGCCTGA-3’	5’-GGATTCCATACCCAAGAAGGA-3’

Table 6: Sequence of primers used for qRT-PCR and semi-quantitative PCR analysis (rat)

Gene	Forward primer	Reverse primer
cJun	5’-CCACCGAGACCGTAAAGAAA-3’	5’-GTCGTCACGGAATTCTTGGT-3’
CD11b	5’-AGGCAGCTGAATGGAAGGAC-3’	5’CGTAGCGAATGATCCCTGCT-3’
CNPase	5’-GGTACTGGTCTGCCATTTCAA-3’	5’-AAGATGGTGTCTGCTGATGCT-3’
GFAP	5’-AGA AAA CCGCAT CAC CATTC-3’	5’-GCACACCTCACA TCACATCC-3’
MAP2	5’-TGT TGCTGCCAAGAAAGATG-3’	5’-ACGTGGCTGGACTCAATACC-3’
PECAM 2	5’-CGA AATCTAGGCCTCAGCAC-3’	5’-CTTTTTGTCCAC GGTCACCT-3’

SMAD2	5’-TTACATCCCAGAAACACCAC-3’	5’-TAAGTAACTGGCTGCAAATCC-3’
TβR1	5’-ACATCAGGGTCTGGATCAGGT-3’	5’-CCATGAACGTTCTTCTCT-3’
Runx1	5’- AAC CCT CAG CCT CAA AGT CA-3’	5’- GGG TGA ACA GAA GAG GTG AT-3’
GAPDH	5’-ACATGCCGCCTGGAGAAACCTGCC-3’	5’-TGCCAGCCCCAGCATCAAAGGGGA-3’

3.22 Agarose gel electrophoresis

3.22.1 Principle

This is a quick and cost effective way to separate DNA based on its size. As DNA carries a negative charge, it migrates through the agarose matrix towards the positive electrode after application of an electric current to the electrophoresis tank. The migration of DNA through the matrix depends on its size, with higher molecular weight fragments running slower while smaller molecular weight frangments running faster towards the positive electrode. Intercalating dyes such as SYBR green or ethidium bromide (EtBr) are added to the agarose gel to enable visualization of the DNA bands (Waring 1965).

3.22.2 Materials and Instrument

- Blue/Orange loading dye 6X (PRG1881, Promega Corporation, ThermoFisher Scientific, USA)

- Certified Molecular biology agarose (Cat. No. 161-3102, Bio-Rad, MO, USA)
- Tris acetate EDTA buffer (BUF-3001-10X1L, 1st Base, Singapore)
- DNA ladder 100bp (Cat # G2101, Promega, Madison, USA)
- Ethidium bromide (EtBr) (Invitrogen, Life Technologies, USA)
- Image Lab ™ (Bio-Rad CA, USA)

3.22.3 Procedure

To prepare a 2% gel, 2g agarose was dissolved in 100ml TAE buffer in a microwave oven. After cooling, 6 µl of EtBr was mixed in the agarose solution and poured onto a gel-tray. 10 µl PCR products were mixed with 2µl of loading dye and loaded onto wells in the agarose gel. 5µl of 100 bp DNA ladder was loading in one well to determine the sie of the product. After running the gel until the dye front reached the end of the gel, the DNA was visualized using the Bio-Rad Image Lab ™ imaging system.

3.23 Immunocytochemistry

3.23.1 Principle

Immunocytochemistry localizes a specific protein of interest in cells. A fluorophore tagged secondary antibody is used to tag the primary antibody and the resulting fluorescent signal is captured using a microscope.

3.23.2 Material

- 4% paraformaldehyde (PF)
- Lectin from *Lycopersicon esculentum* FITC conjugate (Cat # L0401, Sigma-Aldrich, MO, USA)

- Goat anti-rabbit IgG- cy3 antibody (Cat # AP132B, Merck Millipore, Billerica, MA, USA)
- goat anti-mouse IgG-FITC antibody (Cat # AP132F, Merck Millipore, Billerica, MA, USA)
- DAPI (Cat # D3571, Molecular Probes, Invitrogen, Life Technologies, Thermo Fisher Scientific Inc, MA, USA)
- Mounting Medium (Cat # S302380, Dako, Agilent Technologies, USA)
- Goat serum (Cat # S-1000, Vector Laboratories, Burlingame, USA)

Table 7: Antibodies used for immunostaining.

Gene	**Company**	**Species**	**Catalogue #**
TGFβ1	Santa Cruz Biotechnology	Rabbit	sc 28679
TβR1	Santa Cruz Biotechnology	Rabbit	sc 398
NFκB	Santa Cruz Biotechnology	Rabbit	sc 109
SMAD2	Cell Signaling Technology	Rabbit	D43B4
Runx1	Santa Cruz Biotechnology	Rabbit	sc 28679
cJun	Cell Signaling Technology	Rabbit	9165S

phospho-cJun	Cell Signaling Technology	Rabbit	9261S
TNFα	Merck Millipore	Rabbit	AB2148P
iNOS	Santa Cruz Biotechnology	Rabbit	sc 649
Cd11b	Merck Millipore	Mouse	CBL1512

3.23.3 **Procedure**

For performing immunocytochemistry, the first step was to coat glass coverslips placed in each well of a 24-well plate, with poly-l-lysine for 2h at room temperature. 2×10^4 BV2 microglial cells were seeded in each well and allowed to grow for 24h in a 37°C incubator. The following day, the cells were fixed with chilled, freshly-prepared 4% PF for 20 min at room temperature. Following fixation, blocking was performed with 5% goat serum for 30 min at room temperature. The cells were incubated with primary antibody overnight at 4^0C. The next day, after washing, the cells incubated with secondary antibodies for 1h at room temperature. Further, following 3 PBS washes, the nucleus was stained with DAPI. Coverslips were mounted onto glass slides cleaned with 70% alcohol. After air-drying, images were captured with laser scanning Olympus FV1000 confocal microscope.

3.24 Nitrite Quantification

3.24.1 Principle

Nitric oxide (NO) is a secretory product of mammalian cells playing a role in immune response (Moncada and Higgs 1993). NO production and secretion is elevated during an immune response. In biological systems, NO is oxidized to nitrite and nitrate which are used to quantitate NO production (Snyder and Bredt 1992). The Griess reaction involves the conversion of nitrate to nitrite by the enzyme nitrate reductase. This results in the formation of a coloured dye whose absorbance can be measured at 540 nm (Kelm *et al.* 1997).

3.24.2 Materials

- Cell culture medium
- Nitric Oxide Colorimetric BioAssay ^{TM} kit (US Biologicals, MA, USA)

3.24.3 Procedure

Measurement of nitrite in culture supernatant provides a means to measure the NO production in cell culture systems. Culture supernatant was collected from BV2 cells transfected with control and miRNA inhibitors and mimics. 85µl culture supernatant was added to each well of a 96-well ELISA plate and mixed with 5µl each of the enzyme nitrate reductase and enzyme cofactor mixture. This mixture was incubated at room temperature for 1h to allow the conversion of nitrate to nitrite. 50 µl each of Griess reagents provided in the kit, were added to each well. After colour development for 10 min at room temperature, the absorbance was measured at 540 nm using a microplate

spectrophotometer. Nitrate standard curve was used to quantify the nitric oxide produced in the samples.

3.25 ELISA Assay for TNF α release

3.25.1 Principle

Enzyme-linked immunosorbent assays (ELISAs) is a technique used for detecting and quantification of substances such as peptides, proteins, antibodies and hormones. ELISAs have proven to be valuable tools for detection and quantitation of protein analytes from various biological samples: serum, plasma, cell culture supernatants and cell lysates (Engvall and Perlmann 1971; Leng *et al.* 2008).

3.25.2 Materials

- TNF α ELISA kit (Cat No: 88-7324-22, EBiosciences, USA)
- SpectraMax Plus Microplate reader (Molecular Devices, Sunnyvale, USA)

3.25.3 Procedure

BV2 cells were plated in 6-well plates and transfected followed by LPS treatment, as described above. After 48h, the media supernatants were collected, and TNF-α were determined using the EBiosciences ELISA kit that specifically recognizes the mouse cytokine TNF-α. On the first day, the wells of a 96-well ELISA plate were coated with the capture antibody at 4°C overnight. The following day after washing with PBS, the wells were blocked

with the blocking reagent provided in the kit, followed by addition of 100 µl of media supernatant or appropriate dilutions of TNFα standard provided in the kit at 4°C overnight. The next day, the detection antibody was added to each well and incubated at room temperature for 1h followed by washing and colour development. The absorbance was noted at 540 nm and TNF-α standard curve was used to calculate the TNF-α level in the samples.

3.26 Cell Migration assay

3.26.1 Principle

Cell migration is an important multistep process involved in various processes such as development, wound repair and immune surveillance. For quantifiying cell migration, cells are seeded on the upper part of a cell permeable membrane while a chemoattractant is added to the bottom chamber. Cell migration is measured by determining the ability of cells to pass through the membrane towards the chemoattractant. The cells that have migrated through the membrane are stained and counted.

3.26.2 Materials

- Transwell inserts (Corning Life Sciences, MA, USA)
- 100% methanol
- crystal violet (0.5%)

3.26.3 Procedure

BV2 cells were transfected with miR-200b mimics or inhibitors as described above. 48h post transfection, the cells were trypsinized and seeded into

Transwell inserts (Corning Life Sciences, MA, USA) containing free DMEM (no serum). For the control groups, complete medium (10% FBS, DMEM) was added to the wells, while for the LPS activated groups, 1mg/ml of LPS was added to the wells along with complete medium (10% FBS, DMEM). The cells were incubated in the transwell inserts and cultured overnight at 37°C in a humidified atmosphere of 5% CO_2 and 95% air incubator. Migrating cells on the lower membrane surface were fixed with 100% methanol for 15min at room temperature while the non migrated cells were scrapped off gently with a cotton swab. After washing, the inserts were air-dried. The cells were stained with crystal violet (0.5%)/methanol (25%) solution for 30min at room temperature. The inserts were then washed in PBS until the blue stain lightened followed by air drying. Images were captured on Nikon microscope at ×100. Three biological triplicate was performed and ≥5 fields were counted from each sample in each experiment.

3.27 Annexin V Apoptosis Assay

3.27.1 Principle

Apoptosis is a complex multistep process of cell death. Phosphatidyl serine is a phosphoserine membrane component normally expressed on the inner or cytosolic surface of the cell membrane of normal live cells. Upon initiation of apoptosis, the PS residues are “flipped” and appear on the cell surface. On the cell surface, PS can be detected using a protein having high affinity for PS such as Annexin V, conjugated with a fluorescent moiety (van Engeland *et al.* 1998).

3.27.2 Materials

- Annexin V-Cy3 Apoptosis Detection Kit (Cat # ab14142, Abcam, Cambridge, UK)
- BD LSRFortessa™ X-20 analyzer (BD Biosciences, San Jose, CA, USA)

3.27.3 Procedure

Apoptosis assay was carried out using the Annexin V-Cy3 apoptosis detection kit. 0.5×10^5 cells were seeded in each well of a 6 well plate followed by incubation with a 1:1 mixture of fresh complete medium (1 ml) and conditioned medium (1 ml) for 24h. The conditioned medium was obtained from untreated BV2 cells and BV2 cells transfected with anti-miR-200b (inhibitor) or miR-200b mimics or control probes. Following incubation, the cells were gently trypsinized and the staining protocol. Flow-cytometry was performed on a BD LSRFortessa™ X-20 (BD Biosciences) analyzer.

3.28 Western blotting

3.28.1 Principle

Protein content from a tissue or cell can be quantified using western blot technique. The protein samples are separated using poly-acrylamide gel electrophoresis followed by transfer on to a polyvinylidene difluoride (PVDF) membrane. Primary antibody raised against the protein of interest is used to localize the protein. This is followed by using a horseradish peroxidase (HRP) secondary antibody, which binds to the primary antibody. Addition of a

substrate for the HRP emits a signal which can be captured onto an X-Ray film (Kurien and Scofield 2006).

3.28.2 Extraction of total protein

3.28.2.1 Materials

- Mammalian Protein Extraction Reagent (Prod # 78501, Rockford, MI, Thermo Fisher Scientific, USA)
- Protease Inhibitor (Rockford, MI, Prod # 88665, ThermoFisher Scientific, USA)
- Halt Phosphatase inhibitor cocktail (Part No. 23236, ThermoFisher Scientific, USA)

3.28.2.2 Procedure

For total protein extraction 200µl of M-PER reagent containing protease and phosphatase inhibitor cocktail was added to the cells and incubated for 5min on ice. The cells were scrapped out and the resulting lysate was centrifuged at 14,000 rpm at 4ºC for 20min. the supernatant containing the protein was collected in a fresh tube. The protein lysate thus obtained was quantified by Bradford assay and stored at -80ºC.

3.28.3 Extraction of nuclear and cytosolic proteins

3.28.3.1 Materials

- Nuclear extraction kit (Cat # 2900, Merck Millipore, Billerica, MA, USA)

3.28.3.2 Procedure

Total protein was extracted from untransfected BV-2 microglial cells or transfected with miRNA inhibitors and mimics. Following transfections and/or

LPS treatments, the cells were trypsinized to collect the cell pellet. The cell pellet was incubated on ice for 5min with 150µl of 1X cytoplasmic extraction buffer mixed with protease and phosphatase inhibitors followed by pelleting the cells again at 250rpm for 5min at 4ºC. The resulting cell pellet was resuspended in 60 µl cytoplasmic extraction buffer. Cytoplasmic protein was separated by centrifugation at 8000rpm for 20min at 4ºC and collecting the resulting supernatant. This was stored at -80ºC. The pellet was resuspended in protease and phosphatase inhibitor containing nuclear extraction buffer and mixed well using a syringe. Nuclear protein was isolated by centrifuging the lysate at 16,000g for 5min at 4ºC and stored at -80ºC.

3.28.4 Estimation of protein concentration

3.28.4.1 Materials

- Coomassie Bradford Protein Assay Reagent (Cat # 23200, Bio-Rad, CA, USA)

3.28.4.2 Procedure

The extracted protein was quantified using the Bradford calorimetric assay (Bradford 1976). The Bradford assay is a method to quantify protein using the Coomassie Brilliant blue G-250 dye which binds to proteins. Upon binding to proteins in the sample, the dye changes colour which can be measured using a spectrophotometer at a wavelength of 595nm. BSA standard curve was plot using different concentrations of BSA protein (0.006, 0.12, 0.24 and 0.48 mg/ml) was used to quantify the protein amount in a given sample. 1:10 diluted protein sample was added to 200µl of Bradford assay reagent in a 96

well plate and incubated at room temperature for 15 min. The absorbance was read at 595 nm and the protein concentration quantified using the equation obtained from the standard curve.

3.28.5 Gel electrophoresis and protein detection

3.28.5.1 Materials

10% resolving gel:

- H_2O 4.0 ml
- 30% acrylamide mix 3.34 ml
- 1.5M Tris buffer (pH 8.8) 2.5 ml
- 10% SDS 100 µl
- 10% APS 100 µl
- T.E.M.E.D 5 µl

5% stacking gel:

- H_2O 4.1 ml
- 30% acrylamide mix 0.83 ml
- 1.5M Tris (pH 6.8) 0.750 ml
- 10% SDS 50 µl
- 10% APS 50 µl
- TEMED 8 µl

- Tris/glycine/SDS electrophoresis buffer (Cat # 161-0732EDU, Bio-Rad, USA)
  - Tris/glycine buffer (Cat # 161-0734EDU, Bio-rad, CA, USA)

- 2X Laemmli sample buffer (Cat # 161-0737EDU, Bio-Rad, MO, USA)
- Spectra Multicolor protein ladder (Rockford, MI, Prod # 26634, ThermoFisher Scientific, USA)
- Thick Blot paper (Cat # 170-3931, Bio-Rad, MO, USA)
- Immun-blot PVDF membrane (Cat # 162-0177, BioRad, MO, USA)
- Clear Milk blocking buffer (Cat # 37587, Pierce, Thermo Scientific Fisher, Rockford, MI, USA)
- Blot qualified BSA (W3841, Promega, WI, USA)
- Restore PLUS Western Blot Stripping Buffer (Rockford, MI, Prod # 46428, ThermoScientific, USA)
- Goat anti-rabbit HRP antibody (Merck Millipore, Prod # AP307P, Billerica, MA, USA)
- Goat anti-mouse HRP antibody (Merck Millipore, Prod # AP308P, Billerica, MA, USA)
- SuperSignal West Pico Chemiluminescent Substrate (Rockford, MI, Prod # 34077, ThermoFisher Scientific, USA)
- CL-XPosure Film (Rockford, MI, Prod # 34089, Thermo Fisher Scientific, USA)
- Bio-Rad Image Lab ™ imaging system (Bio-Rad, MO, USA)
- 1x TBS (pH7.6)
    - Tris base 2.42 g
    - NaCl 0.8 g

The above salts were mixed in 800 ml of deionised water following which the pH was adjusted to 7.6. Finally, the volume was made up to 1liter.

- 1x TBST
    - 1x TBS 999 ml
    - Tween 20 1ml

Table 8: Antibodies used for western blot.

Gene	**Company**	**Species**	**Catalogue #**
TβR1	Santa Cruz Biotechnology	Rabbit	sc 398
SMAD2	Cell Signaling Technology	Rabbit	D43B4
Phospho SMAD2	Cell Signaling Technology	Rabbit	138D4
Runx1	Abcam	Rabbit	Ab23980
cJun	Cell Signaling Technology	Rabbit	9165S
phospho-cJun	Cell Signaling Technology	Rabbit	9261S
SAPK/JNK	Cell Signaling Technology	Rabbit	9258S
Phospho-SAPK/JNK	Cell Signaling Technology	Rabbit	9251S

Lamin A	Santa Cruz Biotechnology	Rabbit	Sc 20680
β-actin	Sigma-Aldrich	Mouse	A1978

3.28.5.2 Procedure

Total protein (40µg) and nuclear protein (20µg) from each sample was mixed with laemmli buffer and denatured at 95^0C for 5min. The denatured protein was loaded onto a 10% SDS-PAGE. A protein ladder was run alongside the samples for size detection of the proteins. After separation, the proteins were transferred on to a PVDF transfer membrane using the semi-dry teansfer technique. This was followed by blocking the blots with 5% BSA or 5% milk solution for 1h at room temperature. The blots were then incubated with appropriate primary antibodies overnight at 4^0C. The next day after three washing steps, the blots were incubated with secondary anti-mouse or anti-rabbit HRP antibody for 1h at room temperature. Followed by washing with TBST, the blots were developed using a chemiluminescence reagent. The signal was visualized and quantified using the Bio-Rad Image Lab ^{TM} imaging system. All measurements of phosphorylated protein levels were normalized by stripping the blots with stripping buffer and reprobing with antibodies against total protein. To normalize the protein content of each lane, the blots were re-probed with beta actin antibody.

3.29 NFκB Transcription factor assay

3.29.1 Principle

The NFκB Transcription factor assay enables sensitive quantification of the nuclear translocation of NFκB p65 subunit in nuclear extracts. This assay from Merck Millipore is a combination of the electrophoretic mobility shift assay (EMSA) with the 96-well plate based enzyme-linked immunosorbant assay (ELISA). During the assay, the capture probe, a double stranded biotinylated oligonucleotide containing the consenses sequence for NFκB, is mixed with nuclear extract in the streptavidin coated plate. When incubated together, the NFκB in the nuclear extract binds to the biotinylated consenses sequence and is immobilized on the plate. Any unbound material is washed away. The bound NFκB is detected with a specific primary antibody. An HRP-conjugated secondary antibody is used, which binds to the primary antibody. Addition of a substrate for the HRP emits a signal which can be read using a spectrophotometer at 450 nm.

3.29.2 Material

- Universal EZ-TFA Transcription Factor Assay kit Colorimetri (Cat No: 70-500, Merck Millipore, USA)
- SpectraMax Plus Microplate reader (Molecular Devices, Sunnyvale, USA)

3.29.3 Procedure

1X Transcription factor assay buffer (TFA) was prepared by diluting 1 part of 5X TFA in 4 parts distilled water. 1X Enhanced TFA buffer was prepared by

adding blocking reagent to 1X TFA. Following components were added to the plate well directly in sequential order-

1X Enhanced TFA buffer

Oligonucleotide probes

Nuclear extract

This was followed by incubation for 2 hours at room temperature followed by 3 washes with 1X enhanced TFA. 100µl of 1:1000 diluted primary antibody was added to each well followed by incubation for 1 hour at room temperature. Unbound primary antibody was washed off with 3 washes of 1X enhanced TFA followed by incubation with IgG-HRP conjugated secondary antibody for 30 min at room temperature. The wells were then washed with 1X TFA, 4 times followed by color development using TMB substrate for 10 min. the absorbance of the samples was measured using a spectrophotometer at 450 nm.

3.30 Statistical analysis

The data were presented as mean ± SD. Three or more biological and technical triplicates were used for each experiment. Statistical significance was evaluated by the Student's *t- test* or ANOVA with post hoc Tukey test. Results were considered as significant at $p < 0.05$.

4 RESULTS

4.1 miRNA microarray

4.1.1 MiRNA expression profile shows that activated microglia are biologically distinct from control microglia

Microglial cells which have amoeboid morphology in the developing brain, transform into a branched, ramified morphological phenotype in the adult brain (Ling and Wong 1993) (Fig 1 A-B). In the event of pathological insult or external stimuli, these microglial cells become activated and morphologically hypertrophic with spherical in shape. Primary microglia cultured from rodent pup cortices are often used for *in vitro* studies (Fig 1 C-D). Several studies have shown the morphological, molecular and proteomic changes between normal and activated microglia (Hurley *et al.* 1999; Glanzer *et al.* 2007). In the present study, global miRNA expression profiles of control and activated primary rat microglia stimulated by LPS or β-amyloid (Aβ) were analyzed. Exiqon's microRNA microarray platform identified a total of 93 miRNAs differentially expressed between control and activated rat primary microglia. Out of the these 93 miRNAs, top 50 miRNAs having the largest variation across control and activated primary microglia were used to generate a *Principle Component Analysis* (PCA) plot. PCA analysis shows that the biological difference between the microRNA expression of LPS-treated and control microglia is significant as evidenced by the separation of samples in different regions of the PCA plot as per their biology (Fig 2). Two illustrations of the result of the PCA have been provided: a traditional PCA plot (Fig 2) and a matrix plot (Fig 3). The matrix PCA plot gives the possibility to identify

differences in samples arising due to biological or technical factors. PC1 and PC2 describe variation related to sample groups or treatments, whereas PC3 and later PCs describe underlying or less variable factors like sample preparation conditions, operator, storage time etc. Figure 3 shows that the control and activated microglia samples show a difference in PC1 and PC2 as evidenced by a difference in the color code and thus are biologically distinct.

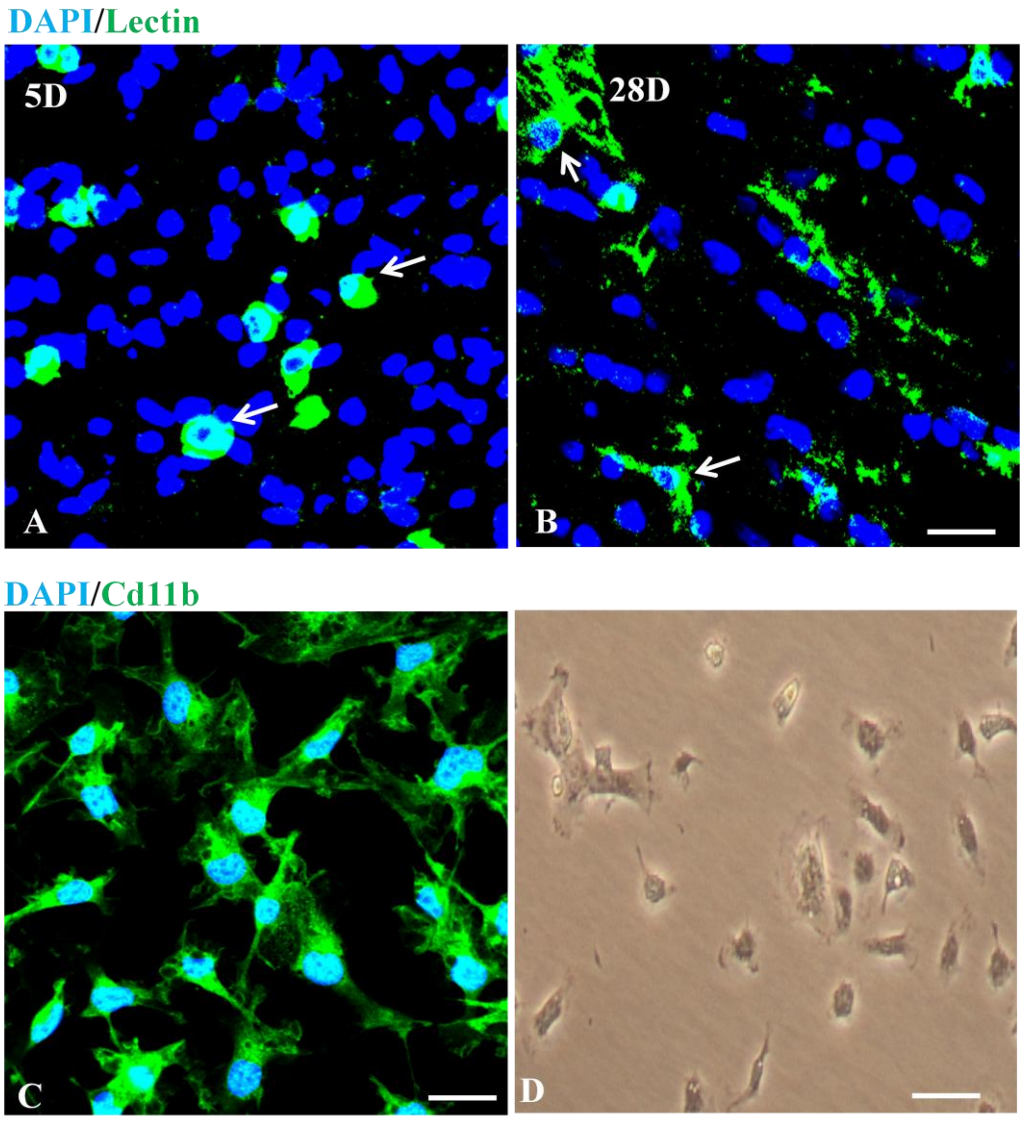

Fig 1 A-B: Immunofluorescense showing lectin-stained microglia (green, arrows) in the corpus callosum of 5 day (A) and 28 day (B) old rat brain. Note the change in morphology of microglia from amoeboid (A, arrows) to ramified with processes (B, arrows) from early post-natal to adult stage. The nucleus is counterstained with DAPI (blue). Scale bar: 20 µm.

C: Immunofluorescense showing Cd11b-stained primary microglia (green) isolated from 3 day old rat pups. The nucleus is counterstained with DAPI (blue). Scale bar: 20 µm.

D: Phase contrast image showing primary microglia purified from mixed glial culture. Scale bar: 20 µm.

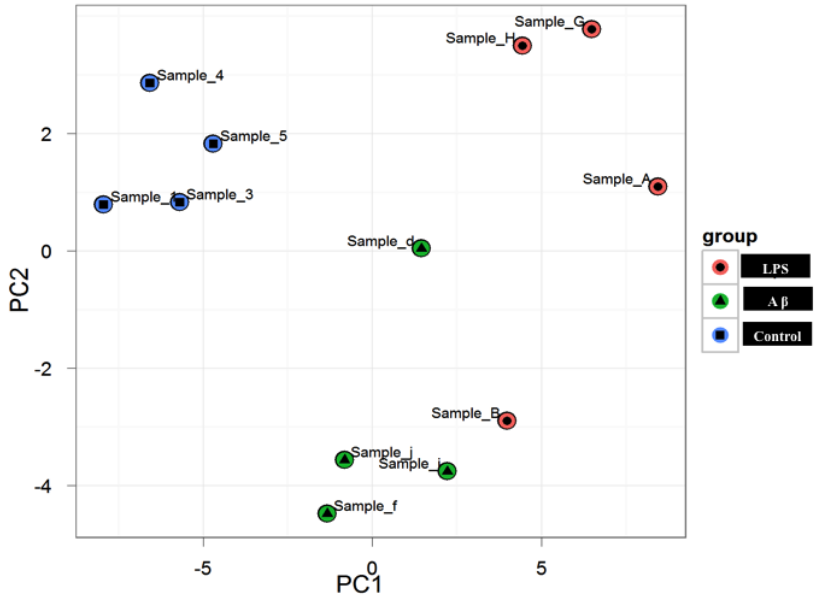

Fig 2: Principle Component Analysis (PCA) performed using the top 50 miRNAs with highest standard deviation, clustered the different samples as per their biological differences. The normalized log ratio values have been used for the analysis. The mean value across samples is shifted to 0 and the variance across samples is scaled to 1 before the analysis.

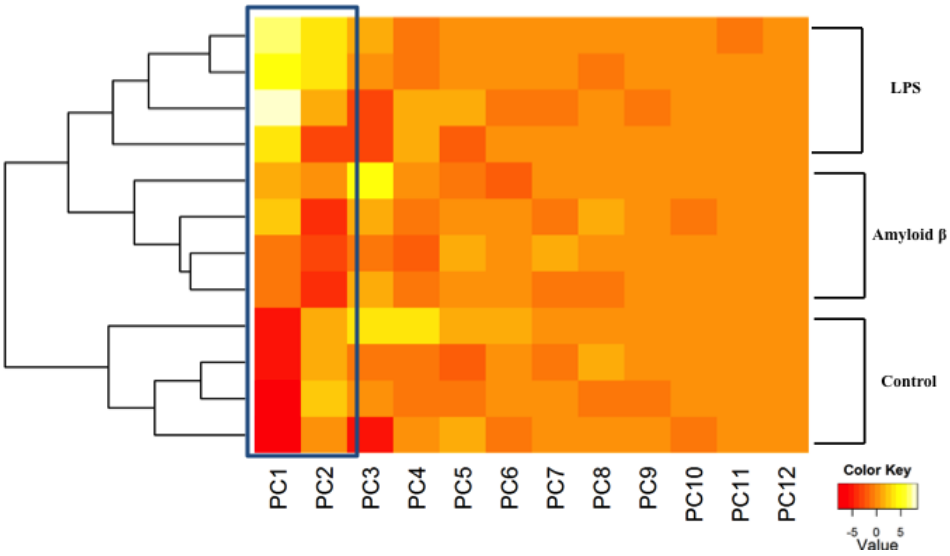

Fig 3: Matrix PCA plot. The analysis was performed on all samples, and on the top 50 microRNAs with the highest standard deviation. The normalized log ratio values have been used for the analysis. The mean value across samples is shifted to 0 and the variance across samples is scaled to 1 before the analysis.

4.1.2 Activated microglia show distinct miRNA expression pattern

The miRNA signature of activated primary microglia was characterized using global miRNA profiling. 93 miRNAs were identified to be differentially expressed between control and activated microglia (Fig 4, Sheet 1).

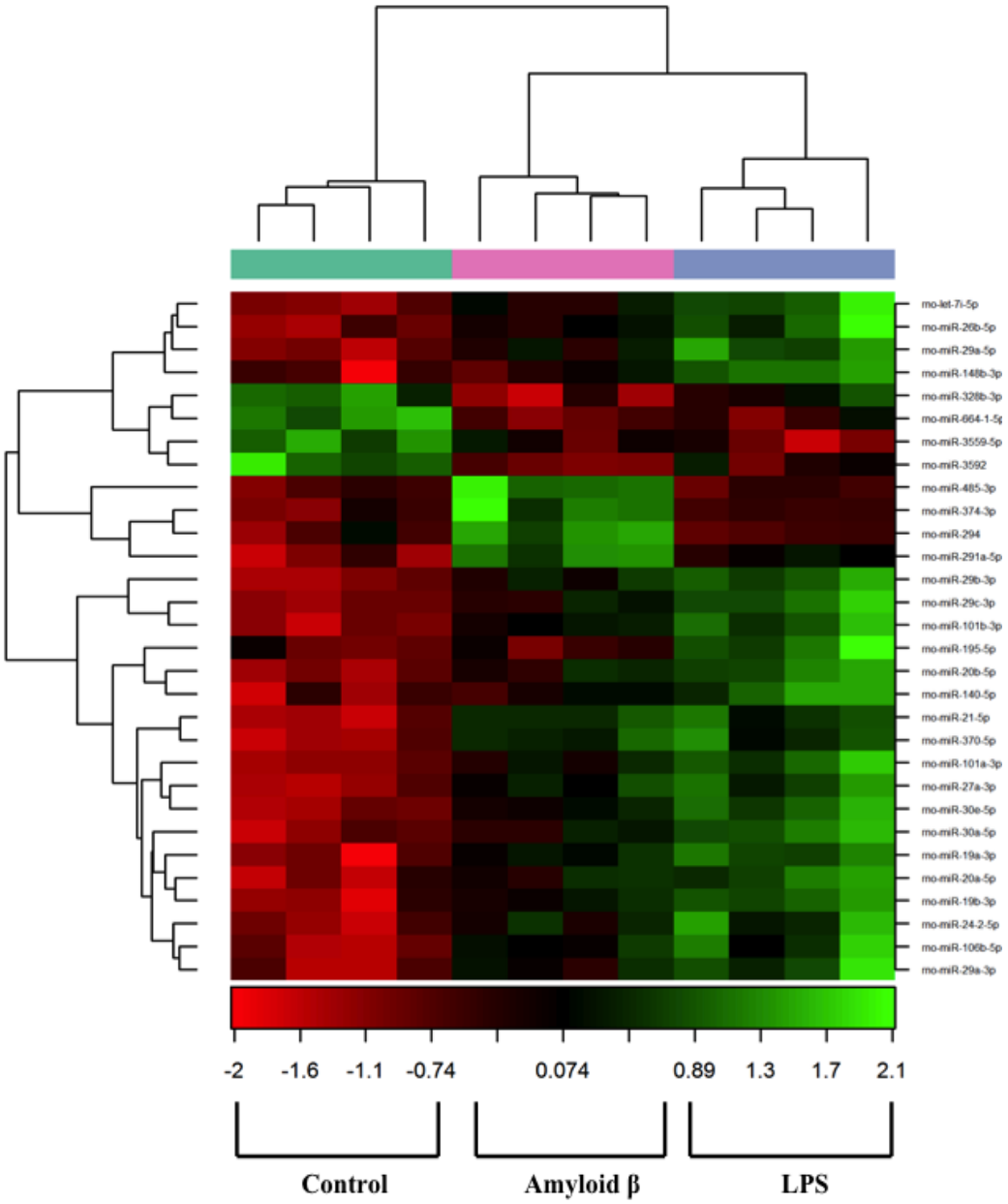

Fig 4: The heat map diagram shows the result of a two-way clustering of miRNAs and samples. Each column represents a biological sample while each row represents a miRNA. The miRNA clustering tree is shown on the left. The colour scale represents the relative expression level of each miRNA in each sample as compared to the reference channel. Red colour indicates an expression that is below the reference channel, while green colour indicates an expression that is higher than the reference.

A volcano plot drawn comparing the expression profile between control and LPS activated microglia (Fig 5) identified members of miRNA -29, -30 and -101 families as most differentially expressed. Sheet 2 lists the differentially expressed miRNAs between control and LPS activated microglia.

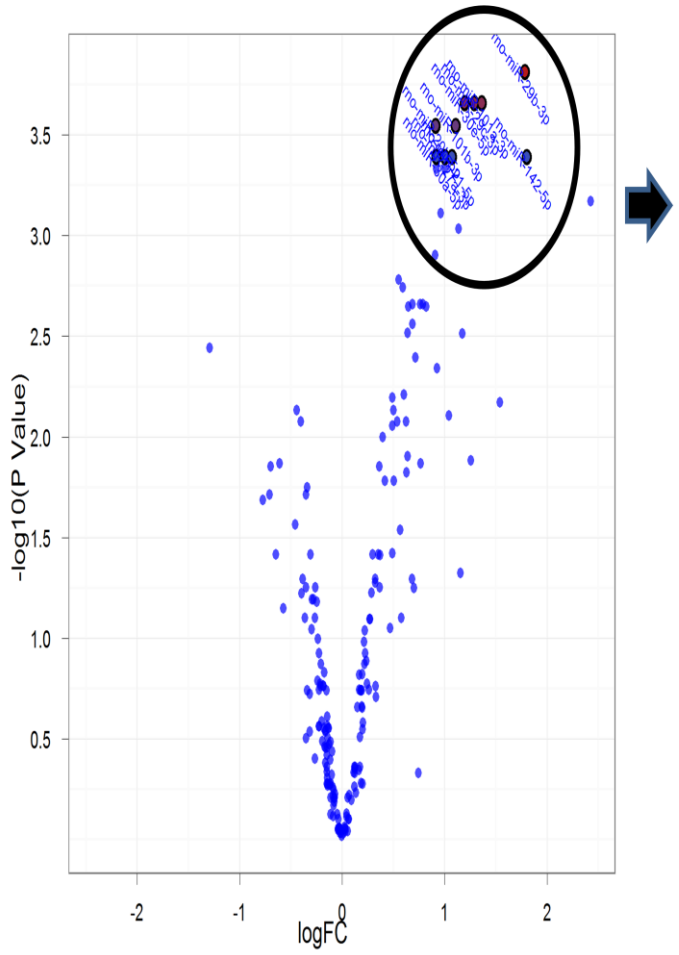

miRNA	LogFc
rno-miR-29b-3p	1.785
rno-miR-30e-5p	1.194
rno-miR-101a-3p	1.362
rno-miR-29c-3p	1.290
rno-miR-20b-5p	0.913
rno-miR-101b-3p	1.109
rno-miR-30a-5p	0.920
rno-miR-27a-5p	1.003
rno-miR-21-5p	1.072
rno-miR-142-5p	1.802

Fig 5: Volcano plot illustrating the relation between the logarithm of the p-values and the log fold change of miRNAs differentially expressed in control

and LPS-activated microglia. The top selected miRNAs are marked with annotation on the plot and tabulated on the right.

Although a large fold change difference was not observed in the Aβ - activated microglia as compared to control, miRNAs-21, -485, -370 were identified as being statistically significant in this comparison (Fig 6, Sheet 3).

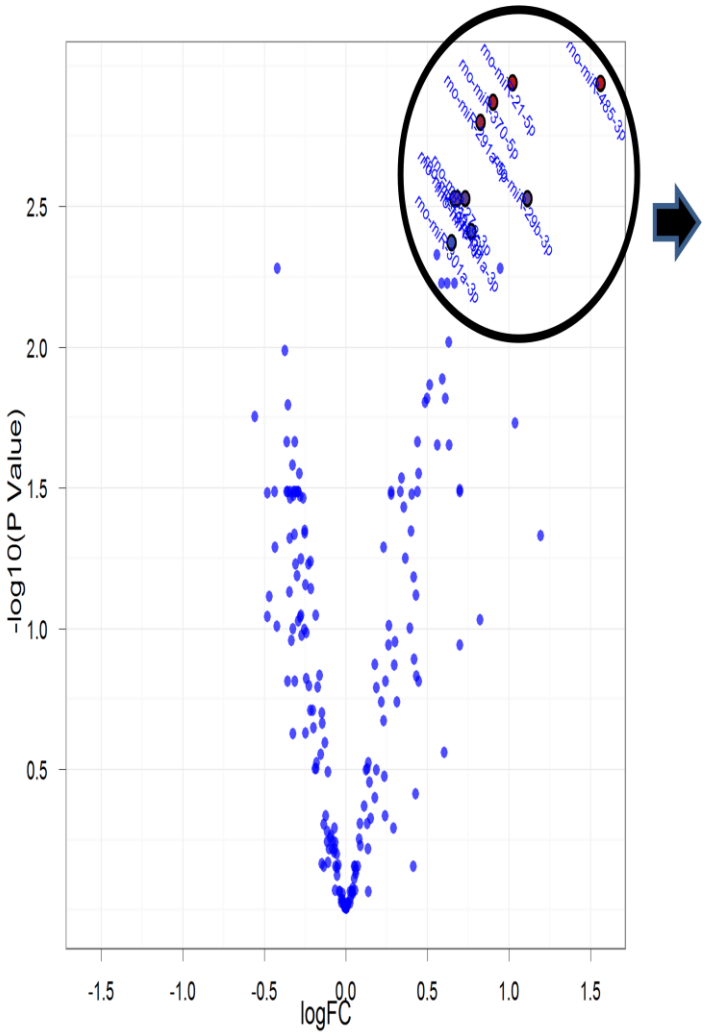

miRNA	LogFc
rno-miR-21-5p	1.022
rno-miR-485-3p	1.561
rno-miR-370-5p	0.902
rno-miR-291a-5p	0.826
rno-miR-30e-5p	0.684
rno-miR-27a-3p	0.733
rno-miR-29b-3p	1.113
rno-miR-101b-3p	0.664
rno-miR-101a-3p	0.768
rno-miR-301a-3p	0.558

Fig 6: Volcano plot illustrating the relation between the logarithm of the p-values and the log fold change of miRNAs differentially expressed in control and Aβ-activated microglia. The top selected miRNAs are marked with annotation on the plot and tabulated on the right.

Further, a comparison between LPS- and Aβ-activated microglia revealed several miRNAs uniquely expressed in either treatment group (Fig 7, Sheet 4).

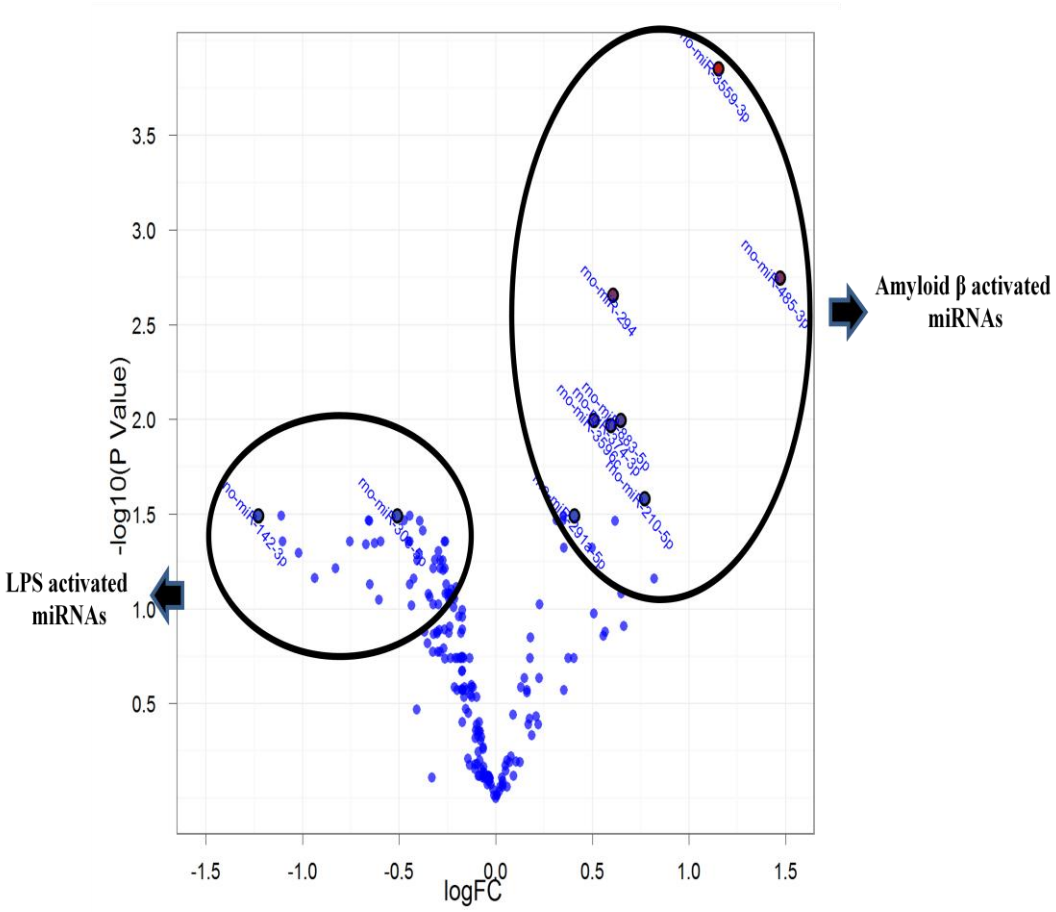

Fig 7: Volcano plot illustrating the relation between the logarithm of the p-values and the log fold change of miRNAs differentially expressed between LPS- (left) and Aβ- (right) activated microglia. The top selected miRNAs are marked with annotation on the plot.

Certain miRNA families were also found to be commonly expressed by both groups (Sheet 5). Thus, this analysis revealed that activation of microglia (by LPS and Aβ) as observed in neuroinflammation and neurodegenerative conditions *in vitro* respectively, induces certain common as well as distinct

group of miRNAs possibly leading to altered gene expression and subsequently perturbed function of microglia in the CNS pathologies.

Selected common miRNAs from the LPS and Aβ activated microglia from the microarray were validated in primary microglia culture by qRTPCR (Fig 8). The PCR products were run on a 15% native PAGE to check for the presence of a single product indicating primer specificity. qRTPCR results for LPS activated microglia were consistent with the results obtained from the miRNA microarray. However a disparity was observed in the Aβ group. Hence further analysis focussed on LPS activated microglia alone in the present study.

A

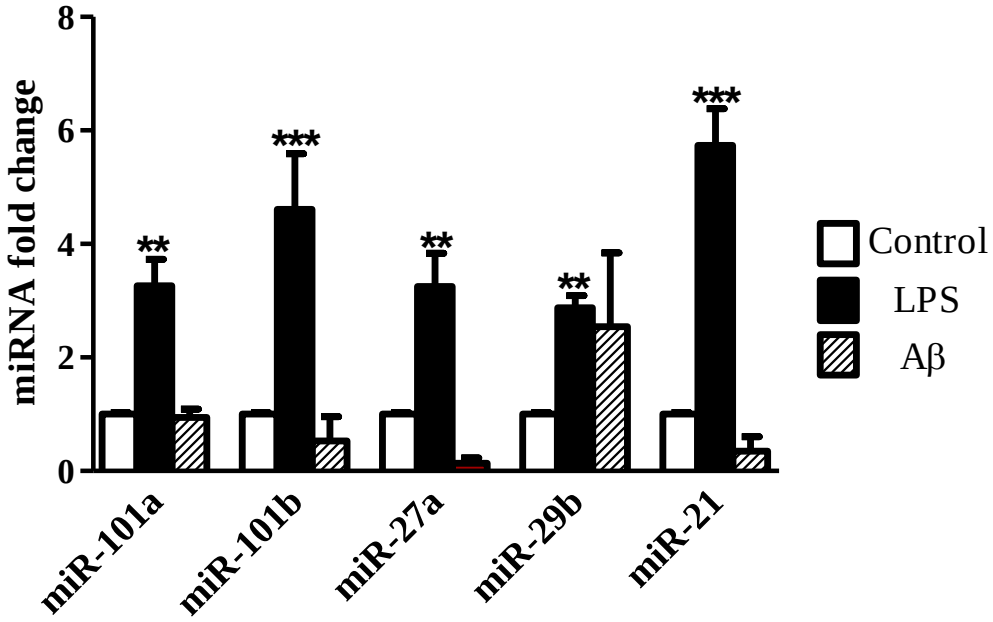

B

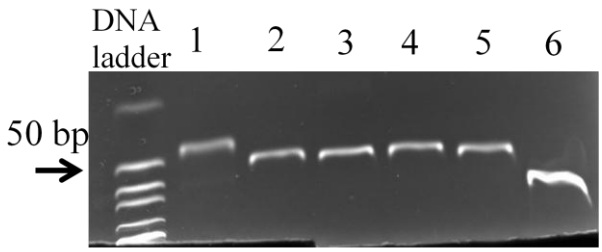

1	miR-21
2	miR-29b
3	miR-27a
4	miR-101a
5	miR-101b
6	U6

Fig 8 A: qRT-PCR analysis in control, Aβ and LPS activated primary microglia. Results are represented as miRNA fold change with respect to untreated controls. Statistical analysis was carried out using ANOVA with post-hoc Tukey test. Data represent the mean ± SD (n=5) $^{**}p<0.01$; $^{*}p<0.05$.

B: 15% native PAGE showing the miRNA bands following amplification.

4.1.3 Pathway analysis predicts miRNAs targeting TGFβ-Smad2 pathway in activated microglia

Ingenuity pathway analysis (IPA) software was employed to identify the signaling pathways targeted by miRNAs that were found to be differentially expressed in activated microglia. A comparison between LPS-activated and control microglia groups predicted several miRNAs targeting different members of the TGFβ-SMAD pathway, including TGFβ2 and TGFβ3, TGFβ receptors 1 and 2 (TβR1 and TβR2), several transcription factors belonging to the SMAD family as well as members of the Runx family (Fig 9). All genes

targeted by the selected miRNAs have been listed in sheet 6. Among other miRNAs, miR-27a was predicted to target 7 members of this family including TβR1, SMAD2 and Runx1. Another bioinformatic search using the miRWALK software confirmed these genes as the putative targets of miR-27a. Given the upregulation of miR-27a in LPS-activated microglia along with the prediction of several genes of the TGFβ-SMAD pathway (which has been shown to exhibit anti-oxidative and anti-inflammatory effects) to be targeted by this miRNA, miR-27a was chosen for further studies with the pathway of choice highlighted in Fig 10 (Hu *et al.* 1995; Paglinawan *et al.* 2003; Kim, Won-Ki *et al.* 2004).

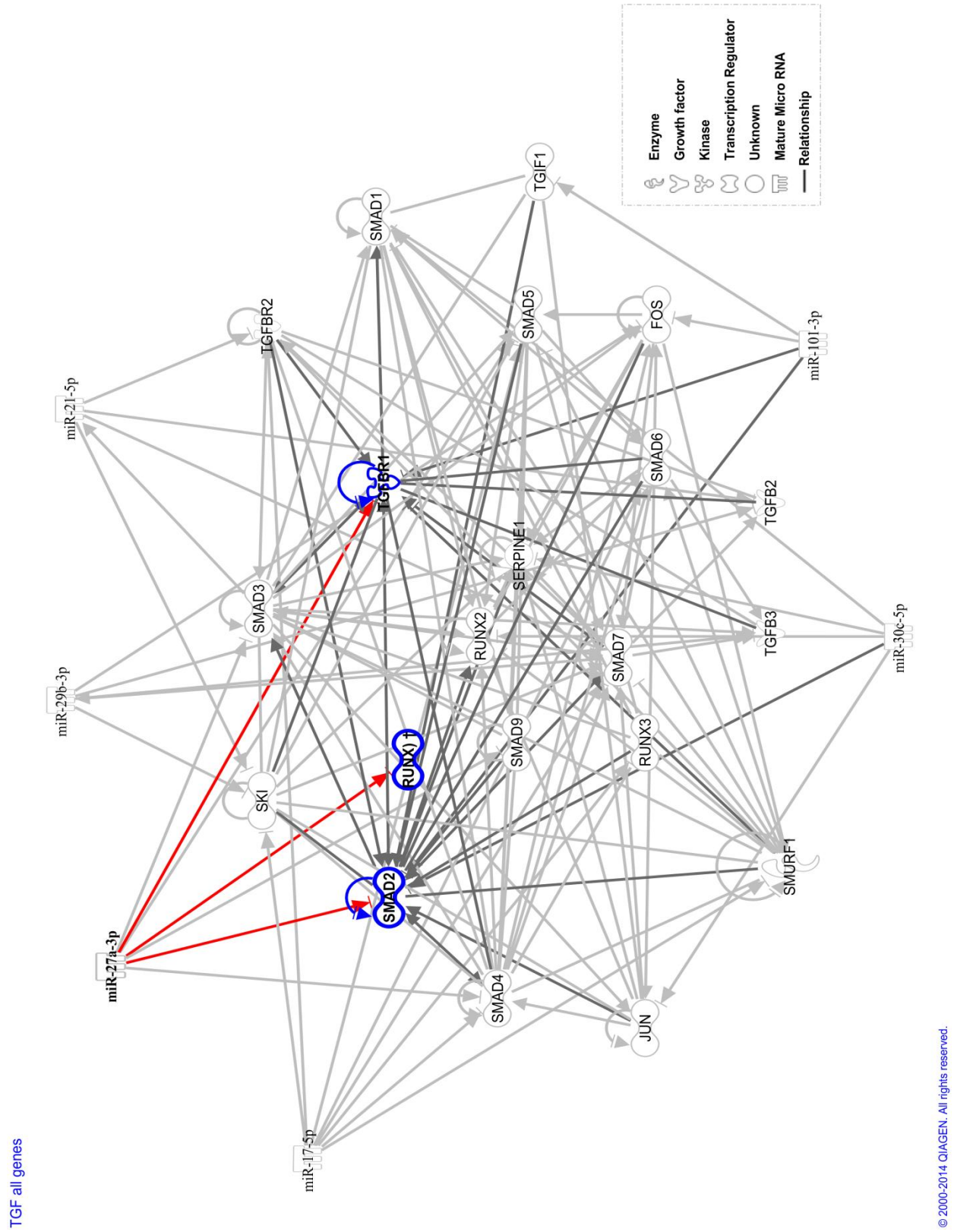

Fig 9: pathway generated using IPA software with selected miRNAs from the miRNA microarray targeting various members of the TGFβ pathway.

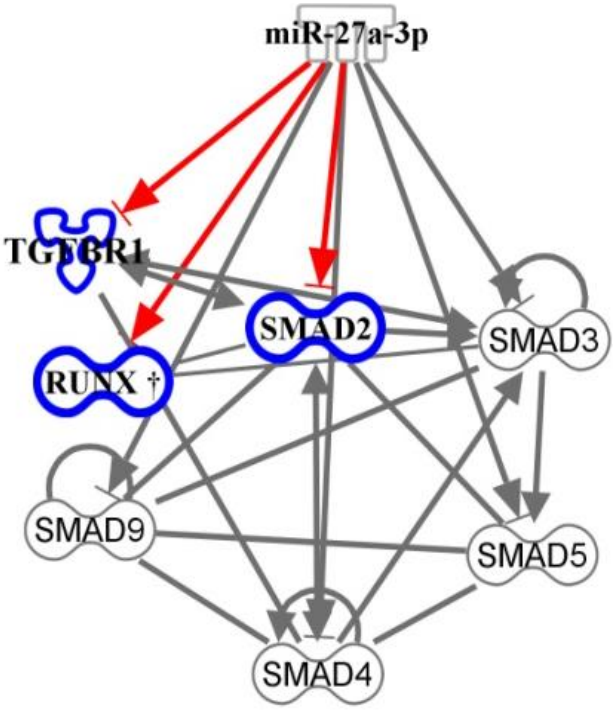

Fig 10: TGFβ pathway selected for analysis highlighting miR-27a targeting TβR1, SMAD2 and Runx1 genes.

4.2 MiR-27a targets TGFβ signalling pathway in microglia

4.2.1 MiR-27a is upregulated in activated microglia *in vitro*

Quantitative RTPCR analysis revealed that expression of miR-27a is upregulated after activation of BV2 microglia by LPS and Aβ for 6h (Fig 11).

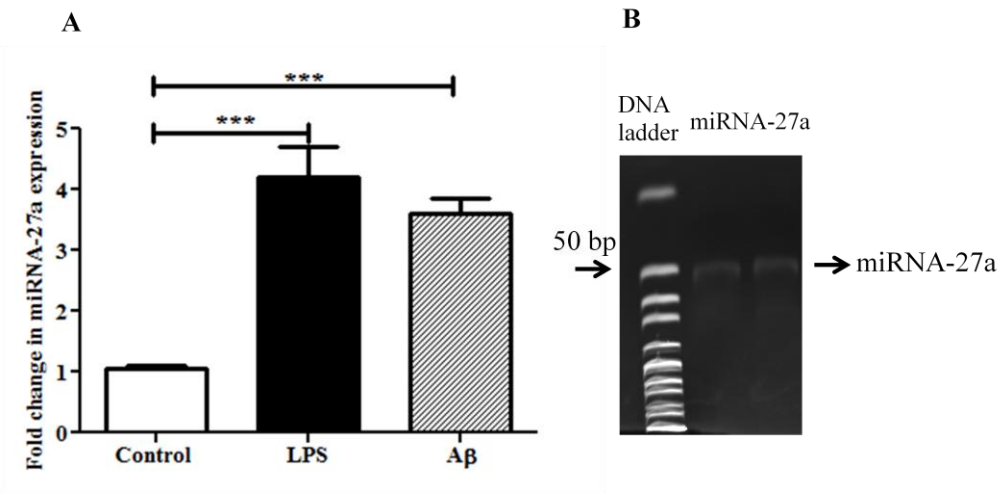

Fig 11 A: qRT-PCR analysis revealing increase in miR-27a expression in LPS (black) and Aβ (shaded) activated BV2 microglia. Results are represented as miRNA fold change with respect to untreated controls. Statistical analysis was carried out using ANOVA with post-hoc Tukey test. Data represent the mean ± SD (n=6) ****p*<0.001.

B: 15% native PAGE showing the band for miR-27a following amplification.

4.2.2 MiR-27a expression is upregulated in microglia *in vivo* in Traumatic brain injury model

In the present study, rat TBI model has been used to study microglia-mediated neuroinflammation, which exaggerates neuronal cell death in the regions of hippocampus thus contributing to increased cognitive dysfunction (Morganti-Kossmann, M.C.; 2007). After inducing TBI, microglial activation after neuronal damage in the hippocampal brain sections in comparison to sham (control) operated animals was confirmed by the induced expression of iNOS (Fig 12 Aa-Bc).

Microglia cells were detected in the hippocampus of sham-operated and TBI rat brain sections using lectin as the marker and isolated by laser capture microdissection (Fig 12 C-F). The cells isolated by LCM were confirmed to be microglia since they were found to express only microglia specific gene

(Cd11b), but not oligodendrocyte (CNPase), astrocyte (GFAP), neuronal (MAP2) and endothelial (PECAM-2) specific genes (Fig 12 G). MiR-27a expression was also observed to be upregulated in laser capture microdissected microglia from traumatic brain injury (TBI) model. This analysis revealed that miR-27a is upregulated in activated microglia both *in vitro* and *in vivo* (Fig 12 H).

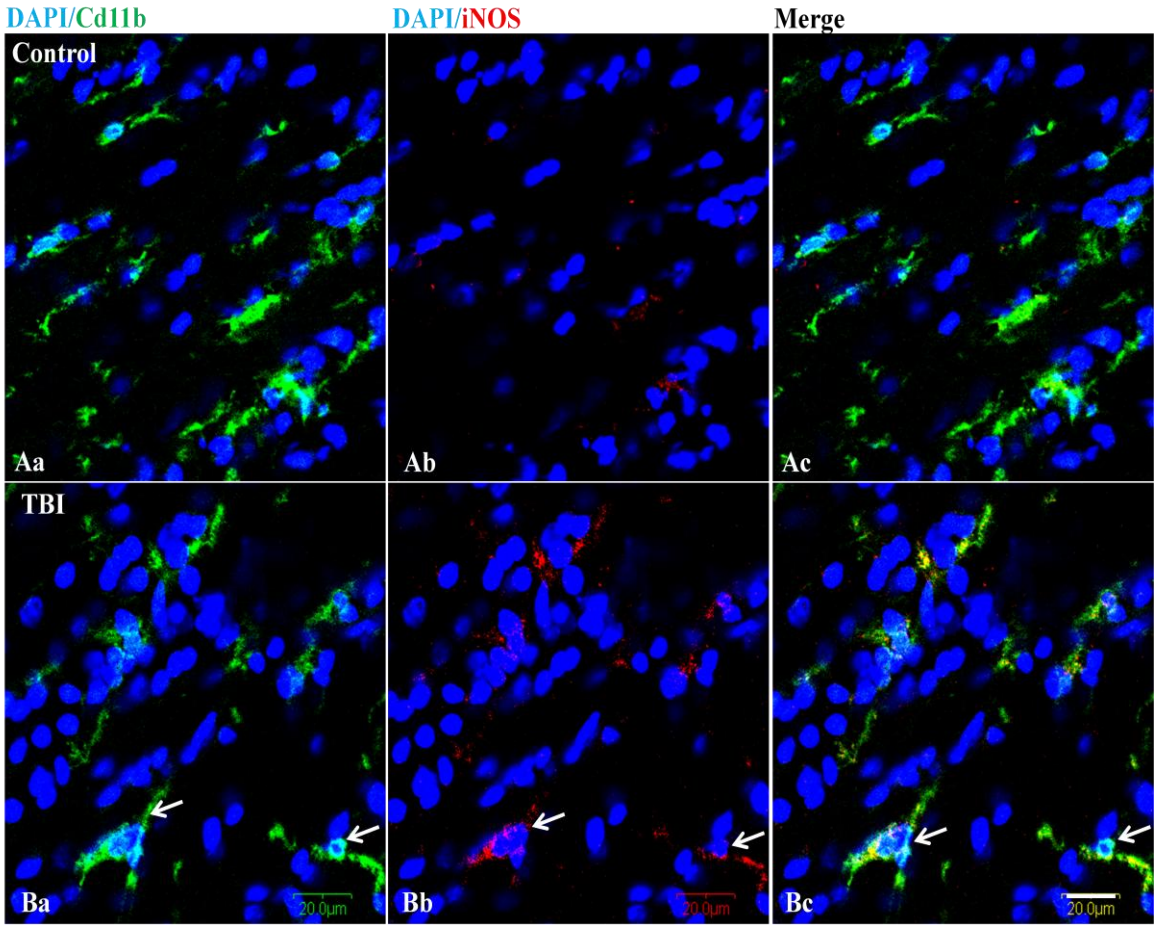

Fig 12 Aa-Bc: Confocal images showing iNOS expression (red) in microglia (green) in the hippocampus of 2-month old sham operated (Aa-Ac) and TBI (Ba-Bc) rat brain by immunofluorescense. Note the expression of iNOS (Bb-Bc, arrows) in microglia after TBI. The nucleus is counterstained with DAPI (blue). Scale bar: 20 μm.

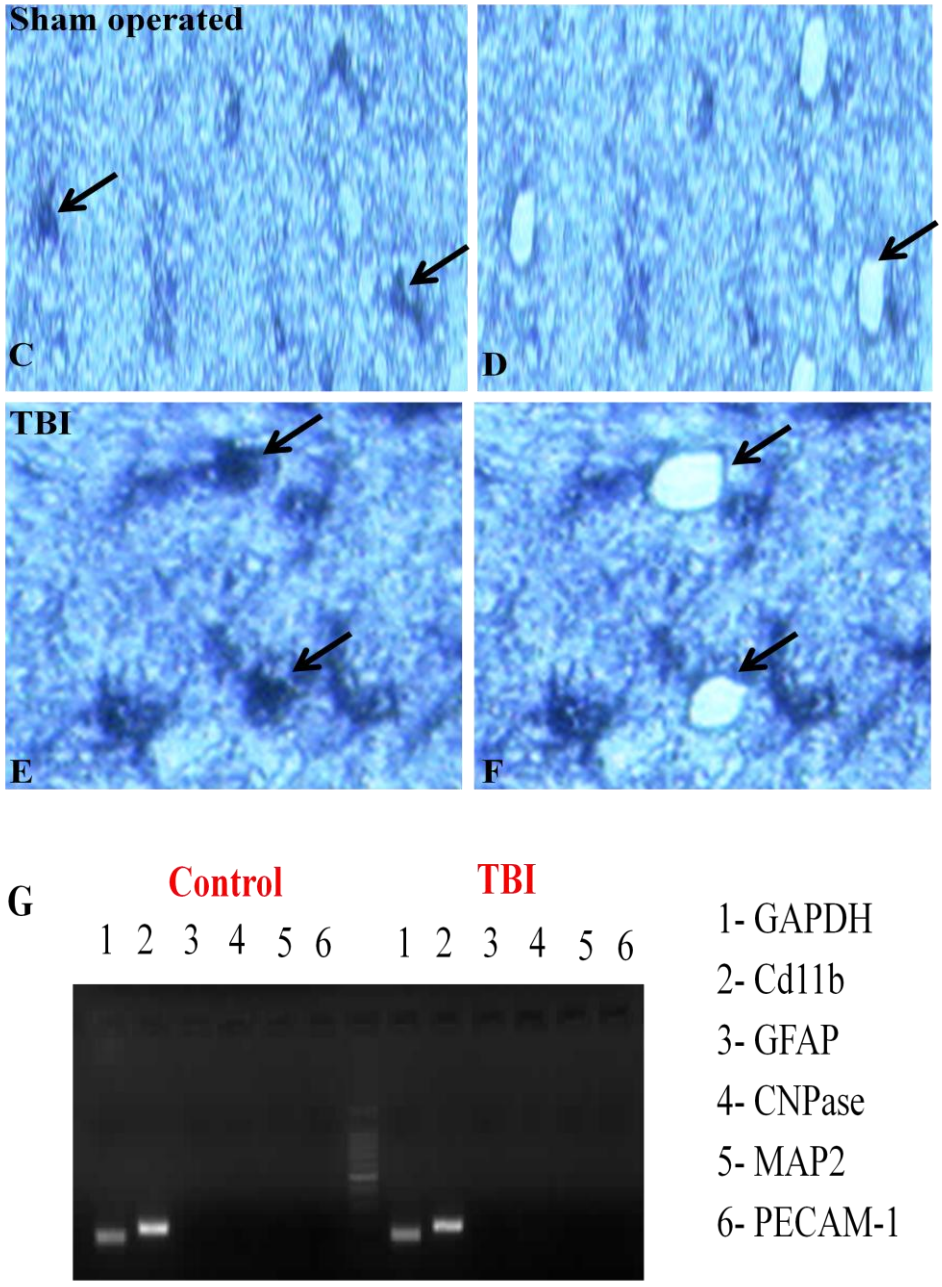

Fig 12 C-F: Light microscopy images showing microglia stained with lectin in the hippocampus of sham operated (C-D) and TBI (E-F) rat brain respectively. Figure C, E show microglia before laser capture microdissection. Figures D and F which are the same sctions shown in Fig C and E respectively, show the stained cells that have been laser cut by laser capture microdissection. Scale bars C-F: 50 µm

G: Agarose gel image showing the semi-quantitative PCR of oligodendrocyte (CNPase), astrocyte (GFAP), neuronal (MAP2) and endothelial cell-specific genes (PECAM-2) in cDNA from LCM extracted rat microglial cells.

H

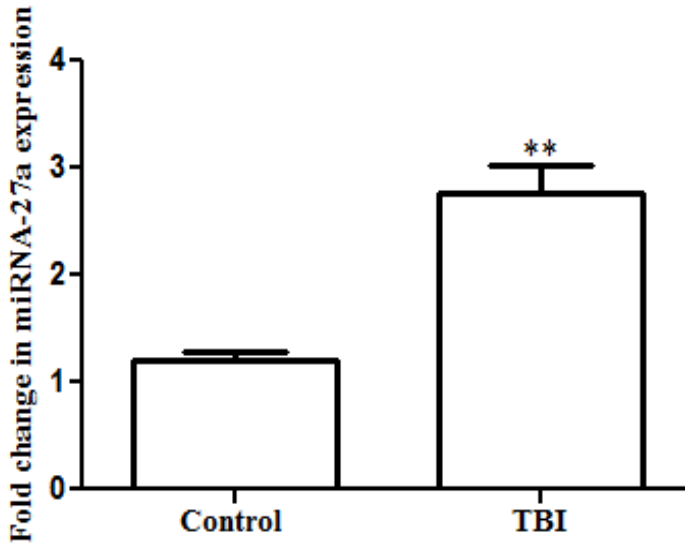

Fig 12 H: qRT-PCR analysis revealing increase in miR-27a expression in LCM extracted activated microglia from TBI model. Results are represented as miRNA fold change with respect to sham-operated control. Statistical analysis was carried out using Student's t-test. Data represent the mean ± SD (n=3) ** $p<0.01$

4.2.3 TGFβ is upregulated in activated microglia *in vivo*

TGFβ expression was observed in microglia in the corpus callosum of 5-day old rat pup by immunoflourescence (Fig 13 A-C). An increase in TGFβ expression was observed upon activation of microglia by LPS *in vivo* (Fig 13 D-E).

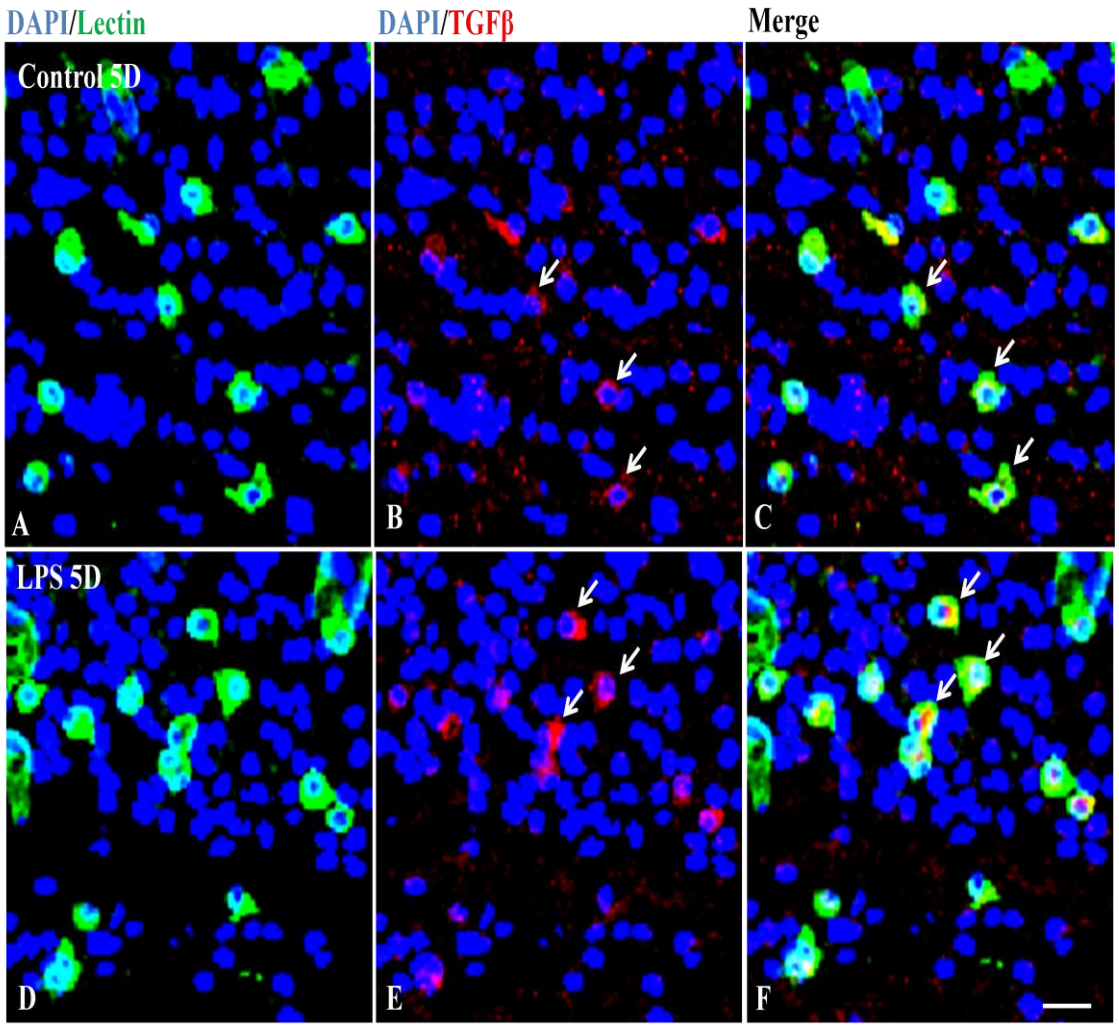

Fig 13 A-F: Confocal images showing TGFβ expression (red) in lectin stained microglia (green) in the corpus callosum of 5-day old control (A-C) and LPS injected (D-F) rat brain by immunofluorescense. Note the increase in TGFβ expression in activated microglia (E-F, arrows). The nucleus is counterstained with DAPI (blue) Scale bar: 20 μm.

4.2.4 Inverse relationship between miR-27a and its targets SMAD2 and TβR1 in activated microglia

IPA predicted miR-27a to target SMAD2 and TβR1. This analysis was confirmed using the bioinformatic tool miRWALK (Fig 14 A, B). qRT-PCR analysis revealed a time-dependent upregulation of miR-27a expression in

activated primary and BV2 microglia exposed to LPS for 1 to 6h. Conversely down-regulation of SMAD2 and TβR1 mRNA expression was observed in primary and BV2 microglia exposed to LPS (1µg/ml) for 1 to 6h, indicating an inverse relationship between miR-27a and its target expression in activated microglia (Fig 14 C-D).

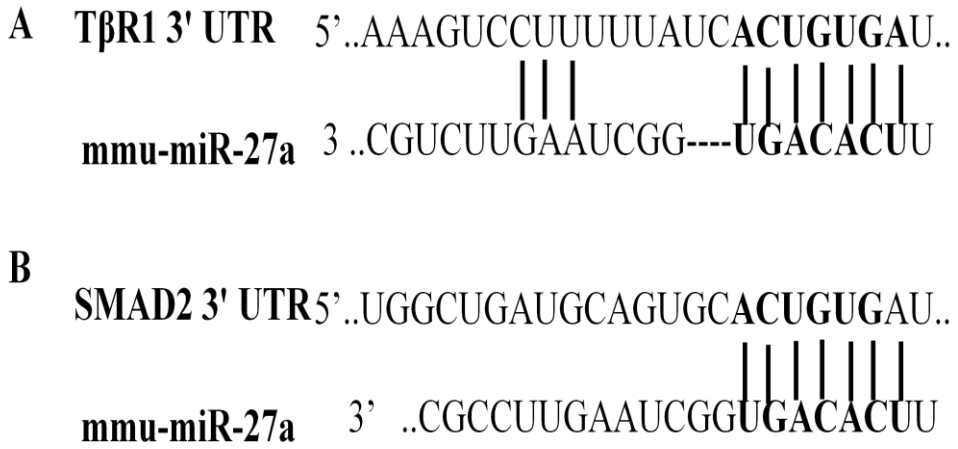

Fig 14 A-B: Alignment of TβR1 3'UTR (A), SMAD2 3'UTR (B) with seed region of miR-27a obtained from Targetscan website.

C

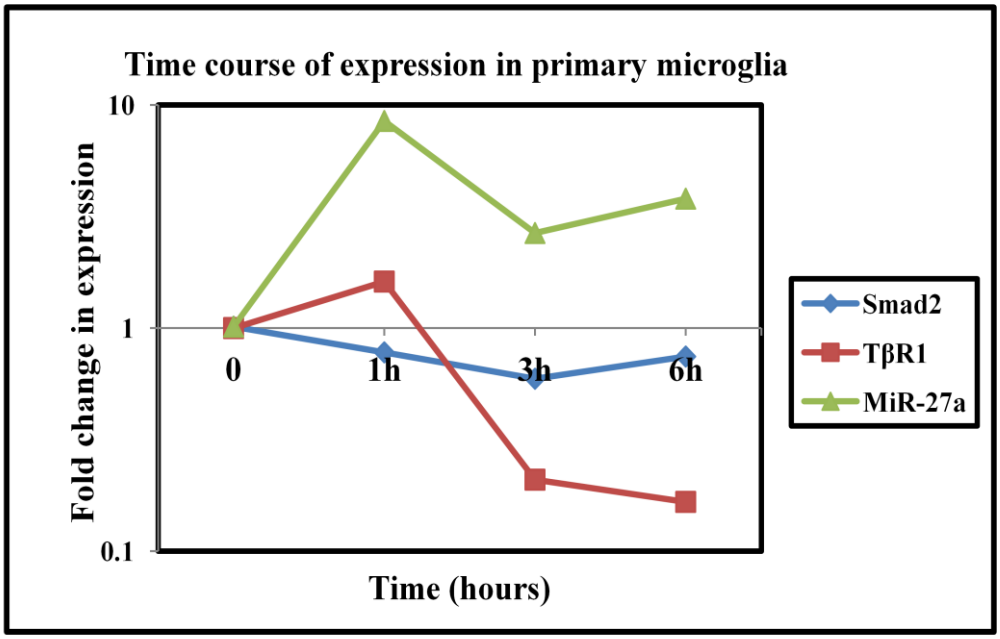

D

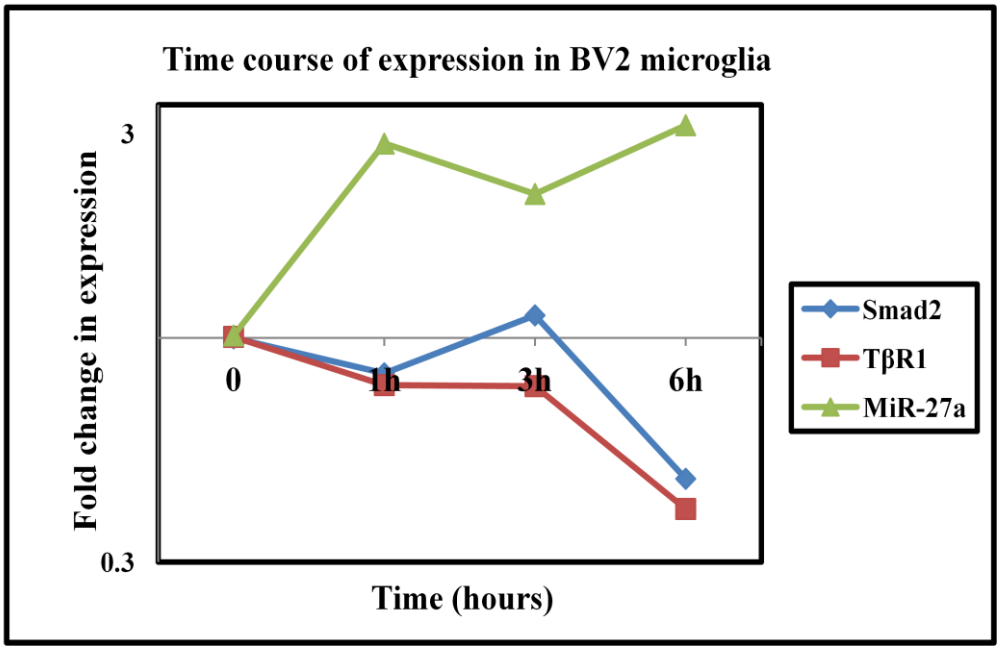

Fig 14 C-D: miR-27a, SMAD2 and TβR1 expression was quantified using qPCR in primary microglia (C) and BV2 microglia (D) after 1-6h of LPS activation revealing increase in miR-27a expression and decrease in SMAD2 and TβR1 expression.

4.2.5 SMAD2 expression is downregulated in activated microglia *in vitro*

It has been shown that in response to stimulus, SMAD2 is phosphorylated at its carboxy terminus on residue Ser465/467 by TGFβ receptor R1, leading to its activation and nuclear transport (Massagué 2000; Khalil *et al.* 2001; Massagué *et al.* 2005). Immunocytochemical analysis showed the expression of total and phospho-SMAD2 in BV2 microglia. The expression of phospho-SMAD2 was observed only on activation of BV2 microglia with TGFβ1 cytokine indicating that SMAD2 is activated only in response to TGFβ signaling in microglia (Fig 15 A-D). A cytoplasmic localisation of total SMAD2 was observed in untreated control microglia. Treatment of microglia with human recombinant TGFβ1 led to an increase in the expression of nuclear SMAD2. Moreover, inhibition of TGFβ signaling by pretreatment of cells using the TβR1 receptor inhibitor, SB 431542 led to a decrease in SMAD2 expression (Fig 15 E-H).

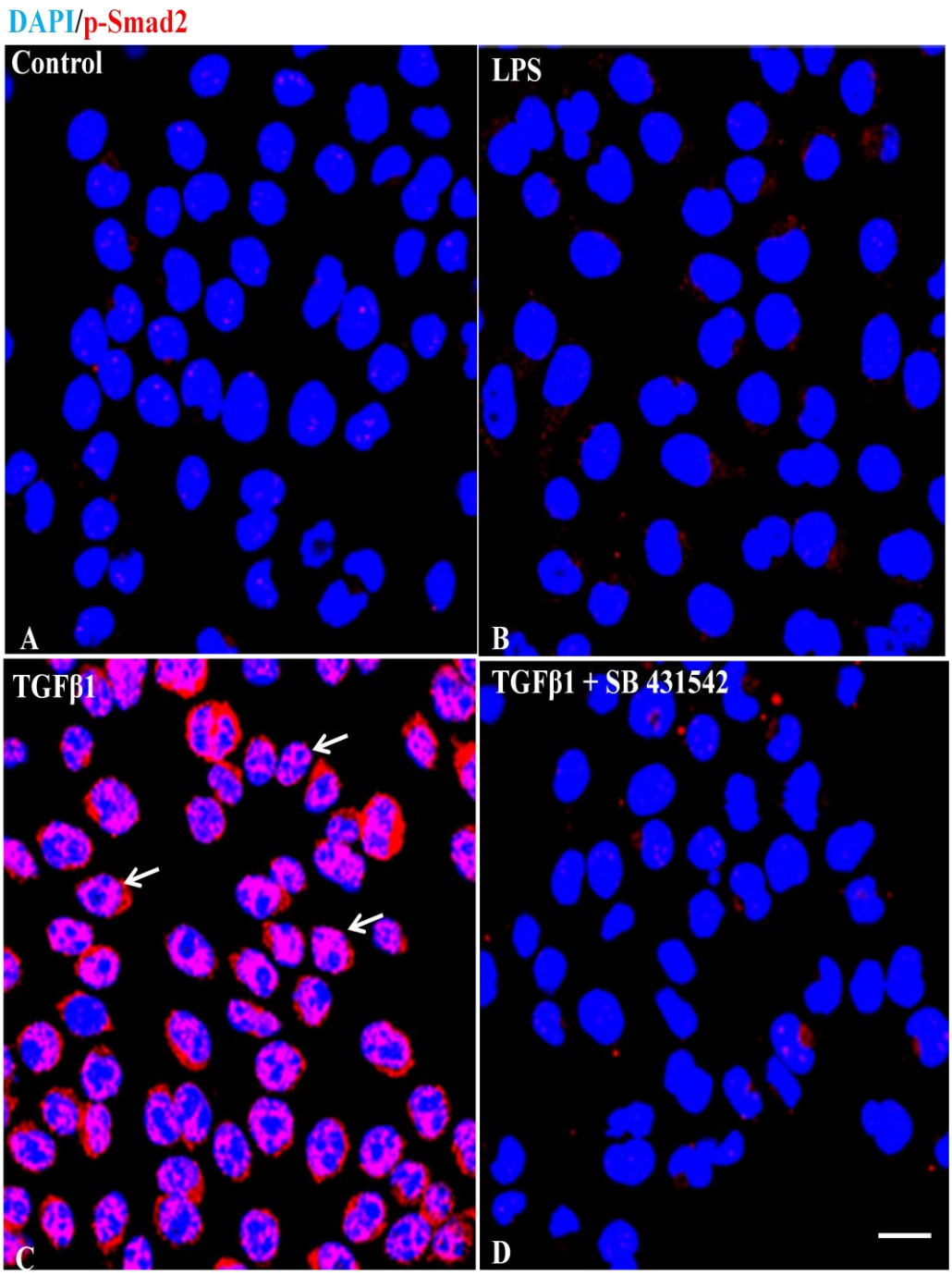

Fig 15 A-D: Immunocytochemistry showing the expression of p-SMAD2 (red) (A-D) after TGFβ1 treatment of BV2 microglia. p-SMAD2 expression is absent in control (A), LPS activated (B) or SB 431542 treated (D) BV2 microglia. Note the expression of phospho-SMAD2 only after TGFβ1 treatment of BV2 microglia (C). The nucleus is counterstained with DAPI (blue) Scale bar: 20 μm.

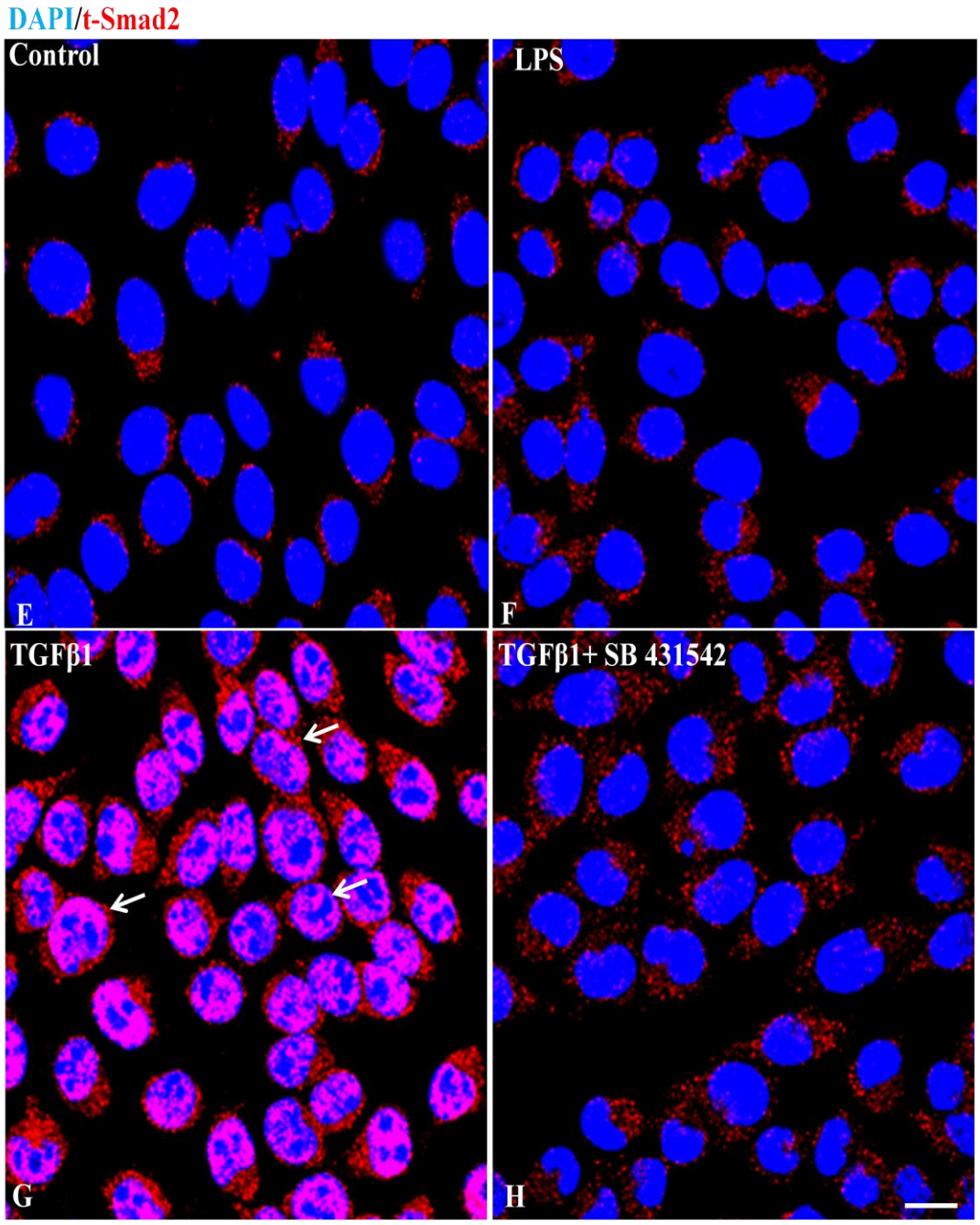

Fig 15 E-H: Immunocytochemical analysis showing total SMAD2 expression in red (E-H). Nuclear expression of total-SMAD2 is observed after TGFβ1 treatment of BV2 microglia (red, G) whereas cytoplasmic expression of total-SMAD2 is observed in control (E), LPS-treated (F) and SB 431542 (H) treated BV2 microglia. The nucleus is counterstained with DAPI (blue) Scale bar: 20 μm.

qRTPCR analysis of SMAD2 in primary microglia revealed its mRNA expression decreasing on LPS activation of microglia. SMAD2 mRNA expression was observed to be increased in primary microglia following TGFβ1 treatment, while the expression was decreased in cells pretreated with SB 431542, TβR1 receptor inhibitor (Fig 16 A). Similarly, western blot analysis in primary microglia indicated an upregulation of SMAD2 protein expression after TGFβ1 treatment and down regulation of SMAD 2 after treatment of SB 431542 (Fig 16 B-C).

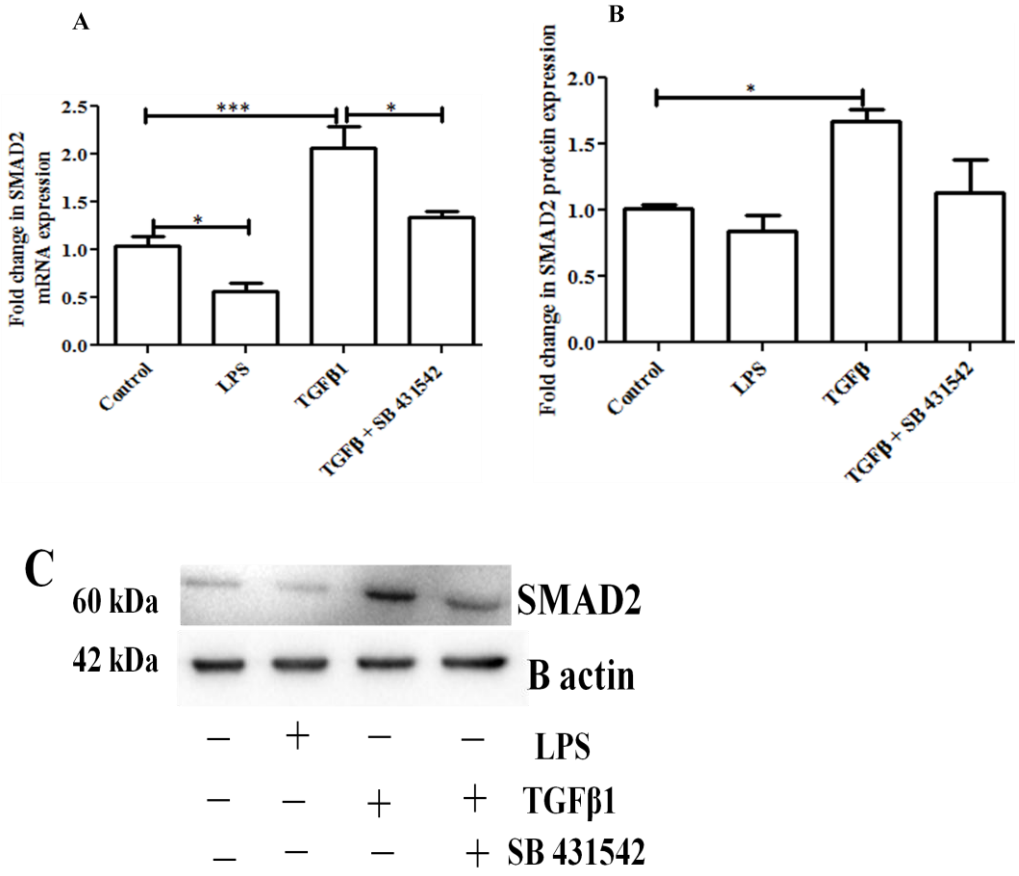

Fig 16 A: qPCR analysis reveals increase in mRNA expression of SMAD2 in primary microglia after treatment of TGFβ1 and SB 431542. Results are represented as mRNA fold change with respect to control. Statistical analysis was carried out using ANOVA with post-hoc Tukey test. Data represent the mean ± SD (n=6) ***p<0.001, **p<0.01, *p<0.05.

B-C: Quantification of protein expression of SMAD2 after western blot reveals an upregulation in expression after TGFβ1 treatment of primary microglia. Statistical analysis was carried out using ANOVA with post-hoc Tukey test. Data represent the mean ± SD (n=4) *p<0.05.

4.2.6 Nuclear translocation of SMAD2 observed in activated microglia *in vivo*

SMAD2 expression was observed in microglia in the corpus callosum of 5D old rat pup by immunoflourescence (Fig 17 A-C). The SMAD2 expression appeared to translocate to the nucleus upon LPS activation of microglia *in vivo* (Fig 17 D-E).

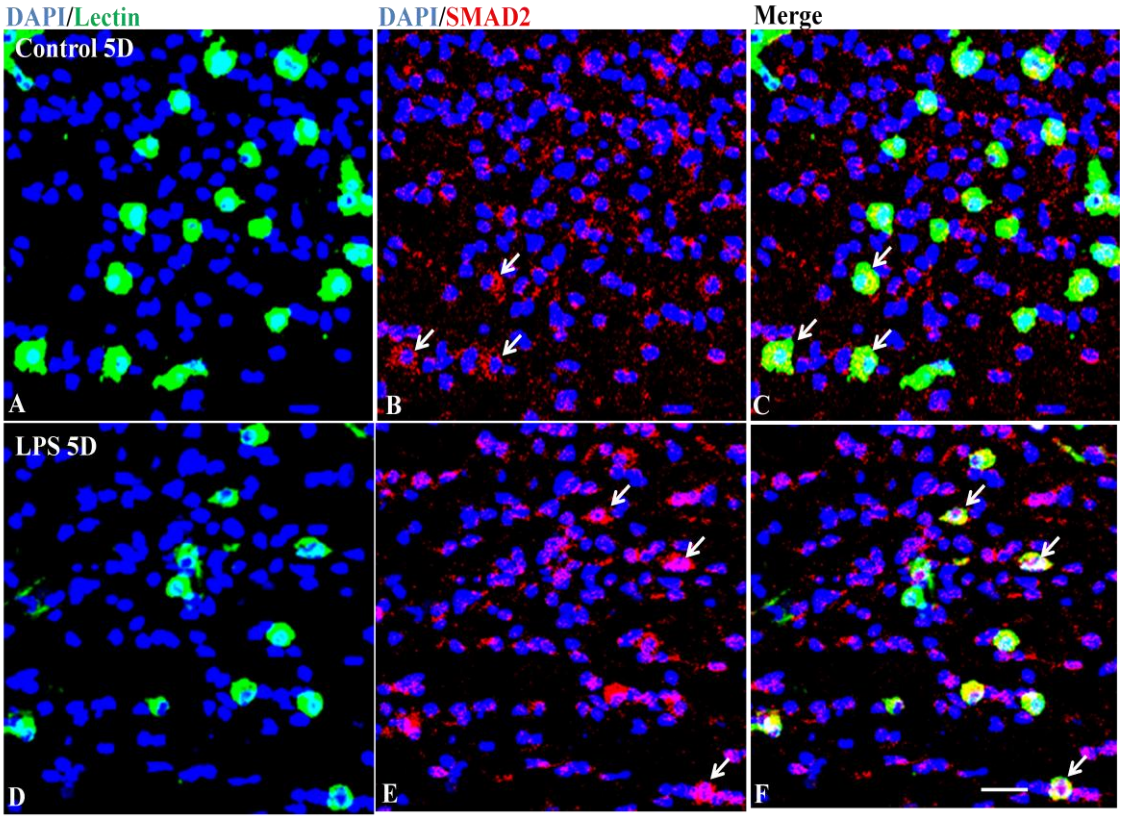

Fig 17 A-F: Confocal images showing the expression of total SMAD2 (red) in microglia (green) distributed in the corpus callosum of 5D pup control (A-C), and LPS injected (D-F) by immunofluorescense. Note the nuclear translocation of SMAD2 upon activation of microglia (E-F, arrows). The nucleus is counterstained with DAPI (blue) Scale bar: 40 µm.

4.2.7 TβR1 expression is downregulated in activated microglia *in vitro*

Confirming with previously published reports, a cytoplasmic expression of TβR1 was observed both in primary and BV2 microglia (Fig 18 A-P). Upon LPS activation, a decrease in TβR1 expression was observed in primary and BV2 microglia. However treatment of cells with TGFβ1 led to an increase in TβR1 expression which was reduced on pretreatment of the cells with the TβR1 inhibitor SB 431542. qRTPCR analysis revealed a significant decrease in TβR1 expression on primary microglia exposed to LPS. This expression peaked upon TGFβ1 treatment followed by a decline after pretreatment of the cells with SB 431542 (Fig 18 Q). Similarly western blot analysis revealed a decrease in TβR1 protein expression in LPS activated primary microglial cells while an upregulation was observed after TGFβ1 treatment of primary microglia followed by a significant decline in its expression upon pretreatment of the cells with SB431542 (Fig 18 R-S).

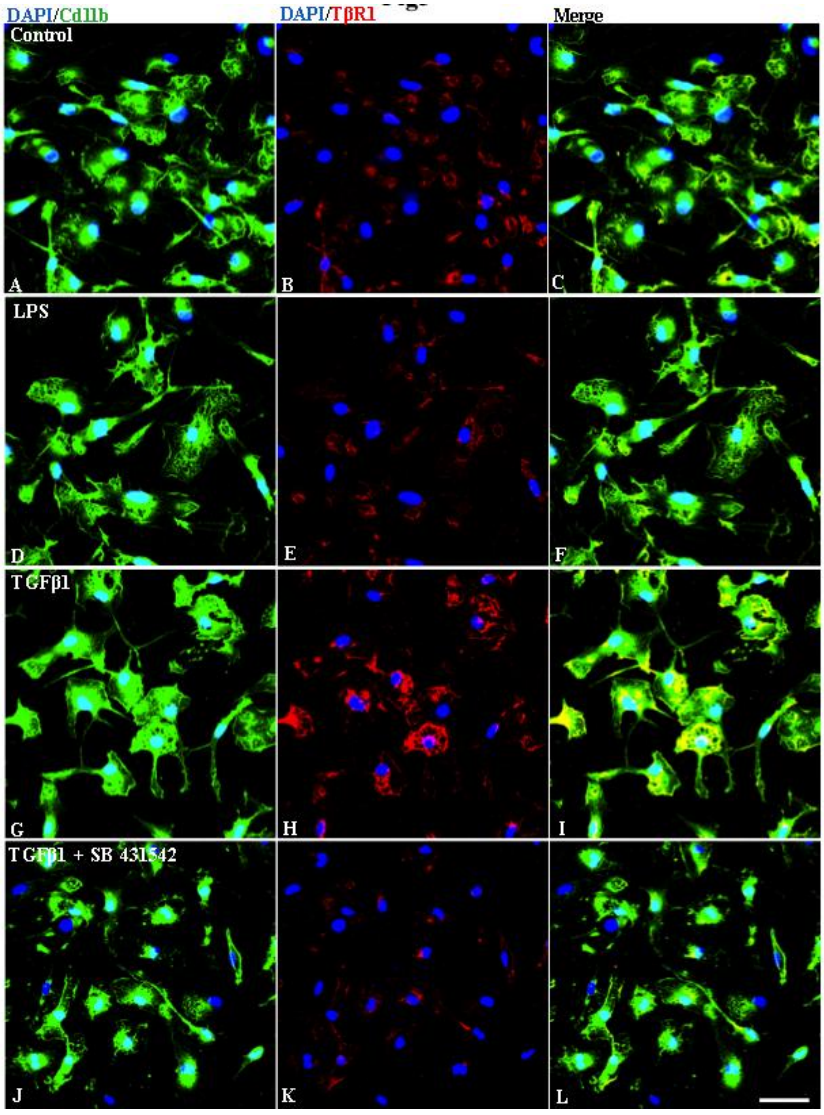
DAPI/Cd11b
DAPI/TβR1
Merge
Control
A
B
C
LPS
D
E
F
TGFβ1
G
H
I
TGFβ1 + SB 431542
J
K
L

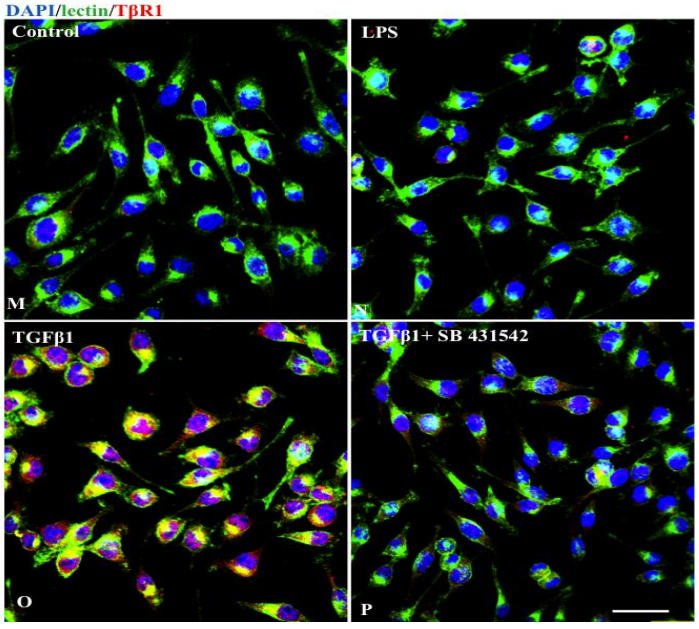
DAPI/lectin/TβR1
Control
M
LPS
N
TGFβ1
O
TGFβ1+ SB 431542
P

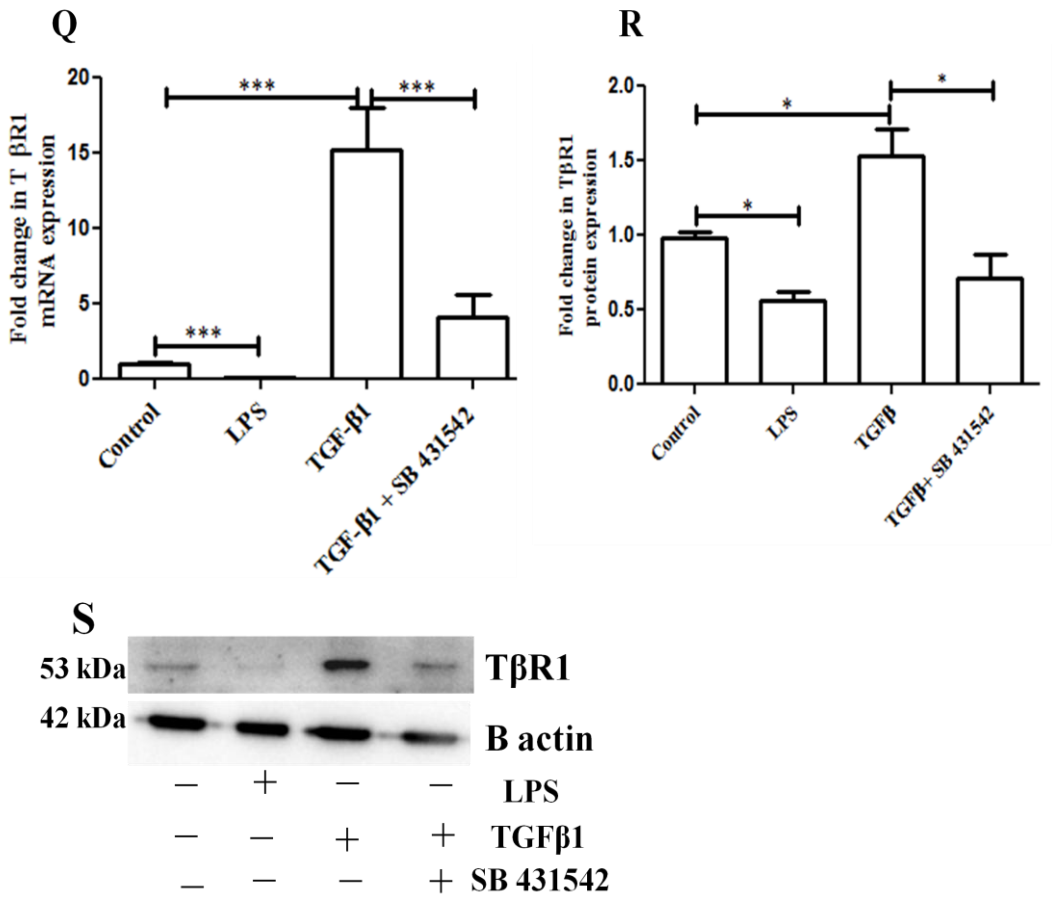

Fig 18 A-S: Confocal images showing TβR1 expression (red) in primary microglia (green) stained with Cd11b (A-L), and BV2 microglia marked with lectin (green) (M-P). The nucleus is counterstained with DAPI (blue) Scale bar: 40 μm.

Q qPCR analysis reveals increase in mRNA expression of TβR1 after TGFβ1 treatment of primary microglia. Statistical analysis was carried out using ANOVA with post-hoc Tukey test. Data represent the mean ± SD (n=4) ***p<0.001, **p<0.01, *p<0.05.

R-S. Quantification of protein expression of TβR1 after western blot reveals an upregulation of TβR1 expression after TGFβ1 treatment of primary microglia. Statistical analysis was carried out using ANOVA with post-hoc Tukey test. Data represent the mean ± SD (n=4) ***p<0.001, **p<0.01, *p<0.05.

4.2.8 TβR1 expression is unaltered in activated microglia *in vivo*

TβR1 expression was observed in microglia in the corpus callosum of 5-day old rat pup by immunoflourescence (Fig 19 A-C). However no change in TβR1 expression was observed on LPS activation of microglia *in vivo* (Fig 19 D-F).

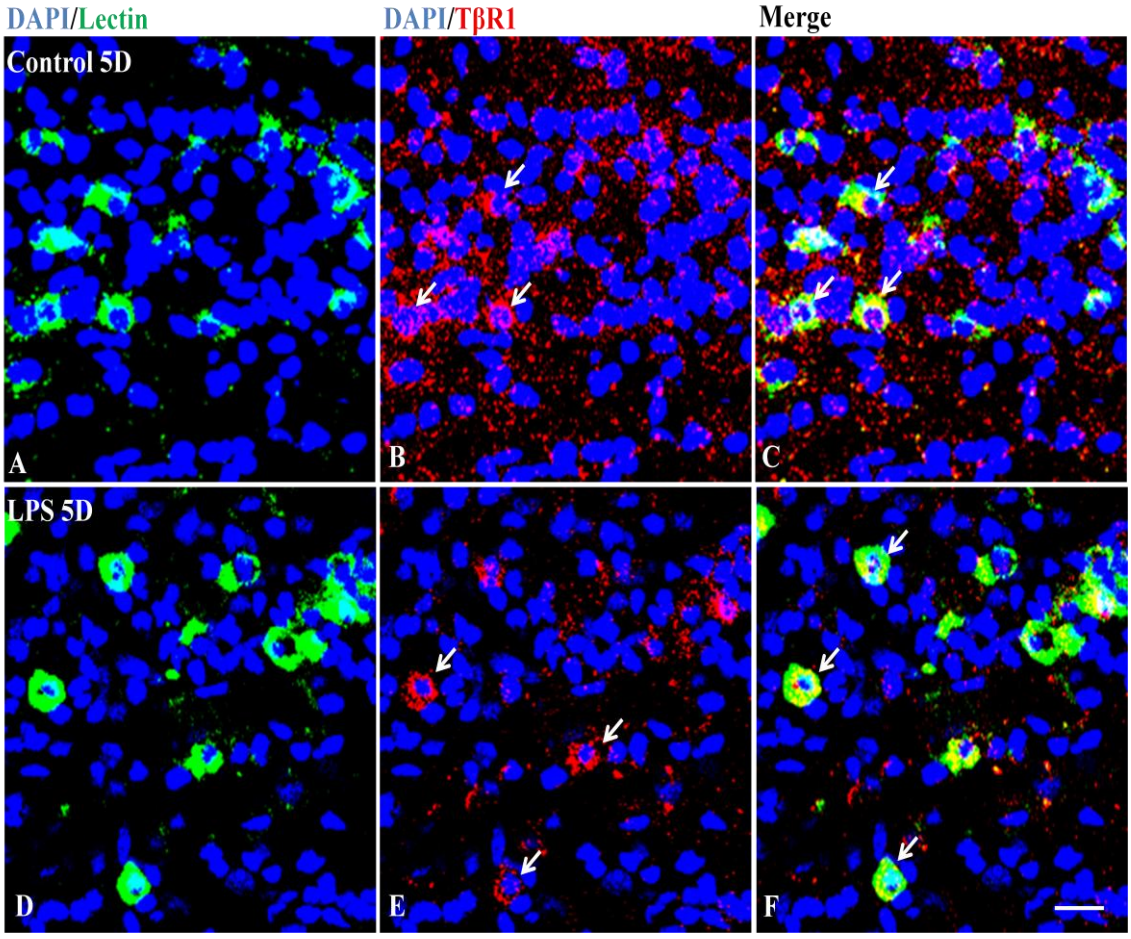

Fig 19 A-F: Confocal images showing the expression of TβR1 (red) in lectin stained microglia (green) from corpus callosum of 5-day old rat pup control (A-C) and LPS injected (D-F) brain. Significant change in TβR1 expression was not observed after LPS activation of microglia *in vivo*. The nucleus is counterstained with DAPI (blue) Scale bar: 20 μm.

4.2.9 MiR-27a targets SMAD2 and TβR1 in microglia

Functional analysis of miR-27a in microglia was carried out using miR-27a inhibitor and miR-27a mimic to mimic knockdown and overexpression of miR-27a in BV2 microglia, respectively. MTS cell viability assay revealed that there was no significant cell death 24h after transfection (Fig 20 A). Knockdown of miR-27a in BV2 microglia revealed an increase in SMAD2 and TβR1 mRNA and protein expression (Fig 20 B-F). On the other hand, overexpression of miR-27a led to a decrease in the protein expression of SMAD2 and TβR1 (Fig 20 B-F) indicating that these genes are targeted by miR-27a in BV2 microglia.

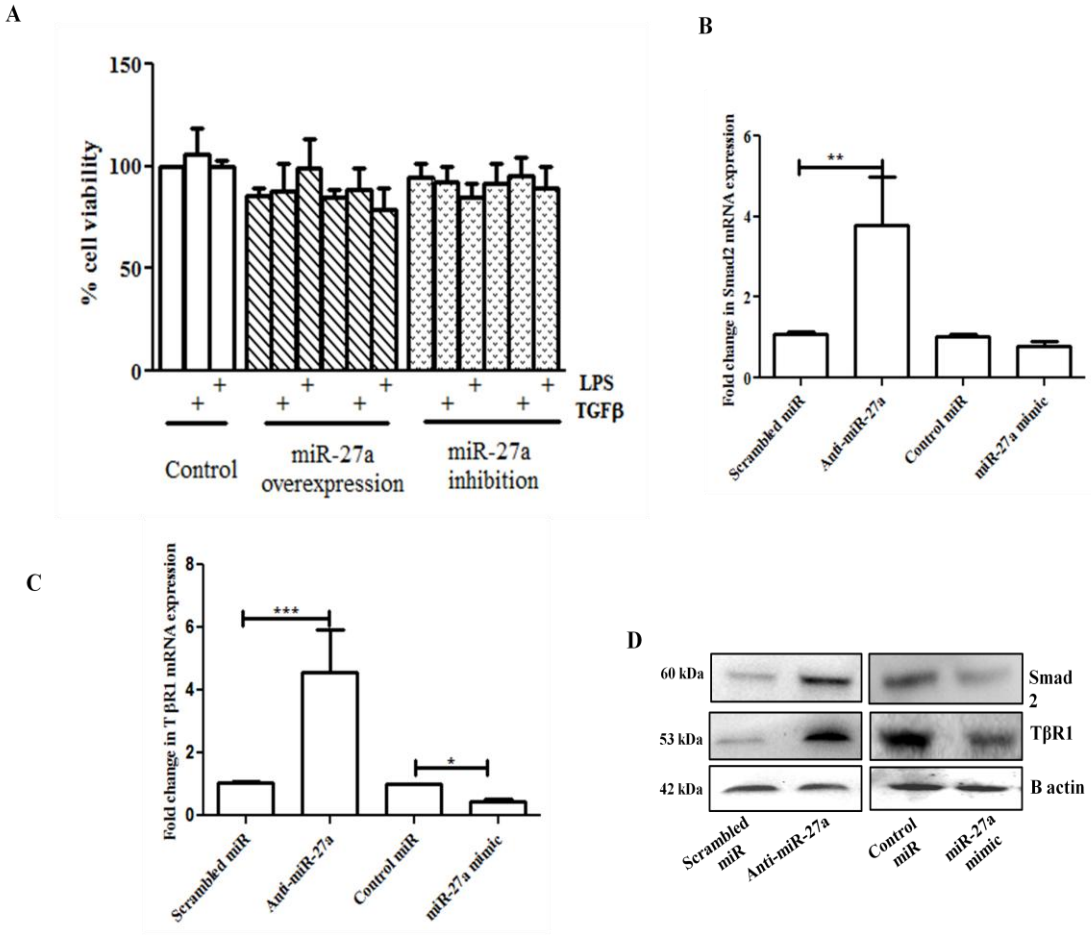

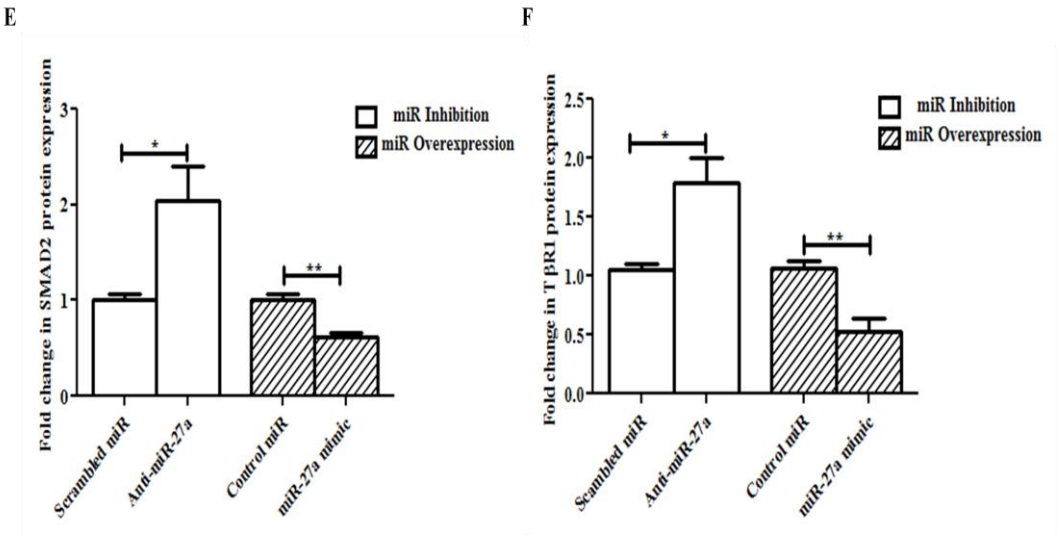

Fig 20 A: MTS assay following miR-27a transfection showed that there was no significant cell death. Statistical analysis was carried out using ANOVA. Data represent the mean ± SD (n=5).

B: SMAD2 mRNA expression was quantified following knockdown and overexpression of miR-27a. The results indicate an increase in SMAD2 expression after miR-27a knockdown.

C: TβR1 mRNA expression was quantified following knockdown and overexpression of miR-27a. The results indicate an increase in TβR1expression after miR-27a knockdown.

D. Western blot analysis of SMAD2 and TβR1 protein expression after knockdown and overexpression of miR-27a.

E: Quantification of SMAD2 protein expression using densitometry analysis showing an increase in SMAD2 protein expression after knockdown and overexpression of miR-27a. Statistical analysis was carried out using ANOVA. Data represent the mean ± SD (n=4) ***p<0.001, **p<0.01, *p<0.05.

F: Quantification of TβR1 protein expression using densitometry analysis showing an increase in TβR1 protein expression after knockdown and overexpression of miR-27a. Statistical analysis was carried out using ANOVA. Data represent the mean ± SD (n=4) ***p<0.001, **p<0.01, *p<0.05.

4.2.10 SMAD2 activity is altered by miR-27a in BV2 microglia

The function of SMAD2 is dependent upon its phosphorylation and thereby activation in response to TGFβ signaling. Hence, SMAD2 activity was evaluated by checking its phosphorylation status after miR-27a knockdown and overexpression in TGFβ treated-BV2 microglia. Western blot analysis revealed an increase in phospho-SMAD2 expression after miR-27a knockdown in TGFβ treated-BV2 microglia (Fig 21 A, C). Conversely a decrease in phospho-SMAD2 expression was observed after miR-27a overexpression in TGFβ treated-BV2 microglia (Fig 21 B, C) indicating that SMAD2 expression as well as function is altered by miR-27a in microglia.

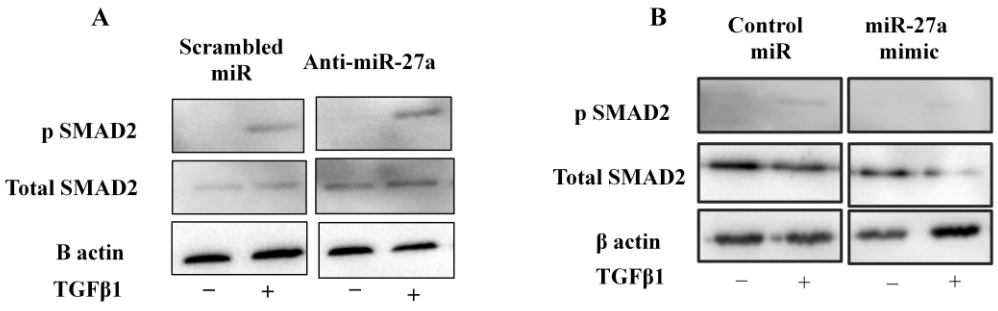

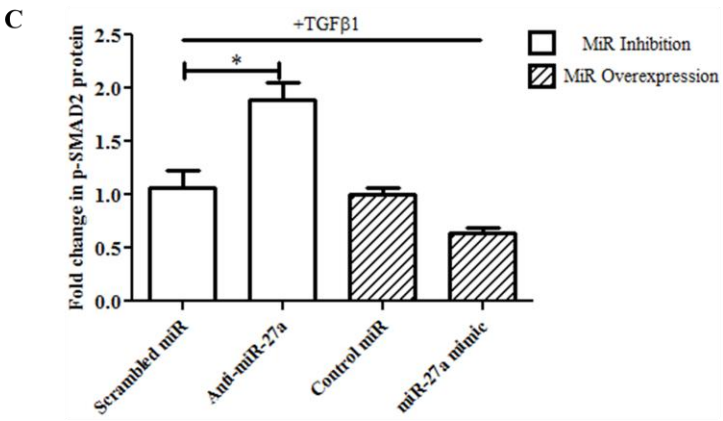

Fig 21 A-B: Western blot of phospho- and total SMAD2 after miR-27a knockdown (A) and overexpression (B) in TGFβ-treated BV2 microglia. Note the expression of phospho-SMAD2 only after TGFβ treatment in microglia.

C. Quantification of phospho-SMAD2 protein expression using densitometry analysis showing an increase in phospho-SMAD2 protein expression after knockdown of miR-27a in BV2 microglia. Statistical analysis was carried out using ANOVA. Data represent the mean $\pm$ SD (n=4),*p<0.05.

4.2.11 Runx1 is upregulated in activated microglia *in vitro* and *in vivo*

Runx1 was identified as the final target of miR-27a in the TGFβ signaling pathway. Immunocytochemical analysis revealed an increase in the protein expression of Runx1 in both TGFβ-treated as well as LPS-activated BV2 microglia. There was a decrease in Runx1 expression upon blockade of TGFβ signaling by SB 431542, indicating that Runx1 is a target of TGFβ pathway in BV2 microglia (Fig 22 A-D). Moreover, qPCR analysis in primary microglia confirmed these findings with an increase in Runx1 mRNA expression after activation of microglia with LPS as well as TGFβ. However, Runx1 expression was found to be decreased followed pre-treatment of BV2 microglia with SB 431542 (Fig 22 E). Further a time-dependent up-regulation of Runx1 expression was observed in primary microglia exposed to LPS (1µg/ml) for 1 to 6h. Maximal Runx1 expression was observed at 3h of LPS exposure in primary microglia (Fig 22 F). Runx1 expression was also observed to be upregulated in laser capture microdissected microglia from traumatic brain injury (TBI) model (Fig 22 G). This analysis revealed that Runx1 is upregulated in activated microglia both *in vitro* and *in vivo*.

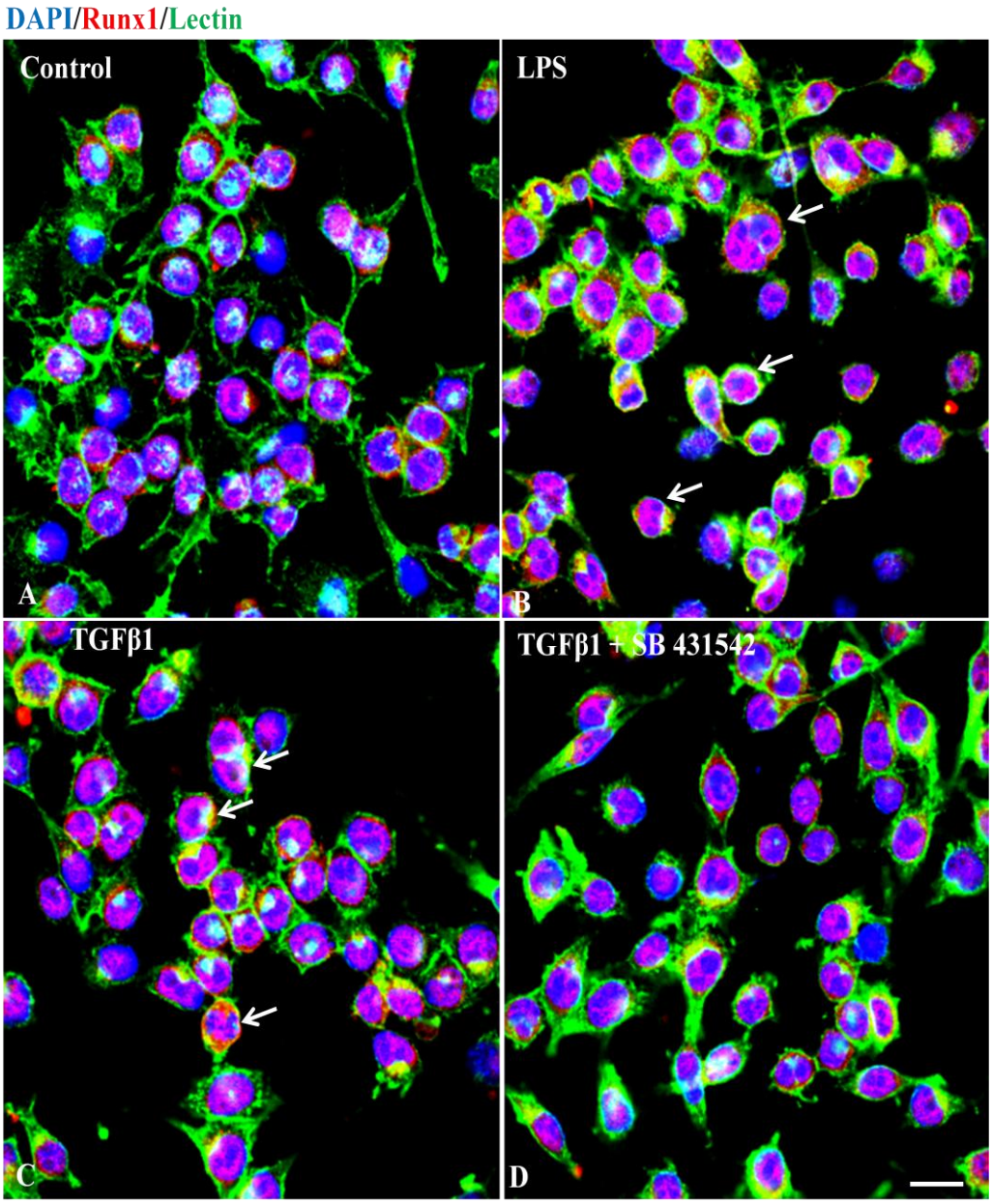

Fig 22: **A-D** Immunocytochemistry showing increase in Runx1 expression (red) in LPS and TGFβ1 activated BV2 microglia (B, C, red). The cells are marked with lectin (green) and nucleus is counterstained with DAPI (blue). Scale bar: 20 μm.

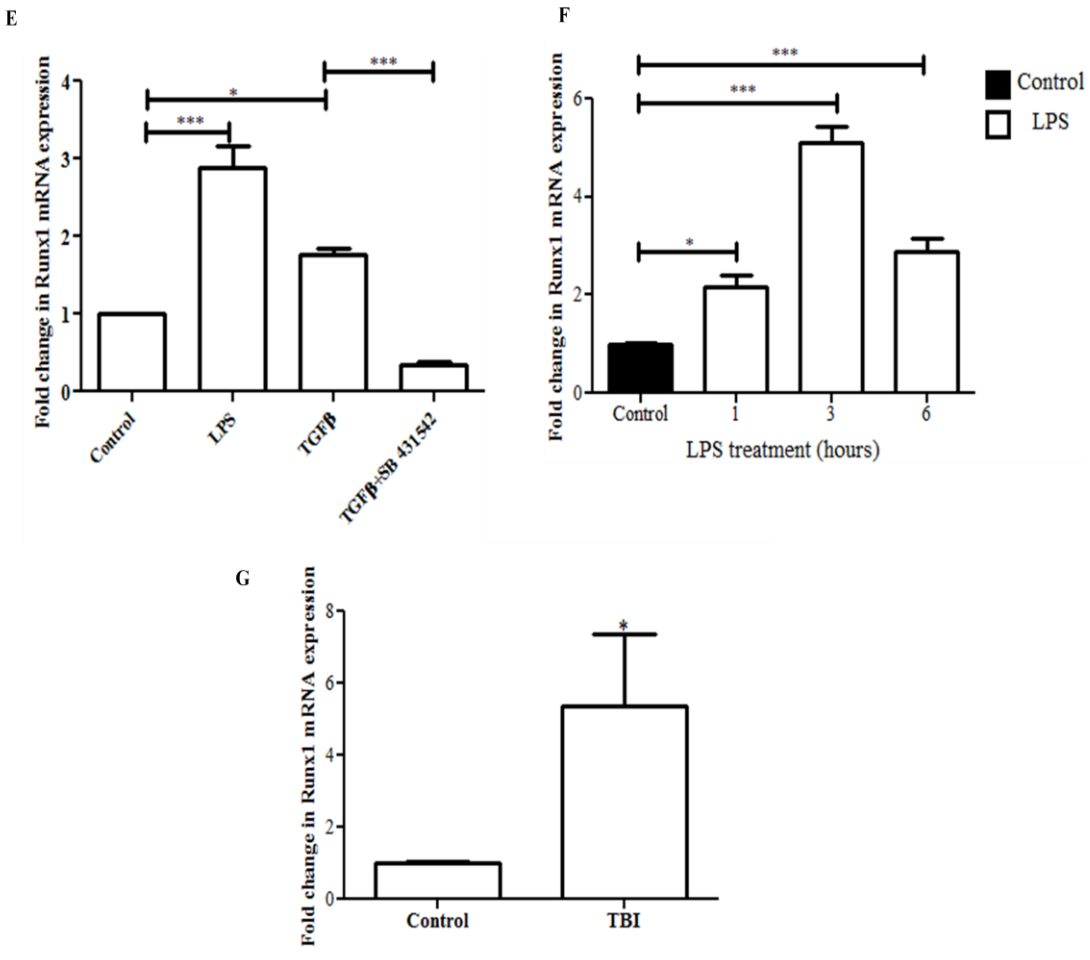

Fig 22 E. qPCR analysis of Runx1 expression showing an increase in LPS and TGFβ1 activated primary microglia and a decrease on SB 431542 pre-treatment of primary microglia. Statistical analysis was carried out using ANOVA. Data represent the mean ± SD (n=4), ***p<0.001, **p<0.01, *p<0.05.

F. qPCR analysis showing an increase in Runx1 mRNA expression in time course of LPS activated primary microglia from 1-6h. Statistical analysis was carried out using ANOVA. Data represent the mean ± SD (n=3), ***p<0.001, **p<0.01, *p<0.05

G. qPCR analysis of Runx1 in LCM-extracted microglia from TBI model. Statistical analysis was carried out using ANOVA. Data represent the mean ± SD (n=3), *p<0.05.

4.2.12 **MiR-27a targets Runx1 in microglia**

Targetscan website shows Runx1 harbouring two conserved miR-27a binding sites in its 3'UTR (Fig 23 A). MiR-27a gain-of-function analysis in BV2 microglia revealed a downregulation of Runx1 mRNA and protein expression after miR-27a overexpression (Fig 23 B-D). Moreover, TGFβ treatment failed to produce a significant increase in Runx1 protein expression after miR-27a overexpression (Fig 23 C-D). Conversely, increase in Runx1 protein was observed on miR-27a knockdown in BV2 microglia (Fig 23 E-F).

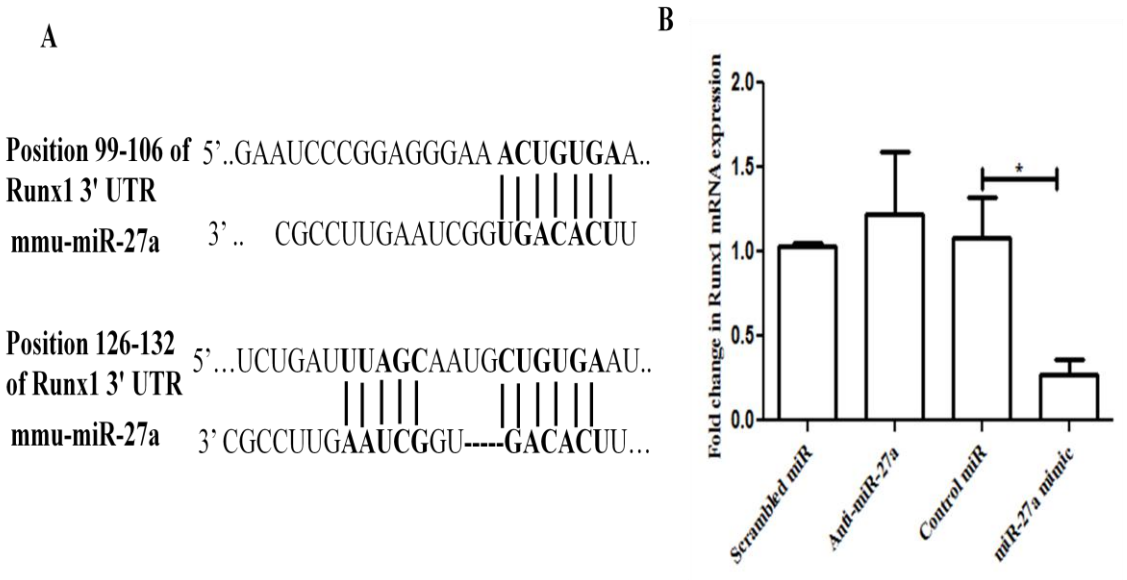

Fig 23 A: Alignment of Runx1 3'UTR with miR-27a seed region obtained from Targetscan website.

B. Runx1 mRNA expression was quantified following knockdown and overexpression of miR-27a using qPCR analysis. The results show a decrease in mRNA expression after miR-27a overexpression. Statistical analysis was carried out using ANOVA. Data represent the mean ± SD (n=4), *p<0.05.

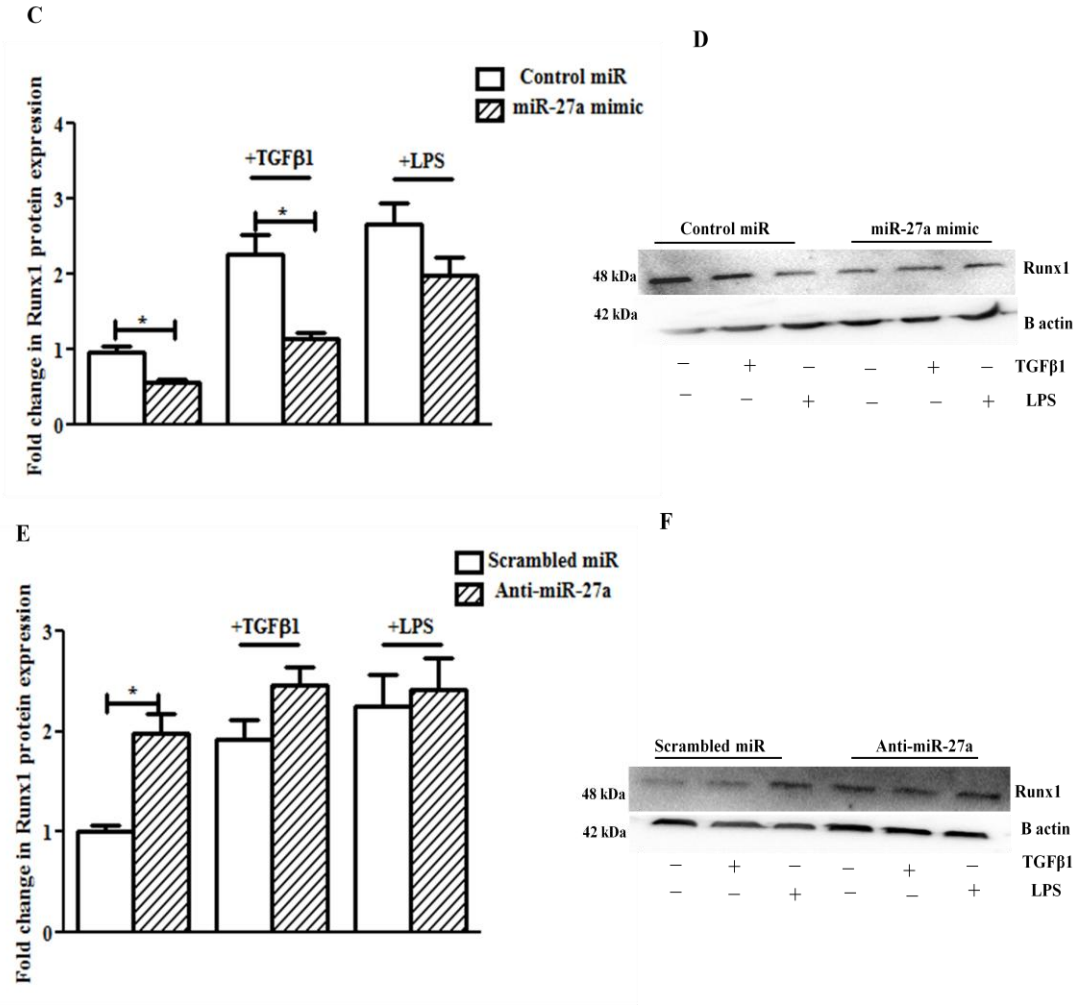

Fig 23 C-D. Densitometry analysis and western blot of Runx1 protein expression after miR-27a overexpression showing a decrease in Runx1 protein expression after miR-27a overexpression in untreated and TGFβ1 treated BV2 microglia. Statistical analysis was carried out using ANOVA. Data represent the mean ± SD (n=3), *p<0.05.

E-F. Densitometry analysis and western blot of Runx1 protein expression after knockdown of miR-27a showing an increase in Runx1 protein expression after miR-27a knockdown. Statistical analysis was carried out using ANOVA. Data represent the mean ± SD (n=3), *p<0.05.

4.2.13 Overexpression of miR-27a increases expression of proinflammatory markers/classical activation markers in activated microglia

MiR-27a was overexpressed in BV2 microglia to check the expression of the proinflammatory cytokines TNFα, IL6, IL-1β and the NO pathway enzyme iNOS. The expression of iNOS was significantly upregulated at the protein level after miR-27a overexpression as compared to control miR+LPS group as evaluated by immunocytochemistry (Fig 24 A-H). Activation of BV2 microglia with LPS led to a significant increase in the mRNA expression of TNFα, IL6, IL-1β and iNOS. The expression of these proinflammatory markers was further enhanced upon miR-27a overexpression followed by activation of BV2 microglia as compared to activated microglia transfected with control mimic (Fig 24 I-L). Further, the TNFα released in the medium by activated microglia was measured using ELISA showing an increase in TNFα release after miR-27a overexpression as compared to control miR (Fig 24 M, grey bars), whereas, a decrease in TNFα release was observed after miR-27a knockdown in BV2 microglia as compared to scrambled miR (Fig 24 N, grey bars).

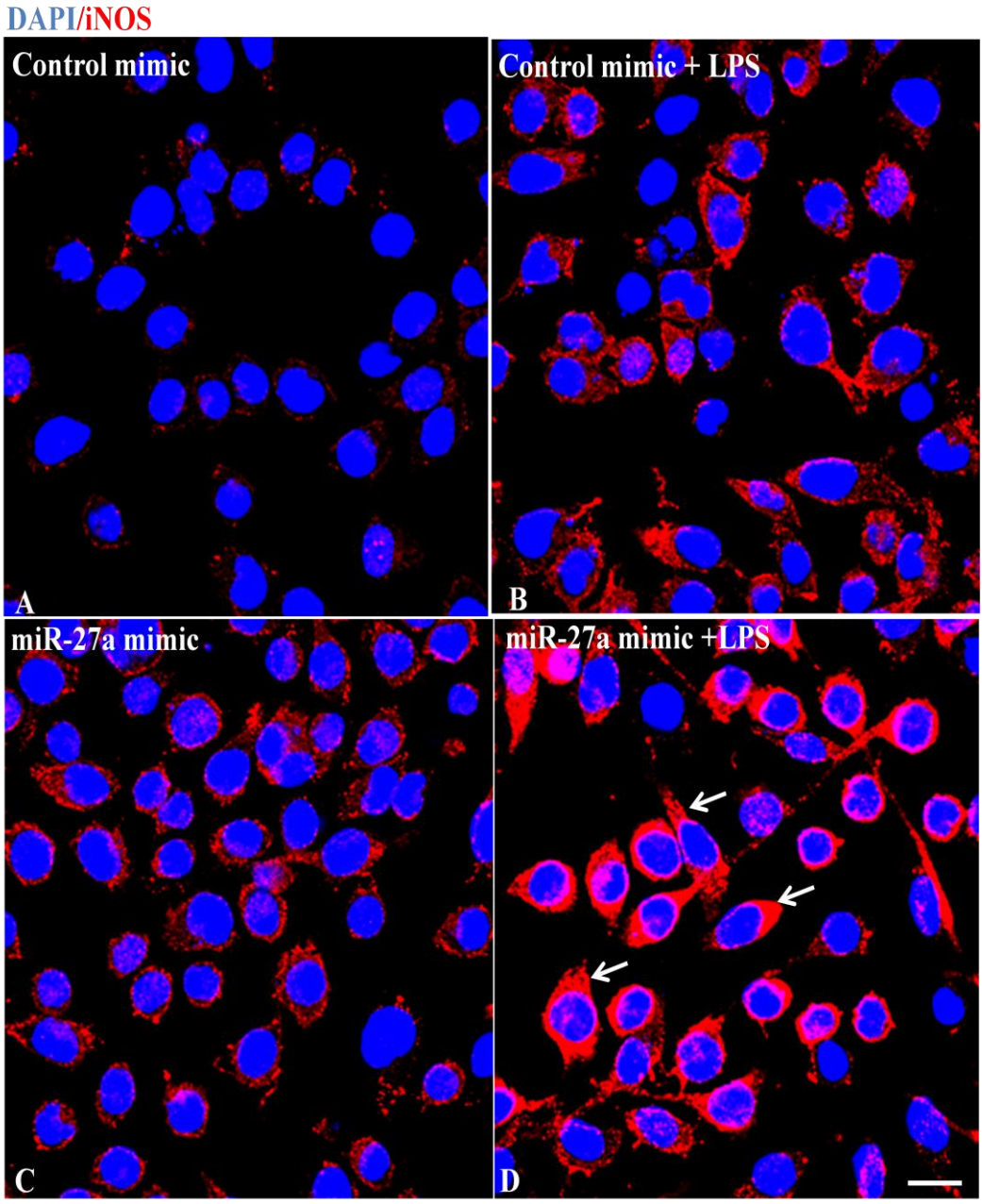

Fig 24 A-D: Confocal images showing the expression of iNOS (red) after miR-27a overexpression in BV2 microglia. The nucleus is stained with DAPI (blue) Scale bar: 20 µm Note the increase in iNOS expression in activated BV2 microglia after miR-27a overexpression (D) as compared to control mimic (B)

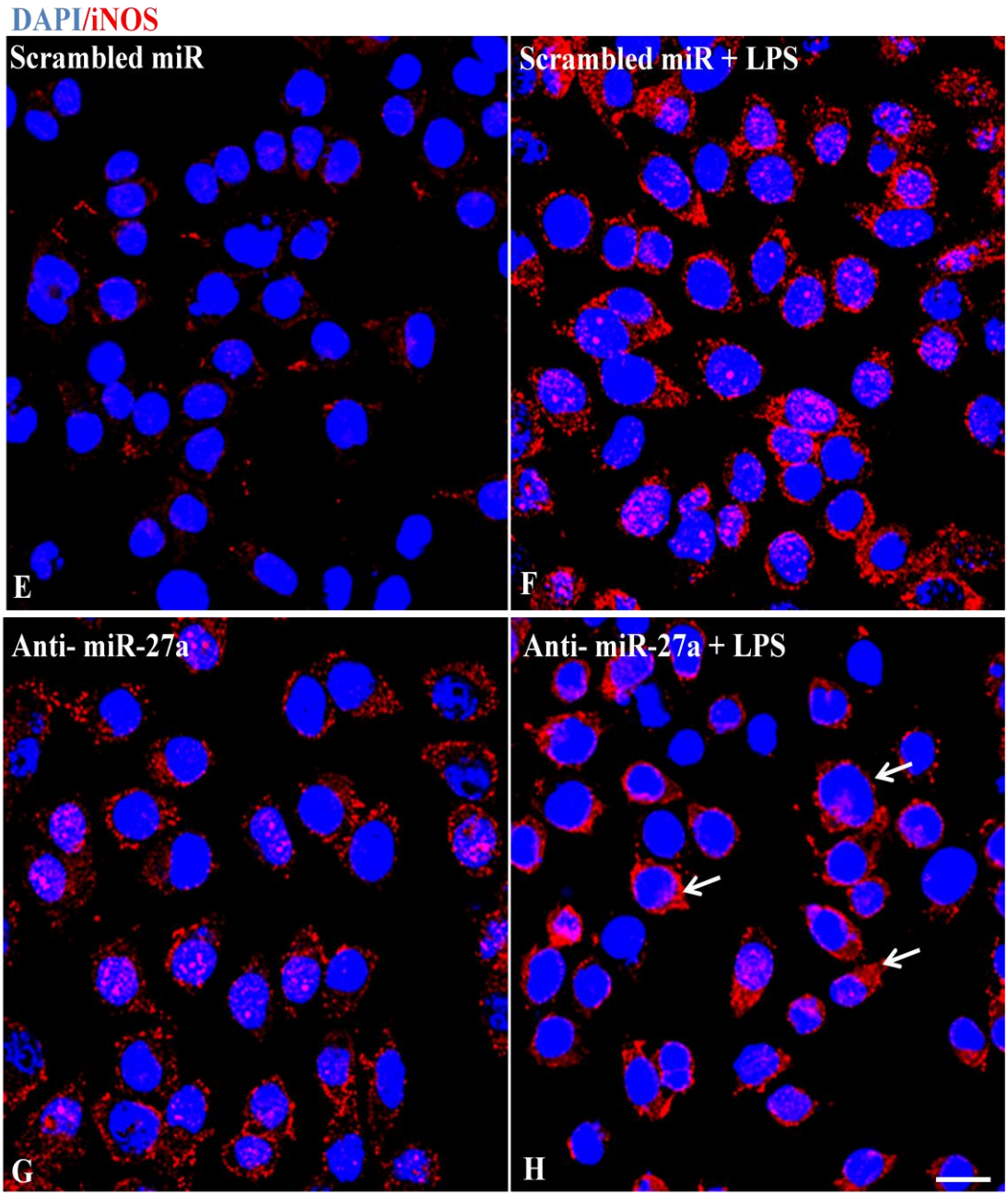

Fig 24 G-H: Confocal images showing the expression of iNOS (red) after miR-27a knockdown in BV2 microglia. The nucleus is stained with DAPI (blue) Scale bar: 20 µm Note the decrease in iNOS expression in activated BV2 microglia after miR-27a knockdown (H) as compared to scrambled control (F).

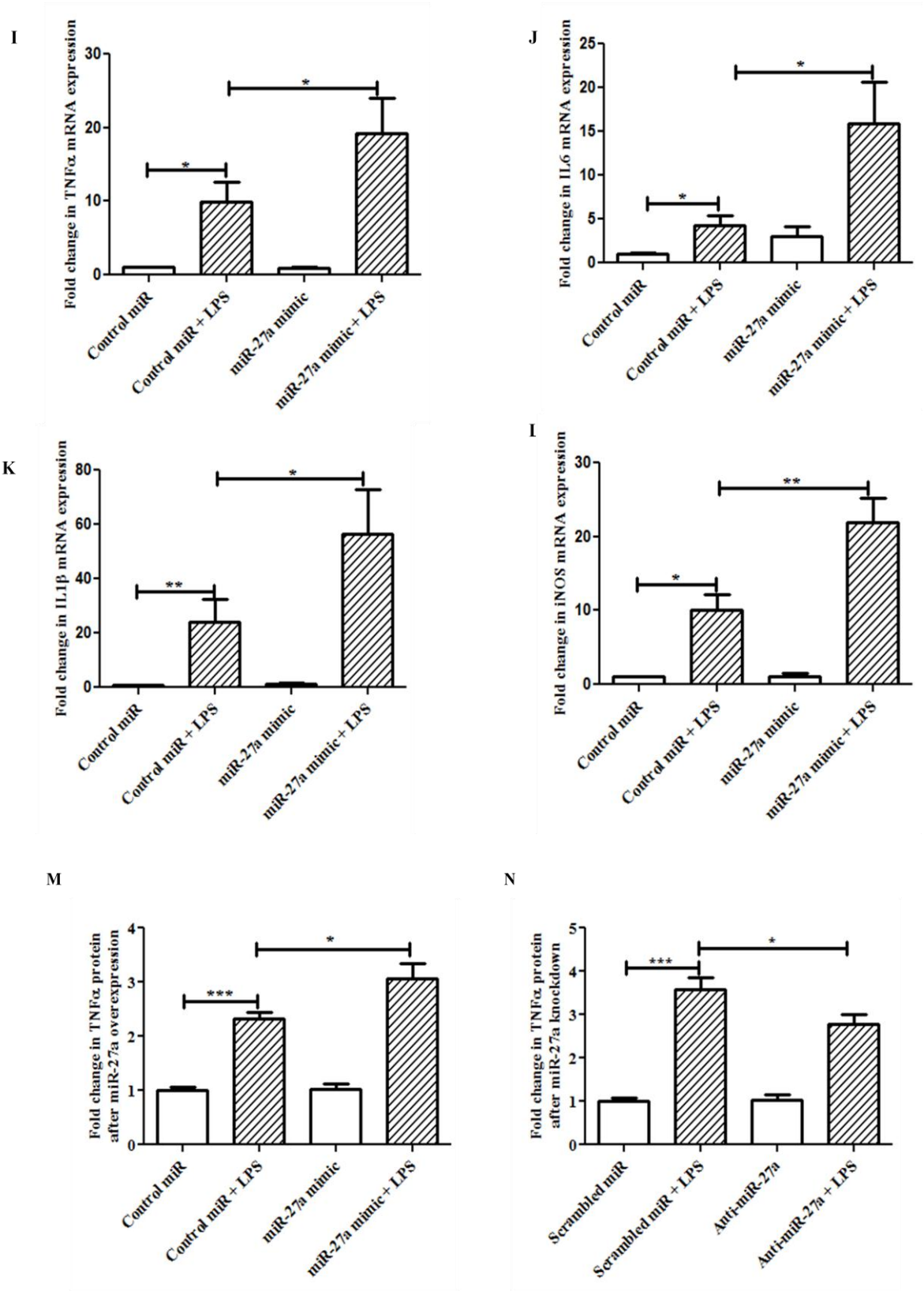

Fig 24 I-L: qPCR analysis showing an increase in TNFα (I), IL6 (J), IL-1β (K) and iNOS (L) expression in BV2 microglia after miR-27a overexpression.

Statistical analysis was carried out using ANOVA with post-hoc Tukey test. Data represent the mean ± SD (n=4), $**p<0.01$, $*p<0.05$.

M: ELISA to measure TNFα protein release in media shows an increase in TNFα release after miR-27a overexpression in activated BV2 microglia. Statistical analysis was carried out using ANOVA with post-hoc Tukey test. Data represent the mean ± SD (n=4), $***p<0.001$, $**p<0.01$, $*p<0.05$.

N: ELISA to measure TNFα protein release in media shows a decrease in TNFα release after miR-27a knockdown in activated BV2 microglia. Statistical analysis was carried out using ANOVA with post-hoc Tukey test. Data represent the mean ± SD (n=4), $***p<0.001$, $**p<0.01$, $*p<0.05$.

4.2.14 Inhibition of TGFβ signaling by miR-27a in microglia leads to suppression of anti-inflammatory/alternative activation markers

Evaluation of expression of alternative activation markers Arginase1 and YM1 revealed an increase in the expression of these genes after treatment of BV2 microglia with recombinant TGFβ1 (Fig 25 A-B). However overexpression of miR-27a followed by treatment of BV2 microglia with recombinant TGFβ1 led to a significant decrease in the expression of these genes as compared to control group treated with LPS. On the other hand, there was a further increase in the expression of Arg1 and YM1 after knockdown of miR-27a and treatment of BV2 microglia with TGFβ1 as compared to scrambled miR.

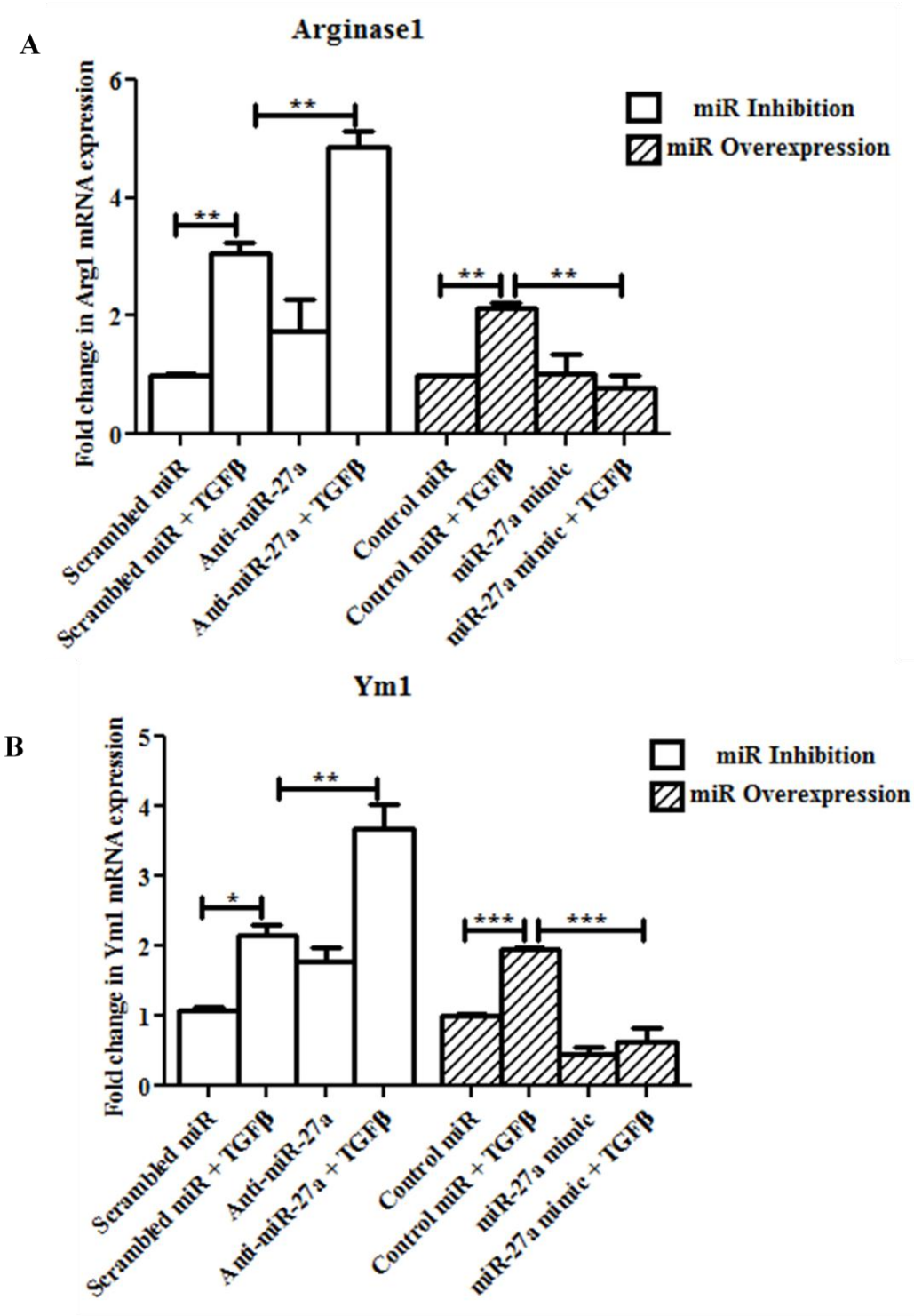

Fig 25 A: qPCR analysis showing an increase in arginase1 expression after miR-27a knockdown in TGFβ1 treated BV2 microglia (light bars) and decrease in arginase1 mRNA expression after miR-27a overexpression in TGFβ1 treated BV2 microglia (dark bars). Statistical analysis was carried out using ANOVA with post-hoc Tukey test. Data represent the mean $\pm$ SD (n=4), *** $p<0.001$, ** $p<0.01$, * $p<0.05$.

B: qPCR analysis showing an increase in YM1 expression after miR-27a knockdown in TGFβ1 treated BV2 microglia (light bars) and decrease in YM1 mRNA expression after miR-27a overexpression in TGFβ1 treated BV2 microglia (dark bars). Statistical analysis was carried out using ANOVA with post-hoc Tukey test. Data represent the mean ± SD (n=4), $**p<0.01$, $*p<0.05$.

4.2.15 MiR-27a knockdown blocks NFKB nuclear translocation in activated microglia

Activation of microglia in response to a stimulus results in the upregulation of the transcription factor, NFKB which is translocated to the nucleus to activate the transcription of several inflammatory genes (Brasier 2006; Gilmore 2006). Thus, NFKB nuclear translocation is an important aspect of inflammatory processes. Immunocytochemistry analysis revealed nuclear translocation of NFKB upon LPS activation of BV2 microglia (Fig 26 B, G). Moreover increased translocation of NFKB was observed on miR-27a overexpression in activated BV2 microglia (Fig 26 A-D). This observation was confirmed using ELISA which detected an increased amount of NFκB p65 subunit in the nuclear extract after miR-27a overexpression in activated BV2 microglia as compared to control miR + LPS group (Fig 26 E). Conversely NFKB nuclear translocation was inhibited on miR-27a knockdown in activated BV2 microglia (Fig 26 F-I). Also, a decrease in the NFκB p65 subunit was observed by ELISA in nuclear extract isolated after miR-27a knockdown in activated BV2 microglia as compared to scrambled miR + LPS group (Fig 26 J).

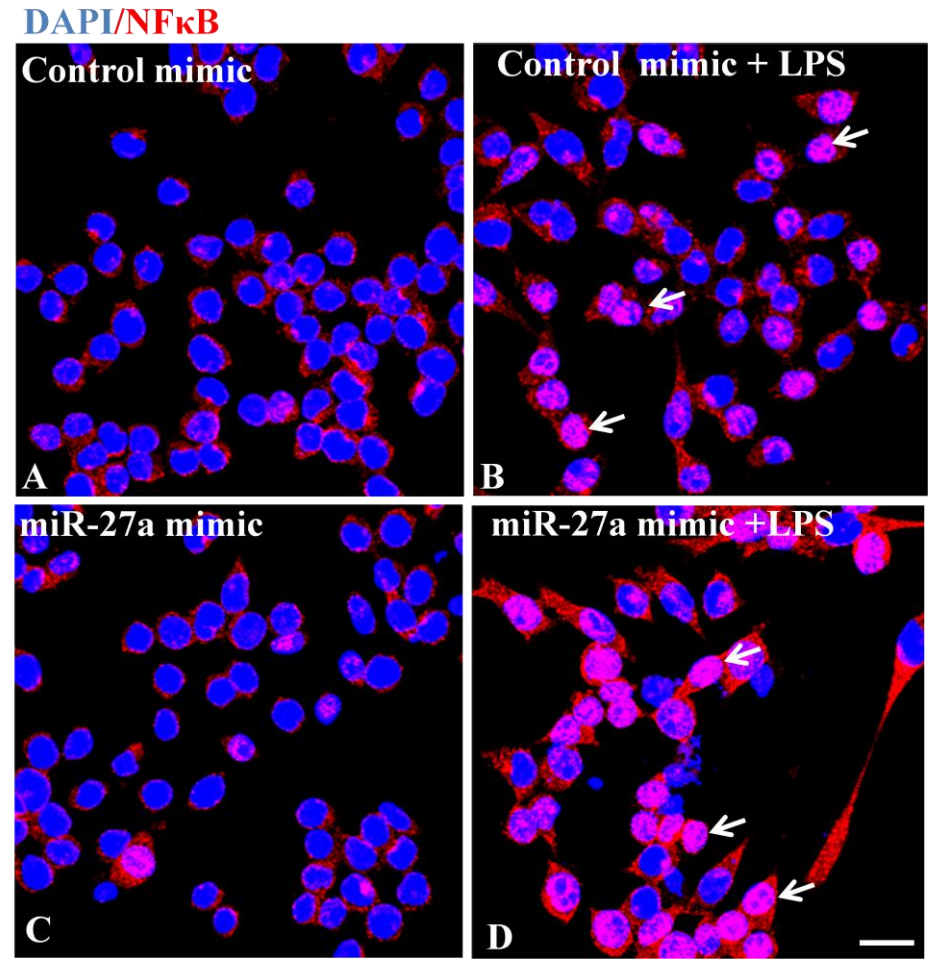
DAPI/NFκB
Control mimic
Control mimic + LPS
A
B
miR-27a mimic
miR-27a mimic +LPS
C
D

E

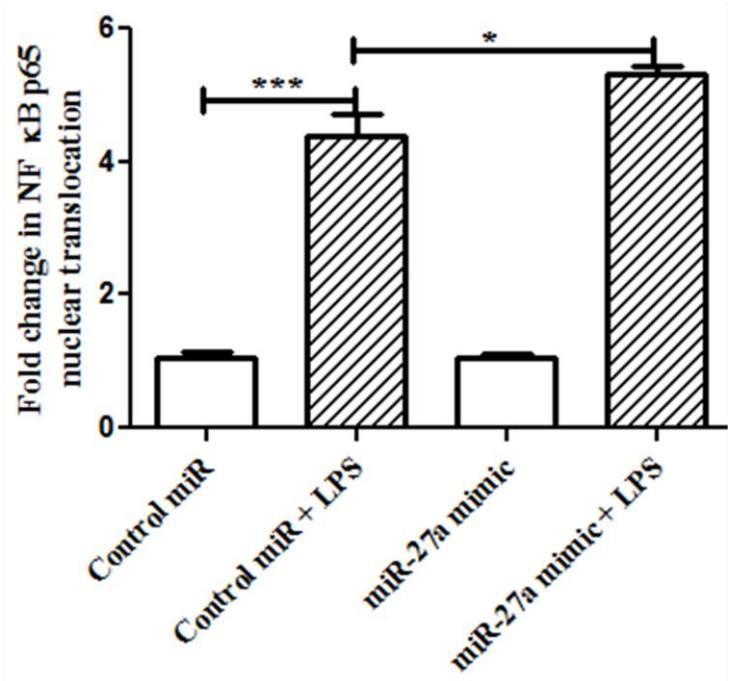
Fold change in NF κB p65 nuclear translocation
6
4
2
0
***
*
Control miR
Control miR + LPS
miR-27a mimic
miR-27a mimic + LPS

Fig 26 A-D: Immunocytochemistry showing the expression of NFκB (red) after miR-27a overexpression Note the increase in NFκB translocation in activated microglia after miR-27a overexpression (D) as compared to control mimic (B). The nucleus is stained with DAPI (blue) Scale bar: 20 μm**. E:** Quantification of nuclear translocation of NFκB p65 subunit using ELISA showing an increase after miR-27a overexpression as compared to control miR in LPS activated BV2 microglia. Statistical analysis was carried out using ANOVA with post-hoc Tukey test. Data represent the mean ± SD (n=3), ***p<0.001, **p<0.01, *p<0.05.

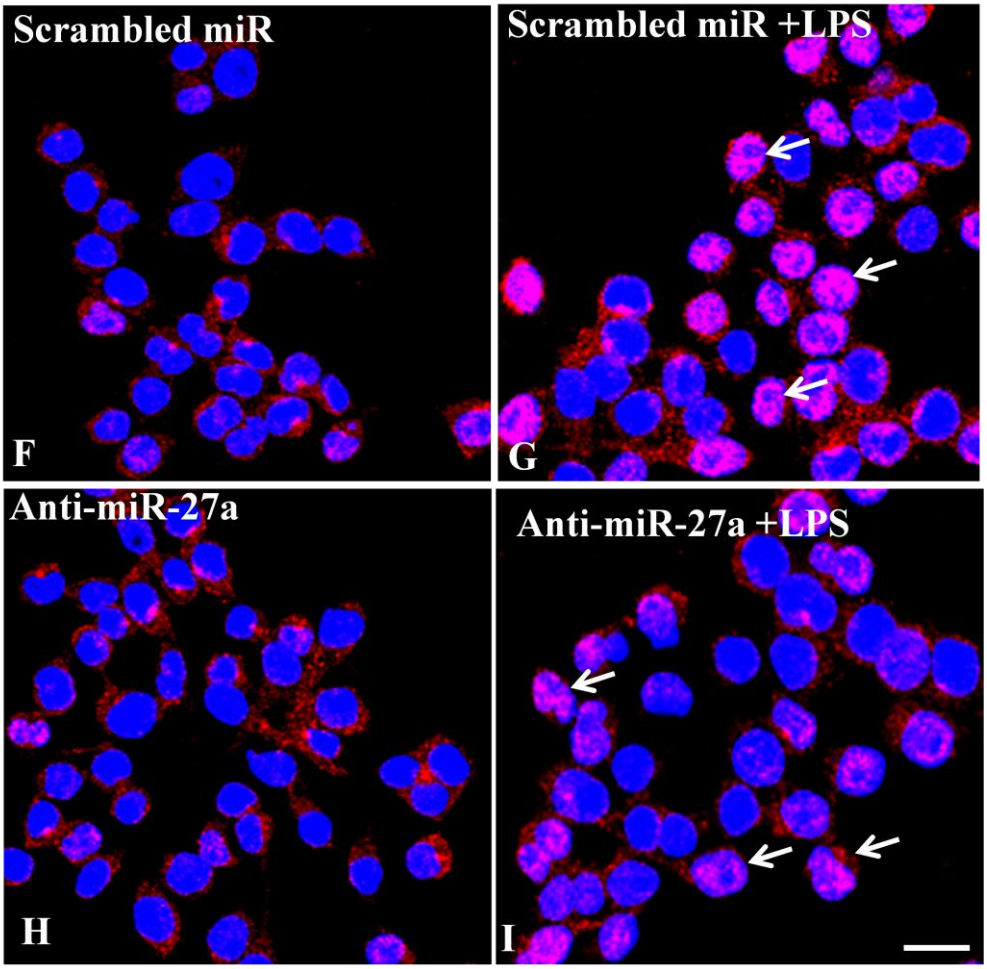

J

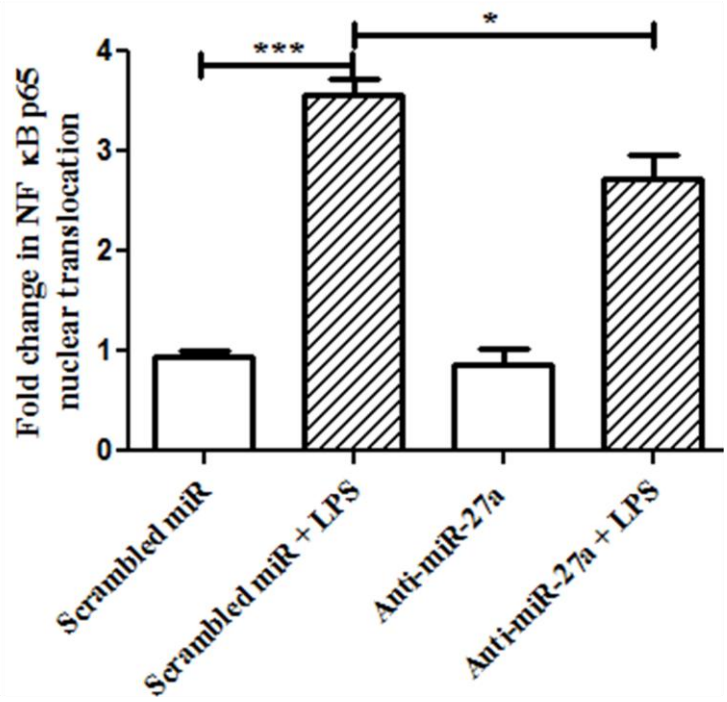

Fig 26 F-I: Immunocytochemistry showing the expression of NFκB (red) after miR-27a knockdown in BV2 microglia. Note the decrease in NFκB translocation in activated microglia after miR-27a knockdown (I) as compared to scrambled control (G). The nucleus is stained with DAPI (blue) Scale bar: 20 μm**. J:** Quantification of nuclear translocation of NFκB p65 subunit using ELISA, showing a decrease after miR-27a knockdown as compared to scrambled miR in LPS activated BV2 microglia. Statistical analysis was carried out using ANOVA with post-hoc Tukey test. Data represent the mean ± SD (n=3), ***p<0.001, **p<0.01, *p<0.05.

4.2.16 MiR-27a knockdown in microglia decreases neuronal apoptosis

Effect of miR-27a modulation in microglia on neuronal survival was examined using MN9D neuronal cells. MN9D cells were treated with BV2 conditioned medium and neuronal cell death was assessed using Annexin V FACS analysis. Apoptosis was observed in neuronal cells treated with conditioned medium (CM) obtained from LPS-activated BV2 microglia transfected with scrambled miR (control for miR inhibitor) or control miR (control for miR

mimic) (Fig 27 A-C). There was a further increase in number of apoptotic cells exposed to CM obtained from miR-27a overexpressing BV2 microglia as compared to control + LPS-treated BV2 microglia (Fig 27 A, C). Conversely, a decrease in apoptotic neuronal cells was observed in culture containing CM obtained from LPS-activated microglia with miR-27a knockdown as compared to control, indicating enhanced neuronal survival (Fig 27 B-C).

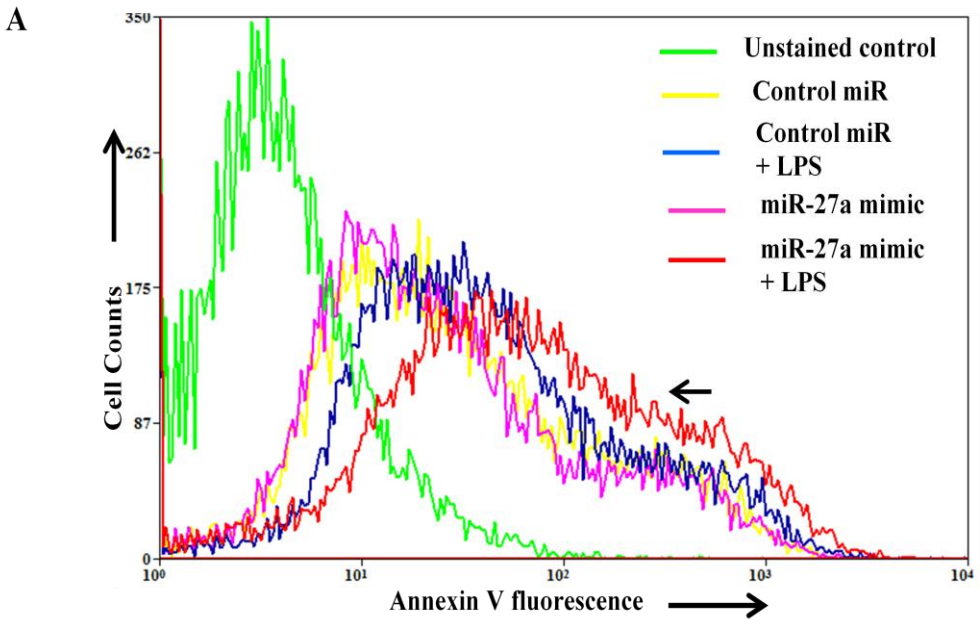

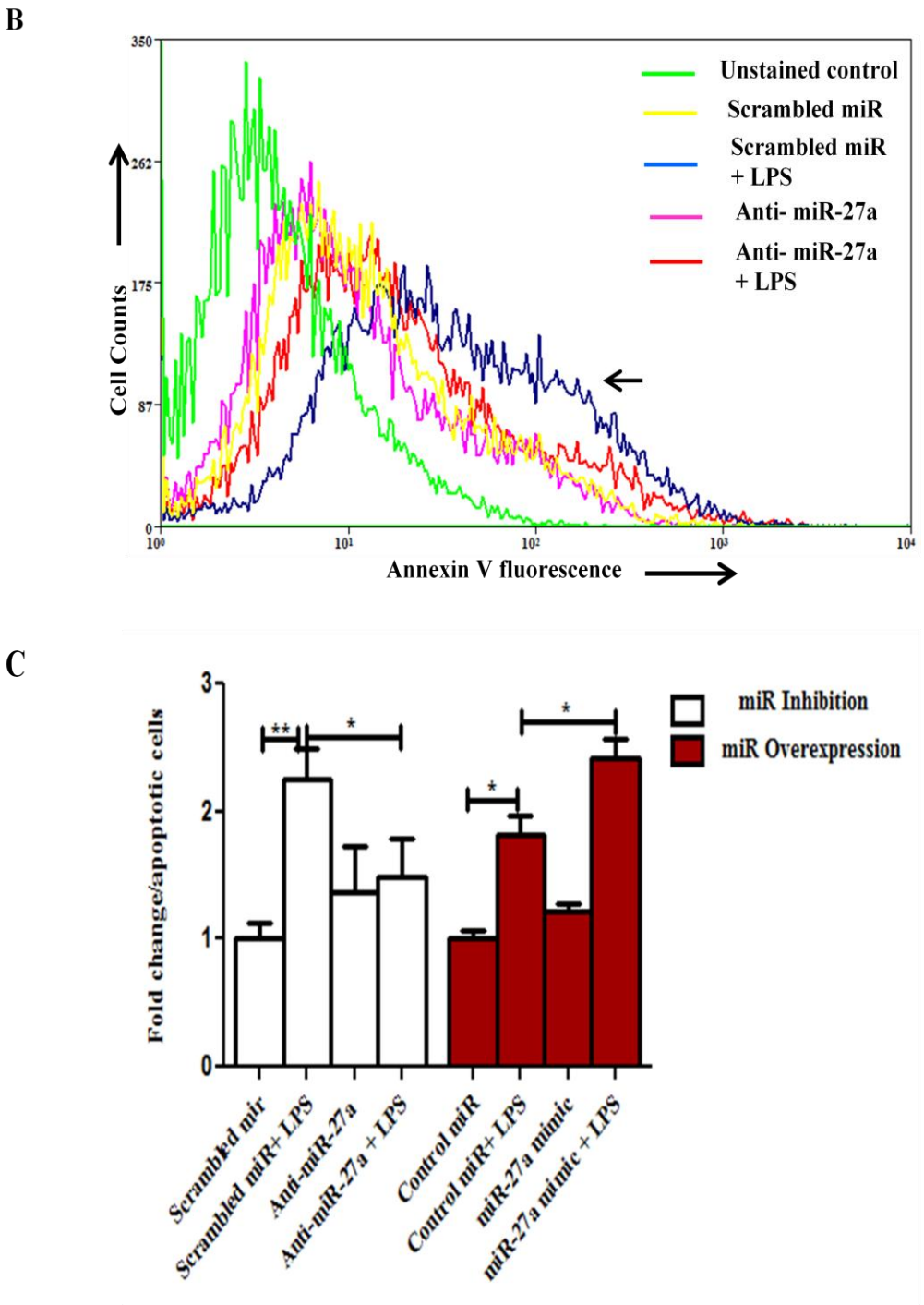

Fig 27 A-B: FACS analysis of annexin V stained apoptotic MN9D neurons after miR-27a overexpression (A) and miR-27a knockdown (B).

C. Quantification of apoptotic MN9D cells assessed using annexin V FACS indicates a decrease in neuronal apoptosis after miR-27a knockdown as compared to scrambled miR (white bars) and increased neuronal apoptosis after miR-27a overexpression as compared to control miR (red bars). Statistical analysis was carried out using ANOVA. Data represent the mean $\pm$ SD (n=3), $^{**}p<0.01$, $^{*}p<0.05$.

4.3 MiR-200b targets cJun/MAPK pathway in microglia

4.3.1 MiR-200b is localized in microglia

In situ hybridization was carried out using a 5'-FITC tagged LNA probe specific for the mature form of miR-200b. U6 was used as a positive control for the experiment (Fig 28 B). The expression of miR-200b was observed in the cytoplasm of BV2 microglia (Fig 28 C) and primary microglial cells (Fig 28 D) indicating that miR-200b is expressed in microglia.

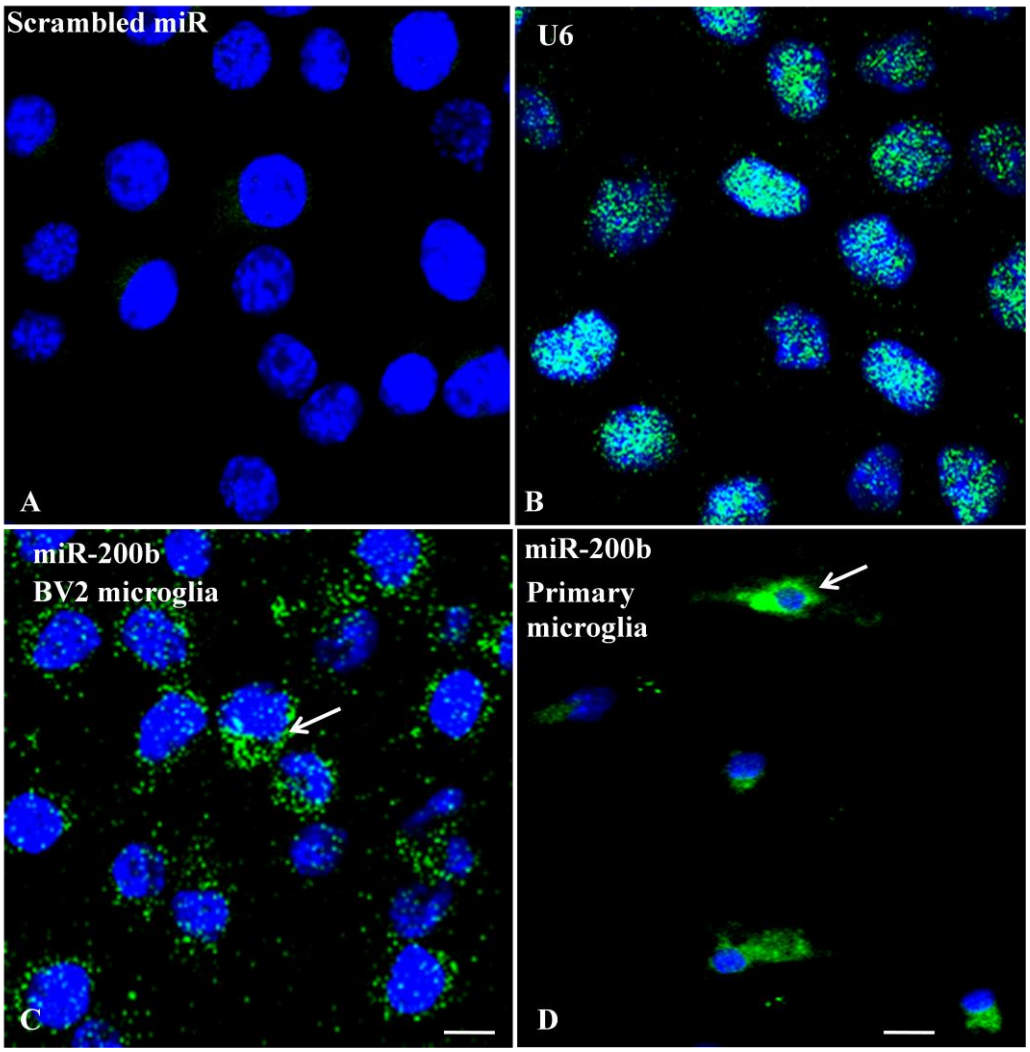

Fig 28 A-D: *in situ* hybridization analysis using 5' fluorescently labeled scrambled microRNA probe (A), U6 reference small RNA (B), mmu-miR-200b in BV2 microglia (C) and primary microglial cells (D) (green). Note the expression of miR-200b in the cytoplasm of BV2 and primary microglia.The nucleus is counterstained with DAPI (DAPI – blue). Scale bars A-D: 20 µm.

4.3.2 MiR-200b expression is altered in activated microglia

A time-dependent down-regulation of miR-200b expression was observed in BV2 microglia exposed to LPS (1µg/ml) for 1 to 6h, indicating that miR-200b expression is altered in activated microglia (Fig 29 A). The PCR products were run on a 15% native PAGE to check for the presence of a single product indicating primer specificity.

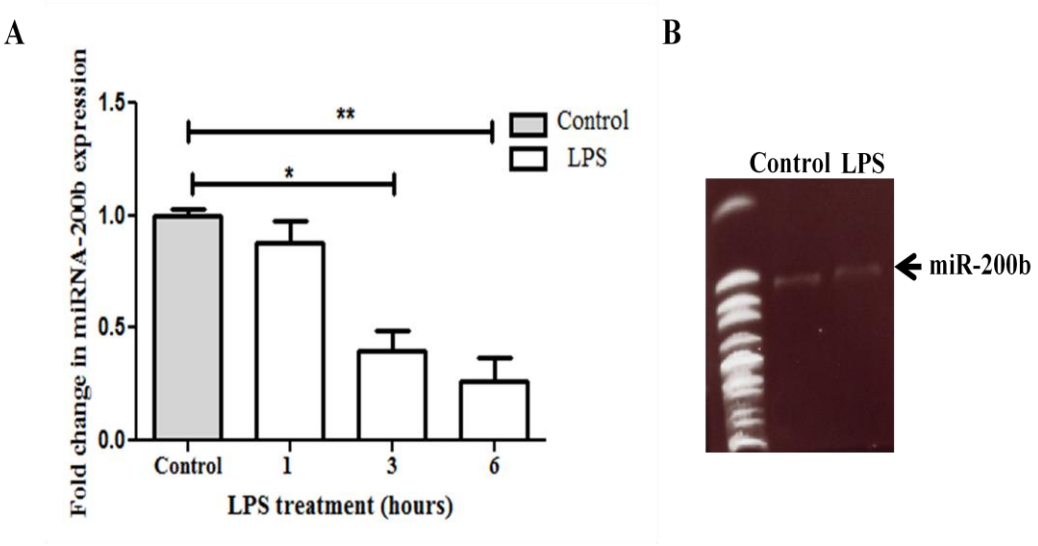

Fig 29 A: miR-200b expression was quantified using Real Time PCR analysis using LNA primers specific for mmu-miR-200b revealing decrease in expression for time course of LPS treatment of 1-6h in BV2 microglia. Statistical analysis was carried out using ANOVA with post-hoc Tukey test. Data represent the mean ± SD (n=4) $^{**}p<0.01$; $^{*}p<0.05$.

B: 15% native PAGE showing the band for miR-200b following amplification.

4.3.3 cJun expression is upregulated in activated microglia

MiR-200b was predicted to target members of the MAPK signalling pathway (Juhila *et al.* 2011). Among the target genes predicted, the transcription factor, cJun, was chosen due to its role in inflammatory response of microglia *via* MAPK signaling pathway. cJun is tightly regulated post-translationally and is phosphorylated in two distinct regions. Activation of cJun occurs by phosphorylation at serine 63 and 73 located at the N terminal (Pulverer *et al.* 1991). Immunocytochemistry analysis revealed an increase in cJun phosphorylation and total protein in activated BV2 microglia (Fig 30 A-D). The mRNA expression level of cJun was evaluated in BV2 microglia after different time points of LPS exposure. cJun expression was greatly enhanced in BV2 microglia at 1h after activation and remained upregulated upto 6h of LPS treatment (Fig 30 D) indicating an inverse relationship between cJun and miR-200b expression in LPS activated microglia *in vitro*.

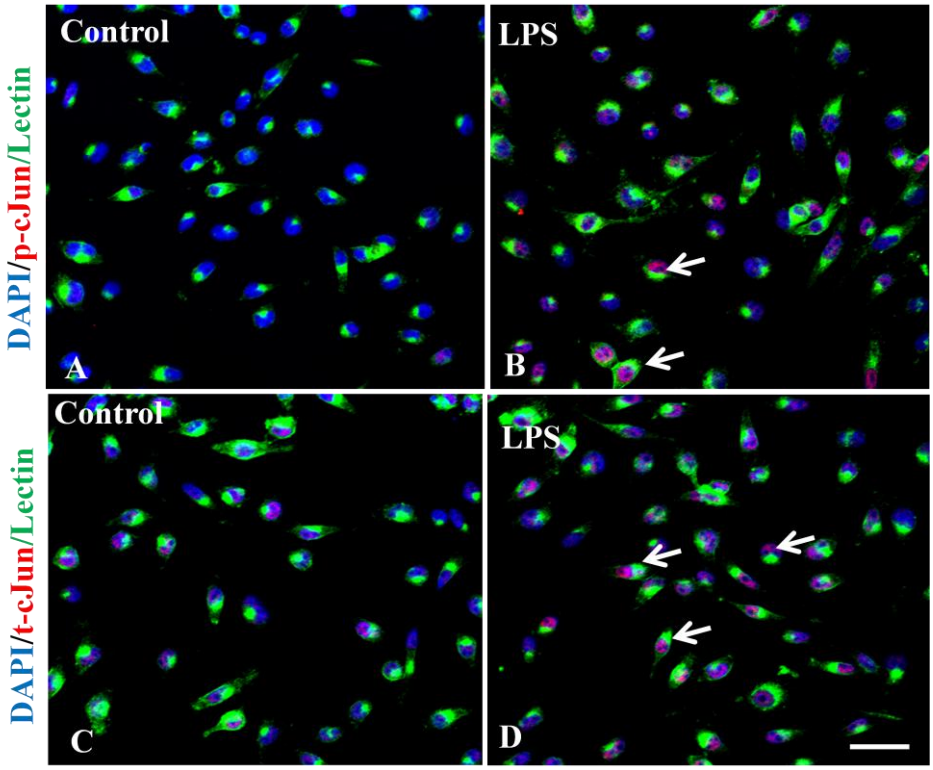

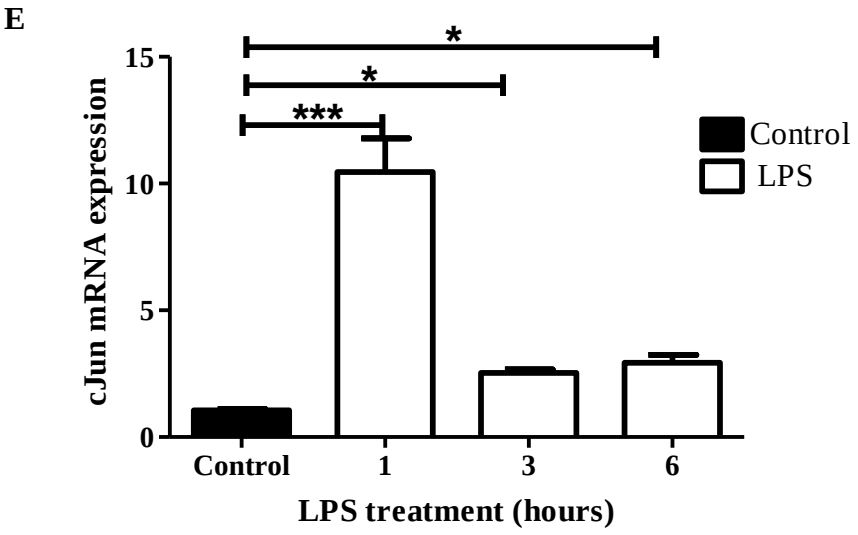

Fig 30 A-D. Immunocytochemistry revealing the increase in phospho cJun (A, B, red) and total cJun (C, D, red) expression after activation of BV2 microglia. The cells are marked with lectin (green) and the nucleus is counterstained with DAPI (DAPI – blue). Scale bars A-D: 50 µm.

E. cJun mRNA expression was quantified using Real Time PCR analysis after 1-6h of LPS activation. Results are represented as mRNA fold change with respect to untreated controls. Statistical analysis was carried out using ANOVA with post-hoc Tukey test. Data represent the mean $\pm$ SD (n=5) *** $p<0.001$;** $p<0.01$; * $p<0.05$.

4.3.4 MiR-200b expression is downregulated in microglia *in vivo* in traumatic brain injury rat model

qRT-PCR analysis revealed a down-regulation of miR-200b expression in activated microglia in vivo in LCM-extracted microglial cells from TBI injury model (Fig 31). On the other hand, miR-200b putative target gene, cJun exhibited increased mRNA expression in microglia following TBI (Fig 31). These results confirmed an inverse correlation between the expression of miR-200b and cJun in activated microglia *in vivo*.

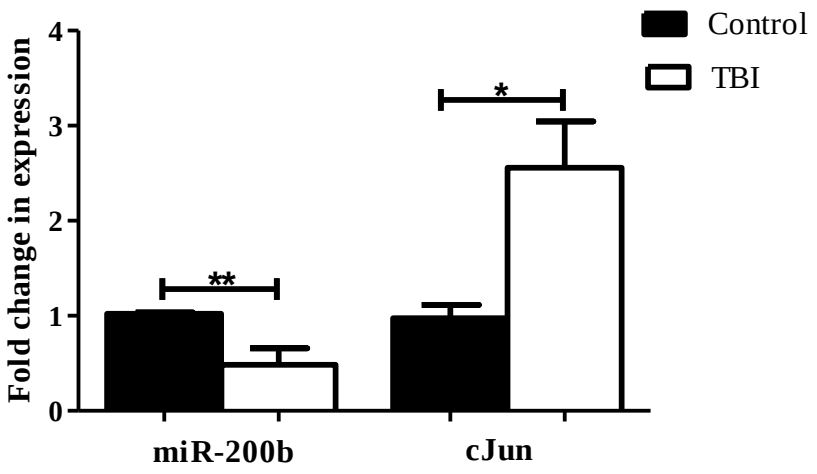

Fig 31: qPCR analysis indicates decrease in miR-200b expression and increase in activated microglia *in vivo* from TBI model using LCM. Statistical analysis was carried out using Student's t-test. Results are represented as miRNA/mRNA fold change with respect to untreated controls. Data represent the mean ± SD (n=4) $^{**}p<0.01$; $^{*}p<0.05$.

4.3.5 MiR-200b binds to the 3'UTR of cJun in microglia

To assess whether cJun is a direct target of miR-200b, a luciferase reporter assay was carried out. cJun 3'UTR was cloned into the pMirTarget reporter vector. RFP expression from the pMirTarget reporter was used for assessing transfection efficiency (Fig 32 A-D). Co-transfection of BV2 cells with miR-200b mimics and the reporter plasmid containing cJun 3' UTR resulted in a significant decrease in luciferase activity as compared to control mimics suggesting that miR-200b directly interacts with the cJun 3'UTR (Fig 32 E).

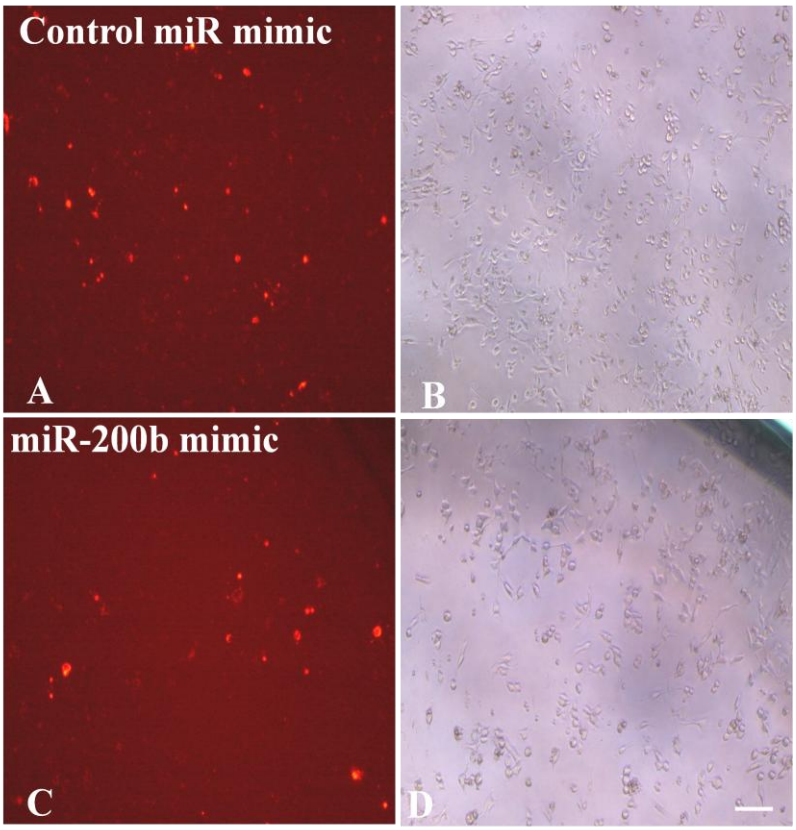

E

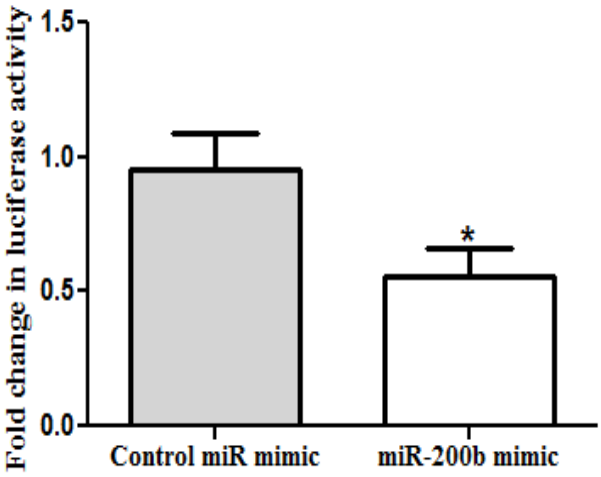

Fig 32 A,C. Confocal images showing the expression of red fluorescent protein (RFP) in BV2 cells co-transfected with control mimic and pMirTarget reporter vector containing mouse cJun 3'UTR (A) and BV2 cells co-transfected with miR-200b mimic and pMirTarget reporter vector containing mouse cJun 3'UTR (C).

B,D. Phase contrast images of BV2 cells co-transfected with control mimic and pMirTarget reporter vector containing mouse cJun 3'UTR (B) and BV2

cells co-transfected with miR-200b mimic and pMirTarget reporter vector containing mouse cJun 3'UTR (D).

E. Luciferase activity assay using reporter pMirTarget with mouse cJun 3′ UTR was performed after co-transfection with miR-200b mimic or control mimic in BV-2 cells. The luciferase activity of the control mimic transfection was set to 1. Low luciferase activity as compared to control after miR-200b overexpression indicates binding of miR-200b to cJun 3'UTR. Statistical analysis was carried out using Student's t-test. Mean ± SD (n=5), *$p<0.05$.

4.3.6 MiR-200b targets cJun in microglia

Gain- and loss-of-function analysis was carried out to substantiate the luciferase assay result. MiR-200b was knocked down using miRCURY LNA™ miR-200b inhibitor while miR-200b was overexpressed using miR-200b *mir*Vana™ mimic, respectively in BV2 microglia (Fig 33 A). MTS assay performed to check cell viability did not show significant cell death 24h after transfection (Fig 33 B). Knockdown of miR-200b resulted in a significant increase in expression levels of cJun mRNA and total protein (Fig 33 C-E). Conversely overexpression of miRNA-200b resulted in a significant decrease in cJun expression at the protein level (Fig 33 D-E). Taken together, these results suggest that cJun is a target of miR-200b in microglial cells.

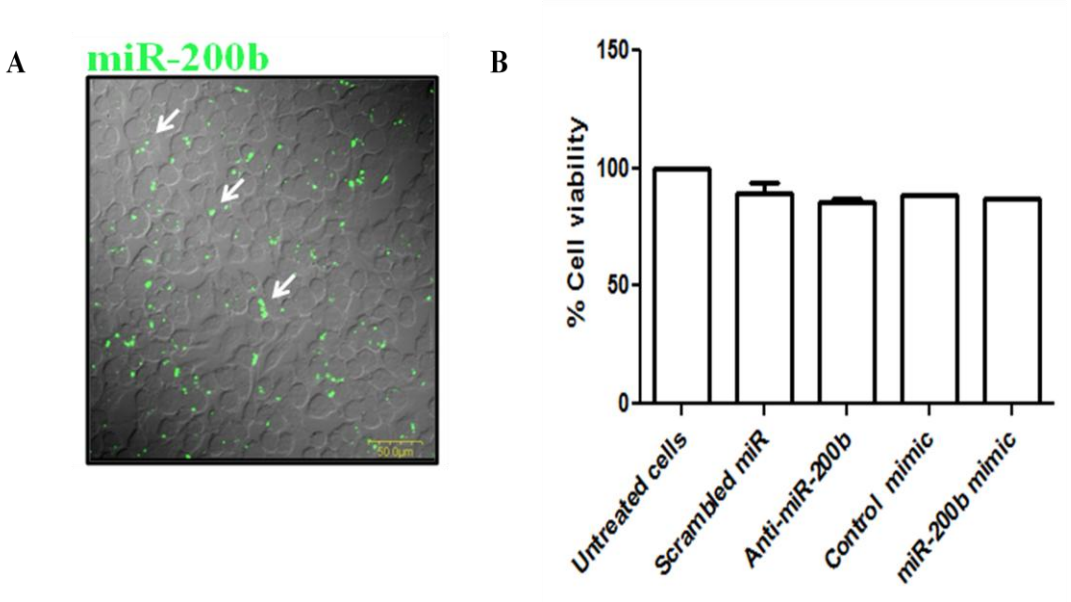

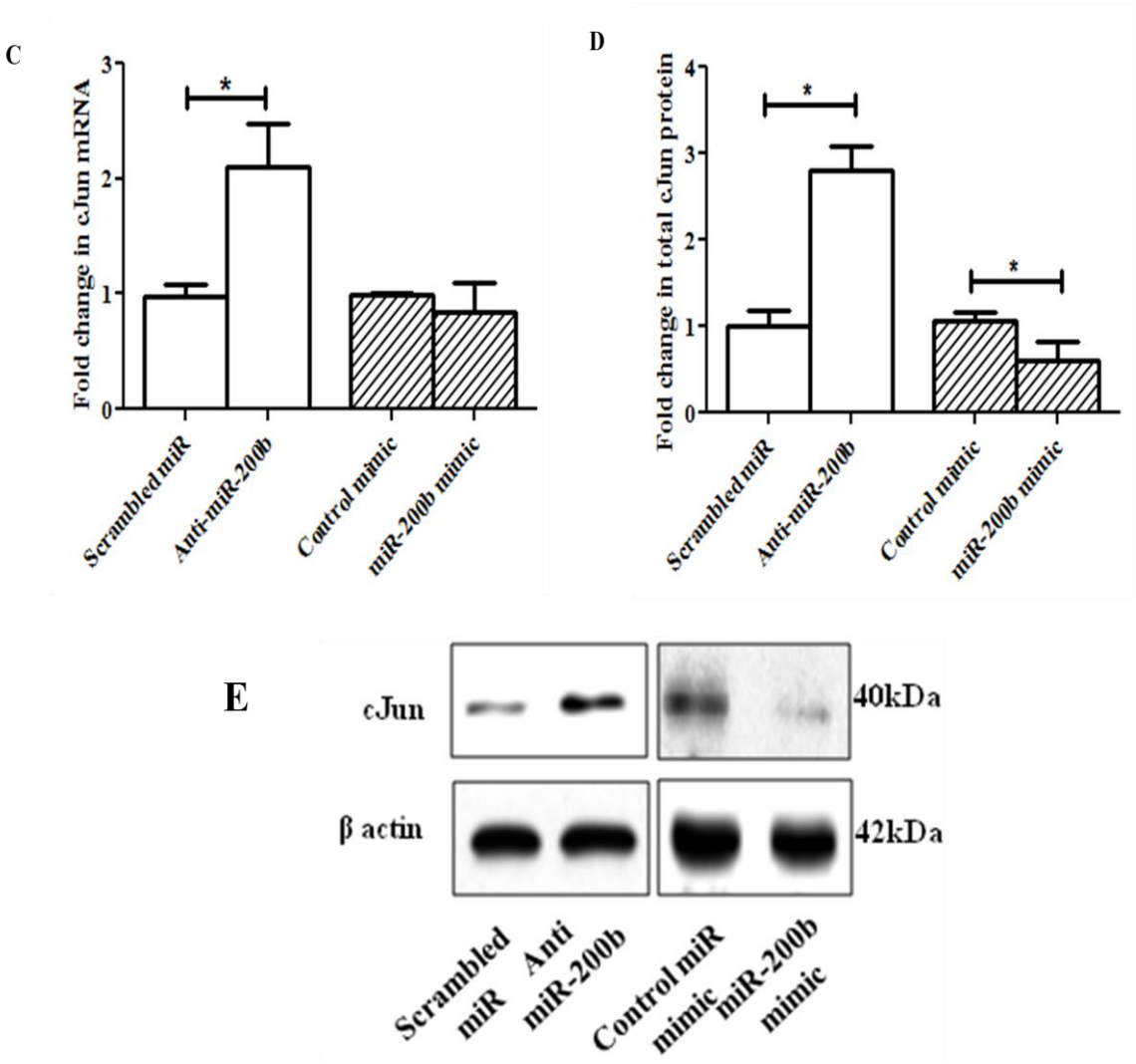

Fig 33 A. Confocal image (transmission) showing anti-miR-200b probe tagged with fluorophore- FITC. Majority of the cells show localization of the probe indicating high efficiency of transfection. Scale bar: 50 µm.

B. MTS assay showing no change in cell viability after miR-200b inhibition and miR-200b overexpression indicating low cell death after these treatments.

C. cJun mRNA expression in BV2 cells quantified using qPCR showing an increase in expression following knockdown of miRNA- 200b. Statistical analysis carried out using Student's t-test. Results are represented as mRNA fold change with respect to untreated controls. Mean ± SD (n=5), *$p<0.05$.

D-E. cJun protein expression after miR-200b knockdown and overexpression was quantified using densitometry analysis following western blot indicating an increase in cJun protein expression following miR-200b knockdown and decrease in expression after miR-200b overexpression. Results are represented as protein fold change with respect to untreated controls. Statistical analysis was carried out using Student's t-test. Mean $\pm$ SD (n=6) *p<0.05.

4.3.7 Knockdown of miR-200b increases cJun phosphorylation in LPS-activated BV2 microglia

cJun activity was assessed by examining its phosphorylation status. Western blot analysis confirmed an increase in cJun phosphorylation in BV2 microglia after LPS treatment (Fig 34 A-D). There was a further increase in phospho-cJun after knockdown of miR-200b in activated microglia (Fig 34 A-B). Conversely overexpression of miR-200b did not increase the phosphorylation of cJun significantly in activated microglia (Fig 34 C-D). These results demonstrate that targeting of cJun by miR-200b in microglia is functionally relevant since cJun activity (phosphorylated levels) was altered by miR-200b in BV2 microglia.

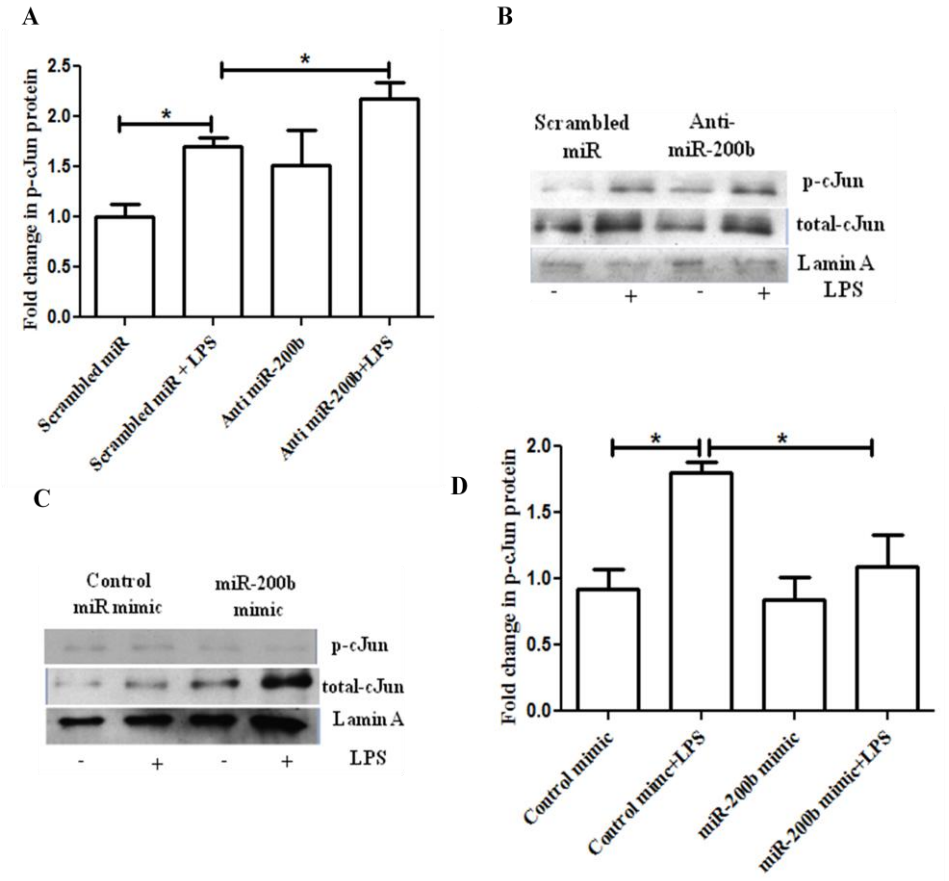

Fig 34 A-B: Activation of cJun in nuclear extracts of activated BV2 microglia was measured by western blotting using antisera against phosphorylated (p) and total cJun and quantified using densitometry analysis shows an increase in phospho-cJun after miR-200b knockdown in activated BV2 microglia. Statistical analysis was carried out using ANOVA with post-hoc Tukey test. Data represent the mean ± SD (n=5), *p<0.05

C-D: Activation of cJun in nuclear extracts of activated BV2 microglia was measured by western blotting using antisera against phosphorylated (p) and total cJun and quantified using densitometry analysis shows a decrease in phospho-cJun after miR-200b overexpression in activated BV2 microglia. Statistical analysis was carried out using ANOVA with post-hoc Tukey test. Data represent the mean ± SD (n=5), *p<0.05.

4.3.8 MiR-200b suppresses JNK activity by downregulating cJun expression

JNKs, members of the MAPK signaling molecules, bind and phosphorylate c-Jun (Hibi et al., 1993). In the present study we examined if suppression of cJun expression by miR-200b alters the JNK protein activity. The expression levels of total-JNK and phospho-JNK protein were examined by western blot after miR-200b knockdown and overexpression in BV2 microglia. JNK activity increased in activated microglia transfected with scrambled miRNA and control mimic (Fig 35 A-D). MiR-200b knockdown further increased the JNK phosphorylation in activated BV2 cells as compared to scrambled miRNA (Fig 35 A-B). Conversely overexpression of miR-200b decreased JNK phosphorylation in activated BV2 cells, as compared to control activated cells confirming the alteration of JNK activity concomitant with cJun activity by miR-200b (Fig 35 C-D).

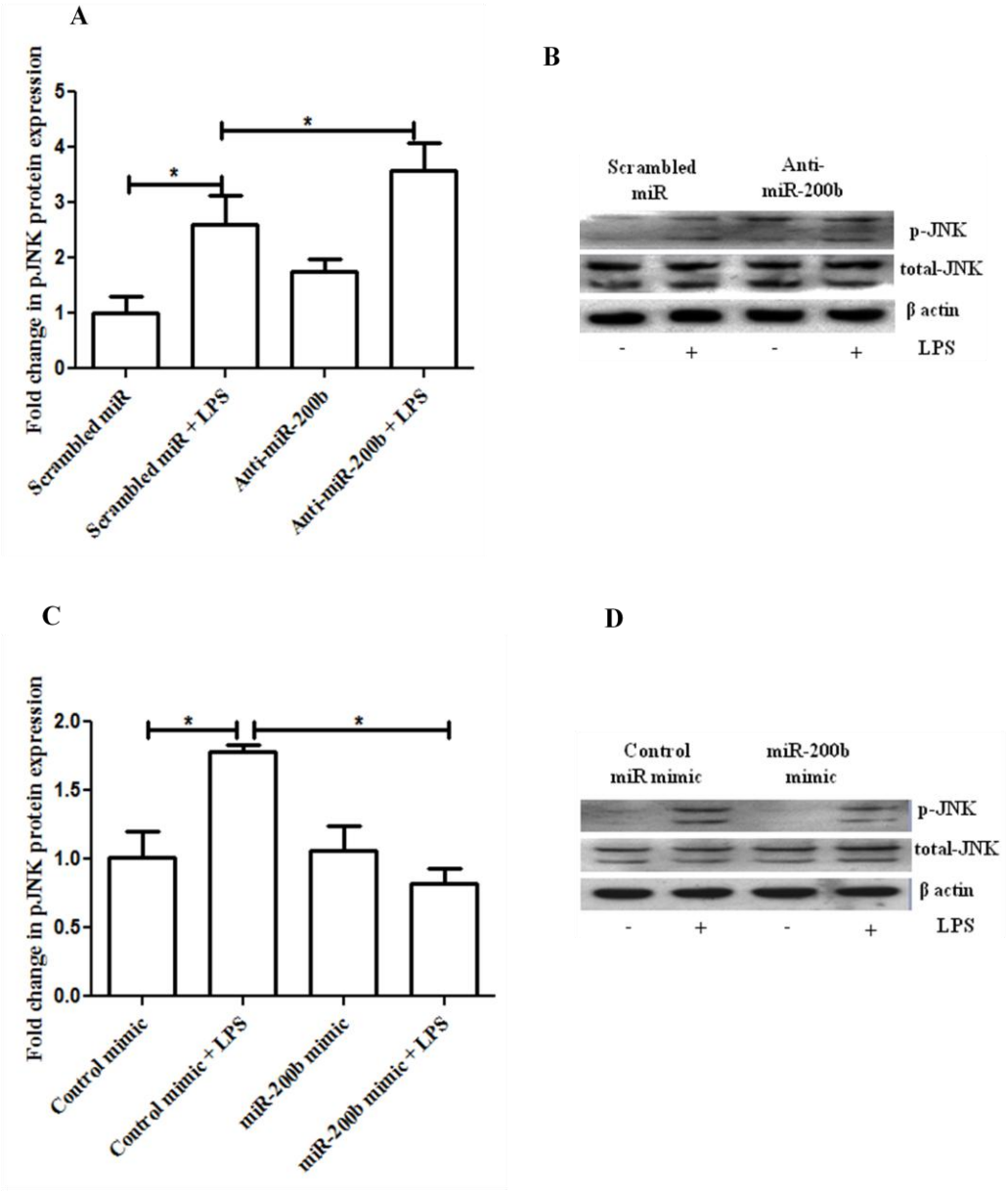

Fig 35 A-B: Activation of JNK in activated BV2 microglia measured by western blotting using antisera against phosphorylated (p) and total JNK and quantified using densitometric analysis shows an increase in phospho-JNK after miR-200b knockdown. Statistical analysis was carried out using ANOVA with post-hoc Tukey test. Data represent the mean ± SD (n=6) *p<0.05.

C-D: Activation of JNK in activated BV2 microglia measured by western blotting using antisera against phosphorylated (p) and total JNK and quantified using densitometric analysis shows a decrease in phospho-JNK after miR-200b overexpression. Statistical analysis was carried out using ANOVA with post-hoc Tukey test. Data represent the mean ± SD (n=6) *p<0.05.

4.3.9 MiR-200b negatively regulates inflammatory cytokine response of microglia

In order to assess the effects of miRNA-200b-mediated cJun suppression on microglial activation, the expression levels of proinflammatory cytokines, TNF-α, IL-6 and IL-1β were evaluated after miR-200b knockdown or overexpression. Knockdown of miR-200b in activated BV2 microglia significantly increased the mRNA expression of TNF-α, IL-6 and IL-1β (Fig 36 A-C). ELISA analysis revealed an increased TNF-α secretion in the medium by activated BV2 cells following miR-200b knockdown (Fig 36 D). In contrast, miR-200b overexpression significantly decreased the LPS-induced TNF-α protein secretion in the medium by BV2 microglia (Fig 36 E). Immunocytochemical analysis also revealed that knockdown of miR-200b increased the expression of TNF-α in activated microglial cells as compared to scrambled miR (Fig 37 Aa-Ad) whereas, miR-200b overexpression decreased the expression of TNF-α in activated microglia (Fig 37 Ba-Bd). Thus both gain- and loss-of-function studies indicate a suppressive role of miR-200b in microglial inflammatory response.

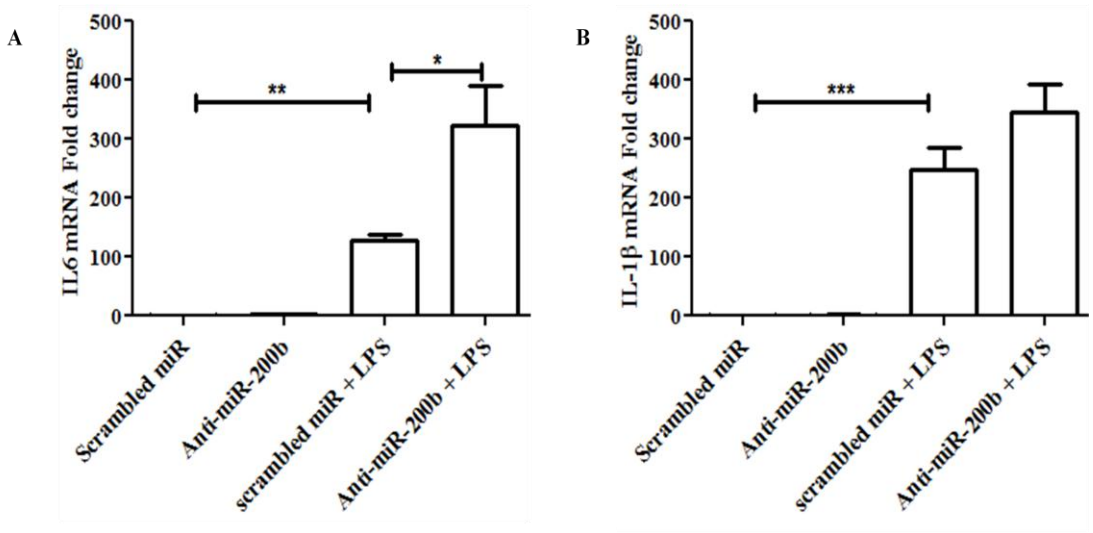

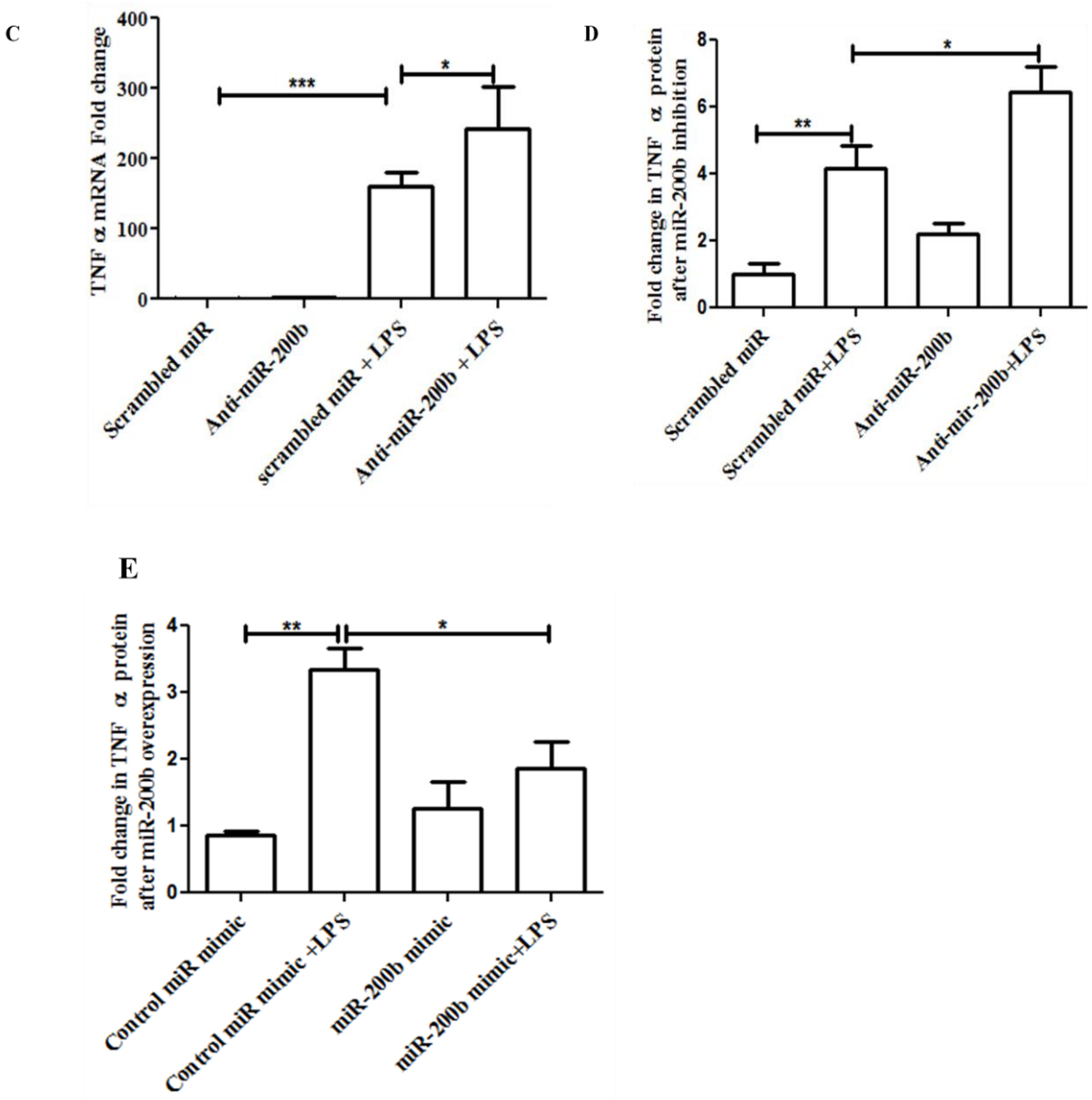

Fig 36: A-C: qRT-PCR analysis of **A**. IL6 **B.** IL-1 β and **C.** TNFα shows an increase in mRNA expression after miR-200b knockdown in activated microglia as compared to control. Data represent the mean ± SD (n=5), ***p<0.001, **p<0.01, *p<0.05.

D: TNFα protein release in media measured by ELISA shows an increase after miR-200b knockdown in activated BV2 microglia. Statistical analysis was carried out using ANOVA with post-hoc Tukey test. Data represent the mean ± SD (n=5), **p<0.01, *p<0.05.

E: TNFα protein release in media measured by ELISA shows a decrease after miR-200b overexpression in activated BV2 microglia. Statistical analysis was carried out using ANOVA with post-hoc Tukey test. Data represent the mean ± SD (n=5), **p<0.01, *p<0.05.

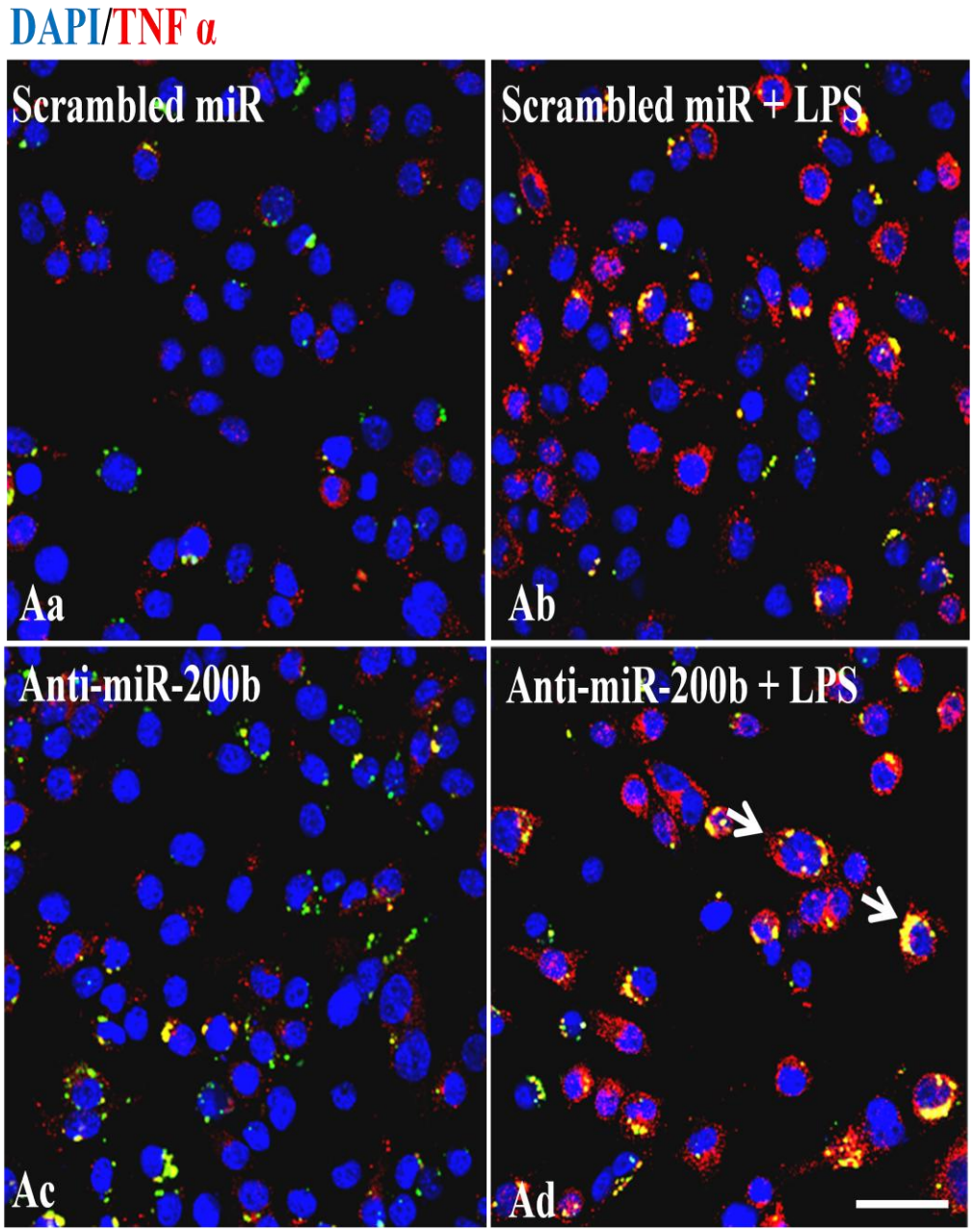

Fig 37 Aa-Ad: Confocal images showing the expression of TNFα (red) in BV2 cells transfected with scrambled probe (green) (Aa, Ab), miR-200b antagomir (green) (Ac, Ad), shows an increase in TNFα expression in activated microglia after miR-200b knockdown (Ad) as compared to scrambled miR (Ab). (DAPI – blue) Scale bars Aa-Ad: 50 µm.

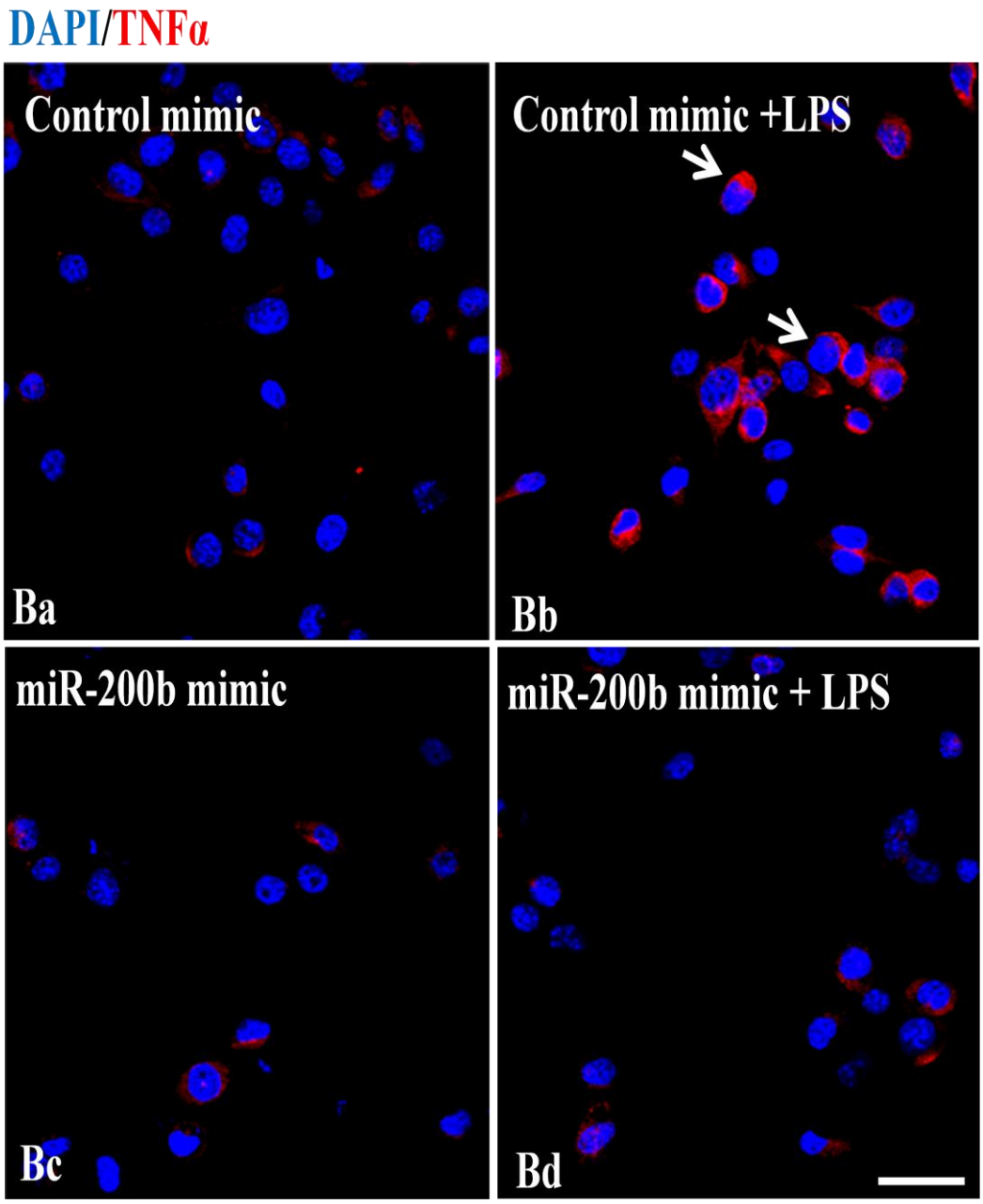

Fig 37 Ba-Bd: Confocal images showing the expression of TNFα (red) in BV2 cells transfected with control mimic (Ba, Bb) and miR-200b mimic (Bc, Bd) shows a decrease in TNFα expression in activated microglia after miR-200b overexpression (Bd) as compared to control mimic (Bb) (DAPI – blue) Scale bars Ba-Bd: 50 µm.

4.3.10 MiR-200b modulates iNOS expression and NO production in activated microglia

The synthesis of nitric oxide (NO), an important mediator of the inflammatory process, is catalyzed by the inducible nitric oxide synthase (iNOS). In microglia, iNOS expression is induced after activation, indicating increased production of NO. Immunofluorescence evaluation revealed that inhibition of miR-200b increased iNOS expression in activated microglia (Fig 38 Aa-Ad), whereas downregulation of the iNOS expression was observed in activated microglia overexpressing miR-200b (Fig 38 Ba-Bd). Moreover, inhibition of miRNA-200b in activated BV2 microglia led to increased production of NO as compared to scrambled miR (Fig 38 C). Conversely, overexpression of miR-200b in activated BV2 microglia significantly decreased the NO release as compared to control (Fig 38 D) indicating both iNOS expression and NO release were altered in response to miR-200b expression.

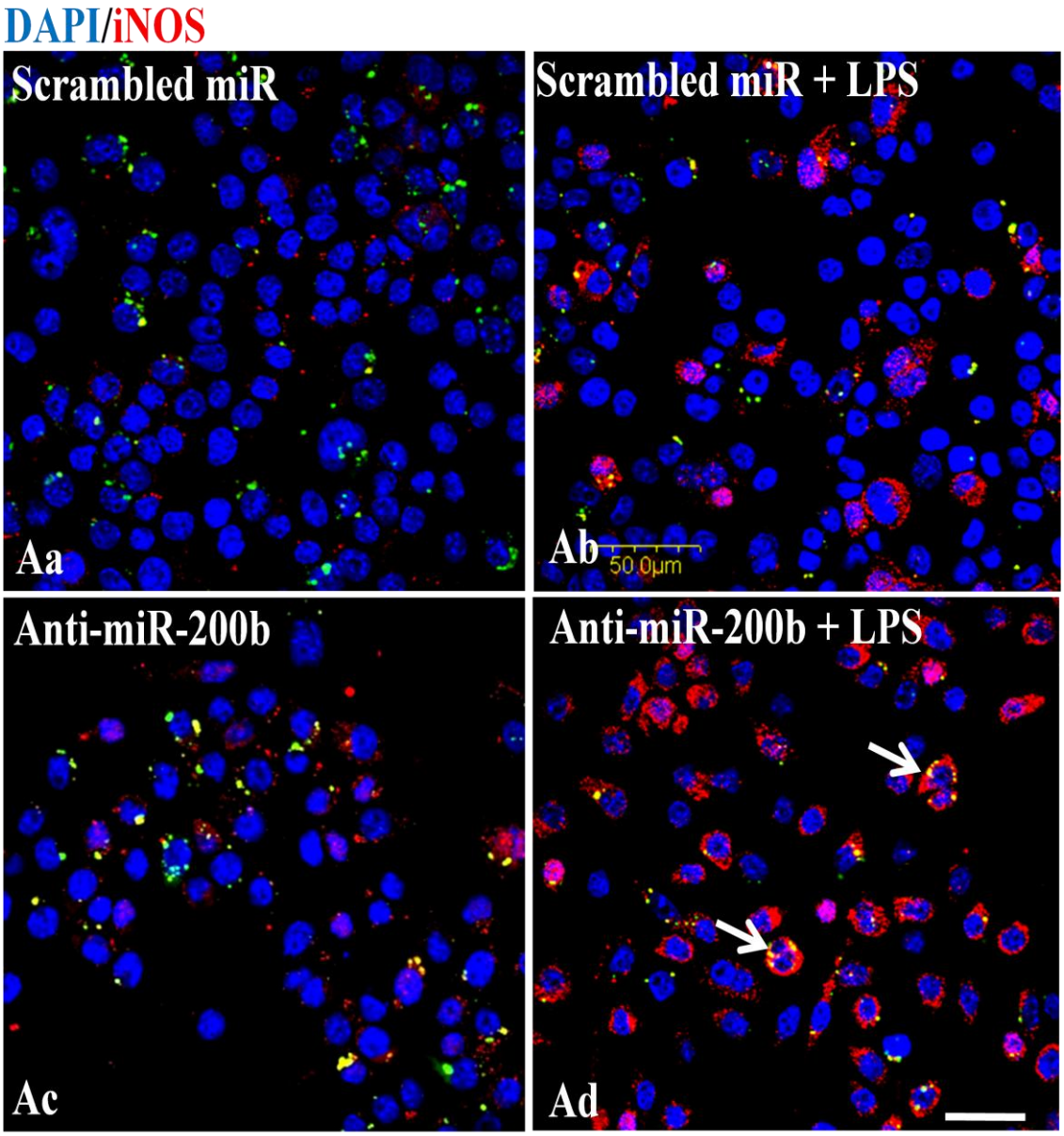

Fig 38 Aa-Ad: Confocal images showing the expression of iNOS (red) in BV2 cells transfected with scrambled probe (green) (Aa, Ab), miR-200b antagomir (green) (Ac, Ad), shows an increase in iNOS expression in activated microglia after miR-200b knockdown (Ad) as compared to scrambled miR (Ab). (DAPI – blue) Scale bars Aa-Ad: 50 µm.

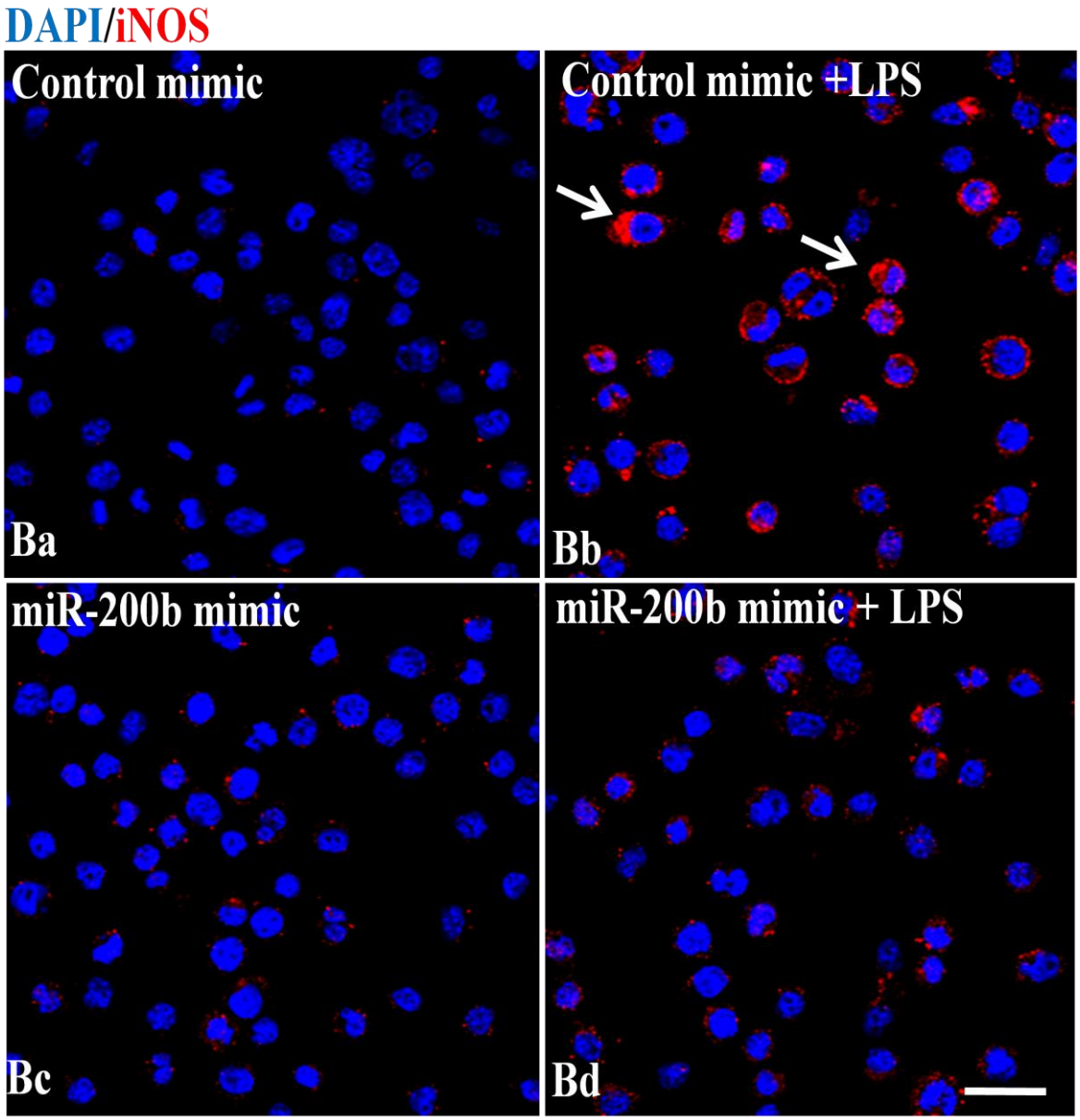

Fig 38 Ba-Bd: Confocal images showing the expression of iNOS (red) in BV2 cells transfected with control mimic (Ba, Bb) and miR-200b mimic (Bc, Bd) shows a decrease in iNOS expression in activated microglia after miR-200b overexpression (Bd) as compared to control mimic (Bb) (DAPI – blue) Scale bars Ba-Bd: 50 µm.

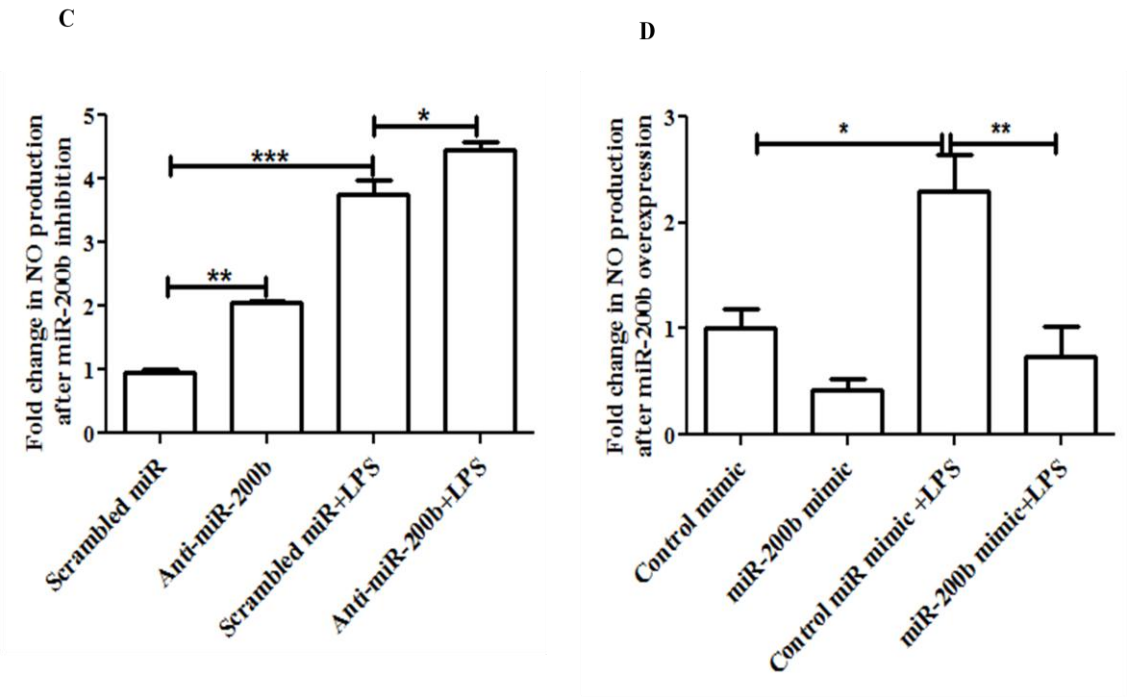

Fig 38 C: Quantitative analysis of NO production using the Greiss assay shows an increase in NO production from activated microglia after miR-200b knockdown (white bars) as compared to scrambled miR (grey bars). Statistical analysis was carried out using ANOVA with post-hoc Tukey test. Data represent the mean $\pm$ SD (n=4), ***p<0.001, **p<0.01, *p<0.05**.**

Fig 38 D. Quantitative analysis of NO production using the Greiss assay shows a decrease in NO production from activated microglia after miR-200b overexpression (white bars) as compared to control mimic (grey bars)**.** Statistical analysis was carried out using ANOVA with post-hoc Tukey test. Data represent the mean $\pm$ SD (n=4), ***p<0.001, **p<0.01, *p<0.05**.**

4.3.11 MiR-200b knockdown increases neuronal cell death following microglial activation

The above results indicate that miR-200b suppresses inflammatory response of microglia by targeting cJun. Next we sought to determine the effect of modulation of miR-200b-mediated microglial immune response on neuronal survival. Immortalized dopamine-containing neuronal hybrid cell line MN9D

was used in this study. Neuronal identity and dopamine production was confirmed by staining fully differentiated MN9D neurons with the neuronal marker Map2 (Fig 39 A) and Tyrosine hydroxylase (Fig 39 B). More than 2-fold change in apoptosis was observed in neuronal cells treated with conditioned medium (CM) obtained from LPS-activated BV2 microglia transfected with scrambled miR (Fig 39 C-E). There was a further increase in number of apoptotic cells exposed to CM obtained from miR-200b knockdown BV2 microglia as compared to scrambled + LPS-treated BV2 microglia (Fig 39 C, E). In contrast, a decrease in apoptotic neuronal cells was observed in culture containing CM obtained from LPS-activated microglia overexpressing miR-200b as compared to miR-200b knockdown BV2 microglia, indicating enhanced neuronal survival (Fig 39 D-E).

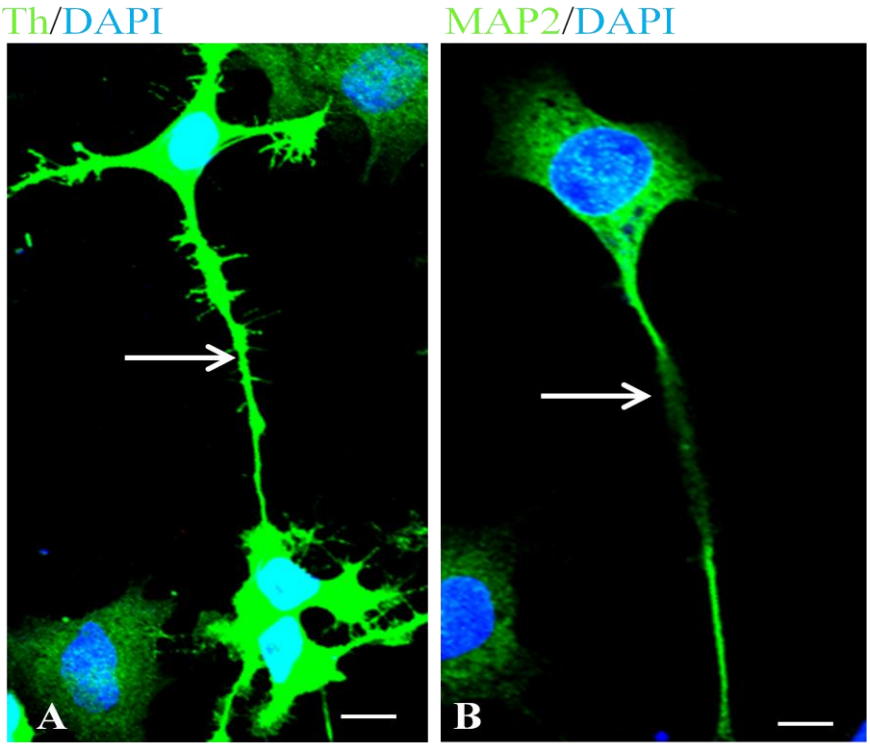

C

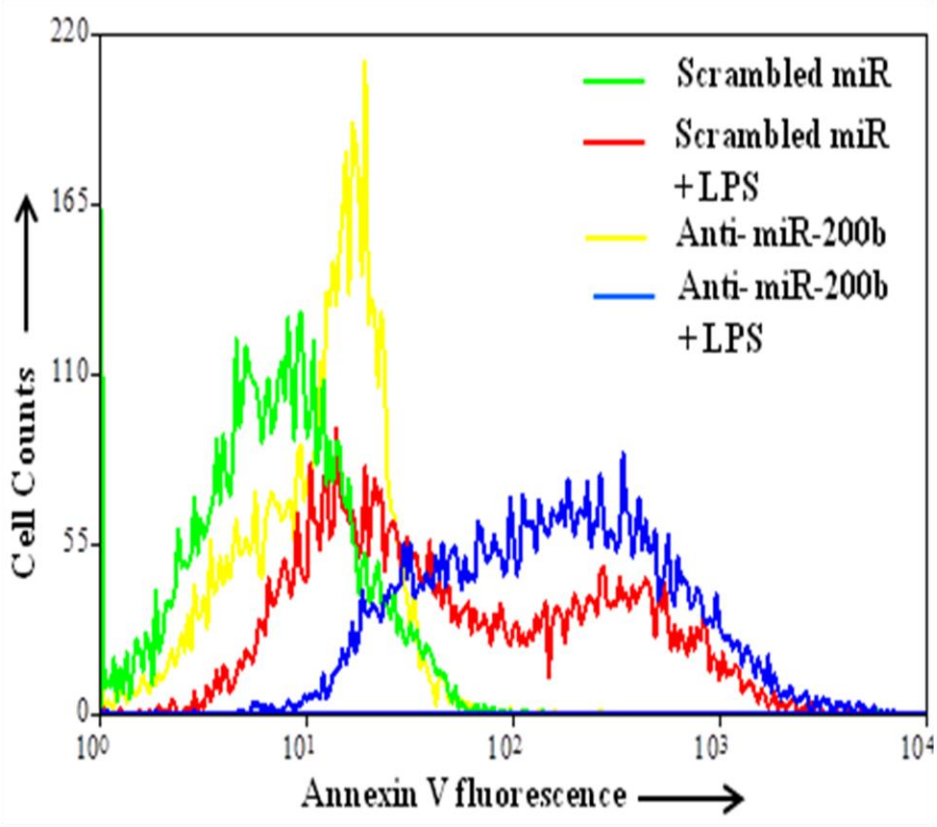
220
165
110
55
0
Cell Counts
Scrambled miR
Scrambled miR +LPS
Anti-miR-200b
Anti-miR-200b +LPS
10⁰
10¹
10²
10³
10⁴
Annexin V fluorescence

D

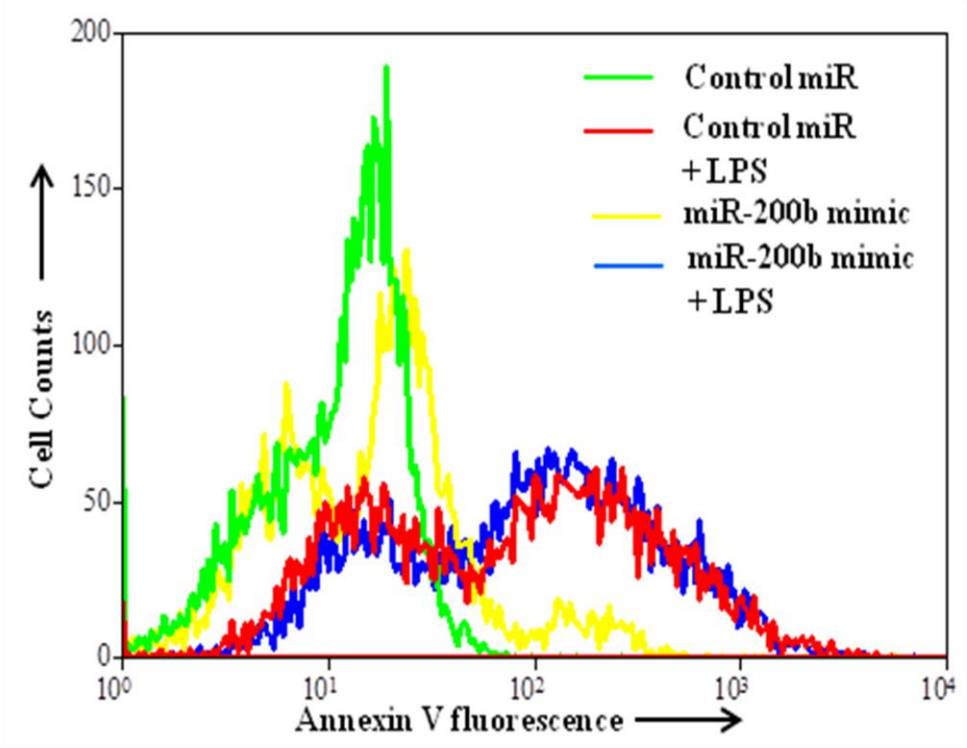
200
150
100
50
0
Cell Counts
Control miR
Control miR +LPS
miR-200b mimic
miR-200b mimic +LPS
10⁰
10¹
10²
10³
10⁴
Annexin V fluorescence

E

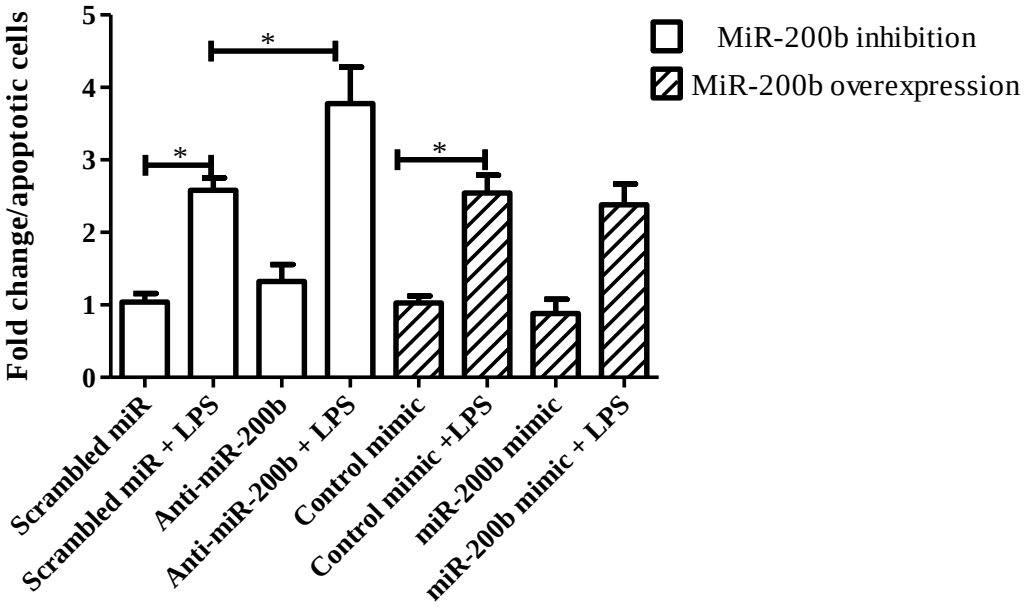

Fig 39 A-B: Confocal image of Tyrosine hydroxylase (green) (A) and Map2 (green) (B) stained fully differentiated MN9D neuron. Arrowhead points towards a long axon-like projection. The nucleus is counterstained with DAPI (DAPI – blue). Scale bar: 20 µm.

C-D: Histogram overlay representing the flow cytometric analysis of Annexin V fluorescence intensity indicates increased neuronal apoptosis after miR-200b knockdown (C) as compared to miR-200b overexpression (D).

E. Quantitative analysis of apoptotic MN9D cells assessed in the presence of microglial conditioned medium (CM) shows an increase in neuronal apoptosis after miR-200b knockdown (white bars). Results expressed as fold change in apoptotic cells with respect to control cells. Statistical analysis was carried out using ANOVA with post-hoc Tukey test. Data represent the mean $\pm$ SD (n=3) *p<0.05.

4.3.12 Overexpression of miRNA-200b reduces the migratory ability of activated microglia

An important feature of activated microglia is the ability to migrate to sites of infection and injury. Activation of microglia by LPS results in increased migration as compared to untreated control (Fig 40 Ab, Bb, C, D). MiR-200b inhibition did not show any significant change in microglial migratory ability (Fig 40 Aa-Ad, C). However miR-200b overexpression significantly impaired microglial migration in response to LPS (Fig 40 Ba-Bd, D).

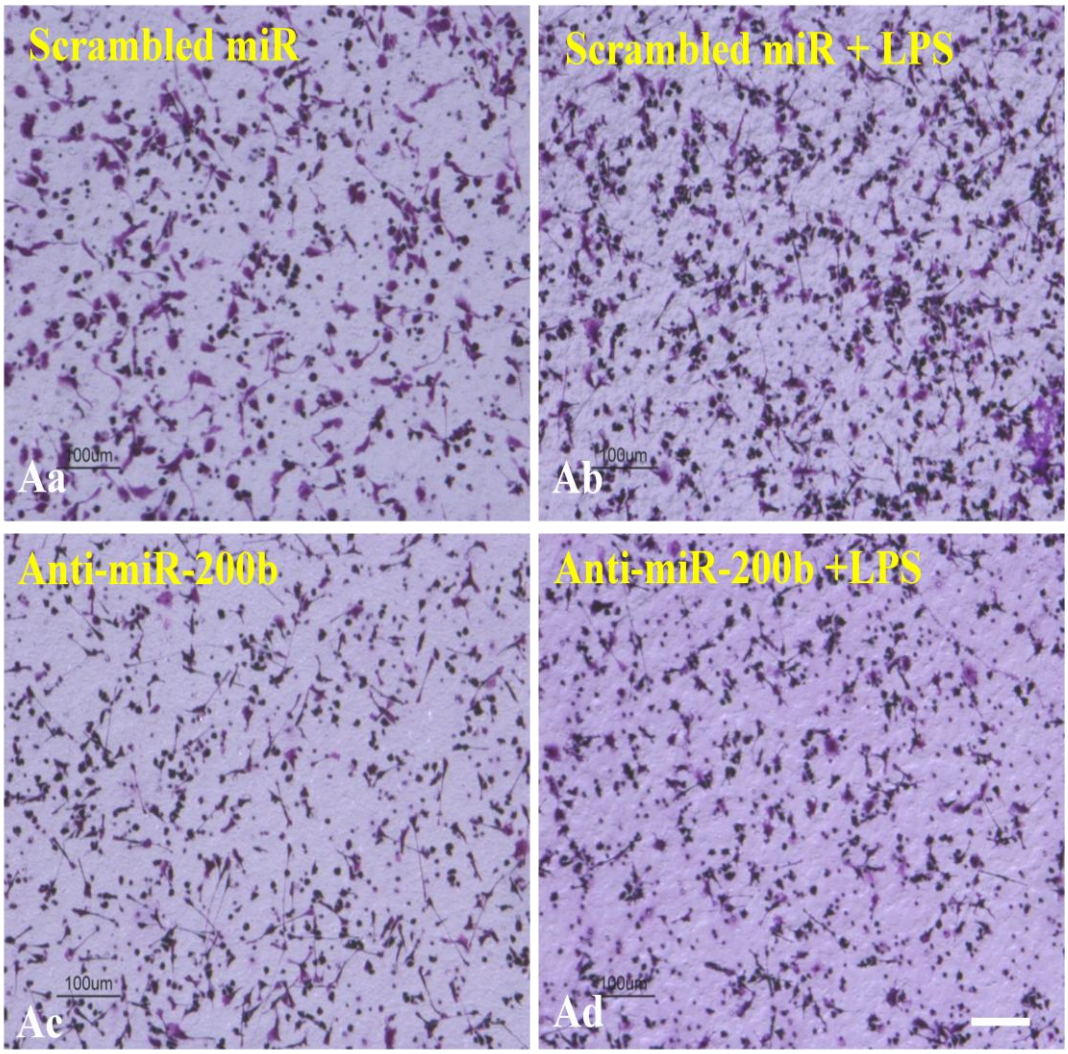

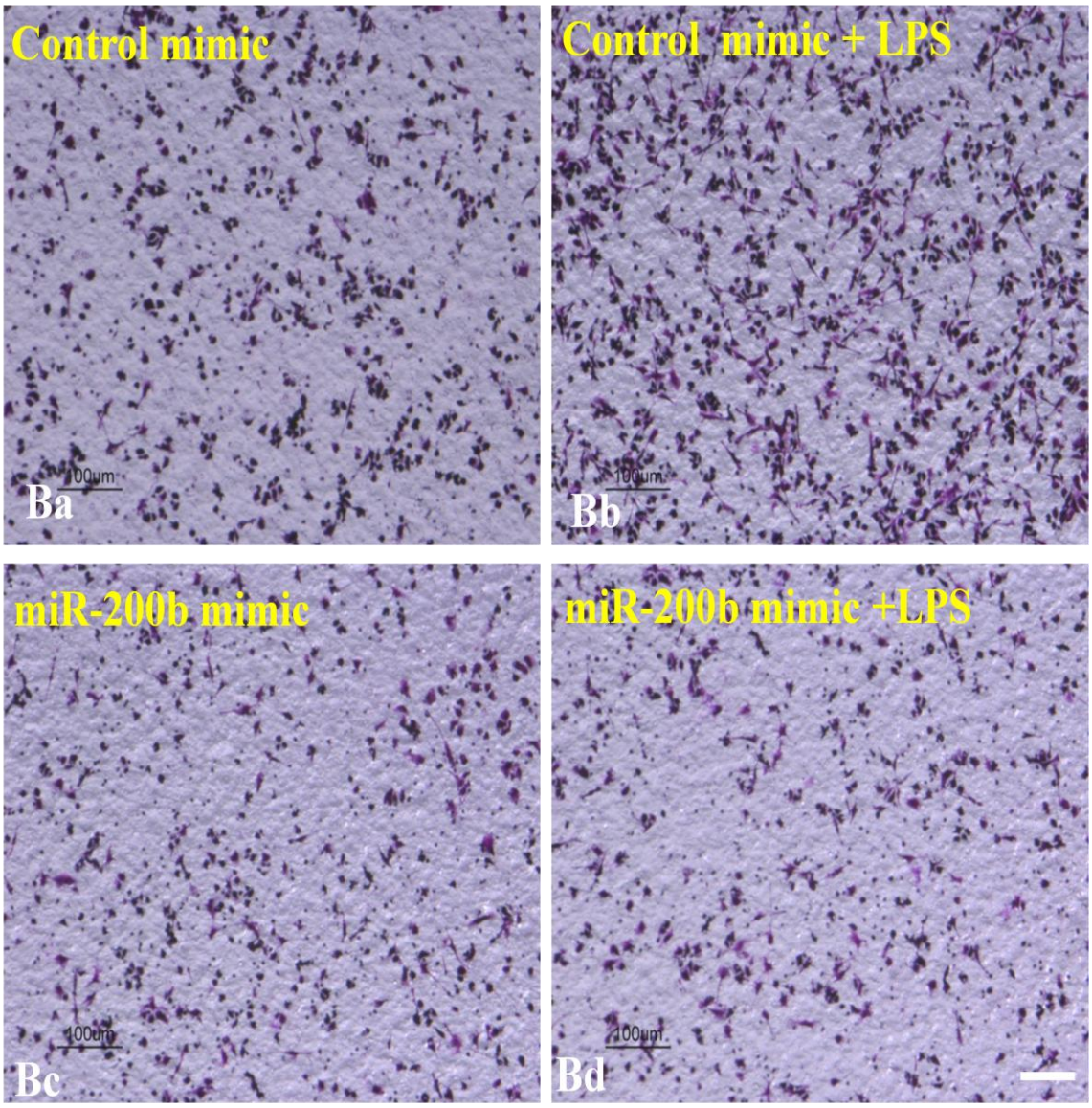

Fig 40 Aa-Bd: Phase contrast images showing migrated BV2 cells (purple) after miR-200b inhibition (Aa-Ad) and miR-200b overexpression (Ba-Bd) in activated microglia. Scale bars A-D: 100 µm.

C: Quantitative analysis of BV2 cell migration shows an increase in BV2 cell migration following activation. However miR-200b knockdown did not affect cell migration significantly. Statistical analysis was carried out using ANOVA with post-hoc Tukey test. Data represent the mean $\pm$ SD (n=3), $^{**}p<0.01$, $^{*}p<0.05$**.**

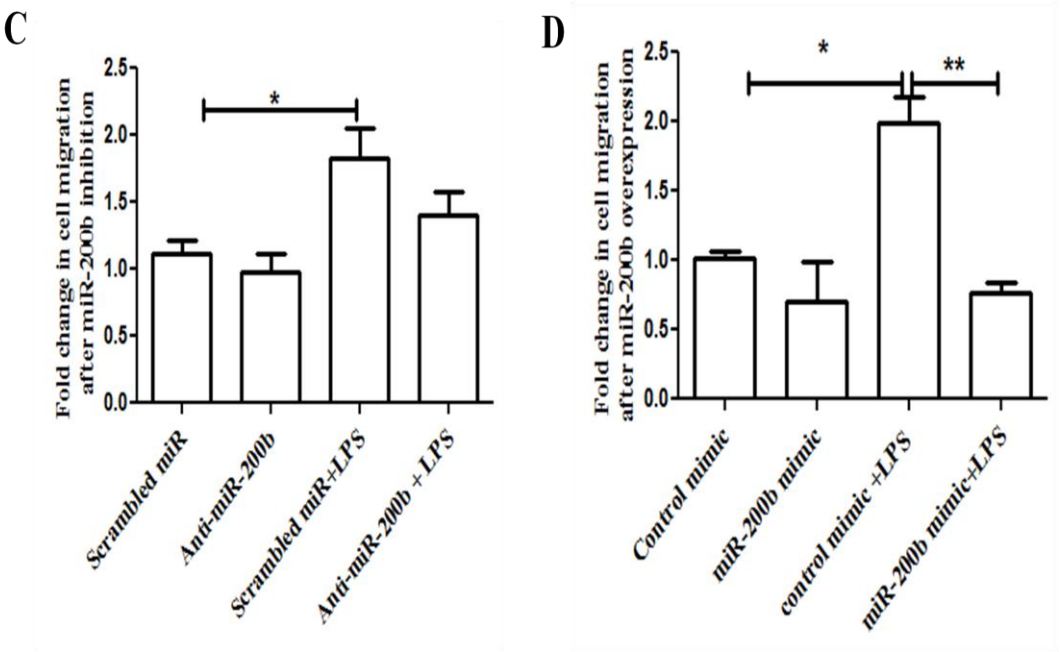

D: Quantitative analysis of BV2 cell migration shows an increase in BV2 cell migration following activation. MiR-200b overexpression resulted in significantly impaired migration of BV2 microglia. Statistical analysis was carried out using ANOVA with post-hoc Tukey test. Data represent the mean $\pm$ SD (n=3), $^{**}p<0.01$, $^{*}p<0.05$**.**

5 DISCUSSION

5.1 Activated microglia display distinct miRNA profile

Microglia, the immune cells of the central nervous system, protect the brain parenchyma against various insults *via* several effector functions such as secretion of proinflammatory cytokines, chemokines, cytotoxic factors as well as phagocytosis of cellular debris. However during an excessive microgliosis in response to chronic neuropathological conditions such as neuroinflammation or neurodegeneration, microglia secrete proinflammatory cytokines and cytotoxic factors excessively, exacerbating neuronal cell death (Dheen *et al.* 2007). Thus, there is a need for optimization of microglial functions to control microglia-mediated neuroinflammation. Recently, miRNAs have been shown to be involved in regulating microglia behavior and functions in diverse CNS pathologies including stroke, ischemic brain injuries (Selvamani *et al.* 2012; Zhao *et al.* 2013), multiple sclerosis (Ponomarev *et al.* 2011), and prion disease (Saba *et al.* 2012), by targeting numerous genes. However, a comprehensive catalogue showing the changes in miRNA expression in activated microglia is lacking. Towards this end, we carried out a microarray of microRNA expression profile and identified several differentially expressed miRNAs in activated microglia. Some miRNAs such as miR-21 and the miR-29 family identified in the microarray, have already been established to play a role in microglia-mediated neuroinflammation (Zhang *et al.* 2012; Thounaojam *et al.* 2014). Several other miRNAs such miR-101, miR-27a, also among the top hits obtained in the miRNA microarray in the present study, have been shown to be expressed in peripheral

macrophages, but their function in microglia remains to be elucidated (Zhu *et al.* 2010; Xie *et al.* 2014).

5.2 MiR-27a regulates the TGFβ-SMAD signaling pathway in microglia

5.2.1 MiR-27a is upregulated in activated microglia

In the current study, miR-27a expression was observed to be upregulated in activated primary microglia *in vitro* as well as *in vivo* (in activated microglial cells isolated from TBI model). Previosly, miR-27a upregulation was reported in peripheral macrophages activated with M1 (LPS + IFNγ) and M2b (LPS + Fcγ receptor) stimuli, indicating its role in peripheral macrophage differentiation toward distinct activation patterns (Graff *et al.* 2012). Additionally, the expression of miR-27b, a close homolog of miR-27a (20/21 nucleotide identity), has been shown to be upregulated 2.3 fold in response to LPS in human primary macrophages (Jennewein *et al.* 2010). These results suggest that upregulation of miR-27a in the present study, is associated with activation of microglia and may regulate the expression of genes involved in the inflammatory response of microglia.

5.2.2 MiR-27a targets key members of the TGFβ signaling pathway in microglia

In microglia, LPS which promotes proinflammation and TGFβ which is anti-inflammatory are mutually antagonistic (Mitchell *et al.* 2014). In the present

study, key regulators of the TGFβ1 signaling pathway, SMAD2 and TβR1 were observed to be downregulated, in activated microglia. *Loss-of-function* and *gain-of-function* studies confirmed that miR-27a targets TGFβ1 signaling pathway molecules including SMAD2 and TβR1 as shown in colon cancer where miR-27a interacts with the 3'UTR of SMAD2 (Bao *et al.* 2014). Although several miRNAs such as miR-140-5p (Yang *et al.* 2013), miR-142-3p (Lei *et al.* 2014) have been reported to target TβR1, this is the first report demonstrating TβR1 as a novel target of miR-27a in microglia.

TGFβ promotes SMAD2 activation by phosphorylation (Massagué 2000; Khalil *et al.* 2001). This SMAD2 phosphorylation was found to be increased in TGFβ activated microglia after knockdown of miR-27a, suggesting that SMAD2 expression and function are regulated by miR-27a in microglia. However, further study is required as the overexpression of miR-27a did not reduce the phosphorylation of SMAD2 significantly.

Runx1 is an important component of the TGFβ superfamily (Ito and Miyazono 2003) and has been shown to control microglial proliferation and activation in the rat brain after TBI (Logan *et al.* 2013). Further, Runx1 has also been shown to inhibit microglial proliferation and help promote the progression of amoeboid microglia to the ramified state (Zusso *et al.* 2012). Taken together these reports suggest that Runx1 is upregulated in activated microglia to control microglial activation possibly *via* inhibition of microglial proliferation. In this study, Runx1 expression was observed to be upregulated in LPS and TGFβ activated primary microglia *in vitro* as well as *in vivo* in LCM-extracted activated microglia cells from TBI rat model. Further, Runx1 was confirmed to be the target of miR-27a, similar to previously published

reports (Ben-Ami *et al.* 2009; Feng *et al.* 2009).Thus, in the current study, it is possible that Runx1 is upregulated in TGFβ activated microglia to control microglial activation. However, miR-27a alters Runx1 expression thereby inhibiting TGFβ signaling in activated microglia.

5.2.3 MiR-27a regulates the inflammatory response of microglia

In activated microglia, in response to various stimuli, such as infection, injury or neurodegeneration, excessive release of proinflammatory mediators such as TNFα, IL6, IL-1β, and NO has been shown to be mediated by the transcription factor, NFκB (Collart *et al.* 1990; Zielasek and Hartung 1996; Ghosh *et al.* 1998). In the current study, overexpression of miR-27a enhanced the proinflammatory response of activated microglia, as evidenced by increased expression of the proinflammatory cytokines, increased nuclear translocation of NFκB and downregulation of the alternate activation genes Arginase1 and Ym1. This enhanced proinflammatory response could be due to the result of inhibition of anti-inflammatory TGFβ signaling pathway by miR-27a in microglia *via* reduction of its mediators SMAD2 and TβR1. However, it needs to be ascertained if miR-27a directly acts on NFκB signaling pathway.

Moreover, mounting evidence suggests that miRNAs (such as miR-155 and miR-124) can regulate the polarization of peripheral macrophages and microglia towards M1 or M2 phenotype (Louafi *et al.* 2010; Martinez-Nunez *et al.* 2011; Ponomarev *et al.* 2011). By suppressing TGFβ signaling members, miR-27a appears to promote the polarization of microglia towards the M1 phenotype in the present study. However further experiments with more

number of alternate activation genes, need to be performed, to ascertain the same.

5.2.4 MiR-27a knockdown in microglia increases neuronal survival

TGFβ is an anti-inflammatory cytokine that functions as an immunomodulatory molecule to limit the potentially injurious effects of sustained or excess inflammatory reaction of microglia in the CNS (Lodge 1996; Kim, Won-Ki *et al.* 2004; Spittau *et al.* 2013). Overexpression or injection of TGFβ1 in the CNS suppresses microglial activation thereby limiting the expression proinflammatory chemokines after hypoxic/ischemic injury (Gross *et al.* 1993). In mixed glial cultures, microglia are the main source of TGFβ (Welser-Alves and Milner 2013), which is produced to inhibit the production of proinflammatory cytokines (Chao and Peterson 1995; Lodge 1996) and reactive oxygen intermediates. It has been postulated that low level of constitutively expressed TGFβ contributes to homeostasis of the healthy brain. Our studies on neuronal apoptosis after treatment with microglial conditioned medium suggest that miR-27a overexpression increases microglia-mediated neurotoxic effect. This observed increase in neuronal apoptosis in the culture exposed to conditioned medium derived from microglia after miR-27a overexpression, is most probably due to the result of an excessive release of proinflammatory cytokines in the conditioned medium, mediated *via* suppression of TGFβ signaling mediators. On the other hand, miR-27a knockdown decreases microglia-mediated neurotoxic effect possibly by reduction in the secretion of proinflammatory cytokines in the conditioned

medium. Overall, our results demonstrate that miR-27a knockdown is able to decrease microglia-mediated neurotoxicity and may, thus, represent a valuable therapeutic strategy in the context of chronic inflammation.

5.3 Mir-200b regulates the cJun/MAPK pathway in microglia

5.3.1 MiR-200b is downregulated in activated microglia

MicroRNA-200b (miR-200b) belongs to a family of five miRNAs with overlapping functions (Pecot *et al.* 2013). MiR-200b and miR-200c have been shown to regulate antibacterial innate immune response by targeting the TLR4 signaling pathway (Wendlandt *et al.* 2012). Further, miR-200c was found to be expressed in microglia, indicating a role for this family of miRNAs in regulating microglial functions in the CNS (Jovičić *et al.* 2013). The present work provides evidence, for the first time, that miR-200b is expressed in microglial cells and its expression is significantly down-regulated in activated microglial cells *in vitro* and *in vivo* model of TBI.

5.3.2 MiR-200b targets cJun in microglia

cJun, a member of the MAPK pathway, is activated in response to a number of stimuli in microglia *in vitro* (Kim *et al.* 2004; Waetzig *et al.* 2005) as well as in a number of neuropathologies *in vivo* such as brain injury (Pennypacker 1997), multiple sclerosis (Bonetti *et al.* 1999). An addition to this data is our result demonstrating the upregulation of cJun expression activated microglia from TBI rat model.

MAPKs have been shown to play critical roles in the pathogenesis of many neurological disorders, including ischemic stroke (Kuan *et al.* 2003), Parkinson's disease (PD) (Chipuk *et al.* 2008; Klegeris *et al.* 2008), amyotrophic lateral sclerosis (Bendotti *et al.* 2005) and Alzheimer's disease (AD) (Tamagno *et al.* 2003, 2005; Colombo *et al.* 2009). Thus inhibitors of MAPK pathways are being explored as potential therapeutic targets for ameliorating neuroinflammation in CNS pathologies (Cui *et al.* 2007). This current study has established miR-200b, a novel epigenetic factor as regulating cJun, a transcription factor of the JNK-MAPK pathway, in microglia, by directly targeting its 3'UTR. This is the first report demonstrating cJun as a novel target of miR-200b in microglia.

cJun function is activated by phosphorylation, which is mediated by JNK (Pulverer *et al.* 1991; Hibi *et al.* 1993). This cJun phosphorylation was found to be significantly increased in activated microglia after miR-200b knockdown and decreased after miR-200b overexpression, suggesting that miR-200b targets cJun and alters its expression and function in microglia.

5.3.3 MiR-200b negatively regulates the inflammatory response in microglia

JNK signaling in MAPK pathway plays a predominant role in secretion of proinflammatory cytokines and chemokines in activated primary microglia by LPS (Waetzig *et al.* 2005), while all three MAPK cascades (ERK, JNK and p38) are activated in BV2 microglia in response to LPS stimulation (Kim *et al.* 2004). In the present study, suppression of JNK activity in microglia by overexpression of miR-200b might be *via* downregulation of cJun expression

and function, suggesting a dysregulation of the JNK pathway in microglia. Further, the observed significant suppression of cytokine production as well as iNOS expression and NO production, by ovreexpression of miR-200b in microglia, might result from the miR-200b caused attenuation of cJun/JNK signaling.

5.3.4 MiR-200b knockdown in microglia increases neurotoxicity

Multiple lines of evidence suggests that chronic activation of microglia exacerbates the neuronal damage in different CNS pathologies (Tuppo and Arias 2005; Phani *et al.* 2012; Rubio-Perez and Morillas-Ruiz 2012). Findings in the present study suggest that inhibition of miR-200b increases microglia-mediated neurotoxic effect. This observed increase in neuronal apoptosis in the culture exposed to conditioned medium derived from culture of microglia treated with miR-200b inhibitor, is most probably due to the result of an excessive release of proinflammatory cytokines and NO in the conditioned medium mediated *via* increased cJun activity. However, further experiments are required to ascertain the possible neuroprotective role of microglial miR-200b since the overexpression of miR-200b in microglia failed to overcome the LPS-mediated neuronal apoptosis.

5.3.5 MiR-200b overexpression impairs microglial migration

It has been well established that activated microglia proliferate and migrate to the site of injury and infection for defense. Impaired microglial migration has been shown to contribute to the pathogenesis of several neuropathologies (Ciesielski-Treska *et al.* 2004; Park *et al.* 2008; Mizuno 2012). Our results

demonstrate that overexpression of miR-200b in activated microglia results in impaired migration. While it is unclear whether these observations are a result of a direct inhibition of cJun activity and its subsequent downstream targets or *via* targeting of other mRNA factors, this study provides a link between miRNA-mediated regulation of various microglial functions.

5.4 CONCLUSION

The smallest of the glial cells, microglia, is one cell with many functions from immune surveillance to neurogenesis (Nayak *et al.* 2014). The remarkable plasticity of these cells enables them to execute such a myriad variety of functions with ease. Morphologically and functionally, microglia are classified as postnatal/amoeboid, resting/ramified and activated (Ling and Wong 1993). Upon encountering any CNS insult, microglia undergo morphological changes and molecular and epigenetic transformation to become activated, accompanied by release of proinflammatory cytokines, chemokines, proteases and cytotoxic molecules such as NO and ROS (Aloisi 2001). Furthermore, chronic activation of microglia leads to excessive release of proinflammatory mediators, exaggerating the neuronal death in several neuropathologies such as neurodegenerative diseases, injury and infection. Thus, it is important to understand the molecular and epigenetic mechanisms underlying microglial activation, to develop therapeutics to control microglial mediated neuroinflammation (Banati and Graeber 1994; Stoll and Jander 1999). While

the molecular changes accompanying this transformation are well documented, the epigenetic changes such as histone modifications and miRNAs need to be examined in detail.

To address this gap in literature, a miRNA microarray comparing control and activated primary microglia was carried out in the present study which established a database of differentially expressed miRNAs in microglia. Two miRNAs were chosen for their putative proinflammatory (miR-27a, since it was upregulated in activated microglia) and anti-inflammatory (miR-200b since its expression was decreased in activated microglia) potential. These miRNAs were shown to target pathways either bringing about microglial quiescence (TGFβ) or in aiding the inflammatory cascade (MAPK), in microglia.

To conclude, two *in vitro* mechanisms of miRNA mediated regulation of microglial functions including inflammatory response, migration and neurotoxicity have been demonstrated in the present study (Illustration 6).

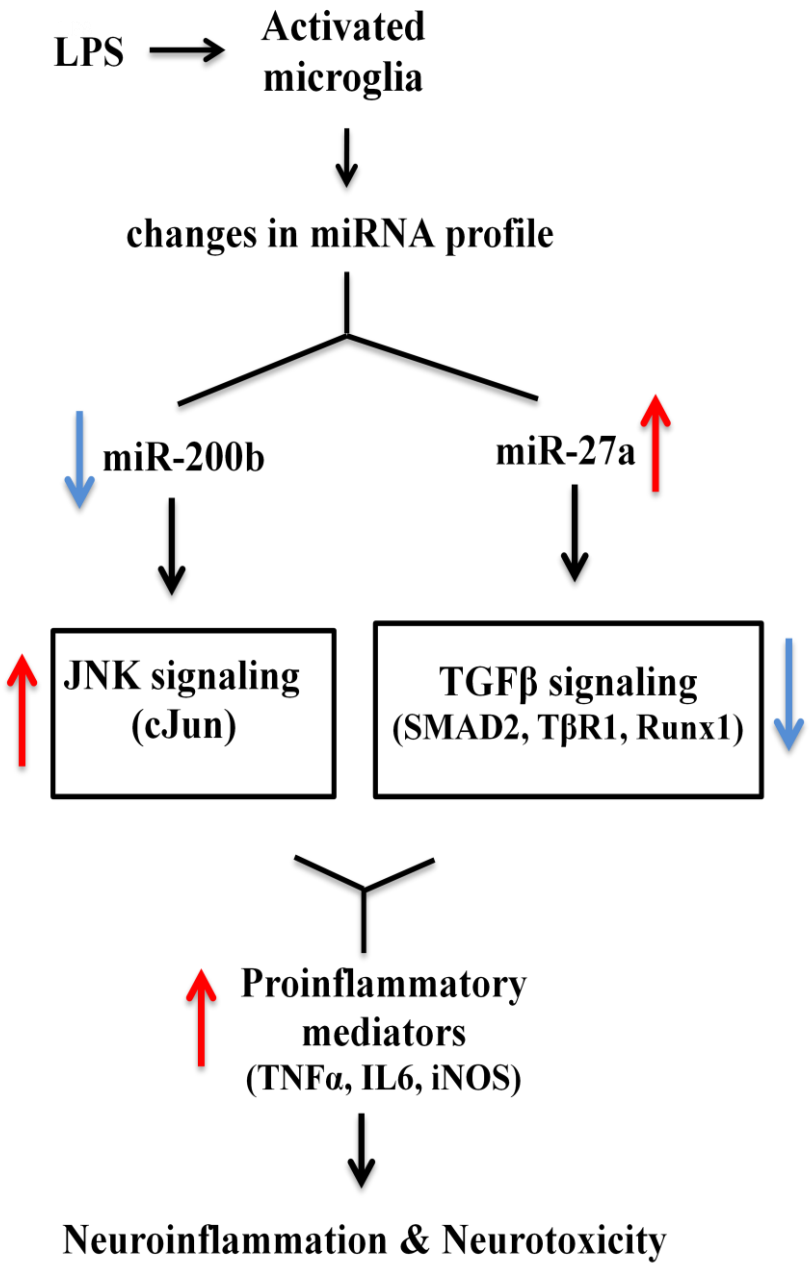

Illustration 6: Epigenetic mechanism of microglial-mediated neuroinflammation. There was a downregulation of miR-200b and in contrast, upregulation of miR-27a in microglia activated by LPS. MiR-200b targets cJun and thus the downregulation of miR-200b in activated microglia enhances the expression of cJun, which subsequently contributes to upregulation of proinflammatory mediators (TNF-α, IL6, iNOS) and neurotoxicity. On the other hand, miR-27a targets TGF-β signaling and its upregulation in activated microglia, downregulates the anti-inflammatory mediators (SMAD2, TβR1), thereby resulting in neuroinflammation and neurotoxicity.

5.5 FUTURE DIRECTIONS

Post-transcriptional reduction of protein expression of selected genes linked to a disease by a particular functional miRNA represents new therapeutic options. The current study identifies two miRNAs in microglia having therapeutic potential and focuses on the *in vitro* mechanism of miRNA mediated regulation of microglial neuroinflammation.

To elucidate the therapeutic potential of the miRNAs under consideration, it is important to study their mechanism of action *in vivo* in an animal model of neuropathy such as traumatic brain injury or stroke. This can be achieved by administration of the miRNA mimic or miRNA inhibitor intracranially. However, since the miRNA mimic/inhibitor would not be targeted towards a particular cell type, such analysis would only provide information on the general effect of the overexpression/knockdown of the specific miRNA under consideration, on the disease condition *in vivo.*

Further studies can also include specifically targeting microglia *in vivo* by exploiting the presence of CX3CR1 receptor which is solely expressed by microglia in the brain and using synthetic delivery materials such as liposomes (Zhang *et al.* 2013).

It has been seen that injection of miR-124 in the brain has the potential to reduce EAE (Ponomarev *et al.* 2011). Further, knockdown of another brain enriched miRNA, miR-181, could provide protection against ischemia induced neuronal death by targeting the chaperone protein GRP78 thus influencing the

outcome of cerebral ischemia (Ouyang *et al.* 2012). Taken together, these results suggest that *in vivo* administration of miRNA inhibitors or mimics could serve as therapeutic agents to reduce microglia-mediated neuroinflammation.

6 REFERENCES

Adle-Biassette, H., Chrétien, F., Wingertsmann, L., Héry, C., Ereau, T., Scaravilli, F., Tardieu, M., and Gray, F. (1999) Neuronal apoptosis does not correlate with dementia in HIV infection but is related to microglial activation and axonal damage. *Neuropathol. Appl. Neurobiol.*, **25**, 123–133.

Aguzzi, A., Barres, B.A., and Bennett, M.L. (2013) Microglia: scapegoat, saboteur, or something else? *Science*, **339**, 156–161.

Åkerblom, M., Sachdeva, R., Barde, I., Verp, S., Gentner, B., Trono, D., and Jakobsson, J. (2012) MicroRNA-124 is a subventricular zone neuronal fate determinant. *J. Neurosci.*, **32**, 8879–8889.

Akira, S. and Takeda, K. (2004) Toll-like receptor signalling. *Nat. Rev. Immunol.*, **4**, 499–511.

Aloisi, F. (2001) Immune function of microglia. *Glia*, **36**, 165–179.

Aloisi, F., De Simone, R., Columba-Cabezas, S., and Levi, G. (1999) Opposite effects of interferon-gamma and prostaglandin E2 on tumor necrosis factor and interleukin-10 production in microglia: a regulatory loop controlling microglia pro- and anti-inflammatory activities. *J. Neurosci. Res.*, **56**, 571–580.

Ameres, S.L. and Zamore, P.D. (2013) Diversifying microRNA sequence and function. *Nat. Rev. Mol. Cell Biol.*, **14**, 475–488.

Baby, N., Li, Y., Ling, E.-A., Lu, J., and Dheen, S.T. (2014) Runx1t1 (Runt-related transcription factor 1; translocated to, 1) epigenetically regulates the proliferation and nitric oxide production of microglia. *PLoS One*, **9**, e89326.

Bala, S., Marcos, M., Kodys, K., Csak, T., Catalano, D., Mandrekar, P., and Szabo, G. (2011) Up-regulation of microRNA-155 in macrophages

contributes to increased tumor necrosis factor {alpha} (TNF{alpha}) production via increased mRNA half-life in alcoholic liver disease. *J. Biol. Chem.*, **286**, 1436–1444.

Balashov, K.E., Rottman, J.B., Weiner, H.L., and Hancock, W.W. (1999) CCR5(+) and CXCR3(+) T cells are increased in multiple sclerosis and their ligands MIP-1alpha and IP-10 are expressed in demyelinating brain lesions. *Proc. Natl. Acad. Sci. U. S. A.*, **96**, 6873–6878.

Banati, R.B. and Graeber, M.B. (1994) Surveillance, intervention and cytotoxicity: is there a protective role of microglia? *Dev. Neurosci.*, **16**, 114–127.

Bao, Y., Chen, Z., Guo, Y., Feng, Y., Li, Z., Han, W., Wang, J., Zhao, W., Jiao, Y., Li, K., Wang, Q., Wang, J., Zhang, H., Wang, L., and Yang, W. (2014) Tumor Suppressor MicroRNA-27a in Colorectal Carcinogenesis and Progression by Targeting SGPP1 and Smad2. *PLoS One*, **9**, e105991.

Bartel, D.P. (2009) MicroRNAs: target recognition and regulatory functions. *Cell*, **136**, 215–233.

Becher, B., Prat, A., and Antel, J.P. (2000) Brain-immune connection: immuno-regulatory properties of CNS-resident cells. *Glia*, **29**, 293–304.

Ben-Ami, O., Pencovich, N., Lotem, J., Levanon, D., and Groner, Y. (2009) A regulatory interplay between miR-27a and Runx1 during megakaryopoiesis. *Proc. Natl. Acad. Sci. U. S. A.*, **106**, 238–243.

Bendotti, C., Bao Cutrona, M., Cheroni, C., Grignaschi, G., Lo Coco, D., Peviani, M., Tortarolo, M., Veglianese, P., and Zennaro, E. (2005) Inter- and intracellular signaling in amyotrophic lateral sclerosis: role of p38 mitogen-activated protein kinase. *Neurodegener. Dis.*, **2**, 128–134.

Benveniste, N. (1992) Inflammatory cytokines within the central nervous sources , function , and mechanism of action system :

Boche, D., Perry, V.H., and Nicoll, J. a R. (2013) Review: activation patterns of microglia and their identification in the human brain. *Neuropathol. Appl. Neurobiol.*, **39**, 3–18.

Boddeke, E.W., Meigel, I., Frentzel, S., Gourmala, N.G., Harrison, J.K., Buttini, M., Spleiss, O., and Gebicke-Härter, P. (1999) Cultured rat microglia express functional beta-chemokine receptors. *J. Neuroimmunol.*, **98**, 176–184.

Bonetti, B., Stegagno, C., Cannella, B., Rizzuto, N., Moretto, G., and Raine, C.S. (1999) Activation of NF-kappaB and c-jun transcription factors in multiple sclerosis lesions. Implications for oligodendrocyte pathology. *Am. J. Pathol.*, **155**, 1433–1438.

Bradford, M.M. (1976) A rapid and sensitive method for the quantitation of microgram quantities of protein utilizing the principle of protein-dye binding. *Anal. Biochem.*, **72**, 248–254.

Brasier, A.R. (2006) The NF-kappaB regulatory network. *Cardiovasc. Toxicol.*, **6**, 111–130.

Brecht, S., Kirchhof, R., Chromik, A., Willesen, M., Nicolaus, T., Raivich, G., Wessig, J., Waetzig, V., Goetz, M., Claussen, M., Pearse, D., Kuan, C.-Y., Vaudano, E., Behrens, A., Wagner, E., Flavell, R. a, Davis, R.J., and Herdegen, T. (2005) Specific pathophysiological functions of JNK isoforms in the brain. *Eur. J. Neurosci.*, **21**, 363–377.

Buss, R.R., Sun, W., and Oppenheim, R.W. (2006) Adaptive roles of programmed cell death during nervous system development. *Annu. Rev. Neurosci.*, **29**, 1–35.

Bustin, S. (2000) Absolute quantification of mRNA using real-time reverse transcription polymerase chain reaction assays. *J. Mol. Endocrinol.*, **25**, 169–193.

Butovsky, O., Jedrychowski, M.P., Moore, C.S., Cialic, R., Amanda, J., Gabriely, G., Koeglsperger, T., Dake, B., Wu, P.M., Camille, E., Fanek, Z., Liu, L., Chen, Z., Rothstein, J.D., Richard, M., Gygi, S.P., Antel, J.P., and Weiner, H.L. (2014) Identification of a unique TGF-b dependent Molecular Functional signature in microglia. *Nat. Neurosci.*, **17**, 131–143.

Campbell, K.S. and Colonna, M. (1999) DAP12: a key accessory protein for relaying signals by natural killer cell receptors. *Int. J. Biochem. Cell Biol.*, **31**, 631–636.

Cao, X., Pfaff, S.L., and Gage, F.H. (2007) A functional study of miR-124 in the developing neural tube. *Genes Dev.*, **21**, 531–536.

Cao, Z., Tanaka, M., Regnier, C., Rothe, M., Yamit-hezi, A., Woronicz, J.D., Fuentes, M.E., Durnin, M.H., Dalrymple, S.A., and Goeddel, D. V (1999) NF-kappa B activation by tumor necrosis factor and interleukin-1. *Cold Spring Harb. Symp. Quant. Biol.*, **64**, 473–483.

Cardona, A.E., Pioro, E.P., Sasse, M.E., Kostenko, V., Cardona, S.M., Dijkstra, I.M., Huang, D., Kidd, G., Dombrowski, S., Dutta, R., Lee, J.-C., Cook, D.N., Jung, S., Lira, S.A., Littman, D.R., and Ransohoff, R.M. (2006) Control of microglial neurotoxicity by the fractalkine receptor. *Nat. Neurosci.*, **9**, 917–924.

Cardoso, A.L., Guedes, J.R., Pereira de Almeida, L., and Pedroso de Lima, M.C. (2012) miR-155 modulates microglia-mediated immune response by down-regulating SOCS-1 and promoting cytokine and nitric oxide production. *Immunology*, **135**, 73–88.

Cazareth, J., Guyon, A., Heurteaux, C., Chabry, J., and Petit-Paitel, A. (2014) Molecular and cellular neuroinflammatory status of mouse brain after systemic lipopolysaccharide challenge: importance of CCR2/CCL2 signaling. *J. Neuroinflammation*, **11**, 132.

Chan, W.Y., Kohsaka, S., and Rezaie, P. (2007) The origin and cell lineage of microglia: new concepts. *Brain Res. Rev.*, **53**, 344–354.

Chao, C. and Peterson, K. (1995) Modulation cytokines of human microglial cell superoxide production by **58**, 65–70.

Chao, C.C., Hu, S., Sheng, W.S., and Peterson, P.K. (1995) Tumor necrosis factor-alpha production by human fetal microglial cells: regulation by other cytokines. *Dev. Neurosci.*, **17**, 97–105.

Chao, C.C., Hu, S., Sheng, W.S., Tsang, M., and Peterson, P.K. (1995) Tumor necrosis factor-alpha mediates the release of bioactive transforming growth factor-beta in murine microglial cell cultures. *Clin. Immunol. Immunopathol.*, **77**, 358–365.

Chaudhuri, A.A., So, A.Y.-L., Sinha, N., Gibson, W.S.J., Taganov, K.D., O'Connell, R.M., and Baltimore, D. (2011) MicroRNA-125b potentiates macrophage activation. *J. Immunol.*, **187**, 5062–5068.

Chipuk, J.E., Fisher, J.C., Dillon, C.P., Kriwacki, R.W., Kuwana, T., and Green, D.R. (2008) Mechanism of apoptosis induction by inhibition of the anti-apoptotic BCL-2 proteins. *Proc. Natl. Acad. Sci. U. S. A.*, **105**, 20327–20332.

Chomczynski, P. and Sacchi, N. (2006) The single-step method of RNA isolation by acid guanidinium thiocyanate-phenol-chloroform extraction: twenty-something years on. *Nat. Protoc.*, **1**, 581–585.

Ciesielski-Treska, J., Grant, N.J., Ulrich, G., Corrotte, M., Bailly, Y., Haeberle, A.-M., Chasserot-Golaz, S., and Bader, M.-F. (2004) Fibrillar prion peptide (106-126) and scrapie prion protein hamper phagocytosis in microglia. *Glia*, **46**, 101–115.

Collart, M.A., Baeuerle, P., and Vassalli, P. (1990) Regulation of tumor necrosis factor alpha transcription in macrophages : involvement of four

kappa B-like motifs and of constitutive and Regulation of Tumor Necrosis Factor Alpha Transcription in Macrophages : Involvement of Four KB-Like Motifs and of Con. *Mol Cell Biol*, **10**, 1498–1506.

Colombo, A., Bastone, A., Ploia, C., Sclip, A., Salmona, M., Forloni, G., and Borsello, T. (2009) JNK regulates APP cleavage and degradation in a model of Alzheimer's disease. *Neurobiol. Dis.*, **33**, 518–525.

Colton, C. a (2009) Heterogeneity of microglial activation in the innate immune response in the brain. *J. Neuroimmune Pharmacol.*, **4**, 399–418.

Cui, J., Zhang, M., Zhang, Y.-Q., and Xu, Z.-H. (2007) JNK pathway: diseases and therapeutic potential. *Acta Pharmacol. Sin.*, **28**, 601–608.

Cunningham, C.L., Martínez-Cerdeño, V., and Noctor, S.C. (2013) Microglia regulate the number of neural precursor cells in the developing cerebral cortex. *J. Neurosci.*, **33**, 4216–4233.

Davalos, D., Grutzendler, J., Yang, G., Kim, J. V, Zuo, Y., Jung, S., Littman, D.R., Dustin, M.L., and Gan, W.-B. (2005) ATP mediates rapid microglial response to local brain injury in vivo. *Nat. Neurosci.*, **8**, 752–758.

De Jong, E.K., de Haas, A.H., Brouwer, N., van Weering, H.R.J., Hensens, M., Bechmann, I., Pratley, P., Wesseling, E., Boddeke, H.W.G.M., and Biber, K. (2008) Expression of CXCL4 in microglia in vitro and in vivo and its possible signaling through CXCR3. *J. Neurochem.*, **105**, 1726–1736.

Delaloy, C., Liu, L., Lee, J.-A., Su, H., Shen, F., Yang, G.-Y., Young, W.L., Ivey, K.N., and Gao, F.-B. (2010) MicroRNA-9 coordinates proliferation and migration of human embryonic stem cell-derived neural progenitors. *Cell Stem Cell*, **6**, 323–335.

Dheen, S.T., Kaur, C., and Ling, E.-A. (2007) Microglial activation and its implications in the brain diseases. *Curr. Med. Chem.*, **14**, 1189–1197.

Dixon, C.E., Lyeth, B.G., Povlishock, J.T., Findling, R.L., Hamm, R.J., Marmarou, A., Young, H.F., and Hayes, R.L. (1987) A fluid percussion model of experimental brain injury in the rat. *J. Neurosurg.*, **67**, 110–119.

Dohi, K., Ohtaki, H., Nakamachi, T., Yofu, S., Satoh, K., Miyamoto, K., Song, D., Tsunawaki, S., Shioda, S., and Aruga, T. (2010) Gp91phox (NOX2) in classically activated microglia exacerbates traumatic brain injury. *J. Neuroinflammation*, **7**, 41.

Doorn, K.J., Drukarch, B., van Dam, A.-M., and Lucassen, P.J. (2014) Hippocampal proliferation is increased in presymptomatic Parkinson's disease and due to microglia. *Neural Plast.*, **2014**, 959154.

Dopp, J.M., Mackenzie-Graham, A., Otero, G.C., and Merrill, J.E. (1997) Differential expression, cytokine modulation, and specific functions of type-1 and type-2 tumor necrosis factor receptors in rat glia. *J. Neuroimmunol.*, **75**, 104–112.

Dünker, N. and Krieglstein, K. (2000) Targeted mutations of transforming growth factor-beta genes reveal important roles in mouse development and adult homeostasis. *Eur. J. Biochem.*, **267**, 6982–6988.

Dweep, H., Sticht, C., Pandey, P., and Gretz, N. (2011) miRWalk--database: prediction of possible miRNA binding sites by "walking" the genes of three genomes. *J. Biomed. Inform.*, **44**, 839–847.

Edbauer, D., Neilson, J.R., Foster, K.A., Wang, C.-F., Seeburg, D.P., Batterton, M.N., Tada, T., Dolan, B.M., Sharp, P.A., and Sheng, M. (2010) Regulation of synaptic structure and function by FMRP-associated microRNAs miR-125b and miR-132. *Neuron*, **65**, 373–384.

Engvall, E. and Perlmann, P. (1971) Enzyme-linked immunosorbent assay (ELISA). Quantitative assay of immunoglobulin G. *Immunochemistry*, **8**, 871–874.

Enright, A.J., John, B., Gaul, U., Tuschl, T., Sander, C., and Marks, D.S. (2003) MicroRNA targets in Drosophila. *Genome Biol.*, **5**, R1.

Epstein, L.G. and Gendelman, H.E. (1993) Human immunodeficiency virus type 1 infection of the nervous system: pathogenetic mechanisms. *Ann. Neurol.*, **33**, 429–436.

Erblich, B., Zhu, L., Etgen, A.M., Dobrenis, K., and Pollard, J.W. (2011) Absence of colony stimulation factor-1 receptor results in loss of microglia, disrupted brain development and olfactory deficits. *PLoS One*, **6**, e26317.

Fabian, M.R. and Sonenberg, N. (2012) The mechanics of miRNA-mediated gene silencing: a look under the hood of miRISC. *Nat. Struct. Mol. Biol.*, **19**, 586–593.

Faraco, G., Pittelli, M., Cavone, L., Fossati, S., Porcu, M., Mascagni, P., Fossati, G., Moroni, F., and Chiarugi, A. (2009) Histone deacetylase (HDAC) inhibitors reduce the glial inflammatory response in vitro and in vivo. *Neurobiol. Dis.*, **36**, 269–279.

Feng, J., Iwama, A., Satake, M., and Kohu, K. (2009) MicroRNA-27 enhances differentiation of myeloblasts into granulocytes by post-transcriptionally downregulating Runx1. *Br. J. Haematol.*, **145**, 412–423.

Fenn, A.M., Smith, K.M., Lovett-Racke, A.E., Guerau-de-Arellano, M., Whitacre, C.C., and Godbout, J.P. (2013) Increased micro-RNA 29b in the aged brain correlates with the reduction of insulin-like growth factor-1 and fractalkine ligand. *Neurobiol. Aging*, **34**, 2748–2758.

Fernandez, E.J. and Lolis, E. (2002) Structure, function, and inhibition of chemokines. *Annu. Rev. Pharmacol. Toxicol.*, **42**, 469–499.

Filipovic, R., Jakovcevski, I., and Zecevic, N. (2003) GRO-alpha and CXCR2 in the human fetal brain and multiple sclerosis lesions. *Dev. Neurosci.*, **25**, 279–290.

Fineberg, S.K., Kosik, K.S., and Davidson, B.L. (2009) MicroRNAs potentiate neural development. *Neuron*, **64**, 303–309.

Follert, P., Cremer, H., and Béclin, C. (2014) MicroRNAs in brain development and function: a matter of flexibility and stability. *Front. Mol. Neurosci.*, **7**, 5.

Franke, H., Schepper, C., Illes, P., and Krügel, U. (2007) Involvement of P2X and P2Y receptors in microglial activation in vivo. *Purinergic Signal.*, **3**, 435–445.

Fritschy Jean-marc, H.W. (2001) *Immunofluorescence*. John Wiley & Sons, Ltd, Chichester.

Garden, G.A. (2013) Epigenetics and the modulation of neuroinflammation. *Neurotherapeutics*, **10**, 782–788.

Garin, J., Diez, R., Kieffer, S., Dermine, J.F., Duclos, S., Gagnon, E., Sadoul, R., Rondeau, C., and Desjardins, M. (2001) The phagosome proteome: insight into phagosome functions. *J. Cell Biol.*, **152**, 165–180.

Garzon, R. and Marcucci, G. (2012) Potential of microRNAs for cancer diagnostics, prognostication and therapy. *Curr. Opin. Oncol.*, **24**, 655–659.

Gemma, C. and Bachstetter, A.D. (2013) The role of microglia in adult hippocampal neurogenesis. *Front. Cell. Neurosci.*, **7**, 229.

Ghafouri, M., Amini, S., Khalili, K., and Sawaya, B.E. (2006) HIV-1 associated dementia: symptoms and causes. *Retrovirology*, **3**, 28.

Ghosh, A. and Chaudhuri, S. (2010) Microglial action in glioma: a boon turns bane. *Immunol. Lett.*, **131**, 3–9.

Ghosh, S., May, M.J., and Kopp, E.B. (1998) NF-kappa B and Rel proteins: evolutionarily conserved mediators of immune responses. *Annu. Rev. Immunol.*, **16**, 225–260.

Gilmore, T.D. (2006) Introduction to NF-kappaB: players, pathways, perspectives. *Oncogene*, **25**, 6680–6684.

Ginhoux, F., Greter, M., Leboeuf, M., Nandi, S., See, P., Gokhan, S., Mehler, M.F., Conway, S.J., Ng, L.G., Stanley, E.R., Samokhvalov, I.M., and Merad, M. (2010) Fate mapping analysis reveals that adult microglia derive from primitive macrophages. *Science*, **330**, 841–845.

Giulian, D. (1999) Microglia and the immune pathology of Alzheimer disease. *Am. J. Hum. Genet.*, **65**, 13–18.

Giulian, D. and Baker, J. (1986) Characterization of Ameboid Mammalian Brain Microglia Isolated from Developing **6**, 2163–2178.

Glanzer, J.G., Enose, Y., Wang, T., Kadiu, I., Gong, N., Rozek, W., Liu, J., Schlautman, J.D., Ciborowski, P.S., Thomas, M.P., and Gendelman, H.E. (2007) Genomic and proteomic microglial profiling: pathways for neuroprotective inflammatory responses following nerve fragment clearance and activation. *J. Neurochem.*, **102**, 627–645.

Gould, S.J. and Subramani, S. (1988) Firefly luciferase as a tool in molecular and cell biology. *Anal. Biochem.*, **175**, 5–13.

Graeber, M.B. (2010) Changing face of microglia. *Science*, **330**, 783–788.

Graeber, M.B., Scheithauer, B.W., and Kreutzberg, G.W. (2002) Microglia in brain tumors. *Glia*, **40**, 252–259.

Graff, J.W., Dickson, A.M., Clay, G., McCaffrey, A.P., and Wilson, M.E. (2012) Identifying functional microRNAs in macrophages with polarized phenotypes. *J. Biol. Chem.*, **287**, 21816–21825.

Gross, C.E., Bednar, M.M., Howard, D.B., and Sporn, M.B. (1993) Transforming growth factor-beta 1 reduces infarct size after experimental cerebral ischemia in a rabbit model. *Stroke*, **24**, 558–562.

Grün, D., Wang, Y.-L., Langenberger, D., Gunsalus, K.C., and Rajewsky, N. (2005) microRNA target predictions across seven Drosophila species and comparison to mammalian targets. *PLoS Comput. Biol.*, **1**, e13.

Gu, X., Meng, S., Liu, S., Jia, C., Fang, Y., Li, S., Fu, C., Song, Q., Lin, L., and Wang, X. (2014) miR-124 represses ROCK1 expression to promote neurite elongation through activation of the PI3K/Akt signal pathway. *J. Mol. Neurosci.*, **52**, 156–165.

Guedes, J.R., Custódia, C.M., Silva, R.J., de Almeida, L.P., Pedroso de Lima, M.C., and Cardoso, A.L. (2014) Early miR-155 upregulation contributes to neuroinflammation in Alzheimer's disease triple transgenic mouse model. *Hum. Mol. Genet.*,.

Hanisch, U.-K. (2002) Microglia as a source and target of cytokines. *Glia*, **40**, 140–155.

Hanisch, U.-K. (2013) Functional diversity of microglia - how heterogeneous are they to begin with? *Front. Cell. Neurosci.*, **7**, 65.

Hanisch, U.-K. and Kettenmann, H. (2007) Microglia: active sensor and versatile effector cells in the normal and pathologic brain. *Nat. Neurosci.*, **10**, 1387–1394.

Hassan, N.F., Rifat, S., Campbell, D.E., McCawley, L.J., and Douglas, S.D. (1991) Isolation and flow cytometric characterization of newborn mouse brain-derived microglia maintained in vitro. *J. Leukoc. Biol.*, **50**, 86–92.

Heneka, M.T., Rodríguez, J.J., and Verkhratsky, A. (2010) Neuroglia in neurodegeneration. *Brain Res. Rev.*, **63**, 189–211.

Henn, A., Lund, S., Hedtjärn, M., Schrattenholz, A., Pörzgen, P., and Leist, M. (2009) The suitability of BV2 cells as alternative model system for primary microglia cultures or for animal experiments examining brain inflammation. *ALTEX*, **26**, 83–94.

Heppner, F.L., Prinz, M., and Aguzzi, A. (2001) Pathogenesis of prion diseases: possible implications of microglial cells. *Prog. Brain Res.*, **132**, 737–750.

Hernandez-Ontiveros, D.G., Tajiri, N., Acosta, S., Giunta, B., Tan, J., and Borlongan, C. V (2013) Microglia activation as a biomarker for traumatic brain injury. *Front. Neurol.*, **4**, 30.

Hibi, M., Lin, A., Smeal, T., Minden, A., and Karin, M. (1993) Identification of an oncoprotein- and UV-responsive protein kinase that binds and potentiates the c-Jun activation domain. *Genes Dev.*, **7**, 2135–2148.

Hirt, U.A. and Leist, M. (2003) Rapid, noninflammatory and PS-dependent phagocytic clearance of necrotic cells. *Cell Death Differ.*, **10**, 1156–1164.

Hoek, R.M., Ruuls, S.R., Murphy, C.A., Wright, G.J., Goddard, R., Zurawski, S.M., Blom, B., Homola, M.E., Streit, W.J., Brown, M.H., Barclay, A.N., and Sedgwick, J.D. (2000) Down-regulation of the macrophage lineage through interaction with OX2 (CD200). *Science*, **290**, 1768–1771.

Hu, S., Chao, C.C., Ehrlich, L.C., Sheng, W.S., Sutton, R.L., Rockswold, G.L., and Peterson, P.K. (1999) Inhibition of microglial cell RANTES

production by IL-10 and TGF- ᴺᴸ mal T cell expressed and secreted) production **65**, 815–821.

Hu, S., Sheng, W.S., Peterson, P.K., and Chao, C.C. (1995) Cytokine modulation of murine microglial cell superoxide production. *Glia*, **13**, 45–50.

Hu, X., Li, P., Guo, Y., Wang, H., Leak, R.K., Chen, S., Gao, Y., and Chen, J. (2012) Microglia/macrophage polarization dynamics reveal novel mechanism of injury expansion after focal cerebral ischemia. *Stroke.*, **43**, 3063–3070.

Hughes, P.M., Botham, M.S., Frentzel, S., Mir, A., and Perry, V.H. (2002) Expression of fractalkine (CX3CL1) and its receptor, CX3CR1, during acute and chronic inflammation in the rodent CNS. *Glia*, **37**, 314–327.

Hurley, S.D., Walter, S.A., Semple-Rowland, S.L., and Streit, W.J. (1999) Cytokine transcripts expressed by microglia in vitro are not expressed by ameboid microglia of the developing rat central nervous system. *Glia*, **25**, 304–309.

Ifuku, M., Färber, K., Okuno, Y., Yamakawa, Y., Miyamoto, T., Nolte, C., Merrino, V.F., Kita, S., Iwamoto, T., Komuro, I., Wang, B., Cheung, G., Ishikawa, E., Ooboshi, H., Bader, M., Wada, K., Kettenmann, H., and Noda, M. (2007) Bradykinin-induced microglial migration mediated by B1-bradykinin receptors depends on Ca2+ influx via reverse-mode activity of the Na+/Ca2+ exchanger. *J. Neurosci.*, **27**, 13065–13073.

Imamoto, K. and Leblond, C.P. (1978) Radioautographic investigation of gliogenesis in the corpus callosum of young rats. II. Origin of microglial cells. *J. Comp. Neurol.*, **180**, 139–163.

Irino, Y., Nakamura, Y., Inoue, K., Kohsaka, S., and Ohsawa, K. (2008) Akt activation is involved in P2Y12 receptor-mediated chemotaxis of microglia. *J. Neurosci. Res.*, **86**, 1511–1519.

Ishizuka, K., Kimura, T., Igata-yi, R., Katsuragi, S., Takamatsu, J., and Miyakawa, T. (1997) Identification of monocyte chemoattractant protein-1 in senile plaques and reactive microglia of Alzheimer's disease. *Psychiatry Clin. Neurosci.*, **51**, 135–138.

Ito, Y. and Miyazono, K. (2003) RUNX transcription factors as key targets of TGF-beta superfamily signaling. *Curr. Opin. Genet. Dev.*, **13**, 43–47.

Jadhav, S.P., Kamath, S.P., Choolani, M., Lu, J., and Dheen, S.T. (2014) microRNA-200b modulates microglia-mediated neuroinflammation via the cJun/MAPK pathway. *J. Neurochem.*, **130**, 388–401.

Jadhav, V.S., Krause, K.-H., and Singh, S.K. (2014) HIV-1 Tat C modulates NOX2 and NOX4 expressions through miR-17 in a human microglial cell line. *J. Neurochem.*, 1–13.

Janabi, N., Mirshahi, A., Wolfrom, C., Mirshahi, M., and Tardieu, M. (1996) Effect of interferon gamma and TNF alpha on the differentiation/activation of human glial cells: implication for the TNF alpha receptor 1. *Res. Virol.*, **147**, 147–153.

Jennewein, C., von Knethen, A., Schmid, T., and Brüne, B. (2010) MicroRNA-27b contributes to lipopolysaccharide-mediated peroxisome proliferator-activated receptor gamma (PPARgamma) mRNA destabilization. *J. Biol. Chem.*, **285**, 11846–11853.

Ji, K., Akgul, G., Wollmuth, L.P., and Tsirka, S.E. (2013) Microglia actively regulate the number of functional synapses. *PLoS One*, **8**, e56293.

Jin, L. and Lloyd, R. V (1997) In situ hybridization: methods and applications. *J. Clin. Lab. Anal.*, **11**, 2–9.

John, B., Enright, A.J., Aravin, A., Tuschl, T., Sander, C., and Marks, D.S. (2004) Human MicroRNA targets. *PLoS Biol.*, **2**, e363.

Jones, M. V, Bell, J.E., and Nath, A. (2000) Immunolocalization of HIV envelope gp120 in HIV encephalitis with dementia. *AIDS*, **14**, 2709–2713.

Jose Luis Marin-Teva, Dusart, I., Colin, C., Gervais, A., Rooijen, N. Van, Mallat, M., Neurone-glie, B.I., and Inserm, U. (2004) Microglia Promote the Death of Developing Purkinje Cells. *Neuron*, **41**, 535–547.

Jose Maria Frade, Y.-A.B. (1998) Microglia-Derived Nerve Growth Factor Causes Cell Death in the Developing Retina. *Neuron*, **20**, 35–41.

Jovičić, A., Roshan, R., Moisoi, N., Pradervand, S., Moser, R., Pillai, B., and Luthi-Carter, R. (2013) Comprehensive expression analyses of neural cell-type-specific miRNAs identify new determinants of the specification and maintenance of neuronal phenotypes. *J. Neurosci.*, **33**, 5127–5137.

Juhila, J., Sipilä, T., Icay, K., Nicorici, D., Ellonen, P., Kallio, A., Korpelainen, E., Greco, D., and Hovatta, I. (2011) MicroRNA expression profiling reveals miRNA families regulating specific biological pathways in mouse frontal cortex and hippocampus. *PLoS One*, **6**, e21495.

Kannan, V., Brouwer, N., Hanisch, U.-K., Regen, T., Eggen, B.J.L., and Boddeke, H.W.G.M. (2013) Histone deacetylase inhibitors suppress immune activation in primary mouse microglia. *J. Neurosci. Res.*, **91**, 1133–1142.

Kaur, C., Hao, A., Wu, C., and Ling, E. (2001) Origin of microglia. *Microsc. Res. …*, **9**, 2–9.

Kawai, T. and Akira, S. (2010) The role of pattern-recognition receptors in innate immunity: update on Toll-like receptors. *Nat. Immunol.*, **11**, 373–384.

Kelm, M., Dahmann, R., Wink, D., and Feelisch, M. (1997) The nitric oxide/superoxide assay. Insights into the biological chemistry of the NO/O-2. interaction. *J. Biol. Chem.*, **272**, 9922–9932.

Kertesz, M., Iovino, N., Unnerstall, U., Gaul, U., and Segal, E. (2007) The role of site accessibility in microRNA target recognition. *Nat. Genet.*, **39**, 1278–1284.

Kettenmann, H., Hanisch, U.-K., Noda, M., and Verkhratsky, A. (2011) Physiology of microglia. *Physiol. Rev.*, **91**, 461–553.

Khalil, N., Parekh, T. V, Connor, R.O., Antman, N., Kepron, W., Yehaulaeshet, T., and Xu, Y.D. (2001) Regulation of the e V ects of TGF- 1 by activation of latent TGF- 1 and di V erential expression of TGF- receptors (T R-I and T R-II) in idiopathic pulmonary fibrosis **1**, 907–915.

Kierdorf, K., Erny, D., Goldmann, T., Sander, V., Schulz, C., Perdiguero, E.G., Wieghofer, P., Heinrich, A., Riemke, P., Hölscher, C., Müller, D.N., Luckow, B., Brocker, T., Debowski, K., Fritz, G., Opdenakker, G., Diefenbach, A., Biber, K., Heikenwalder, M., Geissmann, F., Rosenbauer, F., and Prinz, M. (2013) Microglia emerge from erythromyeloid precursors via Pu.1- and Irf8-dependent pathways. *Nat. Neurosci.*, **16**, 273–280.

Kigerl, K.A., Gensel, J.C., Ankeny, D.P., Alexander, J.K., Donnelly, D.J., and Popovich, P.G. (2009) Identification of two distinct macrophage subsets with divergent effects causing either neurotoxicity or regeneration in the injured mouse spinal cord. *J. Neurosci.*, **29**, 13435–13444.

Kim, H.J., Rowe, M., Ren, M., Hong, J.-S., Chen, P.-S., and Chuang, D.-M. (2007) Histone deacetylase inhibitors exhibit anti-inflammatory and neuroprotective effects in a rat permanent ischemic model of stroke: multiple mechanisms of action. *J. Pharmacol. Exp. Ther.*, **321**, 892–901.

Kim, S.H., Smith, C.J., and Van Eldik, L.J. (2004) Importance of MAPK pathways for microglial pro-inflammatory cytokine IL-1 beta production. *Neurobiol. Aging*, **25**, 431–439.

Kim, V.N. and Nam, J.-W. (2006) Genomics of microRNA. *Trends Genet.*, **22**, 165–173.

Kim, Y.S. and Joh, T.H. (2006) Microglia, major player in the brain inflammation: their roles in the pathogenesis of Parkinson's disease. *Exp. Mol. Med.*, **38**, 333–347.

Kim, Y.S., Kim, S.S., Cho, J.J., Choi, D.H., Hwang, O., Shin, D.H., Chun, H.S., Beal, M.F., and Joh, T.H. (2005) Matrix metalloproteinase-3: a novel signaling proteinase from apoptotic neuronal cells that activates microglia. *J. Neurosci.*, **25**, 3701–3711.

Kim, Won-Ki, Hwang, S.-Y., Oh, E.-S., Piao, H.Z., Kim, K.-W., and Han, I.-O. (2004) TGF-beta1 represses activation and resultant death of microglia via inhibition of phosphatidylinositol 3-kinase activity. *J. Immunol.*, **172**, 7015–7023.

Kitchens, R.L., Thompson, P.A., O'Keefe, G.E., and Munford, R.S. (2000) Plasma constituents regulate LPS binding to, and release from, the monocyte cell surface. *J. Endotoxin Res.*, **6**, 477–482.

Kiyota, T., Ingraham, K.L., Swan, R.J., Jacobsen, M.T., Andrews, S.J., and Ikezu, T. (2012) AAV serotype 2/1-mediated gene delivery of anti-inflammatory interleukin-10 enhances neurogenesis and cognitive function in APP+PS1 mice. *Gene Ther.*, **19**, 724–733.

Klegeris, A., Pelech, S., Giasson, B.I., Maguire, J., Zhang, H., McGeer, E.G., and McGeer, P.L. (2008) Alpha-synuclein activates stress signaling protein kinases in THP-1 cells and microglia. *Neurobiol. Aging*, **29**, 739–752.

Koizumi, S., Shigemoto-Mogami, Y., Nasu-Tada, K., Shinozaki, Y., Ohsawa, K., Tsuda, M., Joshi, B. V, Jacobson, K.A., Kohsaka, S., and Inoue, K. (2007) UDP acting at P2Y6 receptors is a mediator of microglial phagocytosis. *Nature*, **446**, 1091–1095.

Kong, H., Omran, A., Ashhab, M.U., Gan, N., Peng, J., He, F., Wu, L., Deng, X., and Yin, F. (2014) Changes in microglial inflammation-related and brain-enriched MicroRNAs expressions in response to in vitro oxygen-glucose deprivation. *Neurochem. Res.*, **39**, 233–243.

Korte, M., Carroll, P., Wolf, E., Brem, G., Thoenen, H., and Bonhoeffer, T. (1995) Hippocampal long-term potentiation is impaired in mice lacking brain-derived neurotrophic factor. *Proc. Natl. Acad. Sci. U. S. A.*, **92**, 8856–8860.

Kreutzberg, G.W. (1996) Microglia: a sensor for pathological events in the CNS. *Trends Neurosci.*, **19**, 312–318.

Kuan, C.-Y., Whitmarsh, A.J., Yang, D.D., Liao, G., Schloemer, A.J., Dong, C., Bao, J., Banasiak, K.J., Haddad, G.G., Flavell, R.A., Davis, R.J., and Rakic, P. (2003) A critical role of neural-specific JNK3 for ischemic apoptosis. *Proc. Natl. Acad. Sci. U. S. A.*, **100**, 15184–15189.

Kulp, A. and Kuehn, M.J. (2010) Biological functions and biogenesis of secreted bacterial outer membrane vesicles. *Annu. Rev. Microbiol.*, **64**, 163–184.

Kumar, A. and Loane, D.J. (2012) Neuroinflammation after traumatic brain injury: opportunities for therapeutic intervention. *Brain. Behav. Immun.*, **26**, 1191–1201.

Kuo, M.H. and Allis, C.D. (1998) Roles of histone acetyltransferases and deacetylases in gene regulation. *Bioessays*, **20**, 615–626.

Kurien, B.T. and Scofield, R.H. (2006) Western blotting. *Methods*, **38**, 283–293.

Kyriakis, J.M. and Avruch, J. (2001) Mammalian mitogen-activated protein kinase signal transduction pathways activated by stress and inflammation. *Physiol. Rev.*, **81**, 807–869.

Kyriakis, J.M. and Avruch, J. (2012) Mammalian MAPK signal transduction pathways activated by stress and inflammation: a 10-year update. *Physiol. Rev.*, **92**, 689–737.

Lai, L., Song, Y., Liu, Y., Chen, Q., Han, Q., Chen, W., Pan, T., Zhang, Y., Cao, X., and Wang, Q. (2013) MicroRNA-92a negatively regulates Toll-like receptor (TLR)-triggered inflammatory response in macrophages by targeting MKK4 kinase. *J. Biol. Chem.*, **288**, 7956–7967.

Lawson, L.J., Perry, V.H., Dri, P., and Rlksn, S.G. (1990) HETEROGENEITY IN THE DISTRIBUTION AND MORPHOLOGY OF M ~ CROGLIA IN THE NORMAL ADULT MOUSE IBRAIN. *Neuroscience*, **39**, 151–170.

Lee, Y.B., Schrader, J.W., and Kim, S.U. (2000) p38 map kinase regulates TNF-alpha production in human astrocytes and microglia by multiple mechanisms. *Cytokine*, **12**, 874–880.

Lei, Z., Xu, G., Wang, L., Yang, H., Liu, X., Zhao, J., and Zhang, H.-T. (2014) MiR-142-3p represses TGF-β-induced growth inhibition through repression of TGFβR1 in non-small cell lung cancer. *FASEB J.*, **28**, 2696–2704.

Leng, S.X., McElhaney, J.E., Walston, J.D., Xie, D., Fedarko, N.S., and Kuchel, G.A. (2008) ELISA and multiplex technologies for cytokine measurement in inflammation and aging research. *J. Gerontol. A. Biol. Sci. Med. Sci.*, **63**, 879–884.

Leonard, W.J. and O'Shea, J.J. (1998) Jaks and STATs: biological implications. *Annu. Rev. Immunol.*, **16**, 293–322.

Lewis, B.P., Shih, I., Jones-Rhoades, M.W., Bartel, D.P., and Burge, C.B. (2003) Prediction of mammalian microRNA targets. *Cell*, **115**, 787–798.

Li, T., Pang, S., Yu, Y., Wu, X., Guo, J., and Zhang, S. (2013) Proliferation of parenchymal microglia is the main source of microgliosis after ischaemic stroke. *Brain*, **136**, 3578–3588.

Li, W. and Graeber, M.B. (2012) The molecular profile of microglia under the influence of glioma. *Neuro. Oncol.*, **14**, 958–978.

Liang, K.J., Lee, J.E., Wang, Y.D., Ma, W., Fontainhas, A.M., Fariss, R.N., and Wong, W.T. (2009) Regulation of dynamic behavior of retinal microglia by CX3CR1 signaling. *Invest. Ophthalmol. Vis. Sci.*, **50**, 4444–4451.

Limatola, C. and Ransohoff, R.M. (2014) Modulating neurotoxicity through CX3CL1/CX3CR1 signaling. *Front. Cell. Neurosci.*, **8**, 229.

Ling, E.A. and Wong, W.C. (1993) The origin and nature of ramified and amoeboid microglia: a historical review and current concepts. *Glia*, **7**, 9–18.

Linnartz, B., Wang, Y., and Neumann, H. (2010) Microglial immunoreceptor tyrosine-based activation and inhibition motif signaling in neuroinflammation. *Int. J. Alzheimers. Dis.*, **2010**.

Liu, G.J., Nagarajah, R., Banati, R.B., and Bennett, M.R. (2009) Glutamate induces directed chemotaxis of microglia. *Eur. J. Neurosci.*, **29**, 1108–1118.

Livak, K.J. and Schmittgen, T.D. (2001) Analysis of relative gene expression data using real-time quantitative PCR and the 2(-Delta Delta C(T)) Method. *Methods*, **25**, 402–408.

Lodge, A. (1996) Regulation of microglial by TGF- , **60**.

Logan, T.T., Villapol, S., and Symes, A.J. (2013) TGF-β superfamily gene expression and induction of the Runx1 transcription factor in adult neurogenic regions after brain injury. *PLoS One*, **8**, e59250.

Louafi, F., Martinez-Nunez, R.T., and Sanchez-Elsner, T. (2010) MicroRNA-155 targets SMAD2 and modulates the response of macrophages to transforming growth factor-{beta}. *J. Biol. Chem.*, **285**, 41328–41336.

Lu, Y.-C., Yeh, W.-C., and Ohashi, P.S. (2008) LPS/TLR4 signal transduction pathway. *Cytokine*, **42**, 145–151.

Lue, L.F., Rydel, R., Brigham, E.F., Yang, L.B., Hampel, H., Murphy, G.M., Brachova, L., Yan, S.D., Walker, D.G., Shen, Y., and Rogers, J. (2001) Inflammatory repertoire of Alzheimer's disease and nondemented elderly microglia in vitro. *Glia*, **35**, 72–79.

Luo, X.-G. and Chen, S.-D. (2012) The changing phenotype of microglia from homeostasis to disease. *Transl. Neurodegener.*, **1**, 9.

Maas, A.I.R., Stocchetti, N., and Bullock, R. (2008) Moderate and severe traumatic brain injury in adults. *Lancet. Neurol.*, **7**, 728–741.

Magill, S.T., Cambronne, X.A., Luikart, B.W., Lioy, D.T., Leighton, B.H., Westbrook, G.L., Mandel, G., and Goodman, R.H. (2010) microRNA-132 regulates dendritic growth and arborization of newborn neurons in the adult hippocampus. *Proc. Natl. Acad. Sci. U. S. A.*, **107**, 20382–20387.

Marín-Teva, J.L., Cuadros, M. a, Martín-Oliva, D., and Navascués, J. (2011) Microglia and neuronal cell death. *Neuron Glia Biol.*, **7**, 25–40.

Markovic, D.S., Glass, R., Synowitz, M., Rooijen, N. van, and Kettenmann, H. (2005) Microglia stimulate the invasiveness of glioma cells by increasing

the activity of metalloprotease-2. *J. Neuropathol. Exp. Neurol.*, **64**, 754–762.

Marlatt, M.W., Bauer, J., Aronica, E., van Haastert, E.S., Hoozemans, J.J.M., Joels, M., and Lucassen, P.J. (2014) Proliferation in the Alzheimer hippocampus is due to microglia, not astroglia, and occurs at sites of amyloid deposition. *Neural Plast.*, **2014**, 693851.

Martinez-Nunez, R.T., Louafi, F., and Sanchez-Elsner, T. (2011) The interleukin 13 (IL-13) pathway in human macrophages is modulated by microRNA-155 via direct targeting of interleukin 13 receptor alpha1 (IL13Ralpha1). *J. Biol. Chem.*, **286**, 1786–1794.

Massagué, J. (2000) REVIEWS. *Nat. Rev. Mol. Cell Biol.*, **1**, 169–178.

Massagué, J., Seoane, J., and Wotton, D. (2005) Smad transcription factors. *Genes Dev.*, **19**, 2783–2810.

Matos, L.L. de, Trufelli, D.C., de Matos, M.G.L., and da Silva Pinhal, M.A. (2010) Immunohistochemistry as an important tool in biomarkers detection and clinical practice. *Biomark. Insights*, **5**, 9–20.

Mattick, J.S. (2009) The genetic signatures of noncoding RNAs. *PLoS Genet.*, **5**, e1000459.

McIntosh, T.K., Saatman, K.E., Raghupathi, R., Graham, D.I., Smith, D.H., Lee, V.M., and Trojanowski, J.Q. (1998) The Dorothy Russell Memorial Lecture. The molecular and cellular sequelae of experimental traumatic brain injury: pathogenetic mechanisms. *Neuropathol. Appl. Neurobiol.*, **24**, 251–267.

McManus, C.M., Brosnan, C.F., and Berman, J.W. (1998) Cytokine induction of MIP-1 alpha and MIP-1 beta in human fetal microglia. *J. Immunol.*, **160**, 1449–1455.

Même, W., Calvo, C.-F., Froger, N., Ezan, P., Amigou, E., Koulakoff, A., and Giaume, C. (2006) Proinflammatory cytokines released from microglia inhibit gap junctions in astrocytes: potentiation by beta-amyloid. *FASEB J.*, **20**, 494–496.

Merrill, J.E. (1992) Tumor necrosis factor alpha, interleukin 1 and related cytokines in brain development: normal and pathological. *Dev. Neurosci.*, **14**, 1–10.

Min, H. and Yoon, S. (2010) Got target? Computational methods for microRNA target prediction and their extension. *Exp. Mol. Med.*, **42**, 233–244.

Mishra, R., Chhatbar, C., and Singh, S.K. (2012) HIV-1 Tat C-mediated regulation of tumor necrosis factor receptor-associated factor-3 by microRNA 32 in human microglia. *J. Neuroinflammation*, **9**, 131.

Mitchell, K., Shah, J.P., Tsytsikova, L. V, Campbell, A.M., Affram, K., and Symes, A.J. (2014) LPS antagonism of TGF-β signaling results in prolonged survival and activation of rat primary microglia. *J. Neurochem.*, **129**, 155–168.

Mizuno, T. (2012) The biphasic role of microglia in Alzheimer's disease. *Int. J. Alzheimers. Dis.*, **2012**, 737846.

Moncada, S. and Higgs, A. (1993) The L-arginine-nitric oxide pathway. *N. Engl. J. Med.*, **329**, 2002–2012.

Moore, J.P., Kitchen, S.G., Pugach, P., and Zack, J.A. (2004) The CCR5 and CXCR4 coreceptors--central to understanding the transmission and pathogenesis of human immunodeficiency virus type 1 infection. *AIDS Res. Hum. Retroviruses*, **20**, 111–126.

Morganti-Kossmann, M.C., Satgunaseelan, L., Bye, N., and Kossmann, T. (2007) Modulation of immune response by head injury. *Injury*, **38**, 1392–1400.

Nadeau, S. and Rivest, S. (2000) Role of microglial-derived tumor necrosis factor in mediating CD14 transcription and nuclear factor kappa B activity in the brain during endotoxemia. *J. Neurosci.*, **20**, 3456–3468.

Nagamoto-Combs, K., McNeal, D.W., Morecraft, R.J., and Combs, C.K. (2007) Prolonged microgliosis in the rhesus monkey central nervous system after traumatic brain injury. *J. Neurotrauma*, **24**, 1719–1742.

Nayak, D., Roth, T.L., and McGavern, D.B. (2014) Microglia development and function. *Annu. Rev. Immunol.*, **32**, 367–402.

Neumann, H., Kotter, M.R., and Franklin, R.J.M. (2009) Debris clearance by microglia: an essential link between degeneration and regeneration. *Brain*, **132**, 288–295.

Nguyen, V.T. and Benveniste, E.N. (2000) Involvement of STAT-1 and ets family members in interferon-gamma induction of CD40 transcription in microglia/macrophages. *J. Biol. Chem.*, **275**, 23674–23684.

Nimmerjahn, A., Kirchhoff, F., and Helmchen, F. (2005) Resting microglial cells are highly dynamic surveillants of brain parenchyma in vivo. *Science*, **308**, 1314–1318.

Noda, M., Doi, Y., Liang, J., Kawanokuchi, J., Sonobe, Y., Takeuchi, H., Mizuno, T., and Suzumura, A. (2011) Fractalkine attenuates excito-neurotoxicity via microglial clearance of damaged neurons and antioxidant enzyme heme oxygenase-1 expression. *J. Biol. Chem.*, **286**, 2308–2319.

Noori-daloii, M.R. and Nejatizadeh, A. (n.d.) MicroRNAs in Disease and Health : Diagnostic and Therapeutic Potentials. *Gene Ther. Dev. Futur. Perspect.*,.

Nowak, J.S. and Michlewski, G. (2013) miRNAs in development and pathogenesis of the nervous system. *Biochem. Soc. Trans.*, **41**, 815–820.

O'Keefe, G.M., Nguyen, V.T., and Benveniste, E.N. (1999) Class II transactivator and class II MHC gene expression in microglia: modulation by the cytokines TGF-beta, IL-4, IL-13 and IL-10. *Eur. J. Immunol.*, **29**, 1275–1285.

Oliver, C. and Jamur, M.C. (2010) Immunocytochemical methods and protocols. *Methods Mol. Biol.*, **588**, iv – v.

Ouyang, Y.-B., Lu, Y., Yue, S., Xu, L.-J., Xiong, X.-X., White, R.E., Sun, X., and Giffard, R.G. (2012) miR-181 regulates GRP78 and influences outcome from cerebral ischemia in vitro and in vivo. *Neurobiol. Dis.*, **45**, 555–563.

Paglinawan, R., Malipiero, U., Schlapbach, R., Frei, K., Reith, W., and Fontana, A. (2003) TGFbeta directs gene expression of activated microglia to an anti-inflammatory phenotype strongly focusing on chemokine genes and cell migratory genes. *Glia*, **44**, 219–231.

Palin, K., Pousset, F., Verrier, D., Dantzer, R., Kelley, K., Parnet, P., and Lestage, J. (2001) Characterization of interleukin-1 receptor antagonist isoform expression in the brain of lipopolysaccharide-treated rats. *Neuroscience*, **103**, 161–169.

Paolicelli, R.C., Bolasco, G., Pagani, F., Maggi, L., Scianni, M., Panzanelli, P., Giustetto, M., Ferreira, T.A., Guiducci, E., Dumas, L., Ragozzino, D., and Gross, C.T. (2011) Synaptic pruning by microglia is necessary for normal brain development. *Science*, **333**, 1456–1458.

Parakalan, R., Jiang, B., Nimmi, B., Janani, M., Jayapal, M., Lu, J., Tay, S.S.W., Ling, E.-A., and Dheen, S.T. (2012) Transcriptome analysis of amoeboid and ramified microglia isolated from the corpus callosum of rat brain. *BMC Neurosci.*, **13**, 64.

Pareek, S., Roy, S., Kumari, B., Jain, P., Banerjee, A., and Vrati, S. (2014) MiR-155 induction in microglial cells suppresses Japanese encephalitis virus replication and negatively modulates innate immune responses. *J. Neuroinflammation*, **11**, 97.

Park, J., Paik, S.R., Jou, I.L.O., and Park, S.M. (2008) Microglial Phagocytosis Is Enhanced by Monomeric a -Synuclein , Not Aggregated a -Synuclein : Implications for Parkinson ' s Disease. *Glia*, **56**, 1215–1223.

Parkhurst, C.N., Yang, G., Ninan, I., Savas, J.N., Yates, J.R., Lafaille, J.J., Hempstead, B.L., Littman, D.R., and Gan, W.-B. (2013) Microglia promote learning-dependent synapse formation through brain-derived neurotrophic factor. *Cell*, **155**, 1596–1609.

Pasquinelli, A.E. (2012) MicroRNAs and their targets: recognition, regulation and an emerging reciprocal relationship. *Nat. Rev. Genet.*, **13**, 271–282.

Paul, C.A., Beltz, B., and Berger-Sweeney, J. (2008) Perfusion of brain tissues with fixative. *CSH Protoc.*, **2008**, pdb.prot4802.

Pecot, C. V, Rupaimoole, R., Yang, D., Akbani, R., Ivan, C., Lu, C., Wu, S., Han, H.-D., Shah, M.Y., Rodriguez-Aguayo, C., Bottsford-Miller, J., Liu, Y., Kim, S.B., Unruh, A., Gonzalez-Villasana, V., Huang, L., Zand, B., Moreno-Smith, M., Mangala, L.S., Taylor, M., Dalton, H.J., Sehgal, V., Wen, Y., Kang, Y., Baggerly, K.A., Lee, J.-S., Ram, P.T., Ravoori, M.K., Kundra, V., Zhang, X., Ali-Fehmi, R., Gonzalez-Angulo, A.-M., Massion, P.P., Calin, G.A., Lopez-Berestein, G., Zhang, W., and Sood, A.K. (2013) Tumour angiogenesis regulation by the miR-200 family. *Nat. Commun.*, **4**, 2427.

Pennypacker, K. (1997) Transcription factors in brain injury. *Histol. Histopathol.*, **12**, 1125–1133.

Peri, F. and Nüsslein-Volhard, C. (2008) Live imaging of neuronal degradation by microglia reveals a role for v0-ATPase a1 in phagosomal fusion in vivo. *Cell*, **133**, 916–927.

Perry, V.H., Nicoll, J. a R., and Holmes, C. (2010) Microglia in neurodegenerative disease. *Nat. Rev. Neurol.*, **6**, 193–201.

Phani, S., Loike, J.D., and Przedborski, S. (2012) Neurodegeneration and inflammation in Parkinson's disease. *Parkinsonism Relat. Disord.*, **18 Suppl 1**, S207–S209.

Pocock, J.M. and Kettenmann, H. (2007) Neurotransmitter receptors on microglia. *Trends Neurosci.*, **30**, 527–535.

Ponomarev, E.D., Maresz, K., Tan, Y., and Dittel, B.N. (2007) CNS-derived interleukin-4 is essential for the regulation of autoimmune inflammation and induces a state of alternative activation in microglial cells. *J. Neurosci.*, **27**, 10714–10721.

Ponomarev, E.D., Veremeyko, T., Barteneva, N., Krichevsky, A.M., and Weiner, H.L. (2011) MicroRNA-124 promotes microglia quiescence and suppresses EAE by deactivating macrophages via the C/EBP-A-PU.1 pathway. *Nat. Med.*, **17**, 64–70.

Ponomarev, E.D., Veremeyko, T., and Weiner, H.L. (2013) MicroRNAs are universal regulators of differentiation, activation, and polarization of microglia and macrophages in normal and diseased CNS. *Glia*, **61**, 91–103.

Popivanova, B.K., Koike, K., Tonchev, A.B., Ishida, Y., Kondo, T., Ogawa, S., Mukaida, N., Inoue, M., and Yamashima, T. (2003) Accumulation of microglial cells expressing ELR motif-positive CXC chemokines and

their receptor CXCR2 in monkey hippocampus after ischemia-reperfusion. *Brain Res.*, **970**, 195–204.

Pulverer, B.J., Kyriakis, J.M., Avruch, J., Nikolakaki, E., and Woodgett, J.R. (1991) Phosphorylation of c-jun mediated by MAP kinases. *Nature*, **353**, 670–674.

Qin, L., Wu, X., Block, M.L., Liu, Y., Breese, G.R., Hong, J.-S., Knapp, D.J., and Crews, F.T. (2007) Systemic LPS causes chronic neuroinflammation and progressive neurodegeneration. *Glia*, **55**, 453–462.

Rajasethupathy, P., Fiumara, F., Sheridan, R., Betel, D., Puthanveettil, S. V, Russo, J.J., Sander, C., Tuschl, T., and Kandel, E. (2009) Characterization of small RNAs in Aplysia reveals a role for miR-124 in constraining synaptic plasticity through CREB. *Neuron*, **63**, 803–817.

Ramlackhansingh, A.F., Brooks, D.J., Greenwood, R.J., Bose, S.K., Turkheimer, F.E., Kinnunen, K.M., Gentleman, S., Heckemann, R. a, Gunanayagam, K., Gelosa, G., and Sharp, D.J. (2011) Inflammation after trauma: microglial activation and traumatic brain injury. *Ann. Neurol.*, **70**, 374–383.

Raoul, C., Estévez, A.G., Nishimune, H., Cleveland, D.W., DeLapeyrière, O., Henderson, C.E., Haase, G., and Pettmann, B. (2002) Motoneuron death triggered by a specific pathway downstream of Fas. potentiation by ALS-linked SOD1 mutations. *Neuron*, **35**, 1067–1083.

Rappert, A., Biber, K., Nolte, C., Lipp, M., Schubel, A., Lu, B., Gerard, N.P., Gerard, C., Boddeke, H.W.G.M., and Kettenmann, H. (2002) Secondary lymphoid tissue chemokine (CCL21) activates CXCR3 to trigger a Cl- current and chemotaxis in murine microglia. *J. Immunol.*, **168**, 3221–3226.

Rasley, A., Tranguch, S.L., Rati, D.M., and Marriott, I. (2006) Murine glia express the immunosuppressive cytokine, interleukin-10, following

exposure to Borrelia burgdorferi or Neisseria meningitidis. *Glia*, **53**, 583–592.

Ravichandran, K.S. (2010) Find-me and eat-me signals in apoptotic cell clearance: progress and conundrums. *J. Exp. Med.*, **207**, 1807–1817.

Reed-Geaghan, E.G., Savage, J.C., Hise, A.G., and Landreth, G.E. (2009) CD14 and toll-like receptors 2 and 4 are required for fibrillar A{beta}-stimulated microglial activation. *J. Neurosci.*, **29**, 11982–11992.

Rezaie, P. and Male, D. (1999) Colonisation of the developing human brain and spinal cord by microglia: a review. *Microsc. Res. Tech.*, **45**, 359–382.

Rezaie, P. and Male, D. (2002) Mesoglia & microglia--a historical review of the concept of mononuclear phagocytes within the central nervous system. *J. Hist. Neurosci.*, **11**, 325–374.

Ritchie, M.E., Silver, J., Oshlack, A., Holmes, M., Diyagama, D., Holloway, A., and Smyth, G.K. (2007) A comparison of background correction methods for two-colour microarrays. *Bioinformatics*, **23**, 2700–2707.

Rogers, J.T., Morganti, J.M., Bachstetter, A.D., Hudson, C.E., Peters, M.M., Grimmig, B. a, Weeber, E.J., Bickford, P.C., and Gemma, C. (2011) CX3CR1 deficiency leads to impairment of hippocampal cognitive function and synaptic plasticity. *J. Neurosci.*, **31**, 16241–16250.

Rollins, B.J. (1997) Chemokines. *Blood*, **90**, 909–928.

Roumier, A., Béchade, C., Poncer, J.-C., Smalla, K.-H., Tomasello, E., Vivier, E., Gundelfinger, E.D., Triller, A., and Bessis, A. (2004) Impaired synaptic function in the microglial KARAP/DAP12-deficient mouse. *J. Neurosci.*, **24**, 11421–11428.

Rubio-Perez, J.M. and Morillas-Ruiz, J.M. (2012) A review: inflammatory process in Alzheimer's disease, role of cytokines. *ScientificWorldJournal.*, **2012**, 756357.

Ruffell, D., Mourkioti, F., Gambardella, A., Kirstetter, P., Lopez, R.G., Rosenthal, N., and Nerlov, C. (2009) A CREB-C/EBPbeta cascade induces M2 macrophage-specific gene expression and promotes muscle injury repair. *Proc. Natl. Acad. Sci. U. S. A.*, **106**, 17475–17480.

Saatman, K.E., Duhaime, A.-C., Bullock, R., Maas, A.I.R., Valadka, A., and Manley, G.T. (2008) Classification of traumatic brain injury for targeted therapies. *J. Neurotrauma*, **25**, 719–738.

Saba, R., Gushue, S., Huzarewich, R.L.C.H., Manguiat, K., Medina, S., Robertson, C., and Booth, S. a (2012) MicroRNA 146a (miR-146a) is over-expressed during prion disease and modulates the innate immune response and the microglial activation state. *PLoS One*, **7**, e30832.

Saud, K., Herrera-Molina, R., and Von Bernhardi, R. (2005) Pro- and anti-inflammatory cytokines regulate the ERK pathway: implication of the timing for the activation of microglial cells. *Neurotox. Res.*, **8**, 277–287.

Schafer, D.P., Lehrman, E.K., Kautzman, A.G., Koyama, R., Mardinly, A.R., Yamasaki, R., Ransohoff, R.M., Greenberg, M.E., Barres, B.A., and Stevens, B. (2012) Microglia sculpt postnatal neural circuits in an activity and complement-dependent manner. *Neuron*, **74**, 691–705.

Schafer, D.P., Lehrman, E.K., and Stevens, B. (2013) The "quad-partite" synapse: microglia-synapse interactions in the developing and mature CNS. *Glia*, **61**, 24–36.

Schilling, T., Stock, C., Schwab, A., and Eder, C. (2004) Functional importance of Ca2+-activated K+ channels for lysophosphatidic acid-induced microglial migration. *Eur. J. Neurosci.*, **19**, 1469–1474.

Schmid, C.D., Sautkulis, L.N., Danielson, P.E., Cooper, J., Hasel, K.W., Hilbush, B.S., Sutcliffe, J.G., and Carson, M.J. (2002) Heterogeneous expression of the triggering receptor expressed on myeloid cells-2 on adult murine microglia. *J. Neurochem.*, **83**, 1309–1320.

Schratt, G.M., Tuebing, F., Nigh, E.A., Kane, C.G., Sabatini, M.E., Kiebler, M., and Greenberg, M.E. (2006) A brain-specific microRNA regulates dendritic spine development. *Nature*, **439**, 283–289.

Schroeder, A., Mueller, O., Stocker, S., Salowsky, R., Leiber, M., Gassmann, M., Lightfoot, S., Menzel, W., Granzow, M., and Ragg, T. (2006) The RIN: an RNA integrity number for assigning integrity values to RNA measurements. *BMC Mol. Biol.*, **7**, 3.

Schulz, C., Gomez Perdiguero, E., Chorro, L., Szabo-Rogers, H., Cagnard, N., Kierdorf, K., Prinz, M., Wu, B., Jacobsen, S.E.W., Pollard, J.W., Frampton, J., Liu, K.J., and Geissmann, F. (2012) A lineage of myeloid cells independent of Myb and hematopoietic stem cells. *Science*, **336**, 86–90.

Schwab, A. (2001) Function and spatial distribution of ion channels and transporters in cell migration. *Am. J. Physiol. Renal Physiol.*, **280**, F739–F747.

Schwarzmaier, S.M. and Plesnila, N. (2014) Contributions of the immune system to the pathophysiology of traumatic brain injury - evidence by intravital microscopy. *Front. Cell. Neurosci.*, **8**, 358.

Sedel, F., Béchade, C., Vyas, S., and Triller, A. (2004) Macrophage-derived tumor necrosis factor alpha, an early developmental signal for motoneuron death. *J. Neurosci.*, **24**, 2236–2246.

Selvamani, A., Sathyan, P., Miranda, R.C., and Sohrabji, F. (2012) An antagomir to microRNA Let7f promotes neuroprotection in an ischemic stroke model. *PLoS One*, **7**, e32662.

Sempere, L.F., Freemantle, S., Pitha-Rowe, I., Moss, E., Dmitrovsky, E., and Ambros, V. (2004) Expression profiling of mammalian microRNAs uncovers a subset of brain-expressed microRNAs with possible roles in murine and human neuronal differentiation. *Genome Biol.*, **5**, R13.

Shibata, M., Nakao, H., Kiyonari, H., Abe, T., and Aizawa, S. (2011) MicroRNA-9 regulates neurogenesis in mouse telencephalon by targeting multiple transcription factors. *J. Neurosci.*, **31**, 3407–3422.

Sierra, A., Abiega, O., Shahraz, A., and Neumann, H. (2013) Janus-faced microglia: beneficial and detrimental consequences of microglial phagocytosis. *Front. Cell. Neurosci.*, **7**, 6.

Sierra, A., Encinas, J.M., Deudero, J.J.P., Chancey, J.H., Enikolopov, G., Overstreet-Wadiche, L.S., Tsirka, S.E., and Maletic-Savatic, M. (2010) Microglia shape adult hippocampal neurogenesis through apoptosis-coupled phagocytosis. *Cell Stem Cell*, **7**, 483–495.

Sliwa, M., Markovic, D., Gabrusiewicz, K., Synowitz, M., Glass, R., Zawadzka, M., Wesolowska, A., Kettenmann, H., and Kaminska, B. (2007) The invasion promoting effect of microglia on glioblastoma cells is inhibited by cyclosporin A. *Brain*, **130**, 476–489.

Smith, D.H., Chen, X.H., Pierce, J.E., Wolf, J.A., Trojanowski, J.Q., Graham, D.I., and McIntosh, T.K. (1997) Progressive atrophy and neuron death for one year following brain trauma in the rat. *J. Neurotrauma*, **14**, 715–727.

Snyder, S.H. and Bredt, D.S. (1992) Biological roles of nitric oxide. *Sci. Am.*, **266**, 68–71, 74–77.

Spittau, B., Wullkopf, L., Zhou, X., Rilka, J., Pfeifer, D., and Krieglstein, K. (2013) Endogenous transforming growth factor-beta promotes quiescence of primary microglia in vitro. *Glia*, **61**, 287–300.

Stark, K.L., Xu, B., Bagchi, A., Lai, W.-S., Liu, H., Hsu, R., Wan, X., Pavlidis, P., Mills, A.A., Karayiorgou, M., and Gogos, J.A. (2008) Altered brain microRNA biogenesis contributes to phenotypic deficits in a 22q11-deletion mouse model. *Nat. Genet.*, **40**, 751–760.

Stenvang, J., Petri, A., Lindow, M., Obad, S., and Kauppinen, S. (2012) Inhibition of microRNA function by antimiR oligonucleotides. *Silence*, **3**, 1.

Stevens, B., Allen, N.J., Vazquez, L.E., Howell, G.R., Christopherson, K.S., Nouri, N., Micheva, K.D., Mehalow, A.K., Huberman, A.D., Stafford, B., Sher, A., Litke, A.M., Lambris, J.D., Smith, S.J., John, S.W.M., and Barres, B. a (2007) The classical complement cascade mediates CNS synapse elimination. *Cell*, **131**, 1164–1178.

Stoica, B.A. and Faden, A.I. (2010) Cell death mechanisms and modulation in traumatic brain injury. *Neurotherapeutics*, **7**, 3–12.

Stoll, G. and Jander, S. (1999) The role of microglia and macrophages in the pathophysiology of the CNS. *Prog. Neurobiol.*, **58**, 233–247.

Streit, W.J., Walter, S.A., and Pennell, N.A. (1999) Reactive microgliosis. *Prog. Neurobiol.*, **57**, 563–581.

Sun, H.-N., Kim, S.-U., Lee, M.-S., Kim, S.-K., Kim, J.-M., Yim, M., Yu, D.-Y., and Lee, D.-S. (2008) Nicotinamide adenine dinucleotide phosphate (NADPH) oxidase-dependent activation of phosphoinositide 3-kinase and p38 mitogen-activated protein kinase signal pathways is required for lipopolysaccharide-induced microglial phagocytosis. *Biol. Pharm. Bull.*, **31**, 1711–1715.

Suuronen, T., Huuskonen, J., Nuutinen, T., and Salminen, A. (2006) Characterization of the pro-inflammatory signaling induced by protein acetylation in microglia. *Neurochem. Int.*, **49**, 610–618.

Suuronen, T., Huuskonen, J., Pihlaja, R., Kyrylenko, S., and Salminen, A. (2003) Regulation of microglial inflammatory response by histone deacetylase inhibitors. *J. Neurochem.*, **87**, 407–416.

Taft, R.J., Pang, K.C., Mercer, T.R., Dinger, M., and Mattick, J.S. (2010) Non-coding RNAs: regulators of disease. *J. Pathol.*, **220**, 126–139.

Takahashi, K., Rochford, C.D.P., and Neumann, H. (2005) Clearance of apoptotic neurons without inflammation by microglial triggering receptor expressed on myeloid cells-2. *J. Exp. Med.*, **201**, 647–657.

Tamagno, E., Parola, M., Bardini, P., Piccini, A., Borghi, R., Guglielmotto, M., Santoro, G., Davit, A., Danni, O., Smith, M.A., Perry, G., and Tabaton, M. (2005) Beta-site APP cleaving enzyme up-regulation induced by 4-hydroxynonenal is mediated by stress-activated protein kinases pathways. *J. Neurochem.*, **92**, 628–636.

Tamagno, E., Robino, G., Obbili, A., Bardini, P., Aragno, M., Parola, M., and Danni, O. (2003) H2O2 and 4-hydroxynonenal mediate amyloid beta-induced neuronal apoptosis by activating JNKs and p38MAPK. *Exp. Neurol.*, **180**, 144–155.

Thounaojam, M.C., Kaushik, D.K., and Basu, A. (2013) MicroRNAs in the brain: it's regulatory role in neuroinflammation. *Mol. Neurobiol.*, **47**, 1034–1044.

Thounaojam, M.C., Kaushik, D.K., Kundu, K., and Basu, A. (2014) MicroRNA-29b modulates Japanese encephalitis virus-induced microglia activation by targeting tumor necrosis factor alpha-induced protein 3. *J. Neurochem.*, **129**, 143–154.

Trebst, C., Staugaitis, S.M., Kivisäkk, P., Mahad, D., Cathcart, M.K., Tucky, B., Wei, T., Rani, M.R.S., Horuk, R., Aldape, K.D., Pardo, C.A., Lucchinetti, C.F., Lassmann, H., and Ransohoff, R.M. (2003) CC chemokine receptor 8 in the central nervous system is associated with phagocytic macrophages. *Am. J. Pathol.*, **162**, 427–438.

Tremblay, M.-È. (2011) The role of microglia at synapses in the healthy CNS: novel insights from recent imaging studies. *Neuron Glia Biol.*, **7**, 67–76.

Tuan Trang, Simon Beggs, M.W.S. (2011) Pub Med Central CANADA. *Neuron Glia Biol.*, **7**, 99–108.

Tuppo, E.E. and Arias, H.R. (2005) The role of inflammation in Alzheimer's disease. *Int. J. Biochem. Cell Biol.*, **37**, 289–305.

Ueno, M., Fujita, Y., Tanaka, T., Nakamura, Y., Kikuta, J., Ishii, M., and Yamashita, T. (2013) Layer V cortical neurons require microglial support for survival during postnatal development. *Nat. Neurosci.*, **16**, 543–551.

Ueno, M. and Yamashita, T. (2014) Bidirectional tuning of microglia in the developing brain: from neurogenesis to neural circuit formation. *Curr. Opin. Neurobiol.*, **27**, 8–15.

Valastyan, S. and Weinberg, R.A. (2009) Assaying microRNA loss-of-function phenotypes in mammalian cells: emerging tools and their potential therapeutic utility. *RNA Biol.*, **6**, 541–545.

Van Engeland, M., Nieland, L.J., Ramaekers, F.C., Schutte, B., and Reutelingsperger, C.P. (1998) Annexin V-affinity assay: a review on an apoptosis detection system based on phosphatidylserine exposure. *Cytometry*, **31**, 1–9.

Van Rossum, D. and Hanisch, U.-K. (2004) Microglia. *Metab. Brain Dis.*, **19**, 393–411.

Vargas, M.E. and Barres, B. a (2007) Why is Wallerian degeneration in the CNS so slow? *Annu. Rev. Neurosci.*, **30**, 153–179.

Vass, K. and Lassmann, H. (1990) Intrathecal application of interferon gamma. Progressive appearance of MHC antigens within the rat nervous system. *Am. J. Pathol.*, **137**, 789–800.

Vila, M., Teismann, P., Davis, R.J., Hirsch, E.C., Przedborski, S., Rakic, P., and Flavell, R.A. (2004) JNK-mediated induction of cyclooxygenase 2 is

required for neurodegeneration in a mouse model of Parkinson ' s disease. *Proc. Natl. Acad. Sci. U. S. A.*, **101**, 665–670.

Visvanathan, J., Lee, S., Lee, B., Lee, J.W., and Lee, S.-K. (2007) The microRNA miR-124 antagonizes the anti-neural REST/SCP1 pathway during embryonic CNS development. *Genes Dev.*, **21**, 744–749.

Waetzig, V., Czeloth, K., Hidding, U., Mielke, K., Kanzow, M., Brecht, S., Goetz, M., Lucius, R., Herdegen, T., and Hanisch, U.-K. (2005) c-Jun N-terminal kinases (JNKs) mediate pro-inflammatory actions of microglia. *Glia*, **50**, 235–246.

Wake, H., Moorhouse, A.J., Miyamoto, A., and Nabekura, J. (2013) Microglia: actively surveying and shaping neuronal circuit structure and function. *Trends Neurosci.*, **36**, 209–217.

Wang, L.-W., Tu, Y.-F., Huang, C.-C., and Ho, C.-J. (2012) JNK signaling is the shared pathway linking neuroinflammation, blood-brain barrier disruption, and oligodendroglial apoptosis in the white matter injury of the immature brain. *J. Neuroinflammation*, **9**, 175.

Wang, P., Hou, J., Lin, L., Wang, C., Liu, X., Li, D., Ma, F., Wang, Z., and Cao, X. (2010) Inducible microRNA-155 feedback promotes type I IFN signaling in antiviral innate immunity by targeting suppressor of cytokine signaling 1. *J. Immunol.*, **185**, 6226–6233.

Wang, X., Wang, Z.-H., Wu, Y.-Y., Tang, H., Tan, L., Wang, X., Gao, X.-Y., Xiong, Y.-S., Liu, D., Wang, J.-Z., and Zhu, L.-Q. (2013) Melatonin attenuates scopolamine-induced memory/synaptic disorder by rescuing EPACs/miR-124/Egr1 pathway. *Mol. Neurobiol.*, **47**, 373–381.

Wang, Y.-P., Wu, Y., Li, L.-Y., Zheng, J., Liu, R.-G., Zhou, J.-P., Yuan, S.-Y., Shang, Y., and Yao, S.-L. (2011) Aspirin-triggered lipoxin A4 attenuates LPS-induced pro-inflammatory responses by inhibiting

activation of NF-κB and MAPKs in BV-2 microglial cells. *J. Neuroinflammation*, **8**, 95.

Wang, Z. (2011) The principles of MiRNA-masking antisense oligonucleotides technology. *Methods Mol. Biol.*, **676**, 43–49.

Waring, M.J. (1965) Complex formation between ethidium bromide and nucleic acids. *J. Mol. Biol.*, **13**, 269–282.

Welser-Alves, J. V and Milner, R. (2013) Microglia are the major source of TNF-α and TGF-β1 in postnatal glial cultures; regulation by cytokines, lipopolysaccharide, and vitronectin. *Neurochem. Int.*, **63**, 47–53.

Wendlandt, E.B., Graff, J.W., Gioannini, T.L., McCaffrey, A.P., and Wilson, M.E. (2012) The role of microRNAs miR-200b and miR-200c in TLR4 signaling and NF-κB activation. *Innate Immun.*, **18**, 846–855.

Wilms, H., Rosenstiel, P., Sievers, J., Deuschl, G., Zecca, L., and Lucius, R. (2003) Activation of microglia by human neuromelanin is NF-kappaB dependent and involves p38 mitogen-activated protein kinase: implications for Parkinson's disease. *FASEB J.*, **17**, 500–502.

Xie, N., Cui, H., Banerjee, S., Tan, Z., Salomao, R., Fu, M., Abraham, E., Thannickal, V.J., and Liu, G. (2014) miR-27a regulates inflammatory response of macrophages by targeting IL-10. *J. Immunol.*, **193**, 327–334.

Xing, B., Xin, T., Hunter, R.L., and Bing, G. (2008) Pioglitazone inhibition of lipopolysaccharide-induced nitric oxide synthase is associated with altered activity of p38 MAP kinase and PI3K/Akt. *J. Neuroinflammation*, **5**, 4.

Xiong, Y., Mahmood, A., and Chopp, M. (2013) Animal models of traumatic brain injury. *Nat. Rev. Neurosci.*, **14**, 128–142.

Yamagata, T. (1995) Yamagata hgf microglia BBRC.pdf.

Yang, H., Fang, F., Chang, R., and Yang, L. (2013) MicroRNA-140-5p suppresses tumor growth and metastasis by targeting transforming growth factor β receptor 1 and fibroblast growth factor 9 in hepatocellular carcinoma. *Hepatology*, **58**, 205–217.

Yang, Y., Shu, X., Liu, D., Shang, Y., Wu, Y., Pei, L., Xu, X., Tian, Q., Zhang, J., Qian, K., Wang, Y.-X., Petralia, R.S., Tu, W., Zhu, L.-Q., Wang, J.-Z., and Lu, Y. (2012) EPAC null mutation impairs learning and social interactions via aberrant regulation of miR-124 and Zif268 translation. *Neuron*, **73**, 774–788.

Yu, Y. and Ye, R.D. (2014) Microglial Aβ Receptors in Alzheimer's Disease. *Cell. Mol. Neurobiol.*,.

Zanoni, I., Ostuni, R., Marek, L.R., Barresi, S., Barbalat, R., Barton, G.M., Granucci, F., and Kagan, J.C. (2011) CD14 controls the LPS-induced endocytosis of Toll-like receptor 4. *Cell*, **147**, 868–880.

Zhang, J., Malik, A., Choi, H.B., Ko, R.W.Y., Dissing-Olesen, L., and MacVicar, B. a (2014) Microglial CR3 activation triggers long-term synaptic depression in the hippocampus via NADPH oxidase. *Neuron*, **82**, 195–207.

Zhang, L., Dong, L.-Y., Li, Y.-J., Hong, Z., and Wei, W.-S. (2012) miR-21 represses FasL in microglia and protects against microglia-mediated neuronal cell death following hypoxia/ischemia. *Glia*, **60**, 1888–1895.

Zhang, P., Hogan, E.L., and Bhat, N.R. (1998) Activation of JNK/SAPK in primary glial cultures: II. Differential activation of kinase isoforms corresponds to their differential expression. *Neurochem. Res.*, **23**, 219–225.

Zhang, W., Wang, T., Pei, Z., Miller, D.S., Wu, X., Block, M.L., Wilson, B., Zhang, W., Zhou, Y., Hong, J.-S., and Zhang, J. (2005) Aggregated

alpha-synuclein activates microglia: a process leading to disease progression in Parkinson's disease. *FASEB J.*, **19**, 533–542.

Zhang, Y., Wang, Z., and Gemeinhart, R. a (2013) Progress in microRNA delivery. *J. Control. Release*, **172**, 962–974.

Zhao, H., Wang, J., Gao, L., Wang, R., Liu, X., Gao, Z., Tao, Z., Xu, C., Song, J., Ji, X., and Luo, Y. (2013) MiRNA-424 protects against permanent focal cerebral ischemia injury in mice involving suppressing microglia activation. *Stroke.*, **44**, 1706–1713.

Zhou, X., Spittau, B., and Krieglstein, K. (2012) TGFβ signalling plays an important role in IL4-induced alternative activation of microglia. *J. Neuroinflammation*, **9**, 210.

Zhu, Q.-Y., Liu, Q., Chen, J.-X., Lan, K., and Ge, B.-X. (2010) MicroRNA-101 targets MAPK phosphatase-1 to regulate the activation of MAPKs in macrophages. *J. Immunol.*, **185**, 7435–7442.

Zielasek, J. and Hartung, H.P. (1996) Molecular mechanisms of microglial activation. *Adv. Neuroimmunol.*, **6**, 191–22.

Zusso, M., Methot, L., Lo, R., Greenhalgh, A.D., David, S., and Stifani, S. (2012) Regulation of postnatal forebrain amoeboid microglial cell proliferation and development by the transcription factor Runx1. *J. Neurosci.*, **32**, 11285–11298.

7 APPENDIX

7.1 Sheet 1: Top 93 miRNAs from microarray with p<0.05.

No	miRNA	ANOVA *p*-value
1	rno-miR-101a-3p	1.66E-03
2	rno-miR-101b-3p	1.66E-03
3	rno-miR-19a-3p	1.66E-03
4	rno-miR-20b-5p	1.66E-03
5	rno-miR-21-5p	1.66E-03
6	rno-miR-291a-5p	1.66E-03
7	rno-miR-29a-5p	1.66E-03
8	rno-miR-29b-3p	1.66E-03
9	rno-miR-29c-3p	1.66E-03
10	rno-miR-30e-5p	1.66E-03
11	rno-miR-485-3p	1.66E-03
12	rno-miR-19b-3p	1.90E-03
13	rno-miR-27a-3p	1.90E-03
14	rno-miR-30a-5p	1.90E-03
15	rno-miR-370-5p	1.90E-03
16	rno-miR-664-1-5p	1.90E-03
17	rno-let-7i-5p	1.93E-03
18	rno-miR-294	1.93E-03
19	rno-miR-374-3p	3.87E-03
20	rno-miR-3592	4.58E-03

21	rno-miR-106b-5p	6.95E-03
22	rno-miR-20a-5p	6.95E-03
23	rno-miR-26b-5p	6.95E-03
24	rno-miR-140-5p	7.36E-03
25	rno-miR-148b-3p	7.36E-03
26	rno-miR-195-5p	7.36E-03
27	rno-miR-24-2-5p	7.36E-03
28	rno-miR-29a-3p	7.36E-03
29	rno-miR-328b-3p	7.36E-03
30	rno-miR-3559-5p	7.36E-03
31	SNORD110	7.36E-03
32	rno-miR-883-5p	7.47E-03
33	rno-miR-142-3p	8.07E-03
34	rno-miR-34a-5p	9.39E-03
35	rno-miR-1949	9.57E-03
36	rno-miR-16-5p	1.03E-02
37	rno-miR-301a-3p	1.03E-02
38	rno-miR-328a-3p	1.10E-02
39	rno-miR-466b-5p	1.15E-02
40	rno-miR-142-5p	1.15E-02
41	rno-miR-27b-3p	1.25E-02
42	rno-miR-30b-5p	1.25E-02
43	rno-miR-350	1.25E-02
44	rno-miR-351-5p	1.25E-02

45	rno-miR-465-5p	1.25E-02
46	rno-miR-493-5p	1.25E-02
47	rno-miR-181b-5p	1.27E-02
48	rno-miR-3559-3p	1.27E-02
49	SNORD65	1.28E-02
50	rno-miR-17-5p	1.34E-02
51	rno-miR-300-5p	1.39E-02
52	rno-miR-9a-3p	1.39E-02
53	SNORD12	1.39E-02
54	SNORD3@	1.39E-02
55	rno-miR-9a-5p	1.44E-02
56	rno-miR-347	1.46E-02
57	rno-miR-449a-5p	1.47E-02
58	rno-miR-339-5p	1.48E-02
59	rno-miR-338-3p	1.67E-02
60	rno-miR-107-3p	1.68E-02
61	rno-miR-190a-5p	1.68E-02
62	rno-miR-423-5p	1.74E-02
63	rno-miR-214-3p	1.74E-02
64	rno-let-7f-5p	2.32E-02
65	rno-miR-1843-3p	2.32E-02
66	SNORD2	2.52E-02
67	rno-miR-30d-5p	2.57E-02
68	rno-miR-33-5p	2.75E-02

69	rno-miR-299a-5p	2.91E-02
70	rno-miR-331-3p	2.91E-02
71	rno-miR-3568	2.94E-02
72	rno-miR-466c-5p	2.94E-02
73	rno-miR-30e-3p	3.02E-02
74	rno-miR-665	3.08E-02
75	rno-miR-3580-3p	3.09E-02
76	rno-miR-872-5p	3.09E-02
77	SNORD6	3.09E-02
78	rno-miR-21-3p	3.20E-02
79	rno-let-7d-3p	3.30E-02
80	rno-miR-503-5p	3.57E-02
81	rno-miR-22-3p	3.58E-02
82	rno-miR-181a-5p	3.66E-02
83	rno-miR-466d	3.66E-02
84	rno-miR-9b-5p	3.66E-02
85	rno-miR-26a-5p	3.75E-02
86	rno-miR-30c-5p	3.78E-02
87	rno-miR-150-5p	3.85E-02
88	rno-miR-500-3p	3.85E-02
89	rno-miR-98-5p	3.85E-02
90	rno-miR-129-1-3p/rno-miR-129-2-3p	4.29E-02
91	rno-miR-352	4.29E-02

92	rno-miR-34c-5p	4.39E-02
93	rno-miR-125a-5p	4.40E-02

7.2 Sheet 2: Top 63 miRNAs (p<0.05) differentially expressed between control and LPS activated primary microglia.

No	miRNA	logFC	*p*-value
1	rno-miR-29b-3p	1.785	1.54E-04
2	rno-miR-101a-3p	1.362	2.20E-04
3	rno-miR-29c-3p	1.290	2.20E-04
4	rno-miR-30e-5p	1.194	2.20E-04
5	rno-miR-101b-3p	1.109	2.86E-04
6	rno-miR-20b-5p	0.913	2.86E-04
7	rno-miR-142-5p	1.802	4.08E-04
8	rno-miR-21-5p	1.072	4.08E-04
9	rno-miR-27a-3p	1.003	4.08E-04
10	rno-miR-30a-5p	0.920	4.08E-04
11	rno-miR-339-5p	1.083	4.08E-04
12	rno-miR-19a-3p	0.918	4.66E-04
13	rno-miR-19b-3p	1.004	4.68E-04
14	rno-miR-142-3p	2.425	6.76E-04
15	rno-miR-370-5p	0.964	7.73E-04
16	rno-miR-34a-5p	1.135	9.28E-04
17	rno-miR-20a-5p	0.908	1.25E-03
18	rno-miR-29a-5p	0.553	1.65E-03
19	rno-let-7i-5p	0.594	1.81E-03
20	rno-miR-17-5p	0.686	2.19E-03

21	rno-miR-24-2-5p	0.788	2.19E-03
22	rno-miR-29a-3p	0.764	2.19E-03
23	rno-miR-106b-5p	0.822	2.25E-03
24	rno-miR-16-5p	0.648	2.25E-03
25	rno-miR-30b-5p	0.686	2.75E-03
26	rno-miR-140-5p	0.641	3.04E-03
27	rno-miR-9a-5p	1.173	3.07E-03
28	rno-miR-214-3p	-1.291	3.61E-03
29	rno-miR-301a-3p	0.715	4.03E-03
30	rno-miR-9a-3p	0.925	4.55E-03
31	rno-miR-27b-3p	0.603	6.19E-03
32	rno-miR-26b-5p	0.491	6.39E-03
33	rno-miR-146a-5p	1.541	6.74E-03
34	rno-miR-195-5p	0.500	7.37E-03
35	rno-miR-493-5p	-0.441	7.37E-03
36	rno-miR-449a-5p	1.044	7.83E-03
37	rno-miR-190a-5p	0.626	8.39E-03
38	rno-miR-30d-5p	0.537	8.39E-03
39	rno-miR-3559-5p	-0.402	8.39E-03
40	rno-miR-34c-5p	0.490	8.83E-03
41	rno-miR-148b-3p	0.396	1.00E-02
42	rno-miR-338-3p	0.638	1.25E-02
43	rno-miR-146b-5p	1.255	1.31E-02
44	rno-miR-125a-5p	-0.609	1.35E-02

45	rno-miR-33-5p	0.765	1.35E-02
46	rno-miR-145-5p	-0.698	1.40E-02
47	rno-miR-350	0.365	1.40E-02
48	rno-miR-21-3p	0.628	1.51E-02
49	rno-miR-291a-5p	0.419	1.66E-02
50	rno-miR-30c-5p	0.505	1.66E-02
51	rno-miR-664-1-5p	-0.342	1.78E-02
52	rno-miR-150-5p	-0.707	1.93E-02
53	rno-miR-1949	-0.353	1.93E-02
54	rno-miR-99b-5p	-0.775	2.06E-02
55	rno-miR-365-3p	-0.456	2.73E-02
56	rno-miR-34b-5p	0.566	2.89E-02
57	rno-miR-9b-5p	0.491	3.78E-02
58	rno-miR-872-5p	0.352	3.84E-02
59	rno-miR-107-3p	0.299	3.85E-02
60	rno-miR-199a-3p	-0.646	3.85E-02
61	rno-miR-351-5p	-0.307	3.85E-02
62	rno-miR-22-3p	0.369	3.86E-02
63	rno-miR-223-3p	1.156	4.73E-02

7.3 Sheet 3: Top 63 miRNAs (p<0.05) differentially expressed between control and Aβ activated primary microglia.

No	miRNA	logFC	*p*-value
1	rno-miR-21-5p	1.022	1.15E-03
2	rno-miR-485-3p	1.561	1.16E-03
3	rno-miR-370-5p	0.902	1.35E-03
4	rno-miR-291a-5p	0.826	1.59E-03
5	rno-miR-101b-3p	0.664	2.96E-03
6	rno-miR-30e-5p	0.684	2.96E-03
7	rno-miR-29b-3p	1.113	2.96E-03
8	rno-miR-27a-3p	0.733	2.96E-03
9	rno-miR-101a-3p	0.768	3.89E-03
10	rno-miR-301a-3p	0.648	4.24E-03
11	rno-miR-106b-5p	0.558	4.69E-03
12	rno-miR-300-5p	0.946	5.24E-03
13	rno-miR-664-1-5p	-0.420	5.24E-03
14	rno-miR-374-3p	0.666	5.93E-03
15	rno-miR-294	0.586	5.93E-03
16	rno-miR-19a-3p	0.622	5.93E-03
17	rno-miR-29c-3p	0.631	9.59E-03
18	rno-miR-3592	-0.374	1.03E-02
19	rno-miR-143-3p	0.592	1.30E-02
20	rno-miR-20b-5p	0.515	1.36E-02

21	rno-miR-19b-3p	0.610	1.52E-02
22	rno-miR-883-5p	0.498	1.52E-02
23	rno-miR-24-2-5p	0.485	1.57E-02
24	rno-miR-465-5p	-0.355	1.60E-02
25	rno-let-7b-5p	-0.559	1.77E-02
26	rno-miR-3559-3p	1.039	1.86E-02
27	rno-miR-328a-3p	-0.314	2.17E-02
28	rno-miR-29a-3p	0.440	2.17E-02
29	rno-miR-1843-3p	-0.362	2.17E-02
30	SNORD110	-0.335	2.23E-02
31	rno-miR-20a-5p	0.560	2.23E-02
32	rno-miR-193-3p	0.634	2.23E-02
33	rno-miR-3568	-0.327	2.62E-02
34	rno-miR-30a-5p	0.445	2.81E-02
35	rno-miR-328b-3p	-0.285	2.81E-02
36	rno-miR-503-5p	0.342	2.92E-02
37	rno-miR-34a-5p	0.699	3.21E-02
38	rno-miR-34b-3p	-0.357	3.26E-02
39	rno-miR-22-3p	0.334	3.26E-02
40	rno-miR-33-5p	0.440	3.26E-02
41	SNORD2	-0.307	3.26E-02
42	rno-miR-204-3p	0.700	3.26E-02
43	rno-miR-3068-3p	-0.344	3.26E-02
44	rno-miR-299a-5p	-0.312	3.26E-02

45	SNORD65	-0.272	3.26E-02
46	rno-miR-466b-5p	-0.293	3.26E-02
47	rno-miR-92a-3p	-0.324	3.26E-02
48	rno-let-7i-5p	0.278	3.26E-02
49	SNORD12	-0.263	3.26E-02
50	rno-miR-181b-5p	-0.292	3.26E-02
51	SNORD6	-0.257	3.26E-02
52	rno-miR-1949	-0.304	3.26E-02
53	rno-let-7c-5p	-0.436	3.26E-02
54	rno-miR-493-5p	-0.363	3.26E-02
55	rno-miR-125a-5p	-0.483	3.31E-02
56	rno-miR-27b-3p	0.405	3.34E-02
57	rno-miR-29a-5p	0.278	3.34E-02
58	rno-miR-129-1-3p/rno-miR-129-2-3p	-0.323	3.37E-02
59	rno-miR-347	-0.279	3.39E-02
60	rno-miR-466d	-0.341	3.44E-02
61	rno-miR-16-5p	-0.261	3.44E-02
62	rno-let-7d-5p	0.356	3.71E-02
63	rno-miR-17-5p	-0.252	4.49E-02

7.4 Sheet 4: Top 33 miRNAs with $p<0.05$ differentially expressed between LPS and Aβ activated primary microglia.

No	miRNA	logFC	*p*-value
1	rno-miR-3559-3p	1.152	1.41E-04
2	rno-miR-485-3p	1.471	1.79E-03
3	rno-miR-294	0.606	2.21E-03
4	rno-miR-3596c	0.507	1.01E-02
5	rno-miR-883-5p	0.646	1.01E-02
6	rno-miR-374-3p	0.596	1.08E-02
7	rno-miR-210-5p	0.771	2.62E-02
8	rno-miR-449a-5p	-1.109	3.24E-02
9	rno-miR-291a-5p	0.407	3.24E-02
10	rno-miR-195-5p	-0.445	3.24E-02
11	SNORD3@	0.463	3.24E-02
12	rno-miR-30e-5p	-0.510	3.24E-02
13	rno-miR-3573-3p	0.352	3.24E-02
14	rno-miR-142-3p	-1.230	3.24E-02
15	rno-miR-665	0.348	3.41E-02
16	rno-miR-30a-5p	-0.474	3.41E-02
17	rno-miR-29c-3p	-0.658	3.41E-02
18	rno-miR-351-5p	0.315	3.41E-02
19	rno-miR-338-3p	-0.654	3.44E-02

20	rno-miR-300-5p	0.617	3.44E-02
21	rno-miR-19b-3p	-0.394	3.44E-02
22	rno-miR-140-5p	-0.377	3.86E-02
23	rno-miR-101b-3p	-0.445	4.42E-02
24	rno-miR-9b-5p	-0.452	4.42E-02
25	rno-miR-101a-3p	-0.594	4.42E-02
26	rno-miR-9a-5p	-0.756	4.42E-02
27	rno-miR-142-5p	-1.103	4.42E-02
28	rno-miR-500-3p	-0.261	4.42E-02
29	rno-miR-148b-3p	-0.265	4.42E-02
30	rno-miR-9a-3p	-0.627	4.49E-02
31	rno-miR-29b-3p	-0.672	4.58E-02
32	rno-miR-675-5p	0.352	4.78E-02
33	rno-miR-204-3p	0.500	4.78E-02

7.5 Sheet 5: Common miRNAs significantly upregulated in LPS and Aβ activated primary microglia.

No	miRNA	logFC (LPS)	logFC (amyloid β)
1	rno-miR-29b-3p	1.785	1.113
2	rno-miR-29c-3p	1.29	.631
3	rno-miR-29a-3p	.764	.44
4	rno-miR-101a-3p	1.362	.768
5	rno-miR-101b-3p	1.109	.664
6	rno-miR-21-5p	1.072	1.022
7	rno-miR-30e-5p	1.194	.684
8	rno-miR-20b-3p	.913	.515
9	rno-miR-19a-3p	.918	.622
10	rno-miR-19b-3p	1.004	.61
11	rno-miR-24-2-5p	.788	.485
12	rno-miR-106b-5p	.822	.558
13	rno-miR-301a-3p	.715	.648
14	rno-miR-27a-3p	1.003	.733

7.6 Sheet 6: MiRNAs targeting genes from the TGFβ pathway as obtained from Ingenuity pathway analysis software.

No	miRNA	Gene
1	rno-miR-101a-3p	ACVR1C
2	rno-miR-101a-3p	ACVR2B
3	rno-miR-101a-3p	BMPR1B
4	rno-miR-101a-3p	FOS
5	rno-miR-101a-3p	MAPK1
6	rno-miR-101a-3p	SMAD2
7	rno-miR-101a-3p	TGFBR1
8	rno-miR-101a-3p	TGIF1
9	rno-miR-20b-5p	ACVR1B
10	rno-miR-20b-5p	BCL2
11	rno-miR-20b-5p	BMP2
12	rno-miR-20b-5p	BMPR2
13	rno-miR-20b-5p	MAPK1
14	rno-miR-20b-5p	MAPK9
15	rno-miR-20b-5p	RUNX3
16	rno-miR-20b-5p	SKI
17	rno-miR-20b-5p	SMAD4
18	rno-miR-20b-5p	SMAD5
19	rno-miR-20b-5p	SMAD6

20	rno-miR-20b-5p	SMAD7
21	rno-miR-20b-5p	SMURF1
22	rno-miR-20b-5p	SOS1
23	rno-miR-20b-5p	TGFBR2
24	rno-miR-20b-5p	ZFYVE9
25	rno-miR-21-5p	ACVR1C
26	rno-miR-21-5p	ACVR2A
27	rno-miR-21-5p	BCL2
28	rno-miR-21-5p	BMPR2
29	rno-miR-21-5p	MAP2K3
30	rno-miR-21-5p	PITX2
31	rno-miR-21-5p	SKI
32	rno-miR-21-5p	SMAD7
33	rno-miR-21-5p	TGFB2
34	rno-miR-21-5p	TGFBR2
35	rno-miR-27a-3p	ACVR1C
36	rno-miR-27a-3p	ACVR2A
37	rno-miR-27a-3p	ACVR2B
38	rno-miR-27a-3p	BMPR1A
39	rno-miR-27a-3p	GRB2
40	rno-miR-27a-3p	KRAS
41	rno-miR-27a-3p	MAP2K4
42	rno-miR-27a-3p	MAPK14
43	rno-miR-27a-3p	NRAS

44	rno-miR-27a-3p	RNF111
45	rno-miR-27a-3p	SMAD2
46	rno-miR-27a-3p	SMAD3
47	rno-miR-27a-3p	SMAD4
48	rno-miR-27a-3p	SMAD5
49	rno-miR-27a-3p	SMAD9
50	rno-miR-27a-3p	SOS1
51	rno-miR-27a-3p	TGFBR1
52	rno-miR-29b-3p	ACVR2A
53	rno-miR-29b-3p	CDC42
54	rno-miR-29b-3p	FOS
55	rno-miR-29b-3p	MAP2K4
56	rno-miR-29b-3p	MAP2K6
57	rno-miR-29b-3p	NRAS
58	rno-miR-29b-3p	PIAS4
59	rno-miR-29b-3p	SKI
60	rno-miR-29b-3p	TGFB2
61	rno-miR-29b-3p	TGFB3
62	rno-miR-30e-5p	ACVR1
63	rno-miR-30e-5p	BCL2
64	rno-miR-30e-5p	BMP7
65	rno-miR-30e-5p	JUN
66	rno-miR-30e-5p	KRAS
67	rno-miR-30e-5p	RUNX2

68	rno-miR-30e-5p	SERPINE1
69	rno-miR-30e-5p	SMAD1
70	rno-miR-30e-5p	SMAD2
71	rno-miR-30e-5p	SOS1